An Integrated Geochemical and Isotopic Study of the Prieska Province Kimberlites from the Republic of South Africa

A dissertation presented for the degree of
Master of Science

by

Trevor Charles Clark

Bernard Price Institute of Geophysics - Isotope Unit
University of the Witwatersrand
January 1994

Abstract

Rb-Sr emplacement ages of nineteen kimberlites from the Prieska Province vary from 74 to 174 Ma. Their isotopic, whole-rock geochemical signatures and perovskite REE distributions were also determined.

Non-micaceous and micaceous kimberlites from the area show similar petrographic, geochemical and isotopic compositions relative to cratonic kimberlites, indicating similar sub-continental mantle source compositions in the two tectonic environments. Transitional varieties of kimberlite, which can be defined petrographically, geochemically and isotopically are also recognised from the area, but are not prevalent in the cratonic environment. The Prieska Province kimberlites are possibly derived by partial melting processes within a subcontinental reservoir characterised by a spectrum of compositions from time-averaged depleted (HIMU) to enriched (Group II).

The occurrence of these components in both on- and off-craton settings indicates that the kimberlite source area is not strictly linked to the subcratonic lithosphere. Mantle plume sources are not favoured because of the variable source compositions and distribution of emplacement ages within the Province. Transitional kimberlites were derived from a source component with mixed character, not yet noted from within the Kaapvaal Craton. This is the first documented example of isotopically transitional kimberlites from southern Africa.

Declaration

I declare that this dissertation is my own work. It is being submitted for the degree of Master of Science in the University of the Witwatersrand, Johannesburg. It has not been submitted before for any degree or examination in any other University.

Trevor Charles Clark

TREVOR CHARLES CLARK

14th day of January 1994

Acknowledgements

De Beers Consolidated Mines and the Foundation for Research Development are thanked for funding this research. De Beers also provided all the samples for the study and organised a field trip to the area. I would like to thank John Bristow for introducing me to the world of kimberlites, his initial introduction and help in finding my way around the isotope laboratory at the BPI and for co-supervising the early stages of the project. The late Hugh Allsopp and Hans Welke were supervisors prior to their deaths and their passing was a severe blow to the isotope unit.

Craig Smith became my principal supervisor thereafter and grew many grey hairs, particularly towards the end of this project (better late than never !) and is thanked for the suggestions, criticisms, discussions, red ink (will have to buy you a new box of pens!) and patience that has helped the project to mature. In addition, he performed some Rb and Sr analyses for the transitional kimberlites and some of the other kimberlites when I moved to industry. Alaistair Moyes is thanked for all the advice in getting the Sm-Nd work underway. Willie Manton's stay at the BPI enabled me to dabble with the U-Pb system, and Erica Barton gave much advice in this regard too. Moose Kruger is thanked for his suggestions regarding the Rb-Sr system as well as for comments along the way. In addition, some of the VG 354 mass spectrometer analyses were performed by him.

Rodger Hart and Lorraine Roberts are thanked for their advice with the INAA analyses. Dick Rickard analysed the perovskites and Willem van der Westhuizen performed the whole-rock XRF analyses for me.

Janet Moyes helped to keep the lab in running order and Ingeborg Swinley helped to keep the 'accessories' for the mass spec's well stocked. Johan "DD" Holtzhausen is thanked for keeping the mass specs going in spite of the student's attempts to outwit him, as well as for the dirty jokes and threats of chaining me down to the desk (wasn't big enough anyway !). Joe Aphane gave advice on mineral separations and William Nedzibangane helped with keeping the lab's glass supply clean.

GENCOR are acknowledged for sending me to the 5th International Kimberlite Conference against all odds, and the support of Leon Liebenberg and Mossie Mostert is greatly appreciated. Thanks to Brenda Thompson for much of the typing and Thereza Gomes for producing the map of the area.

My wife Dawn has encouraged, supported, advised, and showed incredible patience and understanding during some trying times. Thanks for helping me keep going when it counted and for colouring in all the maps.

Table of Contents

Declaration . . . . . - ii -
List of Figures . . . . . - xxxi -
List of Tables . . . . . - xxxiii -
List of Plates . . . . . - xxxiii -

Chapter 1
Introduction and Review of the Related Literature

1.1 Introduction . . . . . - 1 -
1.2 Research Objectives . . . . . - 3 -
1.3 Review of the Related Literature . . . . . - 4 -
1.3.1. Kimberlite Defined . . . . . - 5 -
1.3.2. Kimberlites located worldwide . . . . . - 10 -
1.3.3. Geochemistry of kimberlite . . . . . - 11 -
1.3.4. Isotopic characteristics of kimberlites . . - 14 -
1.3.5. Unresolved problems . . . . . - 15 -
a. Kimberlite Evolution . . . . . - 15 -
b. Source Region . . . . . - 16 -
c. Plumes, Hot Spots and the Dupal Anomaly . . . . . - 18 -

Chapter 2
Geological Setting and Description of the Kimberlites from the Prieska Province

2.1 Introduction . . . . . - 20 -
2.2 Geological history of the Area . . . . . - 20 -
2.3 Kimberlites from the Prieska Province . . . . . - 22 -
2.4 Descriptions of the Selected Kimberlites . . . . . - 28 -
2.4.1. Brandewynskuil (173/26/K6) . . . . . - 28 -
2.4.2. Britstown (173/26/K35) . . . . . - 29 -
2.4.3. Droogfontein (173/27/K19) . . . . . - 29 -
2.4.4. Eendekuil (173/18/K2) . . . . . - 30 -
2.4.5. Haartebeesfontein (173/27/K1) . . . . . - 30 -
2.4.6. Jonkerwater (173/26/K51) . . . . . - 31 -
2.4.7. Markt (173/26/K15) . . . . . - 32 -
2.4.8. Meltonwold (173/27/K9) . . . . . - 33 -
2.4.9. Middelwater 01 (173/26/K19) . . . . . - 33 -
2.4.10. Pampoenpoort (173/27/K16) . . . . . - 34 -
2.4.11. Sanddrift (173/25/K5) . . . . . - 34 -
2.4.12. Silvery Home (173/27/K11) . . . . . - 34 -
2.4.13. Skietkop (173/27/K23) . . . . . - 35 -
2.4.14. Slypsteen 01 (173/26/K24) . . . . . - 35 -

2.4.15. Sweetput-Soutput (173/26/K40) ..... - 35 -
2.4.16. Vioolkraal West (173/26/K46) ..... - 36 -
2.4.17. Welgevonden (173/26/K67) ..... - 37 -
2.4.18. Witberg Pipe (173/25/K10) ..... - 37 -
2.4.19. Witberg East (173/25/K26) ..... - 38 -
2.5 Other Kimberlites From the Area ..... - 38 -
2.5.1. Uintjiesberg (173/26/K2) ..... - 38 -
2.5.2. Kalkput (173/26/K9) ..... - 39 -
2.5.3. Lushof (173/26/K1) ..... - 39 -
2.6. Summary ..... - 40 -

Chapter 3

Kimberlite Emplacement Ages

3.1 Introduction ..... - 42 -
3.2 Problems With Emplacement Age Determinations ..... - 43 -
3.3 Other Dating Methods ..... - 46 -
3.4 Analyses For This Project ..... - 47 -
3.5 Data Presentation ..... - 48 -
3.5.1. The Britstown Group (173/26/K35) .... - 49 -
3.5.2. The Droogfontein Occurrence (173/27/K19) ..... - 50 -
3.5.3 The Eendekuil Kimberlite (173/18/K2) .. - 53 -
3.5.4. The Haartebeesfontein Occurrence (173/27/K1) ..... - 53 -
3.5.5. The Jonkerwater Kimberlite (173/26/K51) ..... - 54 -
3.5.6. The Markt Kimberlite (173/26/K15/24) . - 56 -
3.5.7. The Meltonwold Kimberlite (173/27/K9) - 58 -
3.5.8. The Middelwater Kimberlite (173/26/K19) - 59 -
3.5.9. The Pampoenpoort Occurrence (173/27/K16/6) ..... - 60 -
3.5.10. The Sanddrift Kimberlite (173/25/K5) . - 61 -
3.5.11. The Skietkop Kimberlite ..... - 63 -
3.5.12. The Sweetput-Soutput Kimberlite (173/26/K40) ..... - 64 -
3.5.13. The Welgevonden Kimberlite (173/26/K67) ..... - 66 -
3.5.14. The Witberg Pipe Kimberlite (173/25/K10) ..... - 67 -
3.5.15. The Witberg Dyke Kimberlite (173/25/K26) ..... - 68 -
3.6 Previous age determinations for kimberlites from the area ..... - 69 -
3.6.1. The Uintjiesburg Kimberlite (173/26/K2) - 69 -
3.6.2. The Kalkput Occurrence (173/26/K9) ... - 69 -
3.6.3. The Lushof Kimberlite (173/26/K1) .... - 70 -

3.7 Samples Not Analysed in This Study ..... - 70 -
3.8 Discussion of Emplacement Age Data ..... - 70 -
3.9 Summary ..... - 72 -

Chapter 4
Whole-rock Isotopic Systematics
4.1 Introduction ..... - 75 -
4.2 Analytical Results ..... - 76 -
4.2.1. Rb-Sr Analyses ..... - 77 -
4.2.2. Sm-Nd Analyses ..... - 80 -
4.2.3. U-Pb Results ..... - 82 -
4.3 Sr-Nd Isotope Compositions ..... - 84 -
4.4 Summary of Isotopic Data ..... - 88 -

Chapter 5
Geochemistry of the Prieska Province Kimberlites
5.1 Introduction ..... - 92 -
5.2 Data used in this work ..... - 94 -
5.3 Major Element Geochemistry ..... - 95 -
5.3.1. General trends ..... - 95 -
5.3.2. Contamination and Alteration ..... - 99 -
5.3.3. Major Element Variation ..... - 105 -
5.4 Trace Element Geochemistry ..... - 111 -
5.4.1. Compatible Elements ..... - 111 -
5.4.2. Incompatible Elements ..... - 112 -
5.5 Discussion ..... - 118 -
5.6 Summary ..... - 118 -

Chapter 6
Geochemistry of Perovskite
6.1 Introduction ..... - 121 -
6.2 Kimberlitic Perovskite ..... - 122 -
6.3 The Prieska Province Perovskites ..... - 124 -
6.4 Discussion ..... - 130 -
6.5 Summary ..... - 131 -

Chapter 7
Discussion
7.1. The Prieska Region as a Province ..... - 133 -
7.2. Prieska Province Kimberlite Age Distribution . - 134 -
7.2.1. Reliability of Emplacement Age Determinations ..... - 134 -
7.2.2. Kimberlite Age Distribution for the Prieska Province ..... - 135 -

7.3 Source Rock Isotope and Geochemical Character . . . . . - 139 -
7.3.1 Petrographic, Geochemical and Isotopic Aspects . . . . . - 139 -
7.3.2. The Transitional Kimberlite Problem . - 143 -
7.3.3. Ages, Hotspots and Tectonic Processes - 146 -
7.3.3.1. Southern African Kimberlite Age Distribution . . . . . - 146 -
7.3.3.2. Hot Spots as Sources ? . . . . . - 152 -
7.3.3.3. Alternative Source Regions . . . - 153 -

Chapter 8
Conclusions . . . . . - 161 -

Appendices

Appendix A . . . . . - 166 -
Sample Descriptions . . . . . - 166 -
A 1. Samples Analysed in this Study . . . . . - 166 -
A.1.1 Brandewynskuil . . . . . - 166 -
A.1.2 Britstown . . . . . - 167 -
A.1.3 Droogfontein . . . . . - 168 -
A.1.4 Eendekuil . . . . . - 168 -
A.1.5 Haartebeesfontein . . . . . - 169 -
A.1.6 Jonkerwater . . . . . - 169 -
A.1.7 Markt . . . . . - 170 -
A.1.8 Meltonwold . . . . . - 170 -
A.1.9 Middelwater 01 . . . . . - 170 -
A.1.10 Pampoenpoort . . . . . - 171 -
A.1.11 Sanddrift . . . . . - 171 -
A.1.12 Silvery Home . . . . . - 172 -
A.1.13 Skietkop . . . . . - 172 -
A.1.14 Slypsteen 01 . . . . . - 172 -
A.1.15 Sweetput-Soutput . . . . . - 173 -
A.1.16 Vioolkraal West . . . . . - 173 -
A.1.17 Welgevonden . . . . . - 174 -
A.1.18 Witberg Pipe . . . . . - 174 -
A.1.19 Witberg East . . . . . - 175 -
A.2. Kimberlites not Analysed in this Work . . . . . - 175 -
A.2.1 Uintjiesburg . . . . . - 175 -
A.2.2 Kalkput . . . . . - 175 -
A.2.3 Lushof . . . . . - 176 -

Appendix B

Analytical Methods

Introduction ..... - 177 -
B 1. Sample Preparation ..... - 183 -
B 1.1 Introduction ..... - 183 -
B 1.2 Whole-Rock Preparation ..... - 183 -
B 1.3 Mineral Separates ..... - 184 -
B 1.3.1 Phlogopite ..... - 184 -
B 1.3.2 Perovskite ..... - 185 -
B 2. Isotope Dilution Analysis ..... - 187 -
B 2.1 Introduction ..... - 187 -
B 2.2 Chemical Procedures ..... - 188 -
B 2.2.1 Reagents, Spikes and Standards - 188 -
B 2.2.2 Beaker Cleaning ..... - 189 -
B 2.2.3 Sample Dissolution ..... - 189 -
B 2.3 Ion Exchange Column Chemistry .... - 191 -
B 2.3.1 Rb-Sr whole-rock chemistry .. - 191 -
B 2.3.2 Rb-Sr phlogopite chemistry ... - 191 -
B 2.3.3 Sm-Nd whole-rock chemistry . - 192 -
B 2.3.4 U-Pb whole-rock chemistry ... - 193 -
B 2.4 Mass Spectrometry ..... - 194 -
B 2.4.1 Loading Samples ..... - 194 -
B 2.4.2 Mass Spectrometer Analysis . - 195 -

B 3 Instrumental Neutron Activation Analysis (INAA) ..... - 196 -

B 4 X-Ray Fluorescence Spectrometry .... - 198 -

B 5 Microprobe Analyses ..... - 198 -

B 6 Standards and Duplicates ..... - 199 -

Appendix C

Data Presentation ..... - 202 -
C 1 : Isotopic Data ..... - 204 -
C1.1 : Rb/Sr Phlogopite Analyses ..... - 204 -
C1.2 : Rb/Sr Whole-Rock Analyses ..... - 206 -
C1.3 : Sm/Nd Whole-Rock Analyses ..... - 207 -
C1.4 : Pb Whole-Rock Anlayses ..... - 208 -
C 2 : XRF Whole-Rock Data ..... - 209 -
C 3 : INAA Whole-Rock Data ..... - 214 -
C 4 : Perovskite Microprobe Analyses ..... - 215 -

Appendix D
Comparison of Analytical Techniques ..... - 218 -
D 1.1 Introduction ..... - 218 -
D 1.2 XRF versus INAA ..... - 218 -
D 1.2 INAA Interlaboratory Correlation ..... - 222 -

Appendix E
Southern African Kimberlite and Related Rock Age Database ..... - 224 -

References ..... - 226 -

List of Figures

Figure 1.1 : Location of Study Area (after Mitchell, 1986) ..... - 1 -
Figure 3.1 : Rb-Sr Isochron Diagram for Britstown ..... - 49 -
Figure 3.2 : Rb-Sr Isochron Diagram for Droogfontein ..... - 51 -
Figure 3.3 : $^{207}Pb/^{206}Pb$ vs $^{238}U/^{206}Pb$ for Droogfontein Perovskite .. - 52 -
Figure 3.4 : Rb-Sr Isochron Diagram for Haartebeesfontein ..... - 54 -
Figure 3.5 : Rb-Sr Isochron Diagram for Jonkerwater ..... - 55 -
Figure 3.6 : Rb-Sr Isochron Diagram for Markt ..... - 57 -
Figure 3.7 : $^{207}Pb/^{206}Pb$ vs $^{238}U/^{206}Pb$ for Meltonwold Perovskite ... - 59 -
Figure 3.8 : Rb-Sr Isochron Diagram for Middelwater 01 ..... - 60 -
Figure 3.9 : Rb-Sr Isochron Diagram for Pampoenpoort ..... - 61 -
Figure 3.10 : Rb-Sr Isochron Diagram for Sanddrift ..... - 62 -
Figure 3.11 : $^{207}Pb/^{206}Pb$ vs $^{238}U/^{206}Pb$ for Skietkop Perovskite .... - 63 -
Figure 3.12 : Rb-Sr Isochron Diagram for Sweetput-Soutput ..... - 65 -
Figure 3.13 : $^{207}Pb/^{206}Pb$ vs $^{238}U/^{206}Pb$ for Sweetput-Soutput
Perovskite ..... - 65 -
Figure 3.14 : Rb-Sr Isochron Diagram for Welgevonden ..... - 66 -
Figure 3.15 : Rb-Sr Isochron Diagram for Witberg Pipe ..... - 67 -
Figure 3.16 : Rb-Sr Isochron Diagram for Witberg Dyke ..... - 68 -
Figure 4.1 : Initial-Sr vs $^{87}Rb/^{86}Sr$ ..... - 79 -
Figure 4.2 : Initial-Nd vs $^{147}Sm/^{144}Nd$ ..... - 81 -
Figure 4.3 : $^{207}Pb/^{204}Pb$ vs $^{206}Pb/^{204}Pb$ ..... - 83 -
Figure 4.4 : $^{208}Pb/^{204}Pb$ vs $^{206}Pb/^{204}Pb$ ..... - 83 -
Figure 4.5 : Epsilon Nd-Sr Diagram ..... - 85 -
Figure 5.1 : Contamination Index for the Frieska Province
Kimberlites ..... - 103 -
Figure 5.2 : Comparison of the CI with the Si/Mg ratio ..... - 103 -
Figure 5.3 : Harker Element Diagram (major elements against
SiO_2) ..... - 106 -
Figure 5.4 : K_2O vs TiO_2 ..... - 110 -
Figure 5.5 : Primitive Mantle Normalised Incompatible Element
Plot ..... 114 -
Figure 5.6 : Rare Earth Element Plot ..... 116 -
Figure 5.7 : Ba/Nb vs La/Nb ..... - 116 -
Figure 5.8 : Ba/Nb vs Zr/Nb ..... - 117 -
Figure 5.8 : Zr/Nb vs La/Nb ..... - 117 -
Figure 6.1 : Chondrite Normalised REE Plot for Perovskite .... - 129 -
Figure 6.2 : Perovskite and Whole-Rock REE Plots ..... - 129 -
Figure 7.1 : Age Histogram of southern African Kimberlites and
Related Rocks ..... - 148 -

List of Tables

Table 2.1 : Characteristics of the Prieska Province Kimberlites . . - 24 -
Table 3.1 : Results of leaching for Markt mica . . . . . - 56 -
Table 3.2 : Summary of Emplacement Ages for the Prieska Province . . . . . - 73 -
Table 4.1 : Summary of Isotopic Data . . . . . - 90 -
Table 5.1 : Ranges and Averages for Major Elements . . . . . - 97 -
Table 5.2 : Compatible Element Trends for the Prieska Province - 111 -
Table 6.1 : Perovskite Microprobe Analyses . . . . . - 127 -
Table 7.1 : Summary of Age Events for southern Africa . . . . . - 151 -

List of Plates

Plate 2.1 : Microphotograph of Typical Non-Micaceous Kimberlite - 25 -
Plate 2.2 : Microphotograph of a Typical Micaceous Kimberlite . . . - 27 -
Plate 2.3 : Example of Typical Transitional Kimberlite . . . . . - 27 -
Plate 3.1 : Microphotograph of Transitional Kimberlite Groundmass . . . . . - 72 -
Plate 6.1 : Perovskite in Transitional Kimberlite . . . . . - 125 -
Plate 6.2 : Perovskite in Non-Micaceous Kimberlite Haartebeesfontein . . . . . - 125 -

Attached Map (in back pocket)

Simplified Geological Map of the Prieska Province Showing Kimberlite Distribution and Localities Investigated (Scale 1:1 000 000)

Chapter 1

Introduction and Review of the Related Literature

1.1 Introduction

This research concerns a suite of kimberlite occurrences situated at the southwestern margin of the Kaapvaal Craton, having intruded, at depth, lithologies of the Natal Namaqua Mobile Belt in South Africa (Figure 1.1, attached map in back folder).

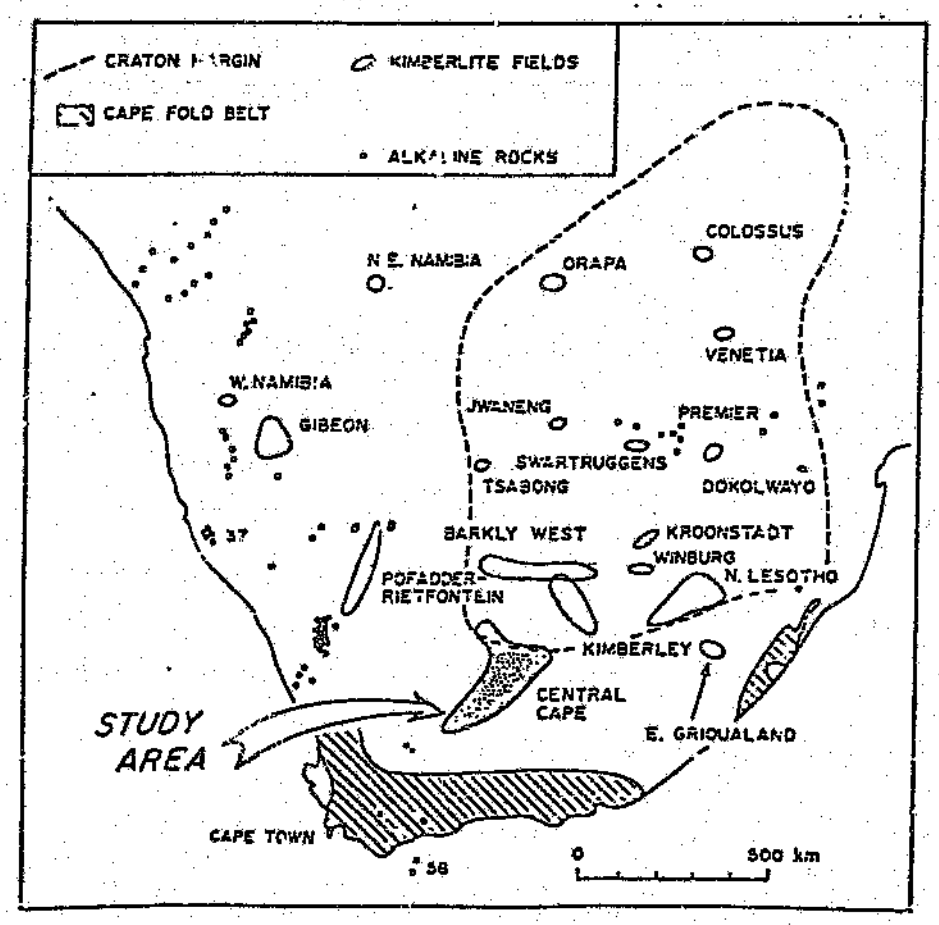

Figure 1.1 : Location of Study Area (after Mitchell, 1986)

They have been termed the Central Cape kimberlites by Mitchell (1986), and the Karoo kimberlites by Robey (1981). This kimberlite suite is referred to in this research as the Prieska Province kimberlites as it is considered that they constitute a number of different kimberlite fields. Very little work regarding the nature of kimberlites from mobile belt terrains has been done in the past. In particular, the Prieska Province kimberlites have received scant attention in terms of their isotopic and geochemical characteristics. This is due mainly to the fact that these kimberlites are considered to be non-diamondiferous, whereas previous work has concentrated on cratonic, diamondiferous kimberlites (eg. Smith, 1983 and others). Some investigations that have been performed on marginal kimberlites and related rocks include those from Griqualand East (Nixon et al., 1983); the Emtilombo dykes of Northern Natal (Colgan et al. 1989); and the geochemical and isotopic character of kimberlites from the Gibeon Province in Namibia (Spriggs, 1988).

Robey (1981) studied many of the occurrences from the Prieska Province, but the emphasis of this research was on the mantle and crustal xenoliths. Major element geochemistry was only undertaken on some of the kimberlites. No isotopic work was performed by him. Smith (1983a,b) and Smith et al (1985) analysed samples from the Uintjiesberg kimberlite for their isotopic and geochemical character and obtained emplacement age data from this occurrence. Davis (1978) analysed zircons to obtain emplacement age data from Kalkput and Lushof. Just south of the area there are a number of olivine melilitites at Sutherland which were examined by Viljoen (1988).

This study is a comprehensive geochemical and isotopic investigation of selected kimberlites from one province. Samples were made available by De Beers following an extensive drilling program to recover fresh

samples, generally unavailable in surface exposures.

1.2 Research Objectives

The objectives of this research are as follows:

1. Determination of the emplacement ages of the kimberlites from the Prieska Province.

   The data will augment the knowledge of southern African kimberlites in space and time.

2. Determination of whole-rock initial isotopic ratios of the Prieska Province kimberlites utilising the Rb-Sr, Sm-Nd and U-Pb isotopic systems.

   This will help to characterise the source material from which the kimberlites were derived and provide insights into the nature of the subcontinental upper mantle of the area.

3. Characterise the Prieska Province kimberlites geochemically, utilising whole-rock major and trace elements.

   This will augment the isotopic data obtained, and will enable the relationship between the geochemistry and isotopic systematics of whole-rock kimberlites to be investigated further.

4. Study of the rare earth element (REE) patterns in both perovskite and kimberlites from the area.

   Perovskite is an important accessory phase in kimberlite and is believed to be a major control of REE and Rb compositions in the kimberlite melt. The distribution of REE's between perovskite and the host rock will be examined to determine more about the distribution of the rare earths in kimberlites.

5. Comparison of the study area rocks to their cratonic counterparts.

   The differences and similarities regarding the geochemical, isotopic and kimberlite source area character of the two tectonic areas will be examined and discussed.

This research therefore complements previous investigations, particularly the ones by Smith (1983b), Smith et al. (1985) and Robey (1981).

The remainder of this chapter is concerned with a review of the related literature pertaining to this research. The reader is therefore referred to the literature quoted below for more detailed explanations.

1.3 Review of the Related Literature

Kimberlite, a rare and volumetrically insignificant rock type, is widely regarded as constituting an important window into the Earth's upper

mantle. Testimony to the importance of this lithology (and its constituents) lies in the fact that five international conferences have been devoted to this unusual rock type, although in recent times, lamproites have also found increasing attention at these conferences.

The range of research available for the study of kimberlites is as varied as kimberlite itself. As such, numerous detailed reviews, dissertations and papers dealing with the various aspects of the geology, petrology and geochemistry of kimberlites exist in the literature. The more significant works include papers submitted to the Proceedings of the five International Kimberlite Conferences (1975, 1979, 1984, 1986, 1992), books by Wagner (1914), Nixon (1973), Dawson (1980) and Mitchell (1986), and articles by Skinner and Clement (1979), Skinner (1989), Smith (1983a,b), Smith et al. (1985) and Ringwood et al. (1992).

Of these, Mitchell (1986) and papers submitted to the Proceedings of the International Kimberlite Conferences give excellent reviews of the current state of knowledge pertaining to kimberlite geology, mineralogy and geochemistry.

1.3.1. Kimberlite Defined

Although kimberlite is only one of many mantle-derived lithologies, it is considered to be one of the key rock types available to study the processes governing the geochemistry and isotopic nature of the subcontinental upper mantle. Despite their rarity, some authors (eg. Eggler, 1989), consider kimberlites to be somewhat "ordinary", with source regions little different to other alkaline magmas in terms of mineralogy or chemistry, and that their rate of ascent is not that much faster than alkaline basalts. Xenolith contents and sizes are not easily

explained by slow ascent rates, however.

Kimberlites commonly intrude as pipes (diatremes) or dykes and occasionally as sills (see Hawthorne, 1975; Dawson, 1980; Clement, 1982, Clement et al. 1985 and Mitchell, 1986 for details). The kimberlite melt may utilise the same conduit to produce a number of distinct intrusions within one diatreme, each of which may be petrographically distinct and geologically mappable.

Mineralogically, kimberlites are complex rocks. Minerals found in kimberlites may have been derived from three sources (Mitchell, 1986) and the proportions from each of these groups which make up the constituent end product varies widely. The three sources include disaggregated mantle-derived xenoliths, megacrysts (discrete nodule suite), and minerals considered to be primary phases of the kimberlite magma. In addition, kimberlites can contain numerous country rock fragments which must be recognised and taken into account when analysing kimberlites geochemically.

There are numerous ways of defining kimberlite. These include the use of geological, mineralogical, isotopic and geochemical parameters. Wagner (1914), Clement et al. (1985) and Mitchell (1986) have attempted to utilise various aspects of these parameters to provide a comprehensive definition. The latter two authors have each provided accepted definitions of kimberlite, although Clement's definition is considered by Mitchell (1986, p.16) to be inadequate as it "omits the characteristic compositions of the kimberlite mineral assemblage and introduces extraneous geological information to a petrological definition". However, the complex mineral assemblages occurring in kimberlite are dealt with separately in the mineralogical classification of Skinner and Clement (1979). Clement et al.'s (1985) definition is

therefore preferred by this author and is reproduced below:

> *"Kimberlite can be defined as a volatile-rich potassic ultrabasic igneous rock which occurs as small volcanic pipes, dykes and sills. It has a distinctive inequigranular texture resulting from the presence of macrocrysts set in a fine grained matrix. This matrix contains as prominent primary phenocrystal and/or groundmass constituents, olivine and several of the following minerals: phlogopite, carbonate (commonly calcite), monticellite, apatite, spinels, perovskite and ilmenite. The macrocrysts are anhedral, mantle-derived, ferromagnesian minerals - which include olivine, phlogopite, picroilmenite, chromian spinel, magnesian garnet, clinopyroxene (commonly chromian diopside) and orthopyroxene (commonly enstatite). Olivine is extremely abundant relative to the other macrocrysts, all of which are not necessarily present. The macrocrysts and relatively early-formed matric minerals are commonly altered by deuteric processes, mainly serpentinisation and carbonatisation. Kimberlite commonly contains inclusions of upper mantle-derived ultramafic rocks. Variable quantities of crustal xenoliths and xenocryst may also be present. Kimberlite may contain diamond but only as a very rare constituent."*

Skinner and Clement's (1979) mineralogical definition is based on the groundmass modal mineralogy and allows for comparison of kimberlites on a worldwide basis (Mitchell, 1986). As olivine is an essential component of kimberlite (both as phenocrysts and xenocrysts), it is excluded from the classification. According to the definition, five varieties of kimberlite are recognised, based upon the predominance of diopside, monticellite, phlogopite, calcite and serpentine. If sufficient quantities of another one of these minerals is present, it may be used

an additional qualifier in the classification. Examples include phlogopite kimberlite, monticellite kimberlite, monticellite-phlogopite kimberlite (where phlogopite > monticellite) and phlogopite-diopside kimberlite (where diopside > phlogopite). Accessory phases such as apatite, perovskite or opaque minerals may also be used in the classification if they are present in significant amounts.

The earlier notion of the existence of two distinct petrographic types of kimberlite (Wagner, 1914) has been upheld, although slightly more refined (Skinner, 1989). The "basaltic" variety of Wagner correlates to the 'non-micaceous' kimberlite type whilst the "lamprophyric" type defined by Wagner is now termed the "micaceous" kimberlite.

Kimberlites have also been subdivided on the basis of isotopic character into two types, termed Group I and Group II (Smith, 1983a) - see Section 1.3.4. This isotopic classification broadly corresponds to the non-micaceous and micaceous varieties respectively. As a result numerous authors (eg. Skinner, 1989) use the Group I and II terminology in a petrographic sense (viz. calling a 'non-micaceous' kimberlite a Group I kimberlite and a micaceous kimberlite a Group II kimberlite). In this research, Group I and II kimberlites refer to the isotopic types, whilst non-micaceous and micaceous kimberlites imply petrographic types. The relationship between the isotopic and petrographic types will be examined further.

Non-micaceous kimberlites are characterised by the presence of olivine, monticellite, phlogopite, calcite and serpentine. Groundmass spinels and perovskite are typically abundant and relatively coarse grained and primary groundmass ilmenite may be present. Apatite is a common accessory mineral. Diopside is not present as a primary phase.

Micaceous kimberlites are characterised by phlogopite being present as both a phenocrystal and macrocrystal phase and primary diopside is common. Groundmass monticellite is usually absent and primary apatite is a common accessory mineral. The megacryst suite is not well represented in micaceous kimberlites and Skinner (1989) believes that ilmenite is characteristically absent. However, garnet-ilmenite megacrysts are reported from the Dokolwayo pipe by Daniels et al. (1989). Garnet megacrysts are also found in the Star, Lace and Kalkput localities and cpx is present at the Lace kimberlite. Group II kimberlites (petrographic and isotopic) have not been recognised anywhere other than in southern Africa (Mitchell, 1989; Skinner, 1989).

Robey (1981) and Skinner (1989) report the occurrence of both micaceous and non-micaceous kimberlites in the Prieska Province in South Africa. In addition, Skinner (1989) reports the presence of some kimberlites which exhibit petrographic features of both micaceous and non-micaceous types in this Province. These kimberlites are essentially micaceous types. However, they are not typical when compared to "classic" micaceous varieties as seen within the Kaapvaal craton in that they contain relatively coarse grained opaque minerals (eg. perovskite) as well as significant amounts of xenocrystic ilmenite, high TiO_2 garnets and chrome-poor macrocrysts. In addition, certain features are similar to olivine lamproites, eg. presence of late-crystallising amphibole, possible presence of sanidine, abundant orange-brown phlogopite and glomeroporphyritic olivine phenocrysts (Skinner et al. 1991). These kimberlites are termed *transitional* in this research.

1.3.2. Kimberlites located worldwide

Known kimberlites are restricted to continental areas. In particular, they are often located within stable, ancient (>2,5 Ga) cratonic regions of continents (Dawson, 1989). They also occur in mobile belts surrounding cratons, but are generally not considered economically significant in mobile-belt terrains (Mitchell, 1986). Possible exceptions to this would include the Venetia kimberlite pipe, situated in the Limpopo Mobile Belt in the northern Transvaal of South Africa and the Argyle lamproite which occurs within the Halls Creek Mobile belt of NW Australia. However, the ages of these mobile-belt terrains are considered to be old enough (ie. "cratonised") to have enabled the formation of diamond within a thickened lithosphere.

Moore and Verwoed (1985), have shown that a zonation of cratonic alkaline igneous activity on a regional scale can be recognised in Eastern Siberia as well as in southern Africa. This zonation consists of diamondiferous kimberlite provinces in cratonic areas and non-diamondiferous kimberlites, alkaline complexes, carbonatites and lamprophyres towards and beyond the craton margins. Atkinson, et al. (1984) noted the occurrence of diamondiferous kimberlites and olivine lamproites from an off-craton setting in northwestern Australia. These observations have lead to a greater interest in kimberlites and related rocks in off-craton settings.

Southern Africa is host to a remarkable number of kimberlite intrusions, in both the ancient cratonic regions and surrounding mobile belt terrains. Economically significant kimberlites are confined to the cratonic regions. Dawson (1980), has noted the absence of kimberlites in the southeast of South Africa. Most of the intrusions tend to occur

clusters and many diatremes are aligned along intersecting fracture patterns within the country rocks.

Mitchell (1986), notes that at least eight periods of kimberlite magmatism can be identified in the southern African Province. The range in ages span from the Precambrian Kuruman kimberlites (1 600 Ma) to the Late Cretaceous Gibeon field (± 70 Ma). The height of kimberlite magmatism in southern Africa was undoubtedly during the Mid- to Late-Cretaceous. Dawson (1980), notes that this period coincides with a period of pronounced regional uplift. The break-up of Gondwanaland also occurred at this time and there is undoubtably a relationship between this event and the magmatic events recorded in southern Africa at this time. Economically, the most important kimberlites are those which are found within regions underlain by the oldest portions of the craton. Dawson (1980), noted that non-diamondiferous kimberlites from the mobile belts tend to be younger than the cratonic (diamondiferous) kimberlites, based on the information available at that time.

These statements by Mitchell and Dawson will be addressed more fully in this research. It will be shown that there is a complex kimberlite age distribution of the Prieska Province alone. This will be related to the rest of the South African kimberlite age distribution.

1.3.3. Geochemistry of kimberlite

Kimberlite is formed from a volatile-rich magma, often has a complex intrusive style (as in the formation of diatremes) and may form a hybrid rock-type, susceptible to high degrees of crustal and mantle contamination and post-intrusive alteration effects. Kimberlite is,

therefore, a problematic rock-type to analyse geochemically. Mitchell (1986), believes that kimberlite whole-rock compositions are not representative of the compositions of the magma from which they formed. Certainly, many earlier investigations have not carefully considered the effects of contamination and some previous geochemical analyses were of crustally contaminated diatreme facies rocks. Nevertheless, it is generally agreed that hypabyssal facies kimberlite provides the most suitable material from which to obtain geochemical data.

Kimberlite is an undersaturated, ultrabasic, volatile- and potassic-rich igneous rock type which exhibits a wide range in composition. Major element geochemistry shows SiO_2 varying between 25 and 40 wt %, MgO ranging from 20 to 30 wt %, up to 10 wt % volatiles (H_2O and CO_2) and up to 4 wt % K_2O. In addition, Al_2O_3 is low (± 2.5 wt %), Na_2O is very low (<1 wt %) and P_2O_5 is high (0.3 to 2.6 wt %), (Dawson, 1980; Clement, 1982; Fraser, 1987).

Trace elements can be broadly grouped into "compatible" and "incompatible" elements as follows:

"Compatible" elements are those elements preferentially incorporated into the phases crystallising from the magma and are therefore rapidly depleted during fractional crystallisation and partial melting. Solid-liquid distribution coefficients are greater than unity. The compatible elements are principally hosted by the spinels and olivine with lesser amounts found in perovskite (Sc), sulphides (Cu, Ni) and diopside (Cr, V, Ni). The abundances are similar to those found in other ultramafic rocks, but relative to basalts the concentrations are much greater. They include the elements, Cr, Ni, Co, Sc, V, Zn and Cd. Mitchell (1986), does not believe these elements to be of any use in geochemical models

of kimberlite evolution.

"Incompatible" elements are those whose abundances are similar to those found in other alkaline rocks such as melilitites, alnoites, carbonatites and potassic lavas (Mitchell, 1989). Solid-liquid distribution coefficients in the common rock-forming silicates are approximately zero. Although their abundances may be decreased by the presence of olivine macrocrysts and/or crustal contamination, the inter-element relationships remain unaffected (Mitchell, 1986). These elements thus provide information regarding the source regions of the magmas. The incompatible elements include Cl, B, Mo, Pt, Y, Sc, Bi, Zr, Tl, Sr, Be, Rb, Pb, Nb, Ta, U, Th, Cs and the rare earth elements. Kimberlites are particularly enriched in the incompatible elements with abundances up to 1 000 times chondritic values.

Nixon et al. (1981) noted that cratonic kimberlites contain greater abundances of REE, Rb, Be, Sr than marginal kimberlites. Smith (1985) presented details of Group IB kimberlites (off craton Group I kimberlites) which occur in the study area, but did not consider differences in incompatible element abundances between these and cratonic Group IA types to be significant. However, IB types showed higher Y and lower LREE enrichment, relative to IA types consistent with the observation of Nixon et al. (1981).

Rogers (1977) also noted a difference in REE and incompatible elements for kimberlites located towards the margin of the Kaapvaal craton.

1.3.4. Isotopic characteristics of kimberlites

Early isotopic studies of kimberlites consisted of attempts to provide emplacement age data. This was hampered by the lack of suitable material since whole-rock kimberlite samples do not provide a spread of $^{87}Rb/^{86}Sr$ ratios on the standard isochron diagram. However, Allsopp and Barrett (1975), showed that reliable emplacement ages could be obtained by the Rb-Sr method on phlogopite. Smith (1983a,b) and Brown et al. (1989) subsequently refined the technique, and Smith (1983a, 1985) also showed that kimberlites could be subdivided on isotopic grounds into Group I and Group II types, which broadly correlate with petrographic "non-micaceous" and "micaceous" types (Wagner, 1914; Skinner and Clement, 1979), respectively.

Group I kimberlites are isotopically defined as having emplacement ages ranging from 90 Ma to 114 Ma, initial-Sr ratios of 0.7033-0.7049 $^{206}Pb/^{204}Pb$ between 18.45 and 20.05 and initial-Nd ratios of between 0.51271 and 0.51277. Smith (1983b) interpreted these kimberlites as being derived from depleted asthenosphere. Group II kimberlites are isotopically defined as having emplacement ages from 11[illegible]-150 Ma, initial-Sr ratios of between 0.7074 and 0.7109, $^{206}Pb/^{204}Pb$ between 17.2 and 17.7, lower U/Pb ratios relative to Group I and initial-Nd ratios of between 0.51208 and 0.51228. These kimberlites are interpreted as being derived from ancient enriched lithosphere (see Section 1.4 for other interpretations of kimberlite source regions). The Frank Smith kimberlite analysed by Smith was found to have an isotopic character between that of Group I and II types, although displaying more Group I character. No fresh kimberlites analysed by Smith (1983b) were seen to display transitional isotopic character (initial-Sr ratios between those for Group I or II kimberlites).

1.3.5. Unresolved problems

Of the numerous problems yet to be solved in kimberlite petrology, the following problems are considered relevant to the Prieska Province:

a. **Kimberlite Evolution**

A number of hypotheses have been put forward to explain the evolution of kimberlites from the mantle. No consensus of opinion has been reached at the present. Mitchell (1986) points out that most petrogenetic schemes are based on the philosophies current at their introduction (current views favour mantle metasomatism and subduction).

There are four main processes thought to be responsible for the generation of kimberlites:

1. **Hybridisation** - whereby kimberlites are hybrids between carbonatites and pre-existing ultramafic rocks (Dawson, 1967);

2. **Zone refining** - partial melting of a slightly hydrated peridotite which rises to the surface by a process of solution stoping, thus leading to an enriched incompatible element liquid (Harris and Middlemost, 1969);

3. **Fractional crystallisation** - partial melting of a four phase garnet lherzolite at ± 80 km depth of produce a liquid with the composition of a hypersthene - normative picrite basalt and a residual peridotitic solid (O'Hara and Yoder, 1967);

4. **Partial melting** - limited melti g of a five- or six-phase garnet lherzolite (phlogopite and carbonate present) to produce the high incompatible element trends observed in kimberlites (Dawson, 1971, 1972; Wyllie, 1979; Eggler and Wendlandt, 1977).

This last option appears to be the favoured model of petrologists today. McKenzie (1985) has shown that extremely small degrees of partial melting (<0.1%) can be invoked to explain the extraction of low-viscosity magmas from the mantle. Zindler (1984) suggests that small isolated eruptions (such as alkali basalts, nephelinites, lamproites and kimberlites) are unlikely to have been derived from deep mantle plumes and could be the results of small degrees of partial melting of small localised fertile regions of the deep subcontinental lithosphere.

b. Source Region

A major unresolved problem regarding the derivation of kimberlites (Group I and Group II types) from the asthenosphere or lithosphere still prevails in kimberlite research. At present, a number of hypotheses have been put forward:

1. Smith (1983a,b) ; Smith et al. (1985) proposed that Group I kimberlites are derived from OIB like sources (asthenosphere), whilst Group II kimberlites are derived from ancient enriched lithosphere. The basis of Smith's arguments rests with isotopic evidence.

2. le Roex (1987), suggests derivation of both Group I and II kimberlites from plumes originating in the asthenosphere. This was based on a study of basalts derived from hotspots which he

attempted to correlate with the spatial distribution of kimberlite pipes.

3. Conversely, McCulloch et al, (1983) and Skinner (1989) propose that both groups of kimberlite have their origin in the lithosphere. Skinner bases his arguments on the similar geochemical character of the two kimberlite types being derived from a heterogeneous lithosphere.

4. Nixon (1981), believes that kimberlites are mixtures of asthenospheric and lithospheric melts. Later work (1987) resulted in the proposal that Group I kimberlites were asthenospherically-derived with Group II kimberlites derived from the lithosphere as a results of heating caused by rising Group I kimberlites.

5. Smith et al. (1992 and pers. comm.) suggests that the isotopic correspondence of kimberlites to OIB signatures is coincidental and that megacrysts and Group I kimberlites are products of the HIMU geochemical reservoir, which he places within a comparatively thick continental tectosphere.

6. Ringwood et al. (1992) propose that both Group I and II kimberlites have source regions similar to OIB's. These are all believed to have been derived from a boundary layer comprised of subducted harzburgite and asthenospheric pyrolite within the transition zone of the upper mantle.

These arguments regarding the source regions of kimberlites will be discussed further in this research, and any model proposed for kimberlite source region should have universal appeal. The Prieska

Province kimberlites have been emplaced in an essentially off-craton setting, with consequent raised heatflow and thinned lithosphere. Data obtained is to be compared to their cratonic counterparts thus enabling a test to be made of the above ideas.

c. Plumes, Hot Spots and the Dupal Anomaly

What is the mechanism causing the generation of kimberlite melts? In the case of the Karoo basaltic magma event, plumes are used to account for their generation (Bristow and Hatton, 199 arsh, et al., 1992) as plumes are considered to have OIB geochemical racter. Bristow and Hatton (1992) also suggests that post-Karoo kimberlite emplacement may be a consequence of localised low-volume continuous plume-tail (hot spot) activity impinging on the Kaapvaal lithosphere.

le Roex (1987) and Skinner (1989) attempted to correlate kimberlite generation to hot spots. These hot spots (now present in the south Atlantic) appeared to be present beneath southern Africa at the time of many Group II kimberlite emplacement ages. However, Smith et al. (1992) present compelling evidence for kimberlites representing lithospheric components of the HIMU geochemical reservoir at shallower levels, and do not favour the deep-seated hot spot theory.

The Dupal Anomaly (Dupre and Allegre, 1983) is an area or band situated in the southern hemisphere between South America and southern Africa. A number of ocean island basalt (OIB) sources fall within this area and show distinct isotopic compositions believed to be a product of mixing of end-member mantle reservoirs (Zindler and Hart, 1986). These Dupal islands (Gough, Tristan da Cunha and Discovery) show high $^{87}Sr/^{86}Sr$ and low $^{143}Nd/^{144}Nd$ (viz. enriched compositions) relative to bulk earth.

Bizzi et al. (1991) suggests that Mesozoic kimberlites from the São Francisco craton in Brazil have a source region similar to that of the Dupal Anomaly. Spriggs (1988) in a study of the Gibeon kimberlite province found that the kimberlites there have a non-Dupal signature, but are more akin to an OIB (Bouvet) type source. Both these kimberlite provinces consist of non-micaceous kimberlite types.

These possible source regions will be discussed with respect to the Prieska Province kimberlites.

Chapter 2

Geological Setting and Description of the Kimberlites from the Prieska Province

2.1 Introduction

The geographic area of the present investigation extends from about 50 km northwest of Prieska to 30 km northeast of Sutherland in the Central Cape Province of South Africa (Figure 1.1, Attached Map).

This area straddles the southwestern margin of the Kaapvaal Craton/Namaqua Mobile Belt. There are about 130 known kimberlites in this area, the majority of which intrude sedimentary rocks of the Karoo Supergroup, thus constraining kimberlite emplacement to post-Karoo times.

This chapter reviews the general geology of the area and describes the various occurrences selected for analysis. The attached map (Plate 1) shows the studied kimberlites in relation to the simplified geology of the area.

2.2 Geological history of the Area

Most of the area is covered by sedimentary rocks of the Karoo Supergroup. To the northwest of the area lies an exposed portion of the Namaqua Metamorphic Complex, and Archaean crystalline basement rocks. Although the full extent of the Namaqua province rocks is unknown due to the sedimentary cover, it is likely to extend eastward

beneath the Karoo cover and link up with the Natal Province (Tankard, et al., 1982). Therefore the Prieska Province kimberlites have intruded, at depth, rocks forming part of the Namaqualand Metamorphic Complex. This is borne out by the fact that xenoliths collected from a number of kimberlite localities in the study area by Robey (1981) include various basic and ultramafic lithologies (eg. granulites, eclogites) that are probable fragments of this complex. Measurements on the PT equilibration conditions for eclogite and granulite xenoliths from some of the kimberlites of the Province give equilibration temperatures of between 800-1000°C and pressures of 15-20kb (Robey, 1981).

The boundary between the Namaqua and Kaapvaal provinces is commonly taken to be the Brakbos fault in the northern part of the study area (Altermann et al., 1991). To the southeast of the study area, this boundary is covered by sedimentary rocks and is inferred. Furthermore, broad 'transitional zones' are present to the northwest of the study area (now termed the Keis Province) which complicates the position of the boundary between the Namaqua and Kaapvaal terrains.

The Namaqua Province developed as an extension of the supracrustal sequences that accumulated on the Kaapvaal craton (continental crust) during the Late Archaean-Early Proterozoic, and was subsequently metamorphosed in the Early Proterozoic. During the Early to Middle Proterozoic, intense orogenic activity disturbed vast areas in the southern and western parts of the continent, which gave rise to the Namaqua and Natal Provinces (Tankard et al., 1982). Accretion of the Namaqua and Natal provinces onto the southern margin of the Archaean Kaapvaal craton took place during a prolonged phase of southwest to northeast directed conveyance (Jacobs et al., 1993). The opening of the proto-South Atlantic Ocean during the Later Proterozoic at about 900 Ma was followed by rifting of the continental crust.

The Gondwana Era was heralded by abortive rifting around the southern and eastern fringe of the Kalahari Province, which gave rise to the Cape Supergroup. During the Carboniferous, the supercontinent had drifted southeast across the Polar regions, giving rise to vast ice sheets. Melting of these sheets during the Permian caused the start of the deposition of the Ecca sediments. The large intercratonic Karoo basin was the site for vast inland seas with fluvial and shoal-water environments resulting in the continued deposition of the Ecca followed by the Beaufort sedimentation. During Beaufort sedimentation (Triassic), tectonic shortening of the Cape and Karoo successions took place. Oceanic crust may have been subducted northward at a low angle at the margin of the supercontinent (Lock, 1980). Vast outpourings of basaltic and rhyolitic lavas heralded the close of Karoo sedimentation and the close of the Gondwana Era.

The Mesozoic was the period during which Gondwana split, and also marks the period of greatest kimberlite magmatism in southern Africa. The fragmentation of Gondwana took place in two stages. From 190 Ma to 160 Ma, separation occurred along the eastern flank of the Mozambique ridge parallel to the trend of the Lebombo lavas (which preceded rifting by about 20 Ma). The second phase of rifting created the South Atlantic Ocean between 135 Ma and 130 Ma during which South America was split from Africa.

2.3 Kimberlites from the Prieska Province

The kimberlites have intruded as dykes, blows (enlargements of dykes) and diatremes. One sill is noted by Skinner et al. (1991). Robey (1981) reports that the diatremes are generally small (<2 ha) in relation to

other southern African examples. Outcrop is poor in the area, due to the inherent weathering characteristics of kimberlites. Some prospecting pits and trenches have been cut into a few of the kimberlites but samples from these prospects are usually too weathered for geochemical and isotopic analyses. However, drilling of many of the kimberlites by De Beers Consolidated Mines has enabled the author to obtain some samples fresh enough for geochemical and isotopic analyses. From this drill-core, nineteen occurrences were selected to give a representative spread from on-craton to far off-craton (Attached Map).

All the kimberlites in the area contain hypabyssal facies rocks, although some occurrences also contain diatreme facies types (Robey, 1981; this study). Non-micaceous types tend to occur as pipes whereas micaceous types often intrude as dykes, in common with cratonic localities. Dykes generally strike NNW to NW, probably reflecting the underlying grain of the basement. Table 2.1 summarises the petrographic types and geological characteristics of the kimberlite occurrences from the area.

In hand specimen, all the samples studied can be described as either macrocrystic or porphyritic hypabyssal facies kimberlite. Samples from Eendekuil are very weathered, but comparatively fresh, large phlogopite macrocrysts are present (from which it was hoped new age data would be obtained). Samples from Slypsteen 01, Mt. Pierre and Witberg East contain numerous thin (<2 mm) veins of calcite and serpentine. Olivines from the majority of the kimberlites studied are serpentinised to varying degrees. The localities Uintjiesberg, Lushof and Kalkput were not examined by this author, but some work has been performed on these localities (Smith, 1983b and Davis 1977 respectively) and they are included for comparative purposes.

Table 2.1 : Characteristics of the Prieska Province Kimberlites

OCCURRENCE	TYPE	FORM	FACIES	STRIKE
Britstown	nm	pipe, dyke	hyp/diat	224
Haartebeesfontein	nm	pipe, dyke	hyp	360
Lushof	nm	pipe, dyke	hyp.diat	54
Pampoenpoort	nm	pipe, dyke	hyp, diat	350
Uintjiesberg	nm	pipe, dyke	hyp	360
Vioolkraal West	nm	pipe	hyp	-
Witberg Pipe	nm	pipe	hyp	-
Droogfontein	t	dyke	hyp	-
Meltonwold	t	pipe, dyke	hyp, diat	360
Silvery Home	t	dyke, blow	hyp	360
Skietkop	t	-	hyp	-
Sweetput-Soutput	t	pipe	hyp	-
Brandewynskuil	m	pipe, dyke	hyp, diat	224
Eendekuil	m	dyke	hyp	270
Jonkerwater	m	dyke	hyp	225
Kalkput	m	pipe	diat	-
Markt	m	pipe	hyp	-
Middelwater 01	m	dyke	hyp	258
Mt. Pierre	m	dyke	hyp	225
Sanddrift	m	dyke, blow	hyp	205
Slypsteen 01	m	dyke	hyp	230
Witberg Dyke	m	dyke	hyp	230

Key to Table 2.1

Hyp = Hypabyssal ; Diat = Diatreme
Types : nm = non-micaceous, m= micaceous, t = transitional

The samples were examined petrographically in order to select the freshest material. Although Skinner (1989) has noted the presence of micaceous kimberlites from this off-craton setting, isotopic Group II kimberlites have not previously been studied in detail from an off-craton setting. The suggestion by Smith (1983b), that Group II kimberlites were restricted to the craton, is incorrect as will be shown in this work.

The ***non-micaceous kimberlites*** are essentially monticellite kimberlites with abundant fairly coarse-grained opaque minerals in the groundmass. Some occurrences contain abundant phlogopite, as groundmass and macrocrystal phases. An example of a typical non-micaceous kimberlite is shown in Plate 2.1 below :-

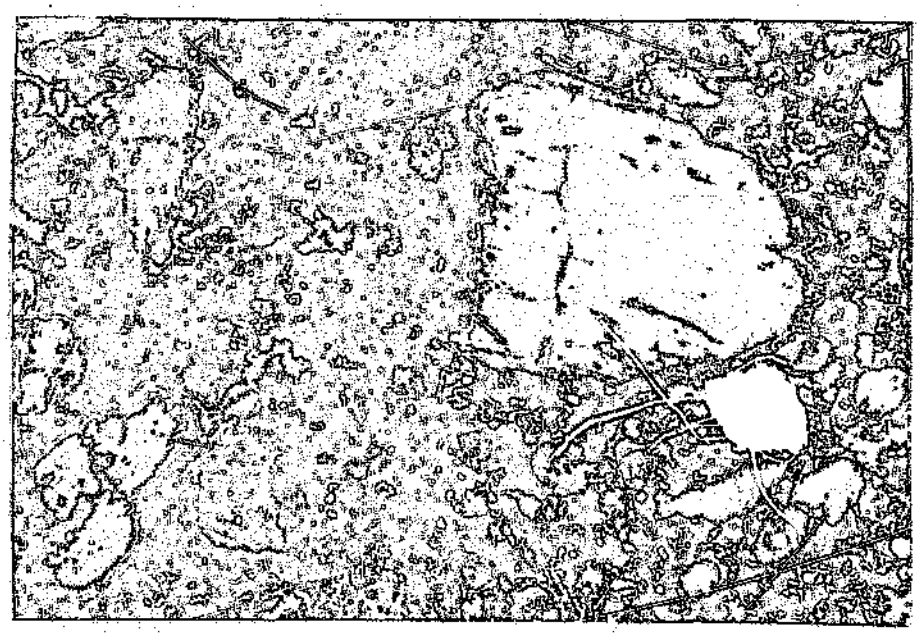

Plate 2.1 : Microphotograph of Typical Non-Micaceous Kimberlite Haartebeesfontein 17

Plane Polarised Light (PPL) Field of View (FOV) = 4.6 mm

Plate 2.1 clearly shows two generations of olivine, monticellite, the opaque-rich nature of the groundmass and calcite as an interstitial phase within the groundmass, all of which are typical features of these non-micaceous varieites of kimberlite. An altered and corroded phlogopite macrocryst is visible towards the top left corner of the photo. Note the alteration of the olivine to serpentine around the edges.

Micaceous kimberlites consist of two varieties :- phlogopite kimberlites and diopside-bearing phlogopite kimberlites. Groundmass opaque minerals are scarce, but where present are seen to be fine-grained. Plate 2.2 shows an example of a typical phlogopite-diopside kimberlite from the Middelwater 01 occurrence. Two generations of corroded olivine are visible with serpentine present along the cracks. Phlogopite is abundant within the groundmass, and often shows darker rims (tetraferri-phlogopite). Note the lack of opaque oxides within the groundmass, which is typical of micaceous kimberlites.

In addition to these kimberlite types, the localities Droogfontein, Meltonwold, Silvery Home, Skietkop and Sweetput-Soutput show petrographic characteristics of both non-micaceous and micaceous types. These kimberlites are termed *transitional types* (or Type 1/2), and have been mentioned briefly by Skinner (1989, 1991), who first examined and described them. Essentially these kimberlites are phlogopite kimberlites, but in addition, contain abundant and relatively coarse grained opaque minerals (especially perovskite). Some occurrences are also diopside-rich. These features are illustrated in Plate 2.3 below.

Plate 2.2 : Microphotograph of a Typical Micaceous Kimberlite

Middelwater 01 15 , PPL , FOV = 9.2 mm

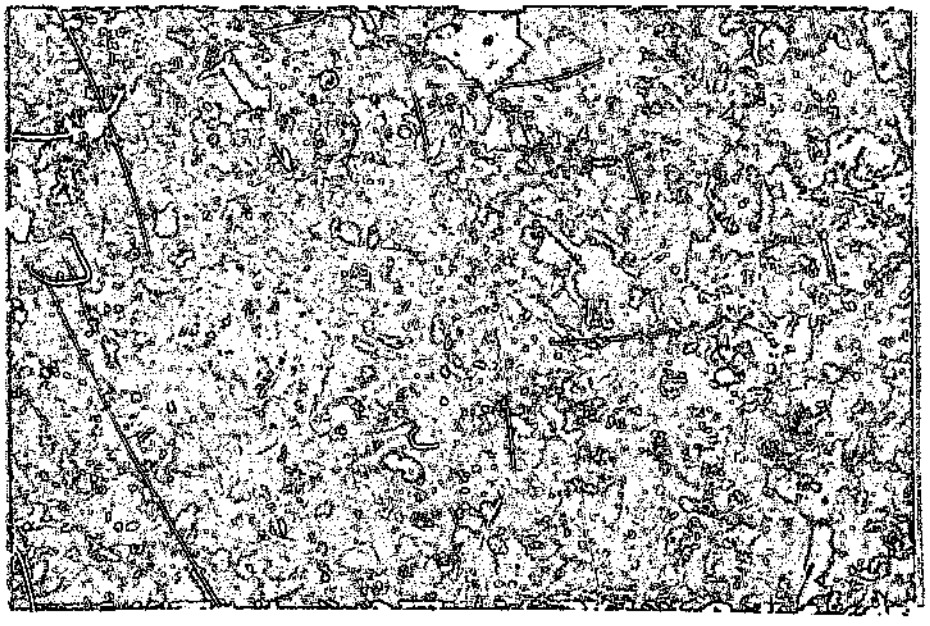

Plate 2.3 : Example of Typical Transitional Kimberlite

Droogfontein 3 , FOV = 2.5mm , PPL

It is clear from Plate 2.3 that this transitional kimberlite resembles a micaceous variety of kimberlite. However, note the relatively abundant and coarse-grained opaque oxides within the groundmass, which is not typical compared to plate 2.2 above. Poikilitic phlogopite is abundant in the groundmass. The large olivine crystal at left centre is fairly euhedral, whilst the second generation of olivine is corroded and serpentinised.

2.4 Descriptions of the Selected Kimberlites

In the following descriptions, locality numbers given are those used by De Beers and consist of three numbers, referring to country, mapsheet, kimberlite number, sample number (eg. 173/26/K5 sample No.). Petrographic descriptions are given in Appendix A.1. All the kimberlite occurrences are non-diamondiferous (Robey, 1981) unless otherwise stated.

2.4.1. Brandewynskuil (173/26/K6)

The Brandewynskuil kimberlite is located approximately 65 km from the craton margin at co-ordinates 30°37'S, 22°41'E. The occurrence consists of two pipes and a dyke northwest of the homestead Brandewynskuil on the Vosburg-Carnarvon road (Robey, 1981). Robey also notes that the larger pipe to the southeast has been pitted and describes the kimberlite as a highly weathered, micaceous type. Numerous crustal xenoliths such as gneisses, schists, granite, dolerite and shale occur in this kimberlite. Other xenoliths include fragments of garnet granulite, garnet peridotite and kyanite garnet granulite..

Samples from the pipe were collected from drill core (numbers 8, 11 and 12) and a whole-rock from sample 12 was prepared for geochemical analysis.

The hand specimen obtained consists of a macrocrystal hypabyssal facies kimberlite with abundant shale fragments. The olivines occur in two generations and are highly serpentinised. The aphanitic groundmass is phlogopite-rich. Petrographically, the sample is classified as a diopside-bearing phlogopite kimberlite.

2.4.2. Britstown (173/26/K35)

This occurrence is located on co-ordinates 30°45'S, 23°28'E and consists of a dyke and pipe immediately west and southwest of Britstown respectively (Robey, 1981). Some pitting of these kimberlites is reported. The occurrence is situated approximately 10 km from the assumed Namaqua-Natal/Kaapvaal craton boundary. A sample from the western portion of the pipe was obtained for geochemical analysis. Robey (1981) reports a garnet granulite from this locality.

The sample consists of a hypabyssal, macrocrystal kimberlite, in which numerous shale fragments are seen. Abundant phlogopite is present, both as macrocrysts and groundmass phases. Petrographically, this kimberlite is described as a phlogopite-monticellite kimberlite.

2.4.3. Droogfontein (173/27/K19)

This is an off-craton kimberlite located at co-ordinates 31°39'S, 22°16'E and is about 177 km from the craton margin. The kimberlite has intruded as a dyke. Drill core samples were obtained (sample number

2) and prepared for geochemical analysis.

This kimberlite consists of hypabyssal macrocrystal kimberlite with two generations of olivine detected in hand specimen. The groundmass is seen to be very fine-grained and phlogopite-rich. Numerous crustal xenoliths (of basement lithologies and sedimentary rocks) are present. Petrographically, the kimberlite is described as a diopside-serpentine-phlogopite kimberlite and is considered to be a transitional variety.

2.4.4. Eendekuil (173/18/K2)

This kimberlite is located at co-ordinates 32°14'S, 20°56'E, and is approximately 307 km form the craton margin, near Sutherland. Samples obtained for this study were from drill core and consist of hypabyssal facies macrocrystic kimberlite, but the samples are extremely weathered. The olivines are completely serpentinised and calcite veining was prevalent in most of the samples. Phlogopite is abundant and comprises macrocrystal and phenocrystal types. Petrographically, this kimberlite is described as a phlogopite kimberlite. The occurrence is not diamondiferous.

2.4.5. Haartebeesfontein (173/27/K1)

Numerous kimberlites are reported form the farm Haartebeesfontein and comprise five pipes, two of which are situated on north-south fissures, on the farm portion Leyfontein (locality co-ordinates 31°17'S, 22°37'E) approximately 120 km from the craton boundary (off-craton). The No. 1 pipe is intrusive into dolerite and has been pitted to a depth of 20m. Two kimberlite types are described by Robey (1981). A tuffisitic breccia is seen as soft "yellow ground" and a hard black

hypabyssal kimberlite described as a serpentine-calcite variety. Ilmenite, olivine, orthopyroxene and clinopyroxene crystals of a large size (the "megacryst suite") were noted and a number of xenoliths are also described from this locality. They include lherzolites, garnet lherzolites, glimmerite and garnet granulites as well as shale and dolerite.

Samples from the No. 1 pipe (173/27/K1) were obtained for geochemical analysis (samples 16, 17 and 19). The samples are fairly fresh, grey-blue hypabyssal macrocrysts and phenocrysts are present in a fine-grained groundmass. Phlogopite macrocrysts are present in two generations. Pyrope garnet was also detected in the groundmass.

In thin section, the kimberlite can be classified as an opaque-rich phlogopite monticellite calcite kimberlite.

2.4.6. Jonkerwater (173/26/K51)

This kimberlite is situated approximately 35 km from the craton margin (off-craton) at co-ordinates 30°10'S, 22°38'E. The kimberlite occurs as a dyke with a strike of ± 225°. A sample (No. 2) was obtained from drill core and prepared for both whole-rock and phlogopite separates. The sample consists of a hypabyssal facies macrocrystic kimberlite. In hand specimen, numerous serpentinised olivine macrocrysts and two generations of phlogopite were observed. Clinopyroxene and pyrope garnet was also noted in the groundmass. A glimmerite was recovered from the sample during the sample preparation.

Petrographically, this kimberlite is a phlogopite-kimberlite. Opaque minerals are numerous but fine grained.

2.4.7. Markt (173/26/K15)

This kimberlite occurrence is located at co-ordinates 30°15'S, 22°21'E on the farm Markt, approximately 55 km southwest of the craton margin (in an off-craton setting). It consists of two pipes and an enlargement (blow) at the intersection of two dykes. The northerly No. 1 pipe is fairly large (300 x 75 m) and a number of pits have been excavated by the farm owner. Samples from this pipe consists of macrocrystic hypabyssal facies kimberlite. Robey (1981) describes the kimberlite as being of the phlogopite-calcite variety, which he likens to the kimberlite seen at Uintjiesberg. Both coarse and fine grained varieties of this kimberlite are described. Numerous xenoliths are reported from the Markt occurrence and include upper crustal xenoliths of amphibolite, schist, gneiss, granite and amygdaloidal basalt; lower crustal xenoliths of granulite and upper mantle xenoliths of eclogite, coarse peridotites and pyroxenite. Diamonds are reported (by the farmer) to have been recovered from the No. 1 pipe, but no confirmation of this is available.

Samples were obtained from the No. 1 pipe and consist of compact dark blue hypabyssal facies macrocrystic kimberlite. Olivine and phlogopite are present in two generations, and the macrocrystal olivine appeared to be fresher than the phenocrystal types. Spherulites were also observed on the surface of the hand specimen.

In thin section the sample is described as a phlogopite kimberlite. Abundant fine-grained opaques and perovskite occur in the groundmass, and calcite is present as a secondary constituent. De Beers personnel report that ilmenite was recovered from the heavy mineral analysis suggesting a transitional character (McGurl, pers. comm.).

2.4.8. Meltonwold (173/27/K9)

This locality (co-ordinates 31°30'S, 22°44'E) consists of a pipe developed at the northern end of a well defined fissure (strike 360°). Two narrower fissures are developed to the east of the pipe parallel to the main fissure, Robey (1981). The pipe has been excavated in a large trench. Fresh hypabyssal kimberlite was obtained from a thick dyke cutting the tuffisitic kimberlite breccia near the northern end of the trench (pers. comm., J Robey). Olivines are serpentinised and in thin section the kimberlite may be described as a calcite-phlogopite kimberlite.

Xenoliths recorded from this locality include lherzolites, garnet lherzolites, garnet harzburgites and gabbroic xenoliths. Robey (1981) reports being shown a diamond allegedly recovered from this locality by the owner of the farm, but no confirmation of it's origin could be made.

2.4.9. Middelwater 01 (173/26/K19)

Middelwater 01 is situated at co-ordinates 22°43'S, 30°10'E approximately 20 km from the craton boundary in an off-craton setting. However, drill core samples were obtained from this locality (samples 13, 14, 15, 17, 18 and 21) and whole-rocks and mica separates were prepared for geochemical and isotopic analysis. All of the samples collected consist of macrocrystic hypabyssal facies kimberlite. Two generations of olivine are evident and the macrocrysts are typically serpentinised. Phlogopite is abundant and occurs in two generations. Thin calcite veining (<1 mm) is evident in some of the samples.

Petrographically, the kimberlite may be classified as a phlogopite

kimberlite. The phlogopites are in many cases chloritised and calcitised.

2.4.10. Pampoenpoort (173/27/K16)

Two pipes are associated with a north-westerly fissure system at co-ordinates 31°07'S, 22°43'E (Robey, 1981). The occurrence is approximately 100 km southwest of the assumed craton boundary, in an off-craton setting. Robey (1981), describes this kimberlite as being "basaltic" with little mica and rare ilmenite and chrome diopside. The sample obtained from drill-core (Sample 6), was prepared for whole-rock and phlogopite separates. The sample consists of a compact hypabyssal facies kimberlite with two generations of olivine and phlogopite present. This section analysis reveals this kimberlite to be an opaque-mineral rich monticellite kimberlite.

2.4.11. Sanddrift (173/25/K5)

The Sanddrift kimberlite is a cratonic kimberlite (about 41 km from the craton margin) located on the banks of the Orange River at co-ordinates 29°30'S, 22°56'E. The kimberlite is diamondiferous and has previously been mined. Samples were obtained from material collected by De Beers. The kimberlite consists of a large blow situated on a dyke and is a hypabyssal macrocrystic variety. Petrographically, the kimberlite is classified as a phlogopite kimberlite.

2.4.12. Silvery Home (173/27/K11)

The Silvery Home occurrence is located at co-ordinates 31°31'S, 22°16'E and consists of a north-south fissure with blows developed at either end

(Robey, 1981). Robey describes two different petrographic types from this locality. One is a phlogopite-diopside kimberlite and the other is a serpentine-phlogopite kimberlite with no diopside.

2.4.13. Skietkop (173/27/K23)

Samples from this locality were received from De Beers and no details regarding their field characteristics are available. The kimberlite is situated northeast of the Meltonwold occurrence and is considered to be transitional in petrographic character, by virtue of the abundant opaque oxides and perovskite present in the groundmass.

2.4.14. Slypsteen 01 (173/26/K24)

Robey (1981) briefly describes this locality (co-ordinates 30°04'S, 23°05'E) as a ENE trending fissure attaining a maximum thickness of 4 m. It is situated about 9 km from the craton boundary in an off-craton setting. Drill core samples were obtained (Nos. 2 and 5) and both are hypabyssal facies types. Sample 5 is more macrocrystic than Sample 2.

Petrographically the kimberlite is described as a diopside-bearing phlogopite kimberlite.

2.4.15. Sweetput-Soutput (173/26/K40)

The Sweetput-Soutput kimberlite is a cratonic kimberlite (16 km from the craton margin) located at co-ordinates 30°15'S, 23°30'E. Two pipes are reported by Robey (1981) from this locality, with diamonds reputed to have been recovered from the No. 1 pipe. Robey does not describe the

kimberlite from this occurrence, but mentions the occurrence of some upper crustal and eclogite xenoliths from this locality.

Samples obtained consist of greenish-blue macrocrystic hypabyssal facies kimberlite. Two generations of olivine are evident and rusty coloured phlogopite is very abundant in the groundmass. On closer inspection with a hand lens, these phlogopites are seen to consist of aggregates of phlogopite, calcite and clinopyroxene. Calcite could be detected in the groundmass and thin calcite veins were present in some of the samples.

Petrographically, this kimberlite is transitional in character, due to the presence of abundant groundmass phlogopite which poikilitically encloses diopside, perovskite and opaque mineral phases. The perovskite is unusually large and optically is very different to perovskites seen in other Prieska Province kimberlites, with respect to size, colour and shape.

2.4.16. Vioolkraal West (173/26/K46)

The Vioolkraal group of kimberlites are located approximately 30km from the craton boundary in an off- craton setting (co-ordinates 30°10'S, 23°35'E). Two pipes are reported by Robey (1981) at this locality. Samples from the western pipe were obtained for analysis. Robey (1981) reports that a variety of crustal xenoliths (gneisses and granites) and a garnet granulite were recovered from this locality.

The kimberlite is described petrographically as a porphyritic, hypabyssal facies opaque mineral-rich, phlogopite, monticellite kimberlite.

2.4.17. Welgevonden (173/26/K67)

This kimberlite is located at co-ordinates 30°05'S, 22°54'E, approximately 2 km from the craton edge (in an off-craton setting). The locality has not been studied before. Samples from the central portion of the pipe were obtained (Sample 14) and prepared for geochemical analysis. The sample consists of a macrocrystic hypabyssal facies kimberlite. Two generations of olivine are evident and are slightly altered to serpentine. The groundmass is phlogopite-rich with numerous opaques and possible clinopyroxene. Small shale and calcareous country rock fragments were noted. In thin section, the kimberlite is classified as a phlogopite kimberlite.

2.4.18. Witberg Pipe (173/25/K10)

The Witberg group is located at co-ordinates 29°10'S, 22°20'E on the farm Homestead. This is within the Kaapvaal craton (approximately 20 km from the craton margin). The occurrence consists of a pipe Witberg Pipe) and north-south trending dyke as well as a NE-SW trending dyke (the Witberg East kimberlite, see 2.4.19). The occurrence has not been studied before. Samples were obtained from drill core from the pipe (Samples 11, 13 and 15), from which whole-rock samples and mica separates were prepared for geochemical analyses.

The hand specimens consisted of macrocrystal olivine (altered to serpentine) set in a fine-grained groundmass. Phlogopite macrocrysts are present. Some thin calcite veins are present cutting obliquely through the sample. A number of small granulites were removed during sample preparation, and shale fragments were also noted. A small lherzolite xenolith is noted from this locality (pers. comm. M

McGurl - a De Beers geologist). In thin section the kimberlite is classified as a phlogopite monticellite type.

2.4.19. Witberg East (173/25/K26)

As mentioned above, this kimberlite dyke occurs near the Witberg pipe. Slightly weathered samples were obtained from drill core, which are seen to contain a few olivine macrocrysts are set in a fine-grained phlogopite-rich groundmass. In thin section, diopside and spinel are seen to be present in the groundmass. Extensive calcite veining is present in the sample. It is not known whether this kimberlite is diamondiferous or not. The kimberlite can be petrographically classified as a diopside-bearing phlogopite kimberlite.

2.5 Other Kimberlites From the Area

There have been some previous isotopic studies performed on kimberlites from the area, but which were not analysed within the present study.

2.5.1. Uintjiesberg (173/26/K2)

This kimberlite is located 350 km southwest of Kimberley (co-ordinates 30°51'S, 22°32'E) and is well outside the Kaapvaal craton. The occurrence consists of a pipe and N trending dyke system. A number of different varieties are present, consisting of a hypabyssal facies phlogopite-serpentine-calcite variety, a hypabyssal facies kimberlite breccia and a tuffisitic variety. Megacrysts of clinopyroxene, cpx-ilmenite intergrowths and brown-orange garnets are abundant. Nodules

recovered by Robey (1981) include MARID suite nodules, garnet lherzolite, lherzolites, eclogite and garnet granulite. Smith (1983b) analysed this kimberlite using the Rb-Sr method on four phlogopite separates and two whole-rock samples as well as Sm-Nd and U-Pb on whole-rocks. Davis (unpubl. data) analysed zircons from this locality using the U-Pb system.

2.5.2 . Kalkput (173/26/K9)

The Kalkput kimberlite is located about 18 km northwest of Vosburg on co-ordinates 30°28'S, 22°46'E. It occurs about 47 km from the craton margin. Davis (1978) analysed zircons for U-Pb on samples supposedly from this locality. However, the Kalkput occurrence is petrographically akin to a Group II (micaceous) type, but carries ilmenite and zircon macrocrysts in addition to garnet and clinopyroxene megacrysts. These macrocrysts are more typical of Group I (petrographic) kimberlites (Skinner, 1991). Material that the author obtained from drill core consisted of diatreme facies kimberlite which is not suitable for isotopic analyses. Robey (1981) notes that poor exposure is present and highly micaceous ground and calcrete marks the site of the kimberlite in two shallow pits.

2.5.3. Lushof (173/26/K1)

This kimberlite is situated approximately 60 km from the craton margin at co-ordinates 30°48'S, 23°01'E in an off-craton setting. Robey (1981) reports that there are two pipes and a fissure at this locality and also mentions that the occurrence has been reported as being diamondiferous to some extent. Davis (1977, 1978) analysed zircons using the U-Pb system to obtain age data from this locality. No

samples from this locality were collected by the author.

2.6 Summary

1. The Prieska Province kimberlites comprise about 130 kimberlite occurrences situated in an essentially off-craton tectonic setting.

2. The kimberlites are small in size and comprise dykes and blows/small pipes. Most of the [illegible] contain hypabyssal facies kimberlite, but in some ca[illegible] [illegible]es t[illegible] [illegible]berlite is present.

3. Xenoliths obtained from the kimberlites [illegible] [illegible]hat have intruded the Namaqua Mobile Belt at depth (Robey, 1981).

4. Nineteen occurrences were selected for study, giving a spread from just on-craton to far off-craton. Three other kimberlites from the area have been studied isotopically and are included for comparison.

5. Both micaceous and non-micaceous types are present, and in addition, transitional (petrographic) varieties of kimberlite occur in the area. These different varieties are described below :-
   - Non-micaceous kimberlites are essentially monticellite kimberlites and some are phlogopite-rich.
   - The micaceous varieties are essentially phlogopite kimberlites but diopside is also common in these kimberlites.
   - Transitional kimberlites show petrographic character of

3.3 Other Dating Methods

There are numerous analytical methods other than the Rb-Sr mica/whole-rock technique which can be used to obtain kimberlite emplacement age data (discussed by Allsopp et al., 1989 and summarised below). They include K-Ar and Ar-Ar step heating on whole-rocks and micas, U-Pb and Pb-Pb on zircon and perovskite and Rb-Sr on clinopyroxenes.

These other methods have been tried in the past because, as stated above, where phlogopite is not present, the Rb-Sr method cannot be used unless other minerals such as clinopyroxene are present (eg. Smith 1983b, using cpx and whole-rock compositions to obtain an age for Premier). In addition, kimberlites may show a complex intrusive style, where diatreme or crater facies rocks are present. Samples obtained from these kimberlite rock types are not amenable to geochemical or isotopic analysis due primarily to country rock contamination. Diatreme facies rocks are particularly problematic in acquiring emplacement age data as they usually contain earlier generations of kimberlite magma (represented by autoliths, pelletal lapilli etc), or may contain crustal biotite.

The K-Ar and Ar-Ar techniques are commonly unreliable, since Ar-loss may have occurred. U-Pb and Pb-Pb on zircons is problematic because zircons are present in extremely small quantities and they are low in U and Pb. Zircon and perovskite analysed by the ion microprobe (SHRIMP) can be useful, but low U contents in zircon require care to be taken in the counting statistics of the instrument.

Fission track dating techniques have been used on zircon grains but the

3.5.1. The Britstown Group (173/26/K35)

A sample from the western portion of the pipe was obtained for isotopic analysis. The sample consists of a hypabyssal, macrocrystic phlogopite-monticellite kimberlite (Chapter 2).

A whole-rock (Sample 16W) and three mica separates (Samples 16M, 16P and 16G) were analysed. The regression calculation with the exclusion of the groundmass fraction (Figure 3.1) gives an isochron age of 74.4 ± 0.8 Ma with an initial-Sr ratio of 0.7040 ± 1. If the groundmass fraction (16G) is included in the regression, an errochron age of 79.1 ± 4.3 Ma is obtained with an initial-Sr ratio of 0.7043 ± 13 (the errors in this case are augmented by Sqrt[MSWD/3.15] as the MSWD of 135 is very high).

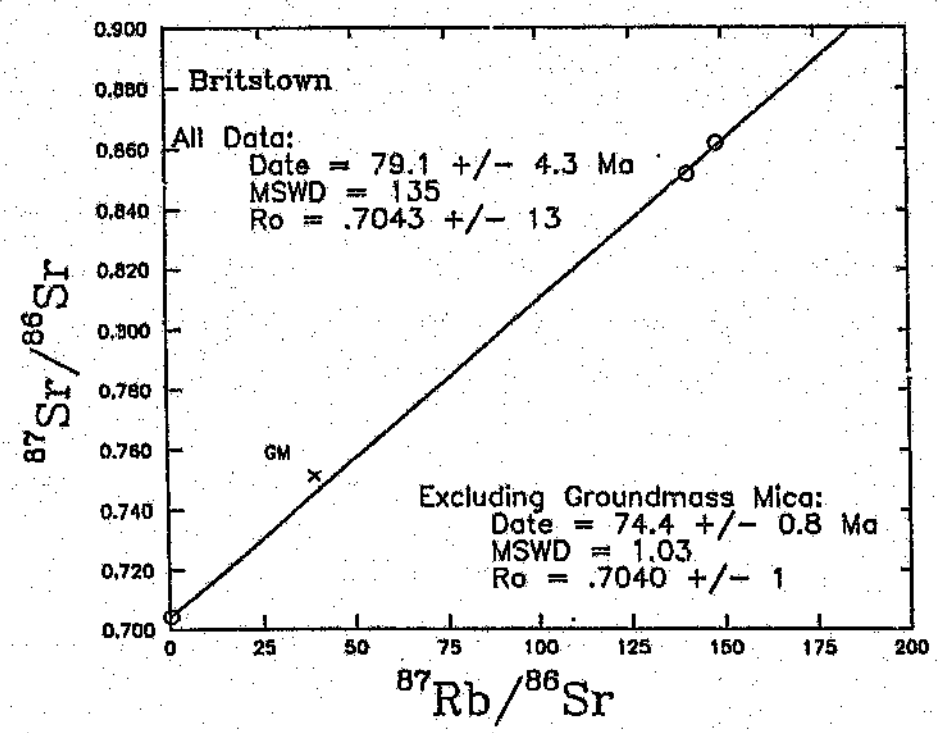

Figure 3.1 : Rb-Sr Isochron Diagram for Britstown

These data, combined with the whole-rock sample give an errochron of 168 ± 18 Ma with a very high MSWD of 316 (Figure 3.2). Where mica sample C is excluded from the regression calculation, an age of 174 ± 2 Ma with an initial-Sr ratio of 0.7063 ± 1 is obtained.

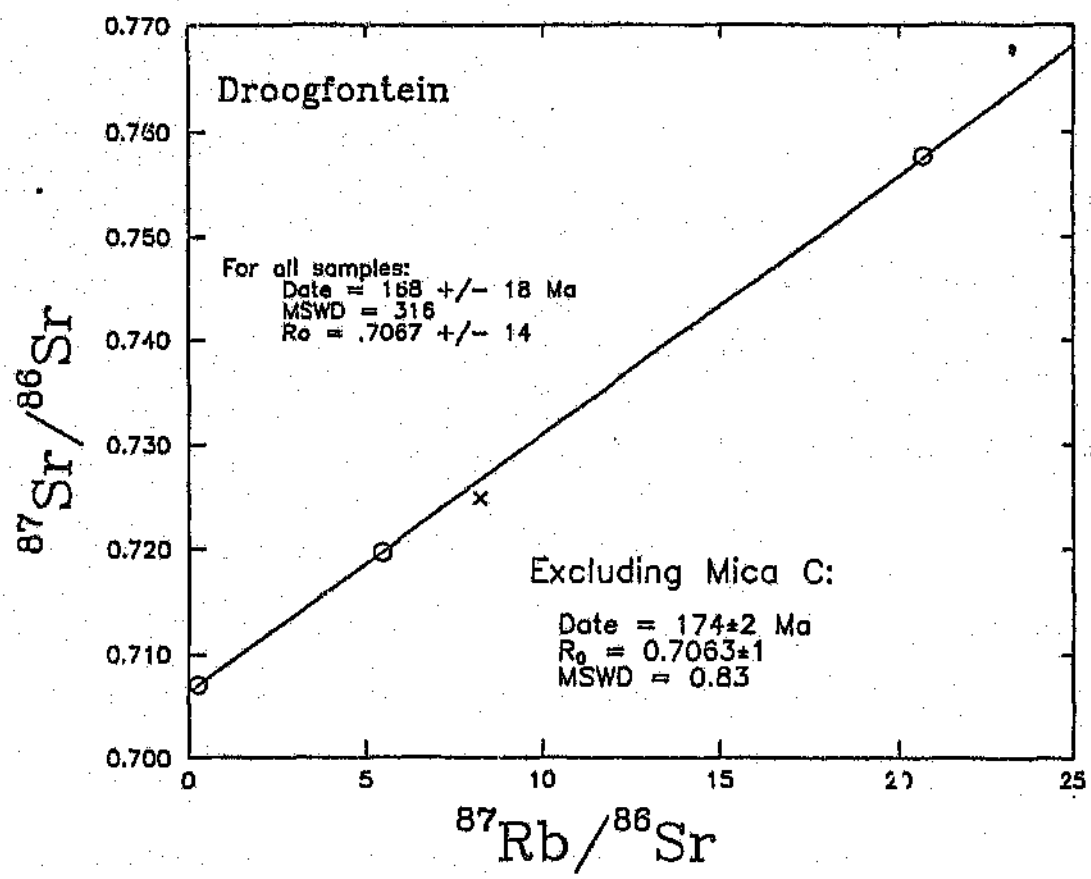

Figure 3.2 : Rb-Sr Isochron Diagram for Droogfontein

As noted above, coarse grained perovskite is present in the samples obtained. Barton (in Smith et al., 1993) analysed four perovskite grains with the ion microprobe and obtained $^{208}Pb/^{238}U$ ages between 105 ± 25 and 143 ± 24 Ma, and $^{208}Pb/^{232}Th$ ages of between 137 ± 45 and 198 ± 44 Ma (Figure 3.3).

both non-micaceous and micaceous types. Perovskites and opaque minerals are abundant and coarse grained (a non-micaceous feature) and in addition contain abundant phlogopite ± diopside (a micaceous feature).

6. Diamonds are reputed to have been recovered from some of the off-craton kimberlites, but the reliability of these reports is uncertain.

Chapter 3

Kimberlite Emplacement Ages

3.1 Introduction

Few emplacement age data have been previously reported for kimberlites occurring in the Prieska Province. Emplacement ages that have been obtained include the Uintjiesberg kimberlite (Smith, 1983b), and the Lushof and Kalkput localities which were investigated by Davis (1978). Allsopp (unpublished data) obtained a model age for the Eendekuil kimberlite. The majority of the kimberlites have intruded Karoo sediments, thus constraining the emplacement ages to post-Karoo times.

This chapter briefly reviews the Rb-Sr technique as applied to kimberlite emplacement age determinations and the problems that are encountered with the technique. Other techniques available for the acquisition of emplacement ages for kimberlites are briefly mentioned. Emplacement age data are then presented for each locality and the reliability of the ages obtained is discussed. No improvements were made on the Rb-Sr technique, but some leaching experiments were carried out and some comments on reliability pertaining to these samples can be made.

Localities analysed in this work are those described in Chapter 2. The ages were determined utilising the Rb-Sr isochron method on phlogopite and whole rock samples (Allsopp et al., 1969, 1975, 1977, 1979; Smith 1983a,b and Brown et al., 1989) and U-Pb on perovskite (Smith et al., in press). The Rb-Sr method allows for the determination of both the

emplacement age and the initial Sr isotopic ratio of the kimberlite whole-rock system. Smith (1983a,b) utilised initial-isotope ratios and emplacement ages in order to isotopically classify kimberlite into Group I and Group II types (refer to Chapter 1.3.4).

Emplacement ages are now available for eighteen kimberlites in the Prieska Province. Eight of these occurrences were dated using the Rb-Sr method by this author. Additional mica separates from six of the locality samples initially prepared by the author were obtained by C.B. Smith to augment the whole-rock data by this author and four localities (two of which were also dated with the Rb-Sr technique) were analysed by E. Barton using U-Pb on perovskites. All these ages are presented in Smith et al., (in press).

3.2 Problems With Emplacement Age Determinations

When phlogopite is scarce within kimberlites, the Rb-Sr isochron method is of little value to emplacement age determinations, although whole-rock isotopic compositions are still of value in determining source character. Kimberlitic phlogopite is commonly altered by weathering effects and/or deuteric processes. The alteration is often reflected by chloritisation. Calcite is also common in kimberlitic mica, occurring between cleavage planes and along grain boundaries. The calcite may have been derived from the kimberlite or country rocks, whilst percolating groundwaters may subsequently redistribute the carbonate. Alteration gives rise to open system behaviour of Rb and Sr, which results in spurious age data obtained from the analysis of such samples. Chloritisation of phlogopite results in Rb loss, whilst calcitisation

results in common Sr gain (Smith, et al., 1985).

In order to improve on the previous methods for the acquisition of reliable emplacement ages on kimberlites, Smith (1983b) and Brown et al., (1989) have shown that leaching of phlogopite samples in weak hydrochloric acid prior to dissolution results in the removal of calcite and common Sr, and increases the $^{87}Rb/^{86}Sr$ and the $^{87}Sr/^{86}Sr$ ratios. This vastly improves the precision of ages calculated for any intrusion. In addition, the leaching often has the effect of causing the weathered micas to become distinctly green in colour, thus allowing for easier removal during the hand-picking stage. Smith (1983b) believes that while the leaching method can produce more reliable ages, leaching of seriously altered phlogopite would not. Brown et al. (1989), however, analysed samples from the Makganyene kimberlite occurrence which contains very altered micas. The leaching technique used enabled an isochron age to be calculated, demonstrating that altered micas can still be of value in age determinations.

Other problems concerned with the acquisition of emplacement age data for kimberlites is the fact that a suite of whole-rock samples from on intrusion cannot be used for reliable age determinations, as there is too small a variation in the $^{87}Rb/^{86}Sr$ ratios. This would, at best, give rise to an errochron. Furthermore, the question of the reliability of whole-rock compositions of kimberlite is a topic of debate and much care is required in the choice of suitably fresh kimberlite for geochemical and isotopic analysis. There are invariably minor crustal contaminants present, even in hypabyssal facies kimberlite. Such material should be removed (wherever possible) prior to analysis, in order to obtain as uncontaminated a sample as possible.

In addition, kimberlite pipes often consist of multiple intrusions, each

of which is a distinct and mappable unit. Each separate intrusion may be petrographically and isotopically distinct from one another, although it is unlikely that separate intrusions within a given pipe would be different in age.

Some uncertainty exists as to the origin of the macrocrystal as opposed to the phenocrystal varieties of phlogopite present in kimberlite. Smith (1983b) has shown that for the Frank Smith kimberlite, groundmass phlogopite from hypabyssal samples may have lower initial-Sr ratios than the macrocrystal mica from the same sample. This raises the question of the validity of using macrocrystal mica which may not be derived from the kimberlite melt. However, provided the macrocrystal mica is in isotopic equilibrium with kimberlite melt, the use of such mica in isotopic analyses enables age determinations to be made.

Macrocrystal mica also generally has higher $^{87}Sr/^{86}Sr$ and Rb/Sr than other micas, which implies that better ages can be obtained (Smith et al., 1985). In addition, macrocrystal mica is easier to handpick and clean prior to analysis further enhancing their use in kimberlite age determinations. Group I kimberlites in particular are usually lacking in groundmass mica but where macrocrystal mica is present, emplacement age estimates may be obtained.

No microprobe analyses of the phlogopite was undertaken for this work, as this was not the primary object of this investigation. Previous microprobe investigations have shown clear distinctions between groundmass and macrocrystal compositions for a number of southern African kimberlites (Smith et al., 1985a).

technique suffers where younger thermal events have reset the zircon isotope systematics.

Although there are numerous techniques available, the Rb-Sr mica and whole-rock technique is still considered to be the most reliable and routine method available (pers. comm. Smith).

3.4 Analyses For This Project

Sample preparation methods are discussed in Appendix B1. In this work, phlogopite was separated into three fractions according to size : macrocrystal (>0.5cm), phenocrystal (0.5 to 0.1cm) and groundmass (<0.1cm). It should be pointed out that this is a subjective distinction and that during the crushing process, macro[illegible]l phlogopite could itself become broken down in size and thus become part of the groundmass fraction picked.

Macrocrystal mica separates generally consist of large anhedral (commonly rounded) grains and phenocrystal mica separates consist of smaller, more euhedral grains. Groundmass mica consists of both euhedral and anhedral types. The micas are usually light or dark brown in colour, although some intrusions (eg. Markt) show a variety of colours. Inclusions (such as ilmenite or rutile) may be present in any of the mica types, but appear to be dominant in the groundmass fraction.

Not all occurrences selected for study were amenable to the Rb-Sr whole-rock/phlogopite dating technique, due to the lack of suitable amounts of phlogopite, or where samples are severely altered. In

addition, phlogopite may also be very fine grained and difficult to obtain as a clean separate for analysis (see plates in Appendix A, particularly for the transitional kimberlites, where phlogopite separates are very difficult to obtain).

In some localities, perovskite is seen to be very coarse grained (up to 0.16mm in diameter). Attempts were made to separate suitable quantities of perovskite by dissolution of whole-rock samples in HF (see Appendix B1.3.2), in order to obtain age data using the U-Pb system. This failed to produce enough perovskite for analysis due to the difficulty in separating this mineral. Subsequently Barton (see Smith et al., in press) analysed individual perovskite grains from samples obtained by the author from four localities using the SHRIMP ion microprobe at the Australian National University. These data are also included in this chapter.

3.5 Data Presentation

The reader is referred to Appendix B2 for descriptions of the analytical techniques employed. Regression calculations were made using a computer program entitled "GEODATE" (Egglinton and Harmer, 1991). In this computer program, regressions are performed using the techniques of York (1969). All reported ages are considered to be reliable unless otherwise noted. Whole-rock sample numbers are suffixed with a W, macrocrystal mica with M, phenocrystal mica with P and groundmass mica with G. All relevant data is presented in Appendix C1.1. All the isochron diagrams are reproduced in Smith et al. (in press). MSWD is an abbreviation for Mean Sum of the Weighted Deviations (see Egglington and Harmer, 1991).

It is not clear as to why the groundmass sample plots off the isochron. Possibilities are that the sample was over-leached resulting in Sr loss, or the sample could be too altered which would have the same effect. Alternatively, there could be chemical differences in the phlogopite populations, as has been previously noted by Smith (1985a), who described the Frank Smith, Rietfontein and Roberts Victor kimberlites as having various chemically distinct populations of micas present for each locality. If macrocrystal mica was incorporated as part of the groundmass sample during the preparation of the sample, then the analysis of the "mixture" would merely move the sample along the isochron towards the macrocrystal fraction and would not therefore be a cause for concern.

The preferred age for this occurrence is 74 Ma.

3.5.2 . The Droogfontein Occurrence (173/27/K19)

Petrographically, this sample is described as a diopside-serpentine-phlogopite kimberlite. In addition, the presence of very coarse-grained perovskite and relatively abundant opaque minerals would suggest that this kimberlite has transitional characteristics. No macrocrystal phlogopite is present in the sample and although the groundmass is very phlogopite-rich, this mica is extremely fine grained and highly poikilitic (inclusions of cpx, opaques and olivine). Extreme difficulty in obtaining a clean mica separate was noted. The whole-rock sample (2W) gave a present day $^{87}Sr/^{86}Sr$ ratio of 0.70706 ± 13.

Smith (in Smith et al., in press) subsequently managed to obtain three mica samples, but also had difficulties in obtaining a pure separate.

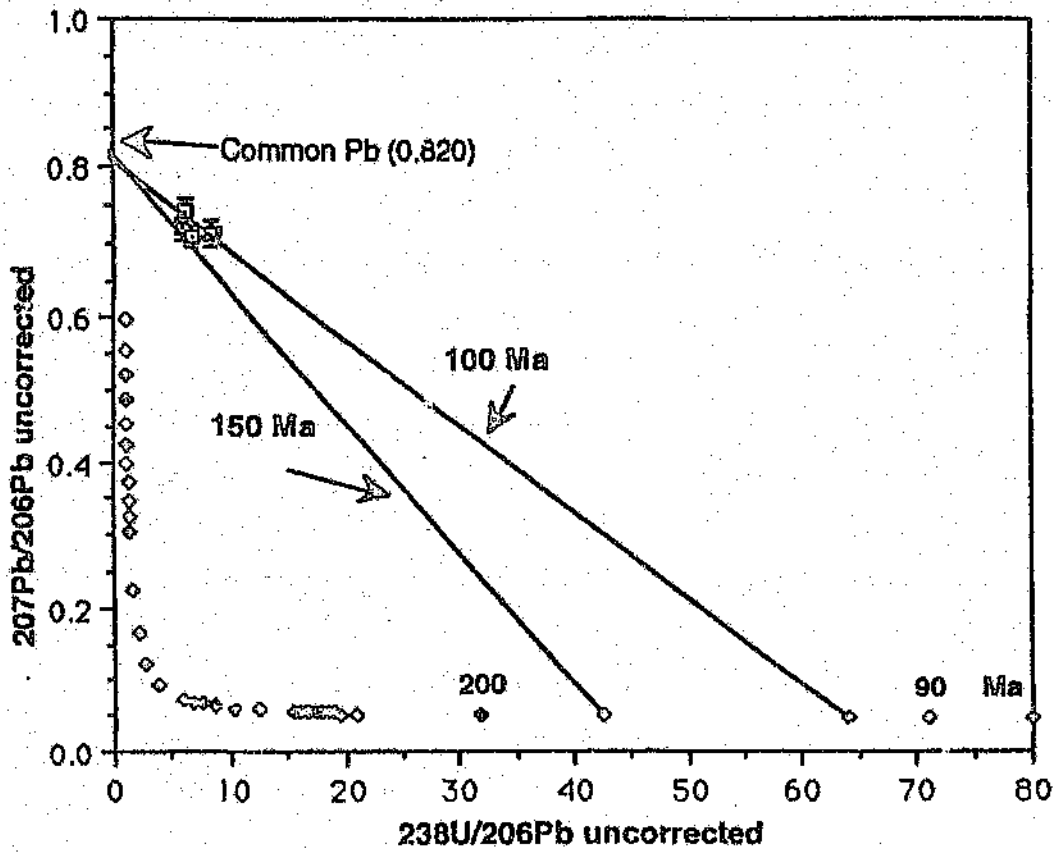

Figure 3.3 : $^{207}Pb/^{206}Pb$ vs $^{238}U/^{206}Pb$ for Droogfontein Perovskite (diamond symbols refer to the concordia in this and subsequent perovskite plots)

There is therefore uncertainty as to which of these is the most reliable age. The Rb-Sr age depends on a mica fraction with the highest Rb/Sr ratio, whilst the range in ages obtained from the perovskite analyses is due to the high common lead present in the samples, which has not been adequately corrected for (Smith et al., in press). There is more common lead in perovskites with unradiogenic compositions for off-craton compared to cratonic localities, implying that such perovskite has lower U/Pb ratios. At this stage, the Rb-Sr age of 174 Ma is considered to be the more reliable emplacement age.

3.5.3 The Eendekuil Kimberlite (173/18/K2)

This kimberlite is the furthest occurrence from the craton margin in the area. Allsopp (unpubl. data) analysed weathered phlogopite samples from this locality and obtained a model age of 110 Ma. The samples obtained in this work are also weathered, but highly micaceous (samples 2, 6, 13), and it was hoped that the leaching technique (discussed above) would be of value in obtaining a more accurate emplacement age. A whole-rock (13W) was analysed for Rb and Sr. This gives a present day $^{87}Sr/^{86}Sr$ ratio of 0.70797 ± 2 (2σ), which is slightly lower than that for Group II kimberlites, but is expected in view of the altered nature of the whole-rock (Smith, 1983). The mica samples are seen to contain calcite along the cleavage planes of individual booklets and the leaching technique was not successful in removing all the (believed) contaminant present. No further tests were performed on this locality.

3.5.4. The Haartebeesfontein Occurrence (173/27/K1)

Samples from the No. 1 pipe were obtained for isotopic analysis (samples 16, 17, 19) and it is seen to be a typical non-micaceous kimberlite, described as a perovskite-serpentine kimberlite. Whole-rock (16W), macrocrystal (17M, 19M), phenocrystal (19P) and groundmass micas (19G) were analysed for Rb and Sr. The regression calculation (excluding 17M and 19P) gives a four-point isochron with an age of 74.3 ± 0.6 Ma (MSWD = 1.85) and an initial-Sr ratio of 0.7040 ± 2 (Figure 3.4). Including 17M and 19P gives an errochron age of 75.9 Ma ± 4.3 Ma an initial-Sr ratio of 0.7040 ± 2 with a very high MSWD value of 198.

The two ages are similar, and the mica samples excluded from the analysis are considered to be altered. The age of this kimberlite is taken to be 74 Ma.

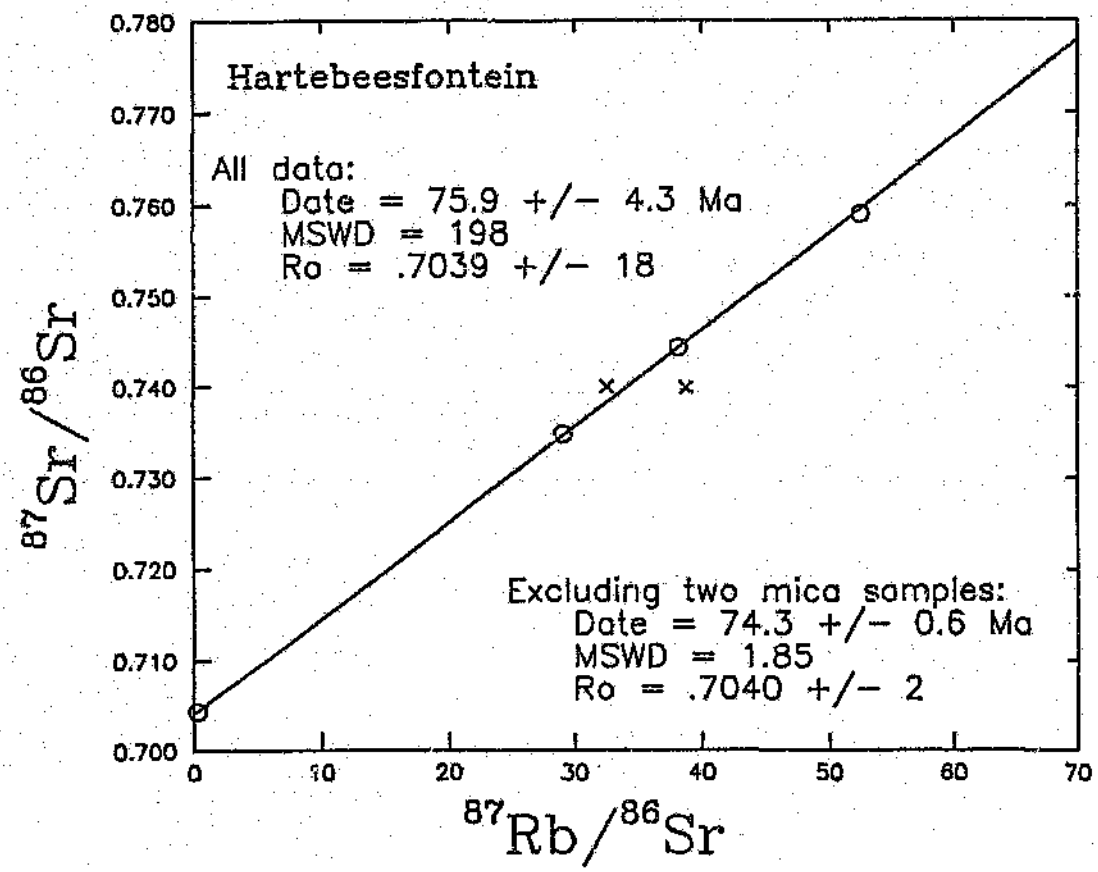

Figure 3.4 : Rb-Sr Isochron Diagram for Haartebeesfontein

3.5.5. The Jonkerwater Kimberlite (173/26/K51)

The Jonkerwater occurrence is classified as a calcite-phlogopite kimberlite. Sample 2 was obtained from drill core and prepared for both whole-rock (2W) and phlogopite separates (2M, 2P, 2G). Analysis

of the samples and regression of these data produced an errochron of 119.5 ± 2.7 Ma (MSWD = 21.8) with an initial-Sr ratio of 0.7084 ± 3 (Figure 3.5).

If the whole-rock data are excluded from the regression calculation, a phlogopite isochron age of 116.2 ± 1.4 Ma (MSWD = 3.59) is obtained. The reason for the discrepancy between the whole-rock age and mica age is unclear. The whole-rock sample is considered to be "fresh" on geochemical grounds (Chapter 5) and if possible contaminants from country rock were present and not removed prior to crushing, the $^{87}Sr/^{86}Sr$ ratio (present day) would have been significantly higher than that obtained. There could be a small degree of isotopic disequilibrium between the whole-rock and phlogopite which would lead to the slight discrepancy. The preferred emplacement age for Jonkerwater is 116 Ma.

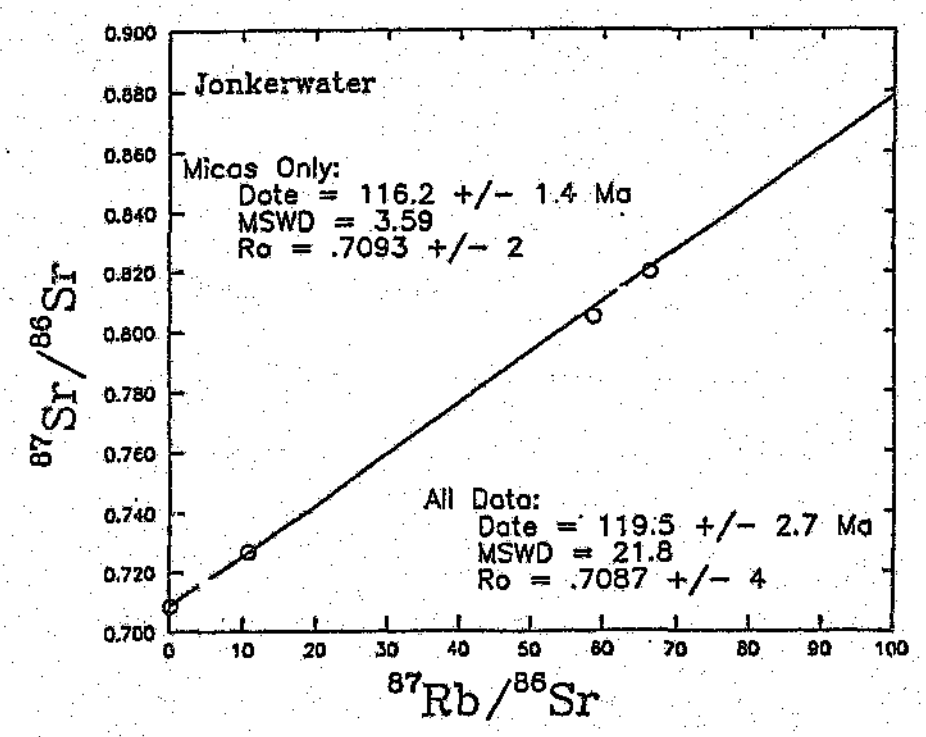

Figure 3.5 : Rb-Sr Isochron Diagram for Jonkerwater

3.5.6. The Markt Kimberlite (173/26/K15/24)

Samples from the Middle pipe were obtained from previous prospecting for geochemical and isotopic analysis. In addition, a mica separate (Sample 10) and whole-rock (Sample 25) are obtained from Dr J.W. Bristow for analysis. The phlogopite (Sample 10) was found to be unusual in that a variety of colours were observed at the handpicking. The sample was split into three colour fractions : light brown, dark brown and bronze. These were then separately analysed for Rb and Sr as well as a "total" mica sample (consisting of all colour fractions together) in order to attempt to obtain a spread in $^{87}Rb/^{86}Sr$ ratios. The total mica sample was split into two parts, one of which was leached twice to determine the effect of the leaching procedure as calcite was very noticeable in the micas. This is corroborated by the high Sr contents (>100 ppm) observed.

Model ages calculated for each fraction yielded the following results (Table 3.1):

Table 3.1 : Results of leaching for Markt mica

MICA FRACTION	MODEL AGE	ERROR	Ro
10 - leached once	174 Ma	± 15	0.708
10 - leached twice	234 Ma	± 50	0.708
10 light brown (10LB)	158 Ma	± 7	0.708
10 dark brown (10DB)	140 Ma	± 10	0.708
10 bronze (10BR)	134 Ma	± 8	0.708

Note that the "double leaching" has seriously affected the isotopic systematics and that Rb loss has occurred. Assumed initial-Sr ratios of 0.708 gives model ages for the colour fractions of between 134 and 158 Ma. The "total" sample, however, gives a much higher model age of 174 Ma. The range of model ages is therefore probably due to alteration, as there is little agreement between the various model ages obtained, implying that the isotopic systematics have been affected by the leaching proceedure. Regression of the data from mica sample 10 gives and age of 147.2 Ma and an initial-Sr ratio of 0.7074 ± 8 (errors augmented by Sqrt[MSWD/2.37]).

When samples 24W, 25W , 24M, 10DB and 10BR are used in the regression calculation, an isochron age of 126,8 ± 2,9 Ma (MSWD = 3,634) is obtained with an initial-Sr ratio of 0,7085 ± 2. It can be seen that mica samples 10BR and 10LB plot far from the isochron (Figure 3.6) which Smith (pers. comm.) considers to be an alteration feature.

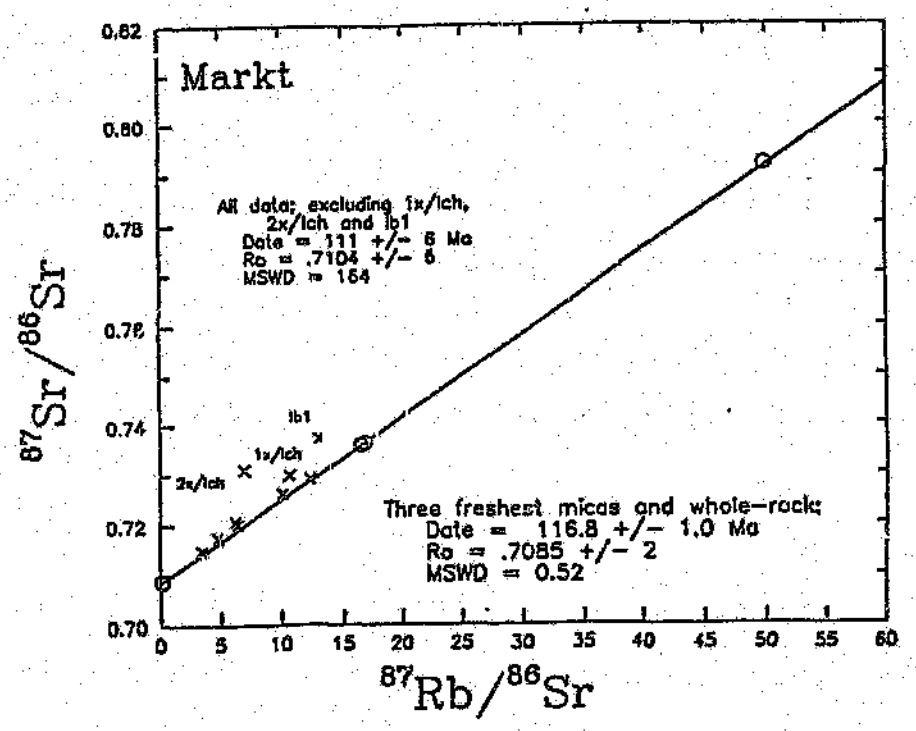

Figure 3.6 : Rb-Sr Isochron Diagram for Markt

Smith (in Smith et al., in press) subsequently picked more mica from this locality and obtained far higher Rb-Sr and $^{87}Sr/^{86}Sr$ ratios for the separates he analysed. In addition, consistent model ages were obtained reflecting the success of careful sample selection. If these phlogopite samples and the whole-rock are used in the calculation, an isochron age of 116.8 ± 1 Ma is obtained. This is considered to be the best estimate of the emplacement age for this locality to date. An initial-Sr ratio of 0.7085 ± 2 is obtained from this calculation.

3.5.7. The Meltonwold Kimberlite (173/27/K9)

This is classified petrographically as a calcite-phlogopite kimberlite but shows transitional characteristics (coarse grained and fairly abundant perovskites present in the groundmass). No Rb-Sr analysis for age purposes were obtained in this work because of the problems in obtaining micas for analysis.

Barton (in Smith et al., in press) analysed perovskite from this locality using the ion microprobe and obtained a linear distribution of four perovskite analyses which intersect the mean $^{207}Pb/^{206}Pb$ composition measured for common Pb in this sample (Figure 3.7). A weighted mean $^{206}Pb/^{238}U$ age of 143 ± 14 Ma was obtained which is considered to be reliable.

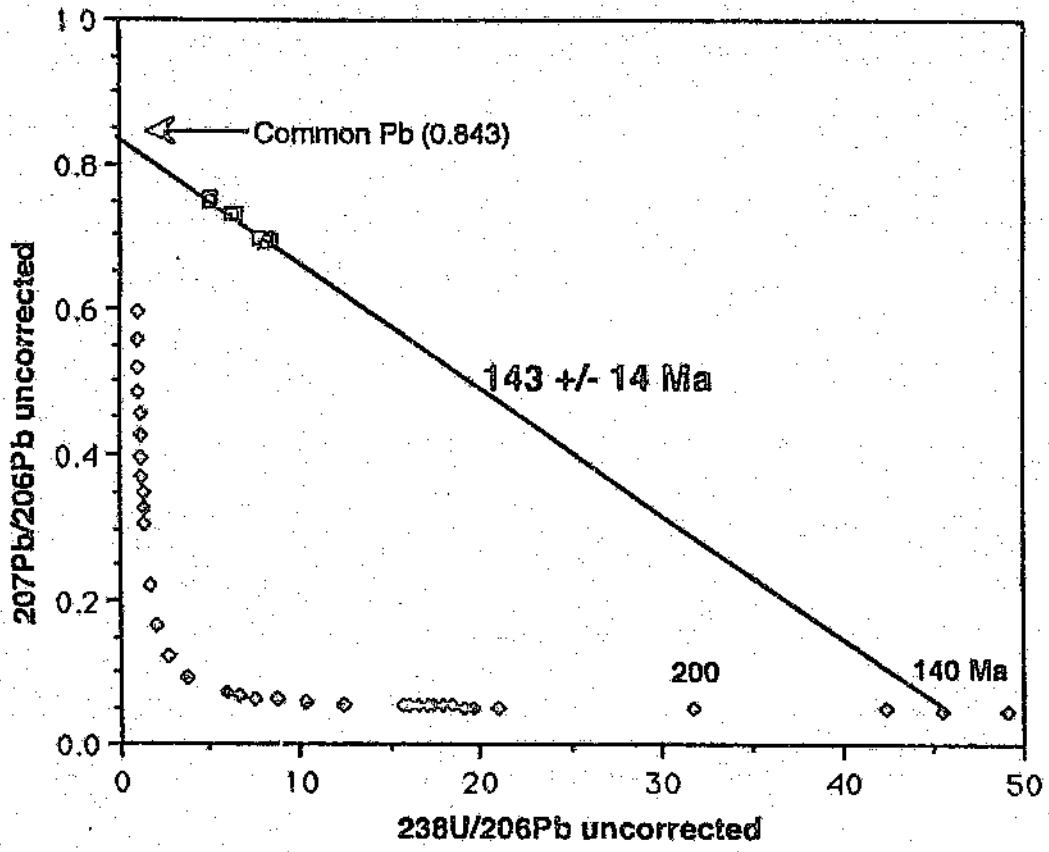

Figure 3.7 : $^{207}Pb/^{206}Pb$ vs $^{238}U/^{206}Pb$ for Meltonwold Perovskite

3.5.8 The Middelwater Kimberlite (173/26/K19)

This is a micaceous (calcite-phlogopite) kimberlite. Drill core samples obtained from this locality include samples 13, 14, 15, 17, 18 and 21. Whole-rocks and macrocrystal mica were prepared for each of the samples as well as phenocrystal mica (13P) and groundmass mica (13G, 14G). Analysis of 13W, 1W, 21W, 13M, 14M, 15M, 18M and 21M gives an eight point isochron with an age of 117.6 ± 0,6 Ma (MSWD = 2.19) and an initial-Sr ratio of 0.7082 ± 2 (Figure 3.8). No change to the age occurs with the exclusion of the whole-rock sample.

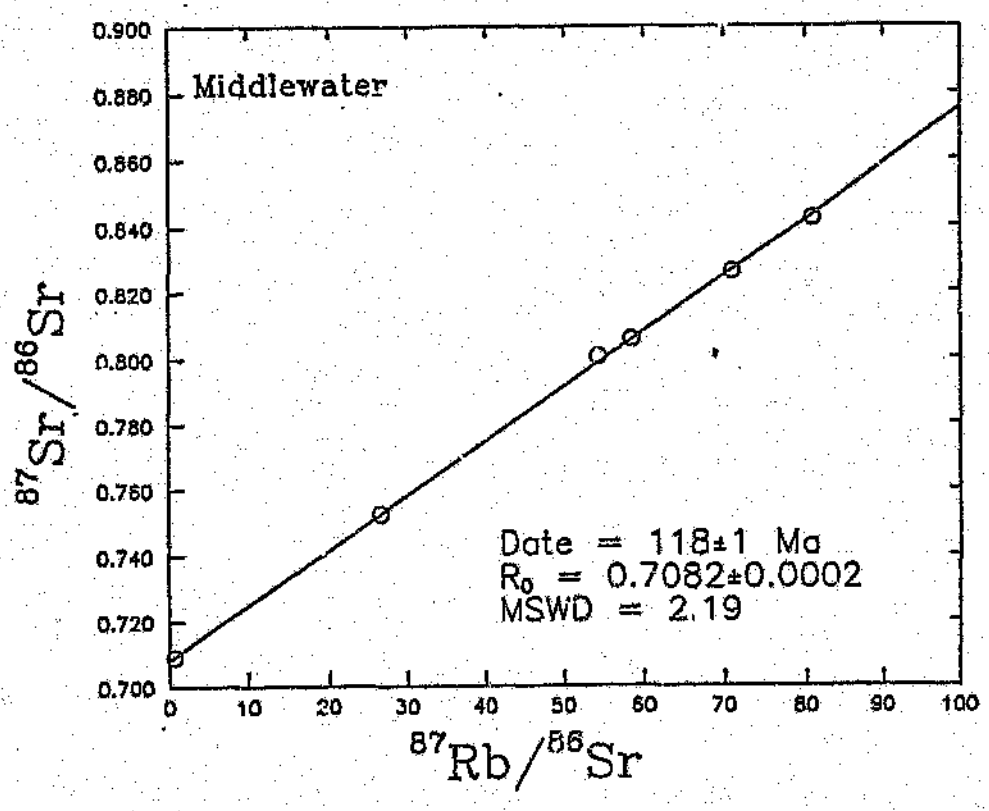

Figure 3.8 : Rb-Sr Isochron Diagram for Middelwater 01

3.5.9. The Pampoenpoort Occurrence (173/27/K16/6)

The drillcore sample collected consisted of an opaque-mineral rich, calcite-serpentine kimberlite. A whole-rock (6W) and macrocrystal (6M), phenocrystal (6P) and groundmass (6G) phlogopite samples were prepared and analysed. In addition Bristow (unpubl. data) analysed a mica separate (1T) for Rb and Sr. This mica separate was subsequently re-analysed by the author (1G).

Regression of the data obtained from sample 6 gives an isochron age of 103.1 ± 0.7 Ma (MSWD = 2,57) and an inital-Sr ratio of 0.7046 ± 2

(Figure 3.9). Inclusion of mica sample 1G gives a five point isochron with an age of 103.4 Ma and initial-Sr ratio of 0.7046 ± 2. No change to the age occurs by excluding the whole-rock sample.

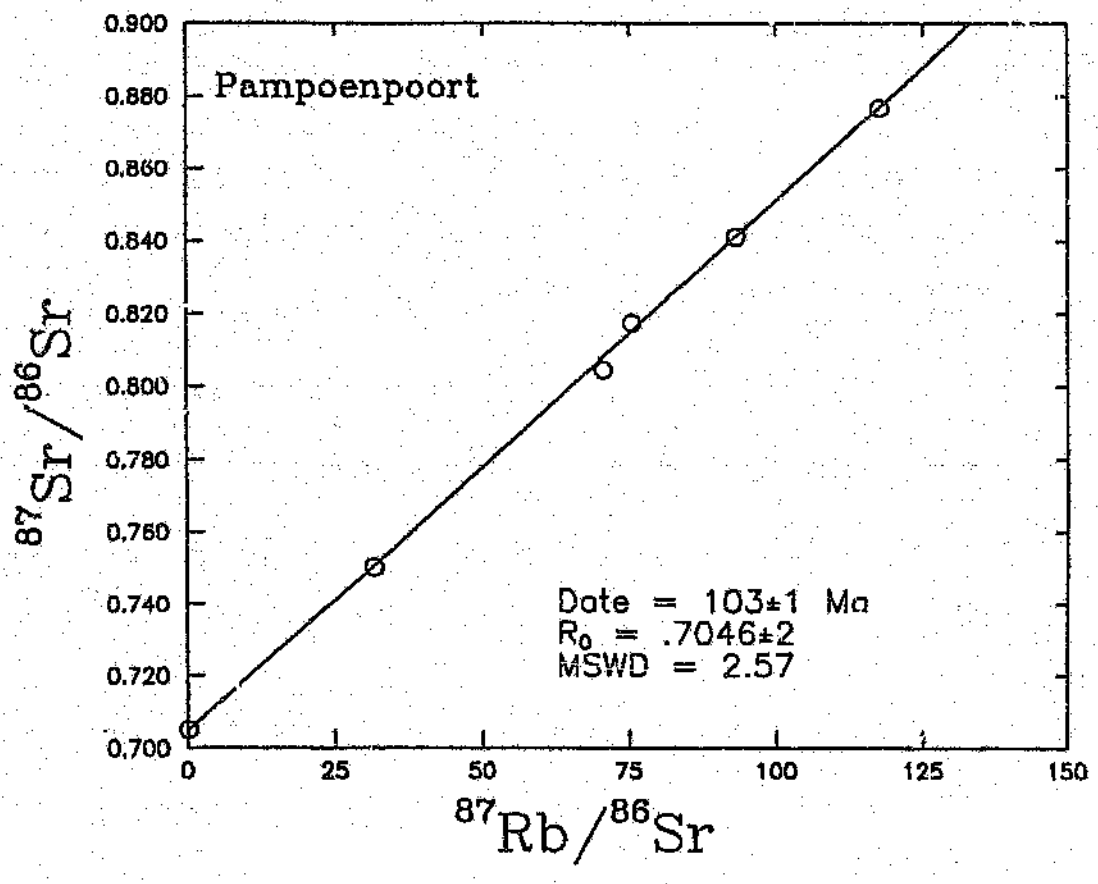

Figure 3.9 : Rb-Sr Isochron Diagram for Pampoenpoort

3.5.10. The Sanddrift Kimberlite (173/25/K5)

Samples of calcite-phlogopite kimberlite were obtained from material collected by De Beers. A previous phlogopite model age of 118 Ma was

obtained by Bristow (unpubl. data). A present day $^{87}Sr/^{86}Sr$ ratio for a whole-rock of 0.7083 ± 1 was obtained by this author, but phlogopite separates were not obtained.

Smith (in Smith et al., in press) obtained other mica separates from this locality and obtained an isochron age of 125.2 ± 3.2 Ma (MSWD = 0.50) (Figure 3.10). Inclusion of another mica separate in the regression calculation gives an errochron of 138 ± 8 Ma (MSWD = 33.2). It is believed that his mica sample represents a contaminate from phlogopite-bearing peridotite xenoliths which are present in the kimberlite. These xenolithic micas give model ages of 2250 Ma which is very much older than the host kimberlite. The isochron age of 125 Ma is the preferred age for this locality.

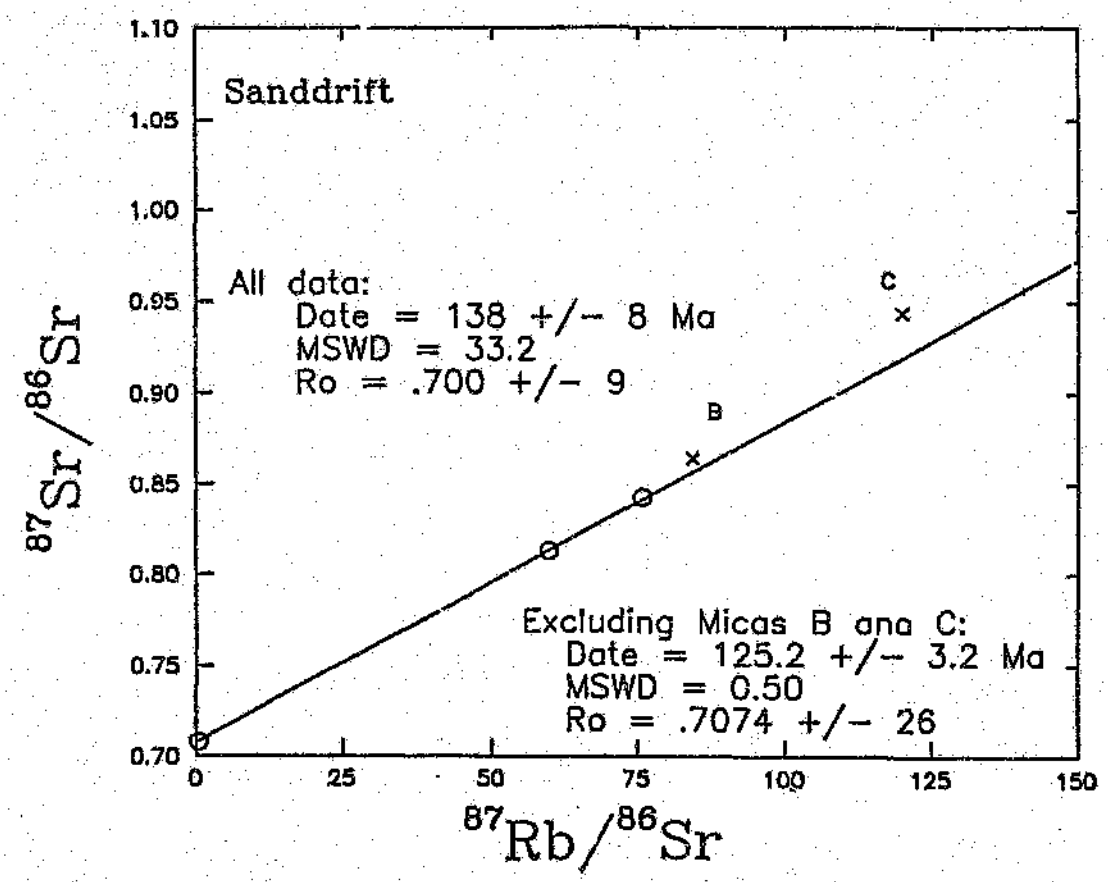

Figure 3.10 : Rb-Sr Isochron Diagram for Sanddrift

3.5.11. The Skietkop Kimberlite

This is a petrographically transitional variety of kimberlite, classified as a phlogopite kimberlite. The groundmass phlogopite is very fine-grained and difficult to separate out. Perovskites analysed by Barton (in Smith et al., in press) give an age of 140 ± 5 ($^{206}Pb/^{238}U$) and 140 ± 8 ($^{208}Pb/^{232}Th$). A weighted mean of this data gives 140 ± 10 (Figure 3.11).

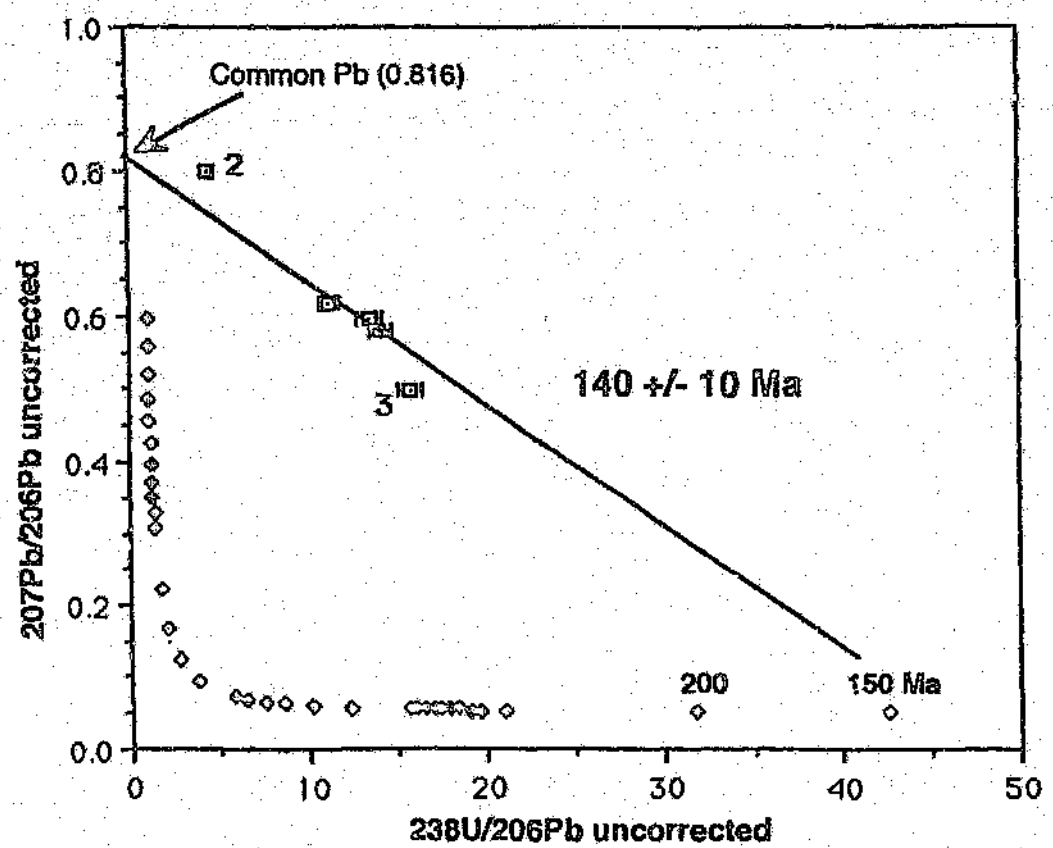

Figure 3.11 : $^{207}Pb/^{206}Pb$ vs $^{238}U/^{206}Pb$ for Skietkop Perovskite

3.5.12. The Sweetput-Soutput Kimberlite (173/26/K40)

This is another petrographically transitional kimberlite which contains abundant perovskite, and is classified as a phlogopite kimberlite.

Three whole-rock samples (10W, 13W and 20W) were prepared. Phlogopite in this occurrence is very fine grained (petrography reveals that the phlogopite is extremely poikilitic, enclosing numerous other minerals) and no clean separates were obtained by this author. Although the regression of the Rb-Sr whole-rock data for these kimberlites produces nonsense results (no spread of $^{87}Rb/^{86}Sr$) in terms of age, the initial-Sr ratio of 0.7069 ± 11 (note the high error) is interesting in that this would appear to be transitional in isotopic character.

Smith (in Smith et al., in press) subsequently managed to further purify the separates initially prepared by this author and analysed the samples, enabling an isochron age of 116 ± 1 Ma to be obtained (Figure 3.12). An initial-Sr ratio of 0.7065 ± 2 is given for this regression. Note that the whole-rock "regression" gives a similar result albeit with a high error.

Five perovskites from this locality were analysed by Barton (in Smith et al., in press) and this gives a weighted mean [illegible]$/^{238}U$ and $^{208}Pb/^{232}Th$ age of 105 ± 14 and 110 ± 18 Ma respectively (Figure 3.13). The ages are within error of the Rb-Sr age of 116 ± 1 Ma.

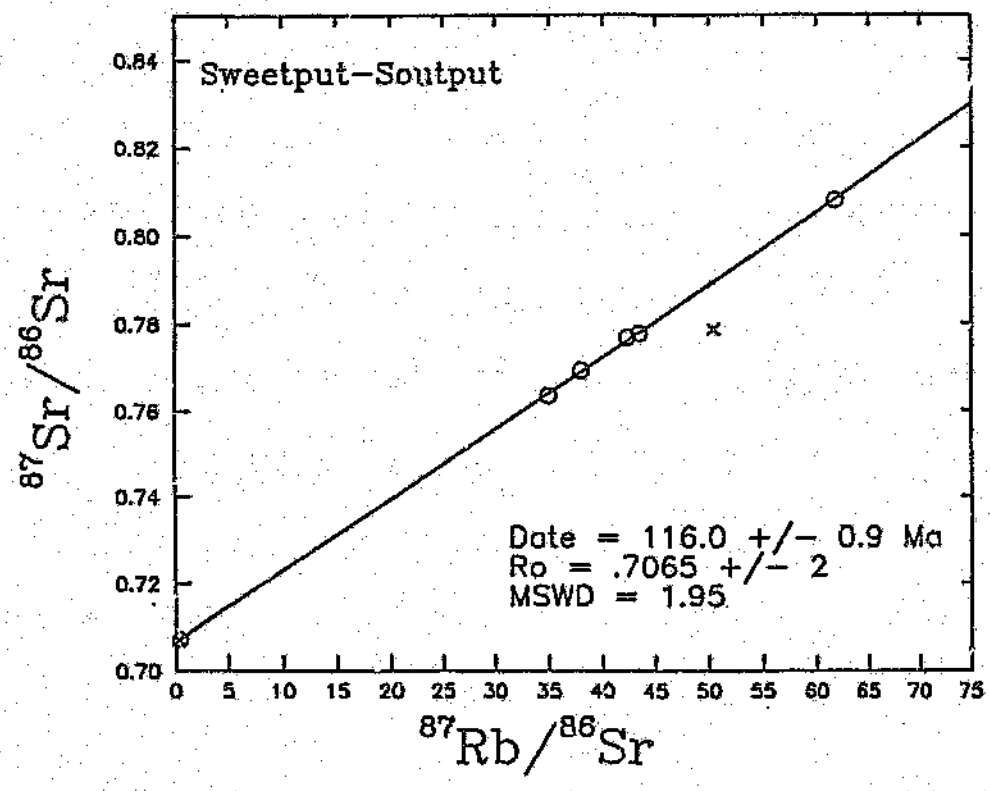

Figure 3.12 : Rb-Sr Isochron Diagram for Sweetput-Soutput

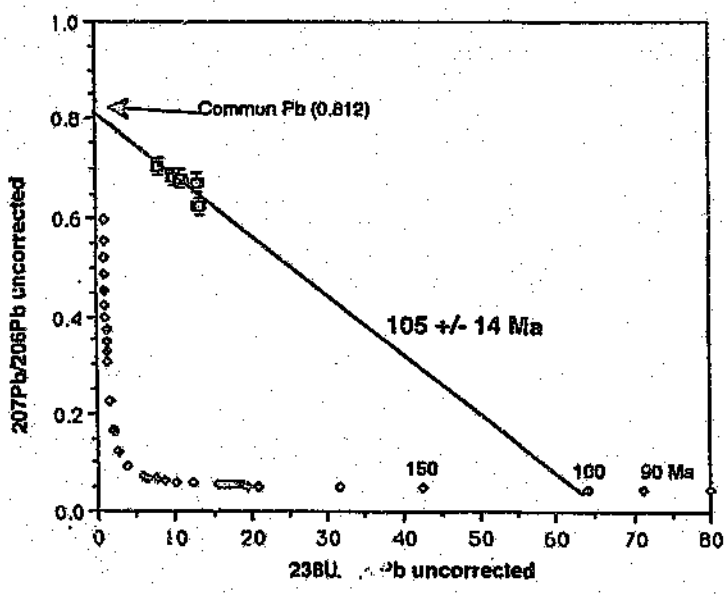

Figure 3.13 : $^{207}Pb/^{206}Pb$ vs $^{238}U/^{206}Pb$ for Sweetput-Soutput Perovskite

3.5.13. The Welgevonden Kimberlite (173/26/K67)

This is a phlogopite kimberlite from which sample 14 was used to prepare a whole-rock (14W) and macrocrystal mica (14M) sample. Smith prepared three further mica separates and the regression of all data gives an isochron age of 116.2 ± 0.2 Ma with an initial-Sr ratio of 0.7088 ± 4 (Figure 3.14). Exclusion of the whole-rock sample does not change the age calculation and the emplacement age of the Welgevonden kimberlite is considered to be 116 Ma.

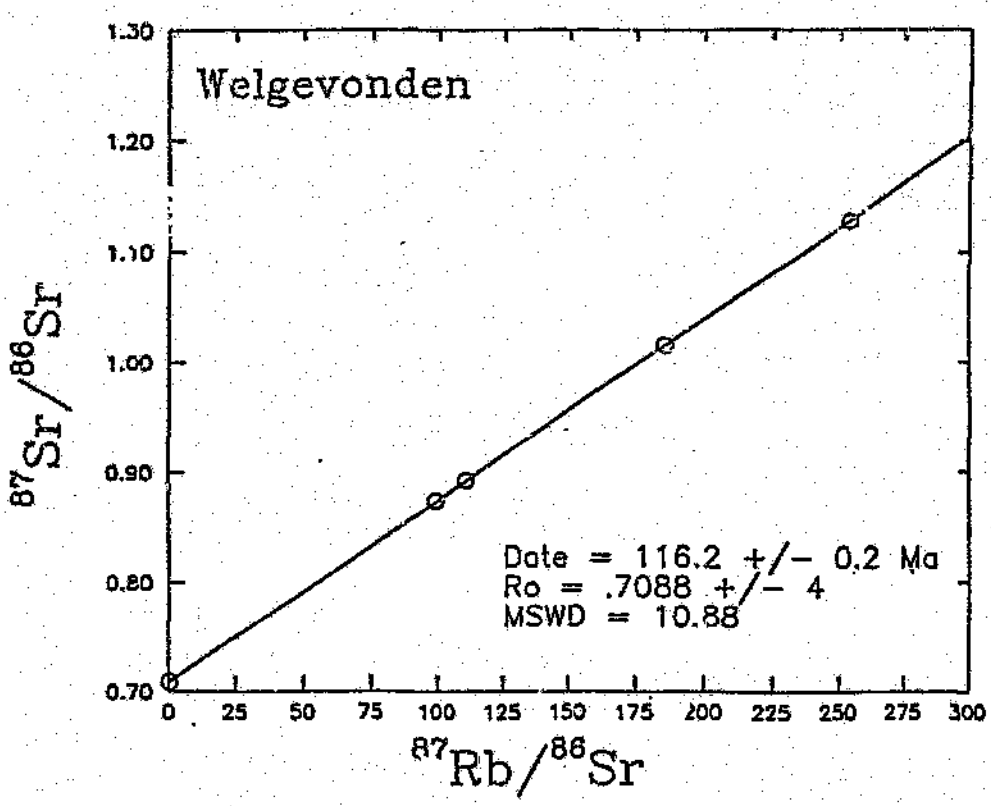

Figure 3.14 : Rb-Sr Isochron Diagram for Welgevonden

3.5.14. The Witberg Pipe Kimberlite (173/25/K10)

Samples 11, 13 and 15 were obtained from drill core from which whole-rocks (11W, 15W) and mica separates (11M, 15M) were prepared and analysed for Rb and Sr. This locality is described as a calcite, serpentine opaque mineral rich kimberlite. Model ages for the mica samples analysed give ages of 114 Ma and 113 Ma assuming initial-Sr ratios of 0.704, in good agreement with one another.

Further mica separates obtained by Smith (in Smith et al., in press) and a whole-rock analysis are regressed to give a seven point isochron of 108.0 ± 0.7 Ma (MSWD = 0.07) (Figure 3.15). Exclusion of the whole-rock gives the same age, but no initial-Sr ratio can be calculated from the micas alone.

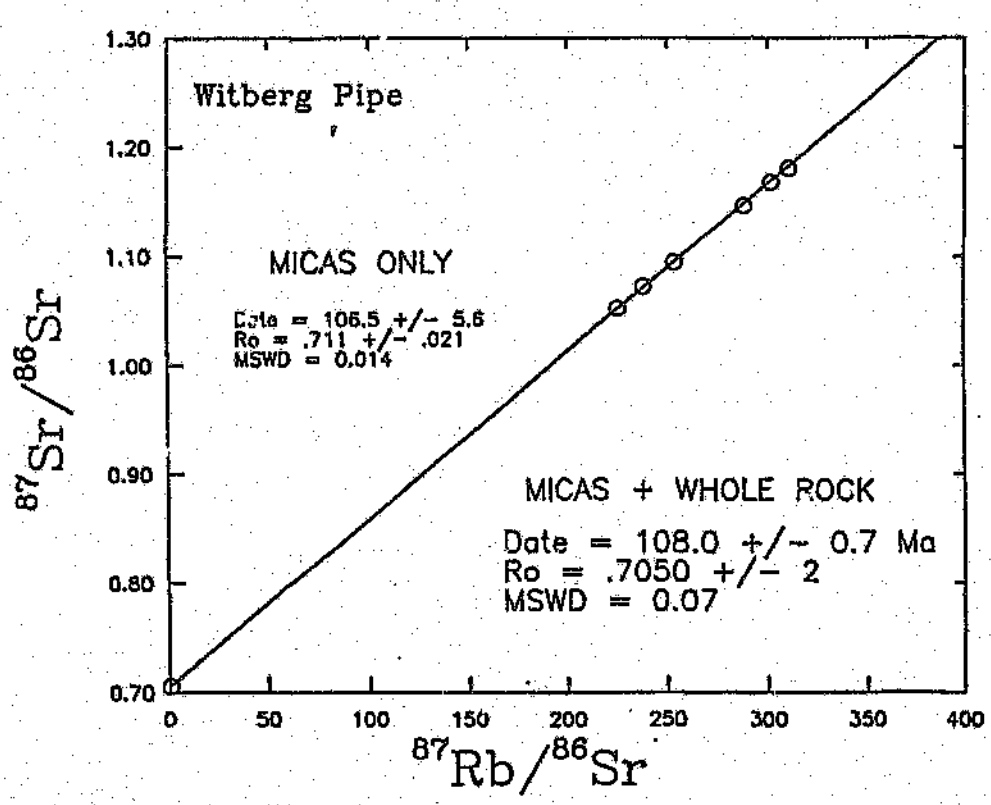

Figure 3.15 : Rb-Sr Isochron Diagram for Witberg Pipe

3.5.15. The Witberg Dyke Kimberlite (173/25/K26)

This dyke is situated a few hundred meters from Witberg Pipe and does not appear to cross cut or have a genetic relationship to the pipe. It is a micaceous kimberlite, from which Smith (in Smith et al., in press) separated and analysed groundmass mica. Regression of the mica data (Figure 3.16) gives an age of 106 ± 39 Ma (model ages are 116-117 Ma assuming an initial-Sr ratio of 0.708).

Inclusion of the whole-rock sample yields an isochron age of 117.7 ± 1 (MSWD = 0.17) and an initial-Sr ratio of 0.7085 ± 2. This shows that the dyke and pipe are not genetically related.

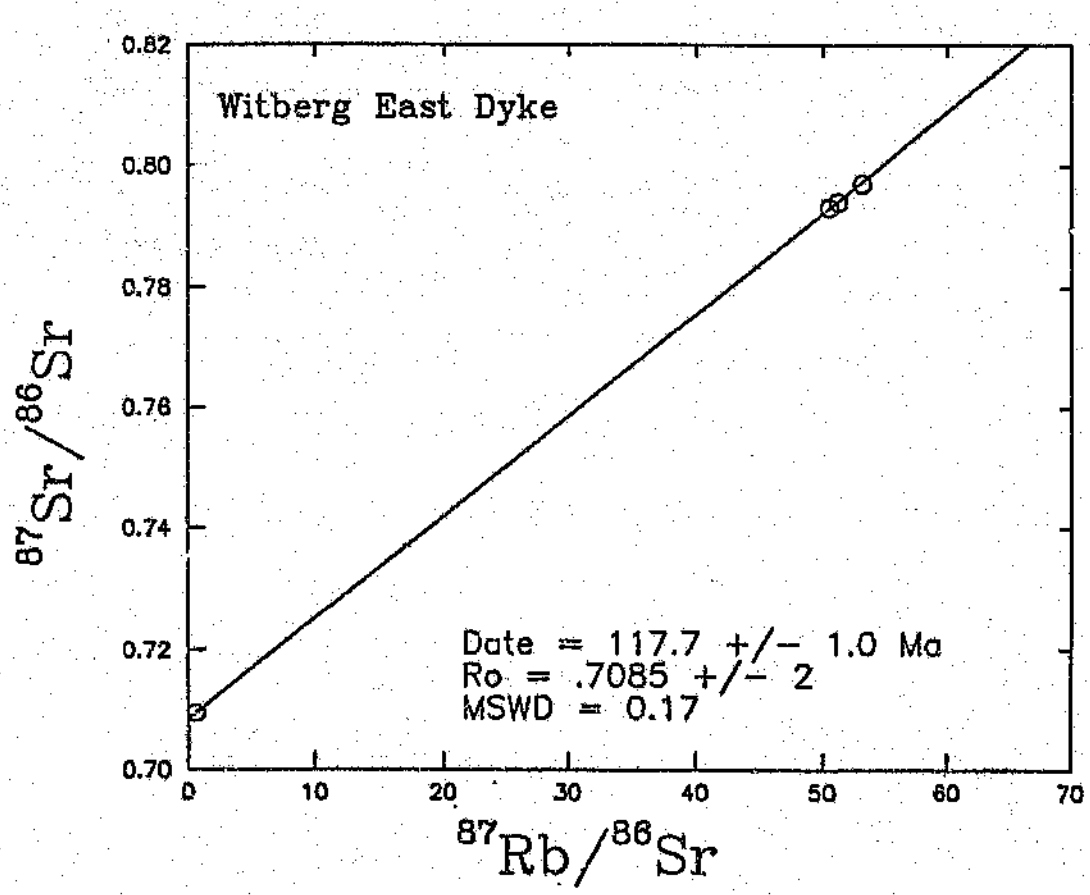

Figure 3.16 : Rb-Sr Isochron Diagram for Witberg Dyke

3.6 Previous age determinations for kimberlites from the area

There have been some previous isotopic studies performed on kimberlites from the area, but which were not analysed in the present study. The results of this previous work are summarised below:

3.6.1. The Uintjiesburg Kimberlite (173/26/K2)

Smith (1983, 1985a) analysed this kimberlite using the Rb-Sr method on four phlogopite separates and two whole-rock samples. The age obtained was 100.7 ± 1.4 Ma with an initial-Sr ratio of 0.7043 ± 2. Davis (unpubl. data) analysed zircons from this locality using the U-Pb system and derived an age of about 100 Ma. The Rb-Sr results obtained by Smith are therefore in good agreement with the U-Pb results of Davis.

3.6.2 . The Kalkput Occurrence (173/26/K9)

Davis (1978) reported two U-Pb zircon ages of 116.4 and 114.1 Ma for this locality. However, this is a micaceous kimberlite variety, and zircon is not commonly seen in micaceous kimberlites. Therefore the age given by Davis requires verification. Material that the author obtained from drill core consisted of diatreme facies kimberlite which is not suitable for isotopic analyses.

3.6.3. The Lushof Kimberlite (173/26/K1)

Davis (1977, 1978) reports U-Pb zircon ages of 68 and 78 Ma for this locality. No samples from this locality were collected by the author.

3.7 Samples Not Analysed in This Study

Localities from which samples were collected and from which no emplacement age data has been obtained include Brandewynskuil, Slypsteen and Eendekuil. As explained in 3.5.3, the micas in the Eendekuil samples are so severely calcitised that leaching alone cannot remove all the obvious contaminant. A possible solution to this may be to gently crush the phlogopite separatcs and leach these fractions, in order to more effectively remove the calcite contaminants.

Samples from the Brandewynskuil kimberlite consist of two different facies - one a hypabyssal facies diopside-phlogopite kimberlite (sample 11) and the other a pelletal TKB (sample 8). Mica could not easily be extracted from sample 11 and sample 8 is not suitable for isotopic analysis.

The Slypsteen 01 kimberlite is fairly altered and typical of a dyke that is extremely phlogopite-rich, but the mica is very fine-grained, often intergrown with diopside and difficult to obtain clean mica separates.

3.8 Discussion of Emplacement Age Data

Table 3.2 summarises the kimberlite emplacement age data available

for the Prieska Province. These data are incorporated in a histogram of kimberlite ages for southern Africa in Figure 7.1, Chapter 7, where the Prieska Province ages are put into context of the South African kimberlite emplacement age events.

Some comments can be made regarding the reliability and acquisition of emplacement age data for kimberlites. With respect to the acquisition of data, the minimum number of phlogopite separates required to obtain an isochron (provided fresh phlogopite is present) would consist of two and preferably three fractions used in conjunction with a whole-rock sample. Model ages calculated for the mica separates should be in agreement and the exclusion of the whole-rock from the isochron should not significantly affect the age. Where a three point isochron is obtained using accurate and precise data from unaltered samples, the addition of further mica analyses is not considered to significantly affect the age obtained. Leaching techniques should be standard practice, but do not always produce better results (eg Markt). Other factors to consider in obtaining good age data are discussed by Smith et al. (1985a) and Smith et al. (in press). These factors are also discussed further in Chapter 7.

The Prieska Province emplacement age data shows some similarity to ages obtained for the Kaapvaal Craton. By the definition of Smith (1983a,b) and Smith et al., (1985a), initial-Sr ratios of kimberlites in the study area show similar Group I and II signatures (ie. 0,704 and 0,708 respectively) to their cratonic counterparts. This will be discussed more fully in Chapters 4 and 7. The petrographic character is correlated with this (viz. non-micaceous types being equivalent to Group I and micaceous types equivalent to Group II) .

Transitional kimberlite varieties are characteristically difficult to date

using the Rb-Sr phlogopite method. This is due to the fine-grained and poikilitic nature of the phlogopite groundmass, illustrated below in Plate 3.1. Here it can be seen that the phlogopite grains are very anhedral in shape, and are full of inclusions (compare to Plate 2.2), which presents difficulties in obtaining clean separates.

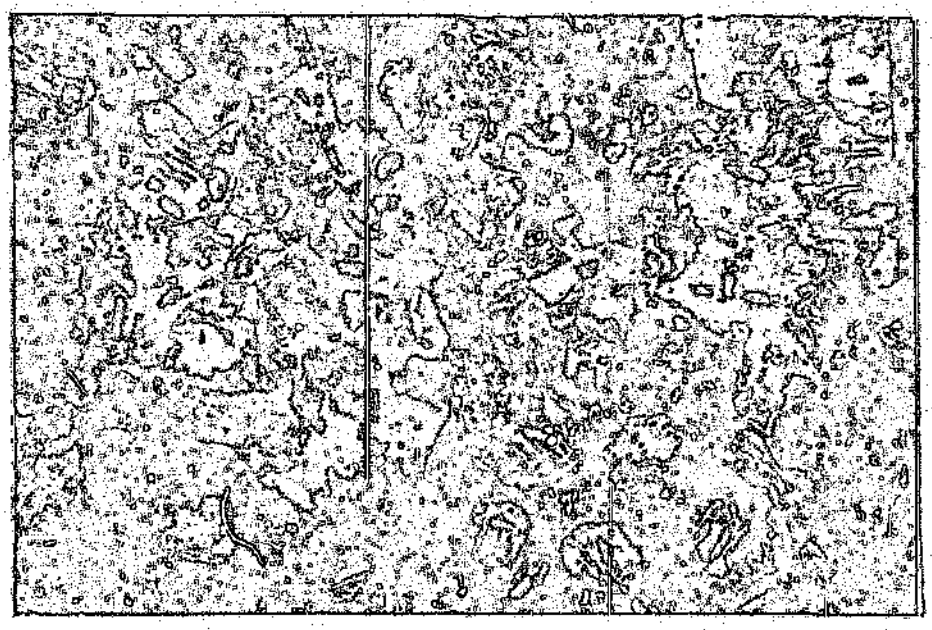

Plate 3.1 : Microphotograph of Transitional Kimberlite Groundmass
Plane polarised light , field of view 2.5 mm - see text for discussion

3.9 Summary

The emplacement age data are summarised in the table below.

Table 3.2 : Summary of Emplacement Ages for the Prieska Province

LOCALITY	AGE (Ma)	INITIAL-Sr
Britstown	74 ± 1	0.7040 ± 1
Haartebeesfontein	74 ± 1	0.7040 ± 2
Pampoenpoort	103 ± 1	0.7046 ± 1
Witberg Pipe	108 ± 1	0.7050 ± 2
Lushof	68 - 73	Zircon U-Pb
Uintjiesberg	101 ± 1	0.7043 ± 2
Eendekuil	±110	Model Age
Kalkput	114 - 117	Zircon U-Pb
Jonkerwater	116 ± 1	0.7093 ± 2
Markt	117 ± 1	0.7085 ± 2
Middelwater 01	118 ± 1	0.7082 ± 2
Sanddrift	125 ± 3	0.7074 ± 26
Welgevonden	116 ± 0.2	0.7088 ± 4
Witberg East (dyke)	118 ± 1	0.7085 ± 2
Droogfontein	174 ± 2	0.7063 ± 1
Meltonwold	143 ± 14	Perov U-Pb
Skietkop	140 ± 10	Perov U-Pb
Sweetput-Soutput	116 ± 1	0.7065 ± 2

From this table the following conclusions can be made :

1. Nineteen kimberlites were analysed using the Rb-Sr whole-rock/phlogopite isochron and U/Pb perovskite methods in order to obtain emplacement age data.

2. Rb-Sr isochron ages tend to be more accurate than U/Pb perovskite ages. The high errors obtained using the latter method are due in part to the high common Pb component within the perovskites.

3. A complex emplacement age history is apparent for the Prieska

Province kimberlites, which are situated in a relatively restricted part of the African subcontinent.

4. The ages obtained generally overlap with the ages for the cratonic kimberlites, but the dominant cratonic Group I 86 Ma event is not represented in the Prieska Province. Off craton Group I kimberlites tend to be either younger or older than this age event. Similarly, the 108 Ma Group I event seen in the Prieska Province is not represented on the Kaapvaal craton, based on the data to date.

5. Transitional kimberlites are difficult to date due to the fine-grained and poikiiitic nature of the phlogopite groundmass.

6. Group II kimberlites are older than Group I kimberlites, in common with cratonic kimberlites. The implication of this is that the kimberlite source area within the subcontinental mantle of South Africa has changed with time.

7. The age data reveal that there is no younging in emplacement events from the north-eastern part of the study area to the southwestern region. This is not supportive of a simple hotspot model for kimberlite generation.

Chapter 4

Whole-rock Isotopic Systematics

4.1 Introduction

Smith (1983b) claimed that the database of twenty four kimberlite analyses provided in his work are almost certainly representative of a large number of localities since kimberlites within a cluster in close proximity to one another are likely to have similar source isotope character (p. 118). He also claims that the kimberlites occurring in off-craton settings (such as those in this study) would not necessarily show the same isotopic character as the cratonic types. These suggestions require modification as will be shown for some of the localities in the Prieska Province.

The petrographic classification of kimberlites into micaceous and non-micaceous types has been correlated with the whole-rock major and trace element geochemistry and also with isotopic and emplacement age data (Smith, 1983a,b; Smith et al., 1985). The Group I and Group II kimberlites terminology arose as a result of the isotopic investigation of mainly cratonic hypabyssal kimberlites.

New whole-rock isotopic analyses are reported for nineteen occurrences selected from the Prieska Province and described in Chapter 2. Twenty eight samples were analysed for Rb-Sr, nineteen for Sm-Nd and thirteen for U-Pb. Some of the samples analysed are considered to be altered (see Chapter 5), but are included to compare to the unaltered varieties. Only hypabyssal facies kimberlites were analysed, and consisted of micaceous, non-micaceous and transitional varieties (see Chapter 2).

Sample preparation methods are given in Appendix B1, whilst analytical methods used to obtain isotopic data are given in Appendix B2.

4.2 Analytical Results

In all of the plots (except the Pb-Pb plots) shown in Chapter 4, the following abbreviations and symbols are used in the legends of the diagrams :

PP G1 = Prieska Province Group I kimberlites
- filled squares

PP G2 = Prieska Province Group II kimberlites
- filled circles

PP GT = Transitional Prieska Province kimberlites
- filled triangles

KC G1= Kaapvaal Craton Group I kimberlites (Smith, 1983a)
- open squares

KC G2 = Kaapvaal Craton Group II kimberlites (Smith, 1983a)
- open circles

Finsch = Finsch kimberlite (Fraser, 1987)
- open square with cross

Gibeon = Gibeon Group I kimberlites (Spriggs, 1988)
- hourglass

Brazil = Brazil "transitional" kimberlites (Bizzi, et al., 1991)
- cross

4.2.1. Rb-Sr Analyses

Rb and Sr concentrations, $^{87}Rb/^{86}Sr$ (atomic), present-day and initial $^{87}Sr/^{86}Sr$ (Rp and Ro respectively) and Epsilon values (ϵ_{Sr}) are presented in Appendix C1.2. For the localities Droogfontein 2W, Eendekuil 13W, Meltonwold 20W, Slypsteen 5W, Vioolkraal West 3W, Welgevonden 14W and Witberg East 11W, Rb concentrations were not obtained by ID and the concentrations obtained by XRF (XRF data presented in Appendix C2) are used for plotting purposes. Initial Sr isotopic ratios were obtained from the emplacement age regression calculations as presented in Chapter 3, but the initial-Sr ratio could also be obtained by back-calculating the whole-rock present-day $^{87}Sr/^{86}Sr$ value for the age.

Rb concentrations vary from 38 ppm to 213 ppm for the Prieska Province kimberlites. There are no correlations or trends between Rb and Sr for the province as a whole, or within (or between) the different petrographic types found in the province. There is, however, a slight positive correlation between Rb and Sr for the petrographically defined transitional varieties of kimberlite. There is also no correlation between the Ro and Rb contents. Sr varies from 449 ppm to 2 289 ppm and no distinctions may be drawn between any of the different types of kimberlites in the area. No correlation exists between Sr and Ro.

Figure 4.1 shows the initial-Sr ratio plotted against the $^{87}Rb/^{86}Sr$ ratio. Smith (1983b) pointed out that a vague inverse correlation between these parameters exists for cratonic types. This is not apparent from this plot. However, an overall positive trend is apparent when all the southern African and Brazilian kimberlite data are plotted together. Note that in this plot, it can be seen that some Group II kimberlites show low Rb/Sr ratios, whilst some Group I kimberlites have slightly

higher Rb/Sr ratios and these rocks plot off the mainly positive trend. More important is the fact that the rocks defined as being transitional in this research, provide the data that create the overall positive effect seen in Figure 4.1, as it can be seen that the Group I and II types plot on two subparallel, slightly positive trends. The calculated initial-Sr ratios are believed to be a real feature and are not due to the effects of alteration (the effects of alteration and contamination of the whole-rocks from this Province are dealt with in Chapter 5). No correlations between Rb, Sr, $^{87}Rb/^{86}Sr$ or Ro and distance from the craton boundary can be determined.

The most important feature of the Rb-Sr data for the Prieska Province is that the distinction between Group I and II [illegible] defined by Smith (1983a,b) is apparent for the Prieska Province kimberlites. In addition, the *transitional kimberlites* as defined petrographically in Chapter 2 and with respect to the initial-Sr ratios in Chapter 3, are seen to exhibit transitional Rb-Sr chemistry as well. Such kimberlites have not been described from southern Africa before. The rocks analysed by Bizzi (1991) from Brazil have also been shown to have intermediate initial-Sr ratios. However, in other respects these are more akin to the Group I kimberlites as defined by Smith (1983a, b), except that the Brazilian kimberlites are extremely rich in Sr relative to the southern African Group I kimberlites. The transitional rocks from the Prieska Province are transitional with respect to the initial-Sr ratio and Sr and Rb contents and plot closer to the Group II kimberlite trend. This will be commented on further in the following sections as well as in Chapters 5 and 7. There is also no correlation between weathered versus altered kimberlites for Rb and Sr concentrations. However, initial-Sr ratios for altered Group II kimberlites tend to be lower than that for the fresh types.

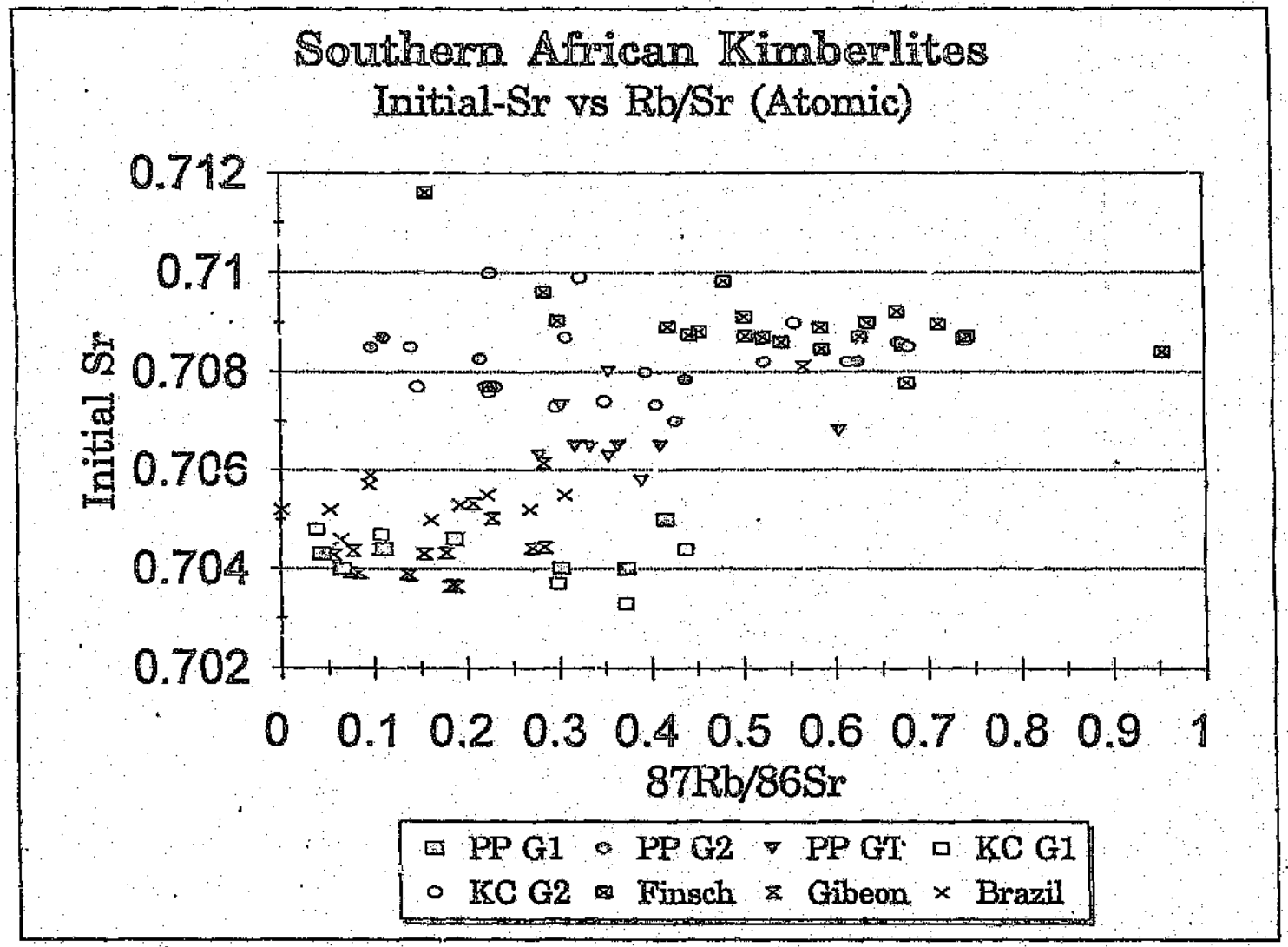

Figure 4.1 : Initial-Sr vs $^{87}Rb/^{86}Sr$

4.2.2 Sm-Nd Analyses

Sm and Nd concentrations, $^{147}Sm/^{144}Nd$ and $^{143}Nd/^{144}Nd$ ratios are presented in Appendix C2.2. Initial Nd ratios were calculated for these data using emplacement age data as presented in Chapter 3.

Sm concentrations range from 8 ppm to 25 ppm and Nd concentrations range from 57 ppm to 194 ppm. There is a strong positive correlation between Sm and Nd for the Prieska Province kimberlites as a whole, but distinctions between the different kimberlite types are not observed. No correlations are evident between the initial-Nd ratio and Nd or Sm concentrations, although the separation of the different kimberlite types is shown by differences in the initial Nd ratios. Group I kimberlites have higher initial-Nd ratios than Group II kimberlites, in accordance with the findings of Smith (1983a,b).

A plot of the initial-Nd ratio against the $^{147}Sm/^{144}Nd$ ratio is shown as Figure 4.2. No trends are evident from this diagram, except that the Group I and II type kimberlites plot with distinctly different initial-Nd ratios, which correlates to the findings of Smith (1983a,b). In this case, the transitional kimberlite types overlap with the kimberlites from Brazil (Bizzi et al., 1991) and both groups of kimberlites are seen to show strong Group II initial-Nd isotopic character. There are only two samples, both from Meltonwold, that plot distictly in the compositional gap between the Group I and II kimberlite types.

No correlations between Sm, Nd or the initial-Nd ratio with distance from the craton margin are evident.

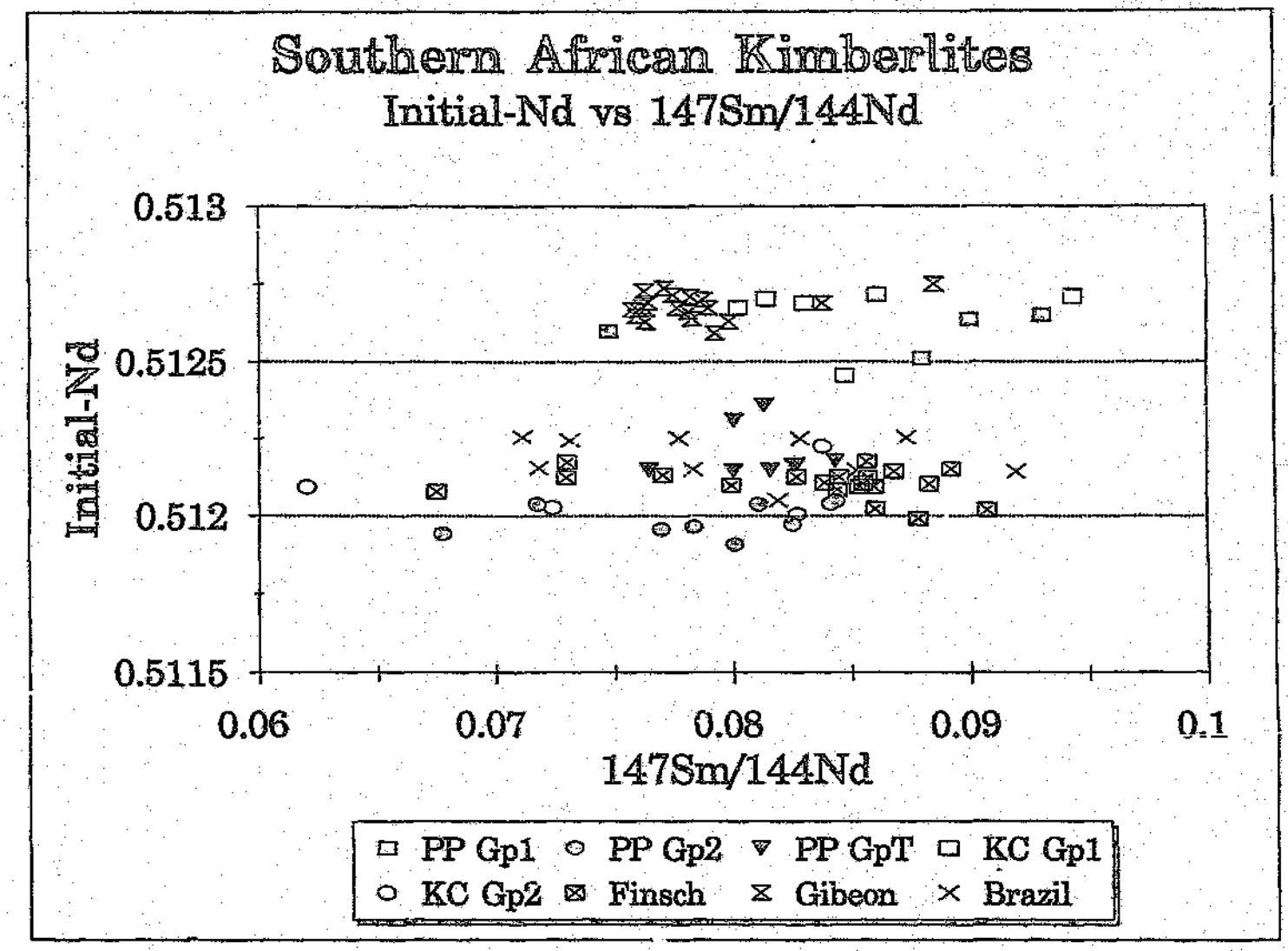

Figure 4.2 : Initial-Nd vs $^{147}Sm/^{144}Nd$

4.2.3 U-Pb Results

Pb isotopic compositions and concentrations for thirteen of the Prieska Province kimberlites are presented in Appendix C1.4. An attempt was made to analyse U by isotope dilution, but this was not sucessful. U concentrations were obtained using XRF and INAA. The U concentrations obtained by XRF are very high (see Appendix C2 and C3 as well as a comparison of the data in Appendix D) relative to those obtained by INAA. Furthermore, the U concenrations obtained by XRF in this study are much higher than the U concentrations obtained for Group I and II kimberlites by Smith (1983). The XRF data are therefore considered to be unreliable and the INAA data are preferred. Thorium data were collected using XRF and INAA.

Figure 4.3 shows the $^{207}Pb/^{204}Pb$ versus $^{206}Pb/^{204}Pb$ compositions, whilst figure 4.4 shows the $^{208}Pb/^{204}Pb$ versus $^{206}Pb/^{204}Pb$ compositions. Note that in these diagrams, only data from South Africa are shown and that in comparison to the Sr-Nd plots, the Pb isotope ratios are not age corrected but are present day values. It is clear that there are two groupings of data. The data showing less radiogenic lead correspond to the Group II kimberlites of Smith (1983a,b), although tending to plot slightly below the established trend of the cratonic Group II field. This observation of the Group II kimberlites showing lower $^{207}Pb/^{204}Pb$ for a given $^{206}Pb/^{204}Pb$ ratio is unexplained. It possibly indicates that the lead compositions beneath the cratonic environment is older than that for the surrounding mobile belt, but further analytical work is required in this regard in order to rule out fractionation effects (pers. comm. C. B. Smith). However, the Group I kimberlites from the Prieska Province (Britstown and Vioolkraal West) show slightly different Pb isotopic compositions relative to their cratonic counterparts, but in keeping with

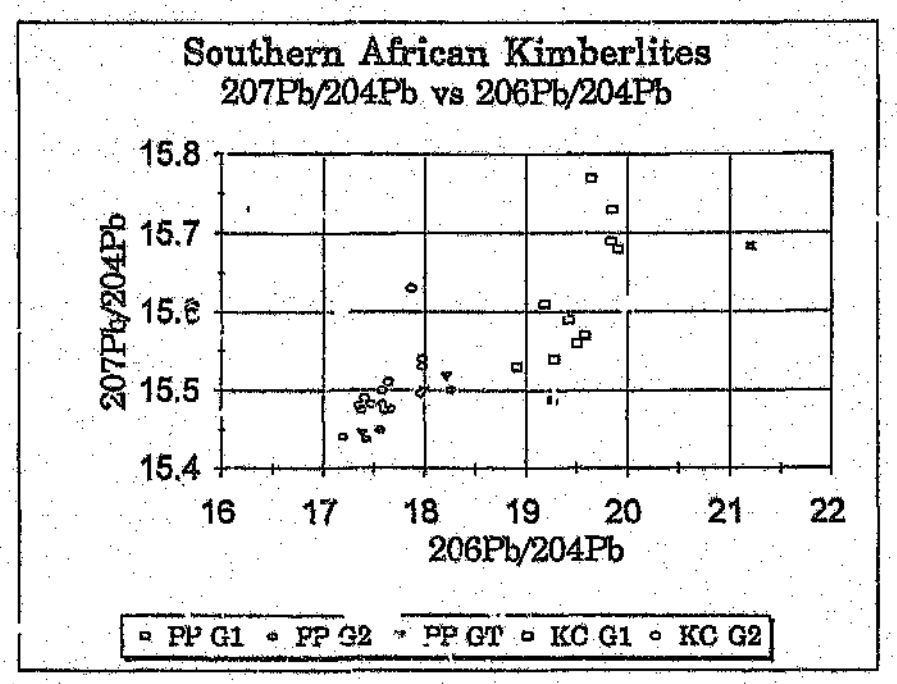

Figure 4.3 : $^{207}Pb/^{204}Pb$ vs $^{206}Pb/^{204}Pb$

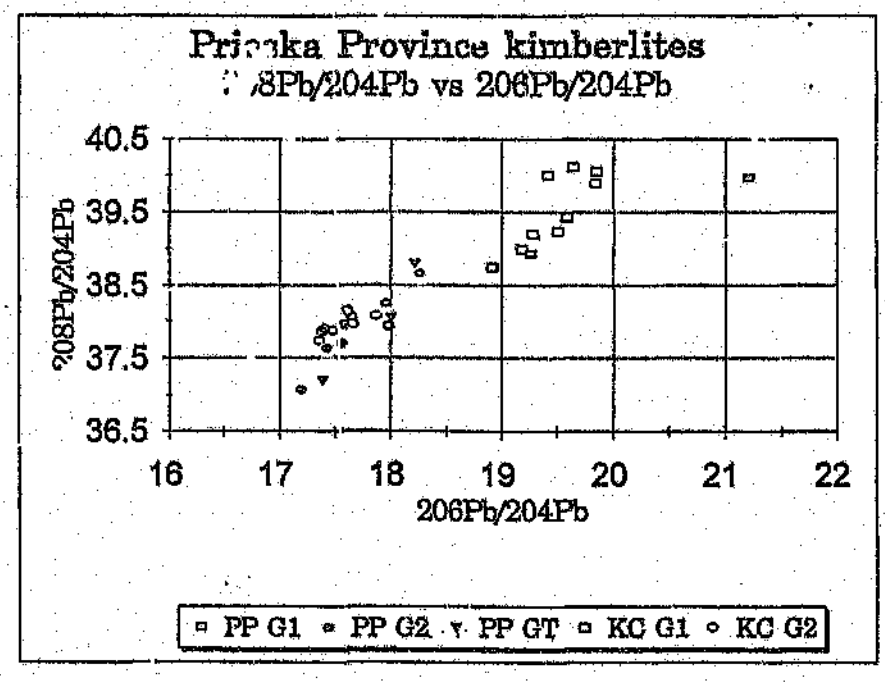

Figure 4.4 : $^{208}Pb/^{204}Pb$ vs $^{206}Pb/^{204}Pb$

the cratonic types show far more radiogenic lead relative to the Group II types. Vioolkraal West shows an extremely high $^{206}Pb/^{204}Pb$ composition, far higher than for previously recorded Group I kimberlites.

With respect to the transitional kimberlites, their lead isotope compositions do not plot between the isotopic fields of the two established kimberlite types, but overlap the Prieska Province Group II field. The Prieska Province Group II field overlaps the cratonic Group II kimberlite field of Smith (1983a).

4.3 Sr-Nd Isotope Compositions

Calculated epsilon values (ϵ_{Nd} and ϵ_{Sr}) are plotted in Figure 4.5. Here the different groups of kimberlite are clearly separated, with the non-micaceous Prieska Province kimberlites plotting within the field defined for the cratonic Group I kimberlites of Smith (1983a). The Pampoenpoort occurrence plots close to the cratonic locality Frank Smith, with both localities plotting close to the Bulk Earth value. The Prieska Province Group II kimberlites plot towards the enriched component of the diagram and overlap the previously defined Group II field (Smith, 1983b) and Finsch (Fraser, 1987) and extend this field towards towards lower ε_{Nd} and ε_{Sr} values.

In terms of the new data obtained from this work, the most important feature displayed by the graph is the position of the transitional kimberlites. They plot close to the Group II field, with one locality Silvery Home) falling within the Group II field. For the most part, the transitional kimberlites plot distictively between the Group I and II

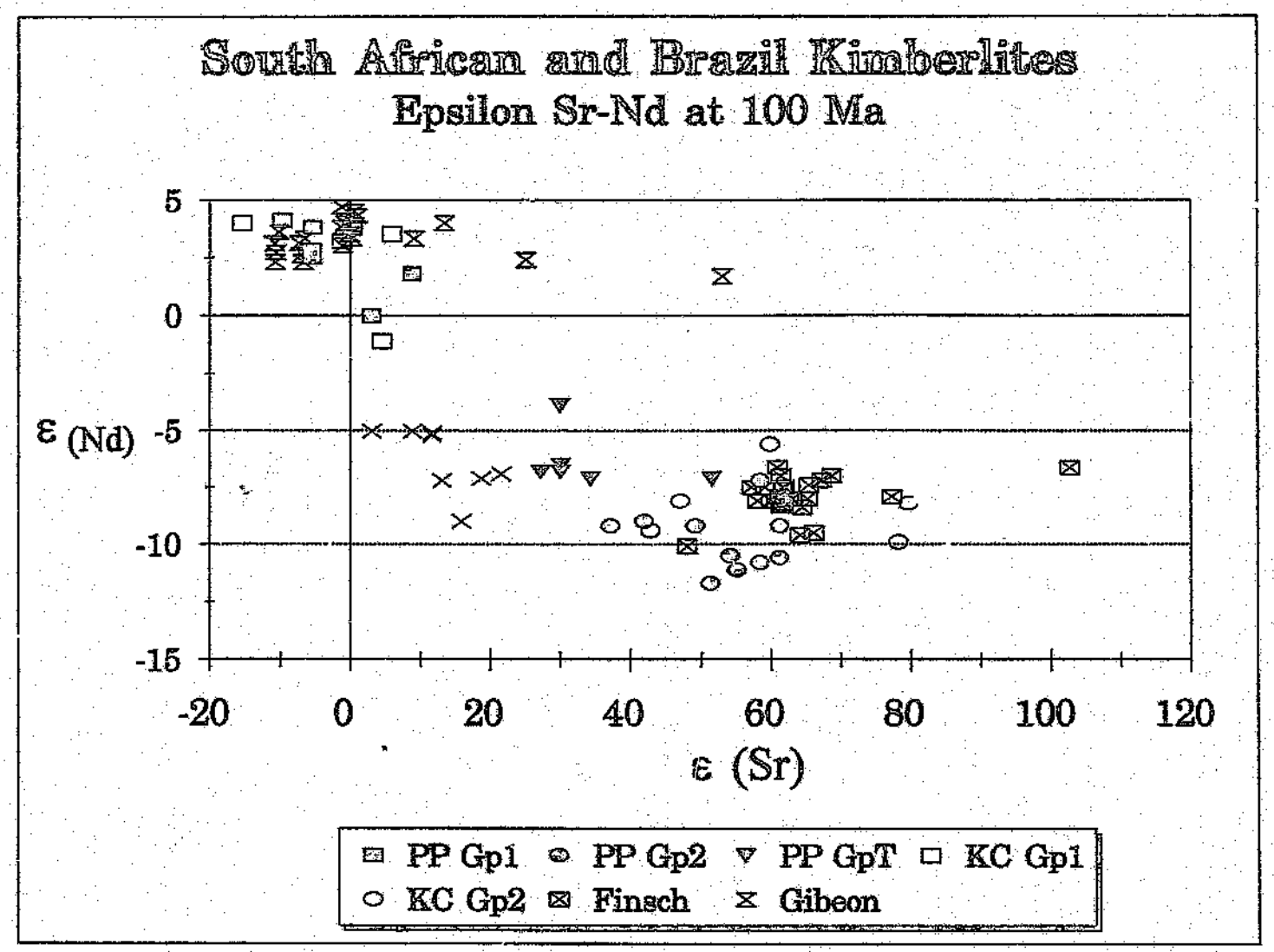
South African and Brazil Kimberlites
Epsilon Sr-Nd at 100 Ma
ε (Nd)
5
0
-5
-10
-15
-20
0
20
40
60
80
100
120
ε (Sr)
PP Gp1
PP Gp2
PP GpT
KC Gp1
KC Gp2
Finsch
Gibeon

kimberlite fields. Two samples from the locality Meltonwold have distictive ε values from one another, but the reason for this is not clear.

Certainly the trend displayed by the transitional kimberlites is not due to fortuitous sampling, nor are they altered samples. Their isotopic compositions must therefore reflect their source area compositions. The transitional kimberlites in this study are problematic to interpret in terms of magma mixing processes due to their generally older ages and the disparate locations within the province. In the study of Smith (1983b), the Group I Frank Smith kimberlite (located ± 50 km northwest of Kimberley) occurs in close association with the Excelsior kimberlite (a Group II occurrence). Data obtained for Frank Smith was seen to reflect Group I character with respect to petrography and isotopes (Sr and Pb), but gave an ϵ_{Nd} value close to Bulk Earth.

Two possible explanations were put forward for this unusual occurrence - either a third kimberlite source or mixing between Group I and II type melts. This was considered possible by mixing 75% of a Group I and 25% of a Group II kimberlite, and was justified in that the Newlands kimberlite (of identical age) is very near by and could possibly have shared the same plumbing system at depth. The Pampoenpoort occurrence in the Prieska Province shows a similar isotopic character to the Frank Smith kimberlite, but no Group II kimberlite of the same age is situated near to Pampoenpoort. Therefore no mixing model can be postulated for Pampoenpoort and it is believed that both the Frank Smith and Pampoenpoort kimberlites show isotopic compositions that reflect their source regions rather than mixing during emplacement.

It is clear from the data presented on the Sr-Nd epsilon diagram that

there are two distinct groups of kimberlites as defined by the Rb-Sr and Sm-Nd systematics, correlative with the results shown by Smith (1983a,b). The kimberlites in the Prieska Province therefore consist of both Group I and Group II (isotopic) types. In addition to these two kimberlite groups, the Prieska Province kimberlites also consist of a third kimberlite component, termed transitional kimberlites, which can be defined using Sr and Nd isotopes. At this stage the Pb isotope characteristics of the transitionals is not definitive in terms of being transitional but the slightly lower $^{207}Pb/^{204}Pb$ ratios may be significant.

As the transitional kimberlites are not considered to be significantly altered, then they either represent a distinct (third) kimberlite source region or are the result of a modification of a Group I or II kimberlite (viz. a Group I or II type which has been modified prior to or during emplacement).

The question of crustal contamination with respect to the isotopic compositions has been addressed by other workers (Berg and Allsopp, 1972; Barrett and Berg, 1975; Kramers, 1977; Smith, 1983b; Mitchell, 1986; Spriggs, 1988). Smith (1983b) concluded that Group II kimberlites could not have been produced by contamination of Group I kimberlites. Although small variations in the isotopic character could be due to such processes, the isotopic differences between Group I and II types could not be ascribed to either alteration or contamination. Spriggs (1988) and Smith (1983b) showed that crustal contamination in amounts of less than 5 % would have little effect on trace element and isotope ratios. It is therefore not believed that the kimberlites in the Prieska Province have been affected to any significant degree by crustal contamination.

Smith (1983b) has on numerous occasions stressed the compositional

gap between the Group I and II type kimberlites. This has been taken as evidence of very different source region characteristics (viz. Group I kimberlites are derived from similar material to OIB, with source regions in the asthenosphere, whilst Group II kimberlites are derived from lithospheric sources characterised by ancient enrichment). This study has demonstrated the occurrence of kimberlites within the compositional gap, with the implication that the conclusions reached above must be modified.

Smith et al. (1992), in studying megacrysts from the cratonic Lace and Frank Smith kimberlites body, has modified his earlier views of kimberlite source regions and suggests that both Group I and II kimberlites are derived from the deep subcontinental lithosphere. Furthermore, there is no hotspot/kimberlite relationship with respect to their material sources. Ringwood, et al., (1992) believe that both kimberlite types are ultimately derived from a deep mantle source, similar to that for OIB's, located within the transition zone and not at depths shallower than about 300 km. These considerations are addressed further in Chapter 7.

4.4 Summary of Isotopic Data

From the data presented above, the following observations of the isotopic characteristics of the Prieska Province kimberlites can be made:

1. Rb concentrations range from 38 to 213 ppm, whilst Sr ranges from 449 to 2 289 ppm. No correlations between these elements are evident. A positive correlation exists between the initial-Sr and $^{87}Rb/^{86}Sr$ ratios for the southern African kimberlites as a

whole.

2. Sm ranges from 8 to 25 ppm and Nd ranges from 57 to 194 ppm for the Prieska Province kimberlites. No correlations between Sm and Nd or between the initial-Nd and $^{147}Sm/^{144}Nd$ ratios are evident for the different kimberlite types of the Prieska Province.

3. There is no correlation between the distance of a locality from the craton margin and the Sm, Nd concentrations.

4. Both Group I and Group II isotopic kimberlites, as previously defined for kimberlites of the Kaapvaal Craton (Smith, 1983a,b), are found in the Prieska Province. Previous investigations have not noted the presence of Group II (isotopic) kimberlites from the off-craton tectonic setting, although Skinner (1989) and Skinner et al. (1991) has noted the presence of micaceous kimber from the study area.

5. The Prieska Province kimberlites consist of three distinct isotopic types of kimberlites, which are correlative with the petrographic distinctions of Skinner et al., 1991. The three kimberlite types are represented by the isotopic ratios presented in Table 4.1 below, where they are compared to their cratonic counterparts.

   It can be seen from this table that the Prieska Province Group I kimberlites encompass the initial-Sr ratio range of the cratonic types and extend it slightly, and fall within the initial-Nd ratio range of the cratonic types. Petrographically, these kimberlites are represented by the non-micaceous type. The present-day Pb isotope ratios (represented only by two localities) are similar to the cratonic Pb-ratios.

Table 4.1 Summary of Isotopic Data

	Setting	Group I	Transitional	Group II
Initial-Sr Ratio	*Prieska*	0.7040-0.7056	0.7056-0.7073	0.7073-0.7090
	Kaapvaal	0.7033-0.7049	nt	0.7074-0.7109
Initial-Nd Ratio	*Prieska*	0.51251-0.51270	0.51214-0.51236	0.51191-0.51214
	Kaapvaal	0.51246-0.51272	nt	0.51200-0.51222
Present-Day $^{207}Pb/^{204}Pb$	*Prieska*	15.49-15.68	15.45-15.52	15.44-15.50
	Kaapvaal	15.53-15.89	nt	15.48-15.63
Present-Day $^{208}Pb/^{204}Pb$	*Prieska*	38.93-38.98	37.20-38.79	37.07-38.67
	Kaapvaal	38.75-48.48	nt	37.88-38.08

Notes to above table:

Prieska = Prieska Province Kimberlites

Kaapvaal = Kaapvaal Craton (Data from Smith, 1983a)

nt = no transitional kimberlite defined from the Kaapvaal craton.

The Prieska Province Group II kimberlites are represented by the petrographically defined micaceous kimberlites. Their initial-Sr ratios fall within the cratonic kimberlite range. The Prieska Province initial-Nd ratios overlap and extend to lower values, the initial-Nd ratios of the cratonic kimberlites. The present-day Pb isotope ratios overlap with those of the cratonic varieties for $^{208}Pb/^{204}Pb$ but are slightly lower for $^{207}Pb/^{204}Pb$ ratios.

The petrographically defined transitional kimberlites (refer to

The petrographically defined transitional kimberlites (refer to Chapters 2 and 3) have not yet been found on the Kaapvaal craton at the present time. (The locality Sweetput-Soutput is situated on-craton, but is close to the craton margin. One locality cannot be considered to be representative of "cratonic transitional kimberlites" unless further transitional types are recorded and analysed). These kimberlite types show initial-Sr ratios between those of the defined Group I and II kimberlites. Only altered cratonic kimberlites were found to plot in this region by Smith (1983b). Initial-Nd ratios for the transitionals overlap the higher ε_{Nd} of the cratonic Group II's and extend to values between those of Group I and Group II kimberlites from the craton. Lead isotopes overlap the Prieska Province Group II trend.

6. The Group I and II kimberlites that occur in both tectonic settings (Prieska Province and Kaapvaal Craton) overlap one another on the Sr-Nd epsilon diagram as well as the $^{208}Pb/^{204}Pb$ and $^{207}Pb/^{204}Pb$ versus $^{206}Pb/^{204}Pb$ diagrams. This indicates that Group I and II type kimberlites on either side of the craton margin are derived from similar source regions.

7. The transitional kimberlites appear, at this stage, to be more common in the off-craton setting, but this does not imply that they do not occur on-craton in greater numbers. Their spatial positions and emplacement ages preclude simple source region mixing between Group I and II kimberlites. Compared to the kimberlites from Brazil, the Prieska Province kimberlites show higher ε_{Sr} values but similar ε_{Nd} values.

Chapter 5

Geochemistry of the Prieska Province Kimberlites

5.1 Introduction

Whole-rock samples were analysed for major, minor and trace element compositions using X-ray Fluorescence Spectrometry (XRF) and Instrumental Neutron Activation Analysis (INAA). Details of the analytical techniques used are given in Appendices B3 and B4 respectively.

In the case of XRF, thirty samples from twenty localities were analysed, whereas for INAA, sixteen samples from twelve localities were analysed. Fewer analyses were done with INAA because samples for some localities (eg. Silvery Home, Skietkop, Vioolkraal West and Slypsteen) only became available after the INAA analyses were performed.

Mitchell (1986) states that "kimberlite whole-rock compositions do not represent the compositions of the magmas from which they formed" (p. 281). In a simplistic sense this is true since kimberlites are the end product of (probably) many processes. In the case of macrocrystal olivine, which is extremely common in kimberlites, it is unlikely that this "contaminant" (commonly accepted as being derived from disaggregated peridotite xenoliths) would affect the trace and incompatible element abundances in the whole-rock, although its presence would be reflected in the MgO content. In spite of the problems associated with the geochemical analysis of kimberlite,

provided suitably fresh hypabyssal facies kimberlite samples are collected and carefully prepared (avoid contamination by country rocks etc.), it is believed that important information can still be obtained regarding the source area of kimberlites.

Of direct relevance to this study is the geochemical investigation performed by Smith et al. (1985), which followed from the isotopic investigation of southern African kimberlites (Smith, 1983b). In the later study, Smith was able to distinguish Group I and II kimberlites geochemically, particularly with the elements SiO_2, Pb, K_2O and TiO_2. These reflect the essential difference in mineralogy and together (with some exceptions) are clearly correlated with the isotope characteristics. Thus both isotope (certainly) and geochemical (probably) signatures are indicative of source character.

Whilst non-micaceous and micaceous kimberlites are generally well correlated with Group I and II (isotopic) kimberlites respectively, it is considered important when giving descriptions of kimberlites to be consistent with the available information. In other words, a micaceous kimberlite should be only termed a Group II kimberlite once the isotopic systematics are known (see chapter 7 for further thoughts on this issue). This study has shown (see Chapter 4) that certain kimberlites, which are essentially micaceous varieties cannot be correlated to Group II types as originally defined. In this study, these kimberlites are termed transitional and their geochemical character will be compared to the previously defined Group I and II kimberlites in order to assess any geochemical differences that they may show.

Smith et al. (1985) believed that Group I kimberlites occurring on the Kaapvaal Craton could be distinguished from Group I kimberlites in the off-craton setting on the basis of whole-rock geochemistry. This led to

the Group IA and IB (on and off-craton respectively) terminology. These geochemical differences could not be correlated with the isotopes however. Group IA and IB kimberlites were found to be effectively discriminated using total Fe. Increased Fe in IB rocks was correlated with increasing TiO_2, CaO, CO_2 and H_2O^+, and decreased MgO and SiO_2 contents compared to IA rocks. In addition, V, Cu and Zn abundances and Ca/Al ratios are higher in IB relative to IA's and II's. Cr and Ni decreases from Group II to IA to IB. However, the trends between IA and IB tend to be gradational, and IB character was found to be not restricted to the off-craton setting (the Mayeng sill complex and the Monastry kimberlite, occurring on the Kaapvaal craton have IB character). It was concluded that IB kimberlites were probably derived from relatively shallow source regions with geothermal gradients between those of continental and oceanic environments.

This study is essentially a continuation of that performed by Smith and includes Group I, II and transitional kimberlites in both an off and on-craton tectonic setting. The major, minor and trace element variations of the Prieska Province kimberlites will be discussed in terms of contamination and alteration, variation within kimberlites and an attempt to relate the geochemical and isotopic variations will be made. These data will also be compared to other southern African localities.

5.2 Data used in this work

Since a variety of methods were employed in the acquisition of the geochemical data, comparisons between techniques for overlapping elements are presented in Appendix D. Some samples analysed by Smith using INAA at the Max Plank Institute were re-analysed by this

author and allow for interlaboratory correlation (also in Appendix D).

Major and most of the trace element element data presented here were obtained by XRF, whilst rare earth element data (whole-rock) were obtained using INAA. Data for Uintjiesberg (Smith, 1985; Robey 1981) and the Meltonwold, Markt, Lovedale, Haartebeesfontein and Silvery Horse (Robey 1981) occurrences which were previously analysed for major and trace elements by XRF are included for comparison and augmentation of the database.

In the diagrams shown in this chapter, the legends use the same abbreviations as was presented on page 76 under section 4.2.

5.3 Major Element Geochemistry

5.3.1. General trends

Major and trace element data are presented in Appendix C2. From this data set, the ranges and averages of the major elements are tabulated in Table 5.1.

From Table 5.1 it is seen that the Prieska Province kimberlites are characterised by a wide range in SiO_2 (28.3-41.4 weight percent), a wide range in MgO (18.5-34.5 weight percent), relatively low Al_2O_3 (2.2-6.7 weight percent) and very low Na_2O (0.01-0.77 weight percent). These data are characteristic of kimberlites reported elsewhere (Mitchell, 1986; Smith, et al., 1985; Fraser, 1987). When data are compared for each group, the ranges are more restricted, as expected. However, considerable overlap between the ranges for each group is noted, with

Group I kimberlites reaching higher limits of Fe_2O_3 and CaO; lower SiO_2, K_2O and Al_2O_3 than the other groups. Transitional kimberlites show intermediate ranges for many elements, but reach higher limits for Al_2O_3 and MgO and lower LOI and show the widest spread of Na_2O. Group II types reach lower limits for TiO_2 and Fe_2O_3 and higher K_2O than the other groups. The overall trends shown in Table 5.1 are similar for all groups. An important feature to note is that data are averaged in order to compare and contrast. In spite of the wide range shown by MgO, the average compositions are very similar. Significant differences in averages are shown by SiO_2 (for Group I and II types), TiO_2, Fe_2O_3, CaO (for Group I and II types) and K_2O. This is a reflection of the different mineralogies of the three kimberlite types, and in all cases the transitional group samples plot between the averages for Group I and II types.

For the most part, the transitional kimberlites are similar to Group II types, but for TiO_2, Fe_2O_3 and K_2O, the presence of "Group I" minerals such as opaque oxides and perovskite, causes their geochemical character to reflect features of both of the two kimberlite groups. Intuitively, the transitional geochemical character is suggestive of mixing between Group I and II types, but as shown in Chapter 3, the emplacement ages and spatial setting of the transitional kimberlites precludes simple magma mixing, but rather the transitional reflect a mixed source region.

It should be noted that care must be exercised whenever averages are used in the comparison of kimberlite data, because kimberlites are inherently variable in their composition. Although most of the localities are small and uneconomic, it is likely that they contain more than one kimberlite variety, as this is a common feature of kimberlite pipes, but not necessarily with dyke systems. Robey (1981) notes that for many

Table 5.1 : Ranges and Averages for Major Elements

SOUTHERN AFRICAN KIMBERLITES									
	Group I		Transitional		Group II		Cratonic Kimberlites		
OXIDE	*Range*	*Avg*	*Range*	*Avg*	*Range*	*Avg*	I A	I B	II
SiO_2	28.3-34.2	30.5	33.3-39.5	35.6	31.9-41.4	36.6	25.7	32.1	36.3
TiO_2	1.98-3.95	2.95	0.92-3.20	1.97	0.71-1.64	1.08	3.0	2.0	1.0
Al_2O_3	2.2-5.6	3.49	2.34-6.70	4.23	2.77-6.38	3.71	3.1	2.6	3.2
Fe_2O_3	10.1-14.9	12.4	8.6-107	9.6	7.3-9.4	8.2	12.7	9.2	8.4
MnO	0.18-0.30	0.24	0.15-0.21	0.17	0.13-0.18	0.16	0.2	0.2	0.2
MgO	18.9-30.8	25.6	18.5-34.5	26.5	21.4-28.8	25.8	23.8	28.5	29.7
CaO	7.3-13.8	9.8	4.4-9.9	6.9	4.6-9.7	6.6	14.1	8.2	6.0
Na_2O	0.04-0.63	0.16	0.01-0.77	0.18	0.03-0.17	0.09	0.2	0.2	0.1
K_2O	1.0-3.4	1.6	1.2-4.6	2.7	1.95-4.92	3.52	0.6	1.1	3.2
P_2O_5	0.8-1.9	1.2	1.2-2.0	1.2	0.04-1.9	1.04	1.1	1.1	1.1
H_2O-	0.7-1.6	1.0	0.1-1.5	0.97	0.7-2.3	1.5	0.5	1.1	0.7
LOI	8.8-12.5	11.1	4.1-14.1	10.0	5.7-14.4	11.3			
TOTAL		99.69		99.87		99.77			
CI	0.99-1.57	1.22	1.07-1.56	1.28	1.12-1.59	1.24			
Si/Mg	0.76-1.34	0.93	0.85-1.51	1.08	0.92-1.5	1.12			

KEY TO TABLE 5.1 :

Group I, II and transitional - Data for Prieska Province (this work)

Cratonic Kimberlites - Averaged Group data from Smith et al. (1985)

IA = Group I (on-craton) kimberlites

IB = Group I (off-craton) kimberlites

II = Group II kimberlites

Avg = Average of all data for that group

CI = Contamination Index (Clement, 1984)

Si/Mg = Contamination Index (Ilupin et al., 1971)

of the localities he visited, two petrographically distinct types of kimberlite from each occurrence could be described, probably implying that the kimberlite bodies are multiply intruded.

This point is well illustrated by the Finsch kimberlite, which although not directly correlative to the kimberlites studied here (certainly in terms of size), shows clearly the effect of a multiply intruded body with respect to averaging data from different intrusions analysed. Fraser (1987) analysed four samples from each of the major intrusions (F2, F3, F4) and two samples each of the minor intrusives (F5/F6, internal dyke and external precursor dyke) from the Finsch kimberlite. An inspection of the major element data ranges of these samples from different intrusions reveals that for this one kimberlite alone, an extremely wide variation of major elements is present, and envelops virtually all of the elements as shown for the Prieska Province kimberlites shown in Table 5.1. This wide range in geochemical composition at Finsch is mirrored in the measured isotopic compositions, which encompasses virtually the whole of the Group II isotopic field of Smith (1983a).

In this study, a number of samples from each of the localities Witberg Pipe, Markt, Middelwater 01, Eendekuil, Droogfontein, Meltonwold, Skietkop and Sweetput-Soutput were selected for analysis. These were taken (for the most part) from one borehole at different depths. Therefore the samples are probably representative of one intrusion from that occurrence. Only in the case of the Brandewynskuil kimberlite, were two intrusive types (hypabyssal and diatreme facies) collected (see Appendix A for descriptions).

5.3.2. Contamination and Alteration

Kimberlites are extremely prone to rapid weathering at surface, which is readily apparent by the serpentinisation of olivine and clay alteration of phlogopite and groundmass phases. In addition, groundwaters may introduce or redistribute carbonates which would be seen as either veins or as segregations within the kimberlite matrix. Calcite may, however, also be present as a primary phase within the kimberlite matrix. Kimberlites may also be altered deuterically (a primary alteration feature, probably occurring during emplacement) which is most notably seen in olivine being altered to fine grained pseudomorphs.

Kimberlites also contain numerous upper mantle and crustal (lower and upper) xenoliths. In hypabyssal facies kimberlites, crustal xenoliths are seen to have baked margins, and it is unlikely that significant crustal contamination of the kimberlite magma has taken place (Mitchell, 1986). Nevertheless, small fragments of country rock could possibly be assimilated, which would have an effect on the geochemistry of the kimberlite.

Thus the effects of crustal contamination and alteration must be taken into account in any geochemical or isotopic study of kimberlites. The "best" material to analyse is of hypabyssal facies rocks, which must be carefully selected to avoid large amounts of crustal xenoliths, and carefully prepared by removing any obvious contaminants at the crushing stage.

Some methods have previously been devised to assess alteration and contamination. Ilupin and Lutz (1971) suggested that contaminated rocks would show a Si/Mg ratio of > 0.88 and Mg/(Mg+Fe) < 0.85. Fesq

et al (1975) also used Si/Mg ratios, but considered a ratio of > 1.2 to indicate crustal contamination. The Si/Mg ratio is based on the fact that crustal rocks contain greater amounts of SiO_2 and lower MgO than ultramafic rocks.

Clement (1982) introduced the concept of a "*contamination index" (CI) defined as :*

$$CI = \frac{(SiO_2 + Al_2O_3 + Na_2O)}{(MgO+2K_2O)}$$

This measures the proportion of clay minerals and tectosilicates relative to olivine and phlogopite and implies that post intrusive alteration effects would be noted with this index. Since crustal rocks have elevated SiO_2 and Al_2O_3 relative to mantle derived rocks, a high index would indicate the presence of crustal contamination. Although fresh kimberlites are characterised by indices < 1.3, Clement (1982) notes that some supposedly uncontaminated phlogopite and diopside rich kimberlites show indices of between 1.0 and 1.5. Spriggs (1988) studied numerous altered kimberlites from the Gibeon Province and showed that despite the obvious alteration observed both macroscopically and microscopically, CI's of 1.03 to 1.28 were obtained. Only where significant (> 20%) crustal contamination was seen to be present, was the index significantly raised above unity for these kimberlites.

Other problems with this index include the fact that fractionation of kimberlite magmas would cause a decrease in olivine content and consequent increase in CI. Similarly, abundant phlogopite (high K_2O) would produce a similar effect. Mitchell (1989) notes that the index does not take into account macrocrystal olivine (which is in reality a contaminant), so numerous published analyses for fresh kimberlites show that they are contaminated when applying the index to them.

Other aspects of contamination and alteration, which are more important with respect to geochemistry, are the behaviour of the trace elements, as these elements are commonly utilised as indicators of source regions. Spriggs (1988) concluded that for the Gibeon kimberlites, slight crustal contamination has little effect on trace element geochemistry, but that slight degrees of alteration had a significant effect on whole-rock geochemistry, with respect to Rb, Ba, K, Sr and the LREE. As Spriggs pointed out, it is commonly believed that the REE are immobile, but in the presence of alkali-carbonate solutions, the LREE are very mobile. Therefore analyses of REE on calcite-rich kimberlites that are only slightly altered should be viewed with caution. Smith et al. (1985) used the CI as one parameter in the selection of samples for the database presented in that work, but also suggested that H_2O would be indicative of alteration.

Whilst the CI is useful, particularly when looking at published analyses for which no other details are available, and attempts to provide a quantitative assessment of contamination, petrographic examination of samples provides a qualitative assessment of the degree of alteration and contamination within a given sample.

Examination of the Prieska Province data (Appendix C2) shows that on average, micaceous kimberlites have slightly higher CI values than non-micaceous varieties and fairly similar values to transitional varieties. Notably altered micaceous varieties show CI > 1.8. A number of samples have CI values between 1.3 and 1.6 (Figure 5.1) and include samples from the Britstown, Vioolkraal West and Droogfontein kimberlites, which are slightly altered petrographically (visible as serpentinisation). The other samples which have high CI values include Brandewynskuil, which microscopically is seen to be a TKB and therefore contains crustal components and which would explain the high

CI, and another sample from Droogfortein, which is less altered than the Droogfontein sample mentioned above, and Sweetput-Soutput, which is considered to be only slightly altered on petrographic grounds. In all cases the alteration consists dominantly of serpentinisation, with some clay alteration of the phlogopite.

The Si/Mg ratio shows a broadly similar pattern but when compared to the CI (Figure 5.2) shows that higher indices are given by the CI relative to the Si/Mg ratio. Strictly speaking, these ratios cannot be compared directly as they measure different combinations of elements, but Figure 5.2 is shown in order to illustrate that the simple index of Si/Mg is probably just as useful as the CI. There is no correlation between either LOI or H_2O and CI. A vague negative correlation exists between H_2O and LOI, but the scatter is high.

Because few samples of both fresh and altered kimberlites were collected from the same locality, it is difficult to accurately quantify the effect of alteration or contamination on the major and trace element geochemistry. In this project, five Group II kimberlites are considered to be altered which is reflected by their high CI values. Comparison of these altered kimberlites to the fresh Group II sample analyses (see Appendix C2) shows the following relative changes : higher SiO_2, Al_2O_3, CaO and lower MgO in the altered samples (except for Eenzaamheidskuil 6 which shows significantly lower SiO_2). In the case of trace elements, few significant differences are apparent, although some discernable trends include Ba, which tends to be lower, whilst Cr and Co are sometimes lower, and Ni is much lower in altered compared to fresh samples. In the case of REE little change is evident, but this may be a reflection of the small dataset used. No discernible trends are seen in trace element ratios for fresh versus altered samples, when one considers data for each group as a whole.

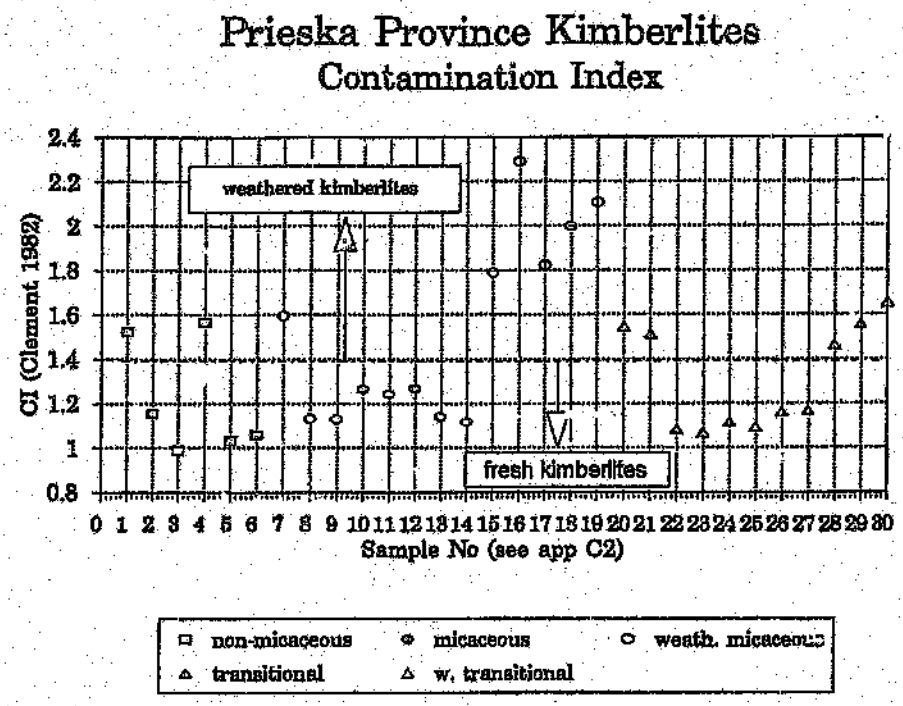

Figure 5.1: Contamination Index for the Prieska Province Kimberlites

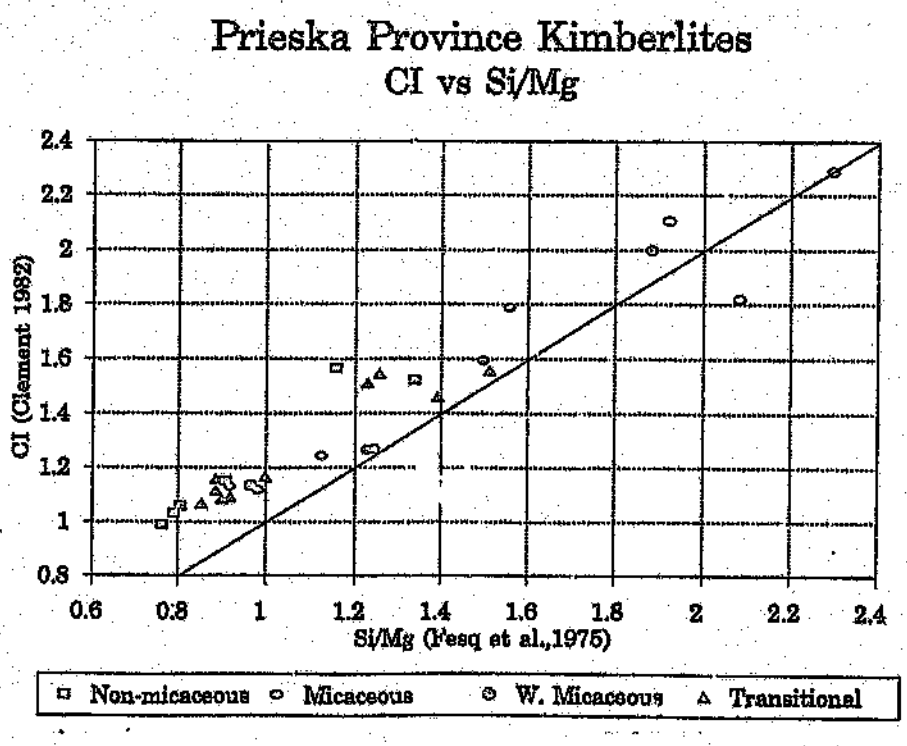

Figure 5.2 : Comparison of the CI with the Si/Mg ratio

Relatively fresh and altered samples from the transitional kimberlite Sweetput-Soutput (analyses 28, 29 and 30 of Appendix C2) show that the more altered sample displays lower Ba, Rb, V and Zn, whilst Sr and Cu are increased in the more altered sample. In the case of Brandewynskuil, samples of hypabyssal and diatreme facies rocks show that the diatreme facies material shows a slight decrease in TiO_2, MgO, CaO, K_2O and P_2O_5 and an increase in Na_2O and LOI relative to the hypabyssal facies rock. With respect to trace elements, Ba is significantly reduced, whilst Rb, Nb, Cr, Co and Ni are slightly reduced relative to the more fresh sample. Sr, V and Zn are slightly increased in the more altered sample. No change is seen for Cu.

There does not appear to be a consistent change for all elements between fresh and altered samples. It is concluded that alteration and contamination are specific to each kimberlite body, dependant on the specific mineralogy of the body and the amount of country rock xenoliths present. The presence of country rock fragments may allow for the circulation of greater amounts of groundwater in the altered zone of the pipe and therefore lead to significant differences in the chemistry of the rock.

In order to properly assess these features in kimberlites, it is suggested that samples are sequentially selected along a length of borehole core, incorporating the most altered samples at surface, through to relatively fresh material at depth. This should be done for each of a suite of kimberlites of different petrographic types, thus allowing for comparison within a body and between bodies of similar mineralogical type. In addition, differences between say xenolith-rich and xenolith-poor hypabyssal facies kimberlite should be investigated to see whether contamination/alteration is different for different textural types of kimberlite (as one would intuitively expect). A comparative study

involving detailed petrography, mineral chemistry and whole-rock geochemistry would be required in order for a realistic assessment of alteration and contamination to be achieved.

5.3.3. Major Element Variation

Harker variation diagrams showing the variation of the major elements against SiO_2 (Figure 5.3) reveal that non-micaceous kimberlites contain greater amounts of TiO_2, Fe_2O_3, MnO and CaO than micaceous varieties. In addition, SiO_2 contents are greater in the micaceous and transi[illegible] as relative to the non-micaceous varieties. These trends a[illegible] to the petrographic distinctions between the two kimbe[illegible] [illegible]ample, non-micaceous kimberlites contain ilmenite (which [illegible] TiO_2 and Fe_2O_3 contents will be higher), and greater amounts of p[illegible]rovskite and calcite (implying greater CaO) than micaceous varieties. In addition, non-micaceous kimberlites contain monticellite, which would also increase the CaO contents relative to micaceous types. MgO concentrations of micaceous and non-micaceous kimberlite types are similar, which is expected in view of the fact that the principal phase containing MgO is olivine - a common mineral in both micaceous and non-micaceous kimberlites.

As expected, K_2O for micaceous kimberlites is greater than for non-micaceous kimberlites. For fresh kimberlites, Na_2O is approximately the same for all groups, but is much greater for weathered kimberlites. P_2O_5 shows extreme variation in all the kimberlites analysed. This oxide would be present in accessory phases (eg. apatite) and a small amount of such a phase would significantly influence the results obtained. No trend can therefore be deduced from this oxide, and it is

Southern African Kimberlites

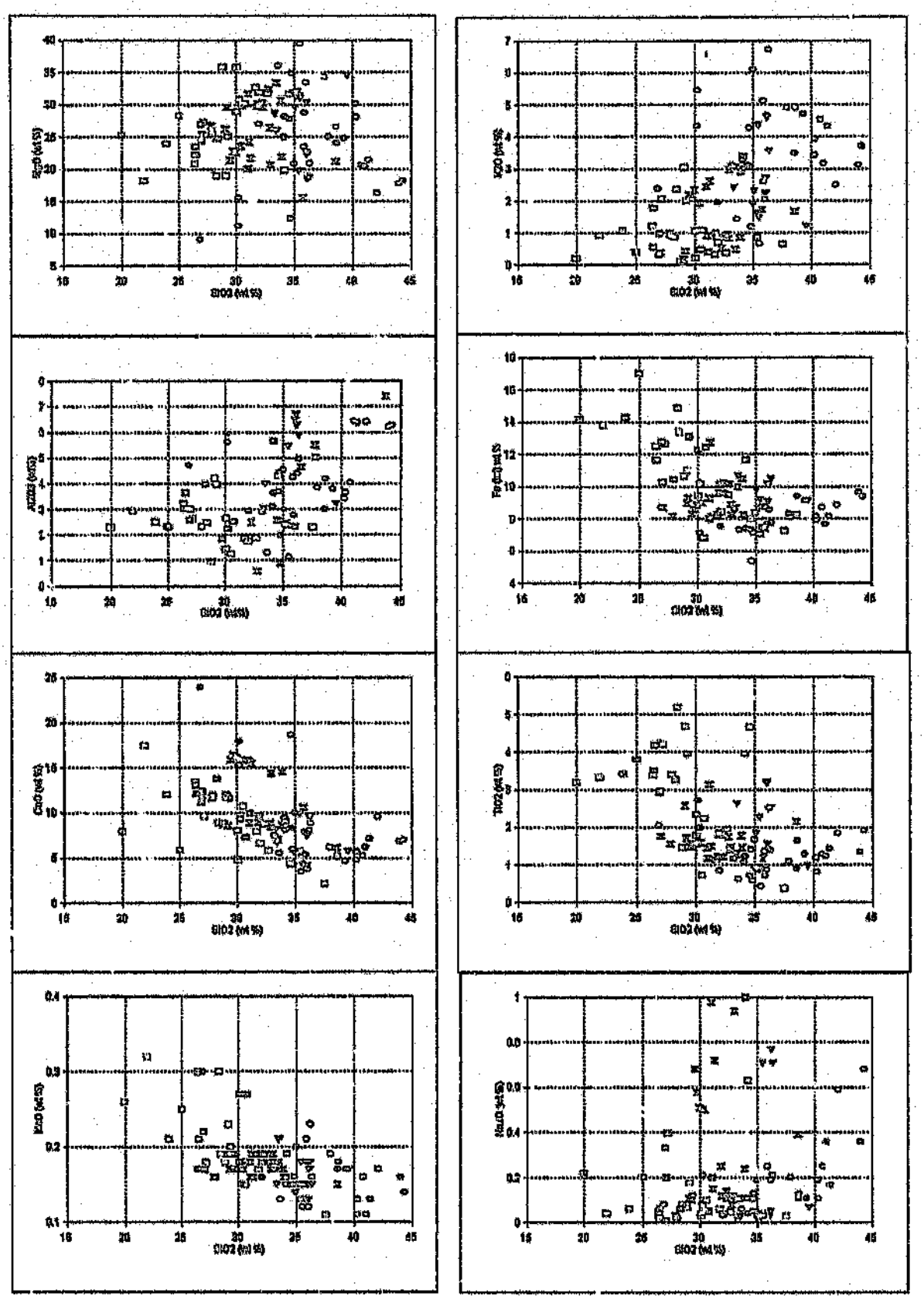

Figure 5.3 : Harker Variation Diagrams

Symbols as for other plots; Colours - blue = Group I, red = Group II, green = transitional, black=Gibeon

not plotted with the other major elements in Figure 5.3. Smith et al. (1985) showed that the different petrographic varieties could be distinguished in a P_2O_5 versus Ce plot. Two kimberlites - Uintjiesberg and a sill from south-west Botswana (off-craton localities) - were found to have extremely high P_2O_5 contents relative to cratonic varieties. However, the Prieska Province kimberlites analysed in this study show similar ranges to those analysed by Smith and no apparent differences between cratonic versus off-craton kimberlites are recognised with this oxide.

Figure 5.3 also shows general negative correlations for TiO_2, Fe_2O_3, MnO and CaO which reflects the points made above regarding the chemical distinctions being correlative with the mineralogy. Similarly, positive trends are noted for K_2O and Al_2O_3, which reflects the petrographic distinctions.

It can be seen in Figure 5.3 that for almost all major element oxides, the transitional kimberlite data plots between those of the micaceous and non-micaceous varieties. There is, however, more overlap between the transitional and micaceous types, which is expected since the transitional varieties are richer in minerals from the micaceous kimberlites relative to non-micaceous kimberlitic minerals. Nevertheless, the isotopic compositions of these kimberlites is distinct (Chapter 4). Therefore, it is considered that the geochemical trends displayed by the major elements show that the transitional kimberlites are also distinct geochemically (reflecting petrography), and this has not been recorded for southern African kimberlites before.

Apart from the Harker variation trends shown above, other major element oxide plots or major elements plotted against trace element data enable further separations of the different kimberlite types to be

distinguished. The most significant plot in this regard is shown in Figure 5.4 which plots K_2O against TiO_2. It is clear from this that the different kimberlites can be easily distinguished from one another. The plot is similar to the Harker variation diagrams in that this reflects mineralogical differences with micaceous varieties contain greater K_2O (phlogopite) and less TiO_2 (ilmenite) than non-micaceous types. The transitional types, however plot distinctly between these two trends, which reflects the micaceous and opaque-mineral rich nature of these kimberlites.

If K_2O is plotted against Rb, a separation into the various petrographic groups is again noted, which reflects phlogopite compositions as this mineral is the principal host of both these elements. In plots reflecting phlogopite contents, weathered micaceous varieties plot within the field of the transitional types. Smith et al. (1985) noted on the basis of isotopic characteristics that weathered kimberlites tended to show isotopic character between that of the two kimberlite types, but did not analyse any kimberlites which could be termed transitional. In this study, the petrographic and isotopically defined transitional kimberlites analysed are not considered to be significantly altered, or seriously affected by crustal contamination. Therefore the geochemical and isotopic characteristics must be indicative of a source region slightly different to that for Group I and II kimberlites.

Mitchell (1986), notes that the use of major element data for whole-rock kimberlite geochemistry is extremely limited. However, from the above, it can be seen that there are distinct differences in whole-rock geochemistry between the two kimberlite varieties, but this correlates to mineralogical differences. Furthermore, the transitional kimberlites (previously defined by isotopes) tend to plot between the micaceous and non-micaceous fields and are therefore considered to be geochemically

They do, however, show a closer geochemical affinity to the micaceous varieties relative to their isotopic signatures, which reflects the similar mineralogies of the two types.

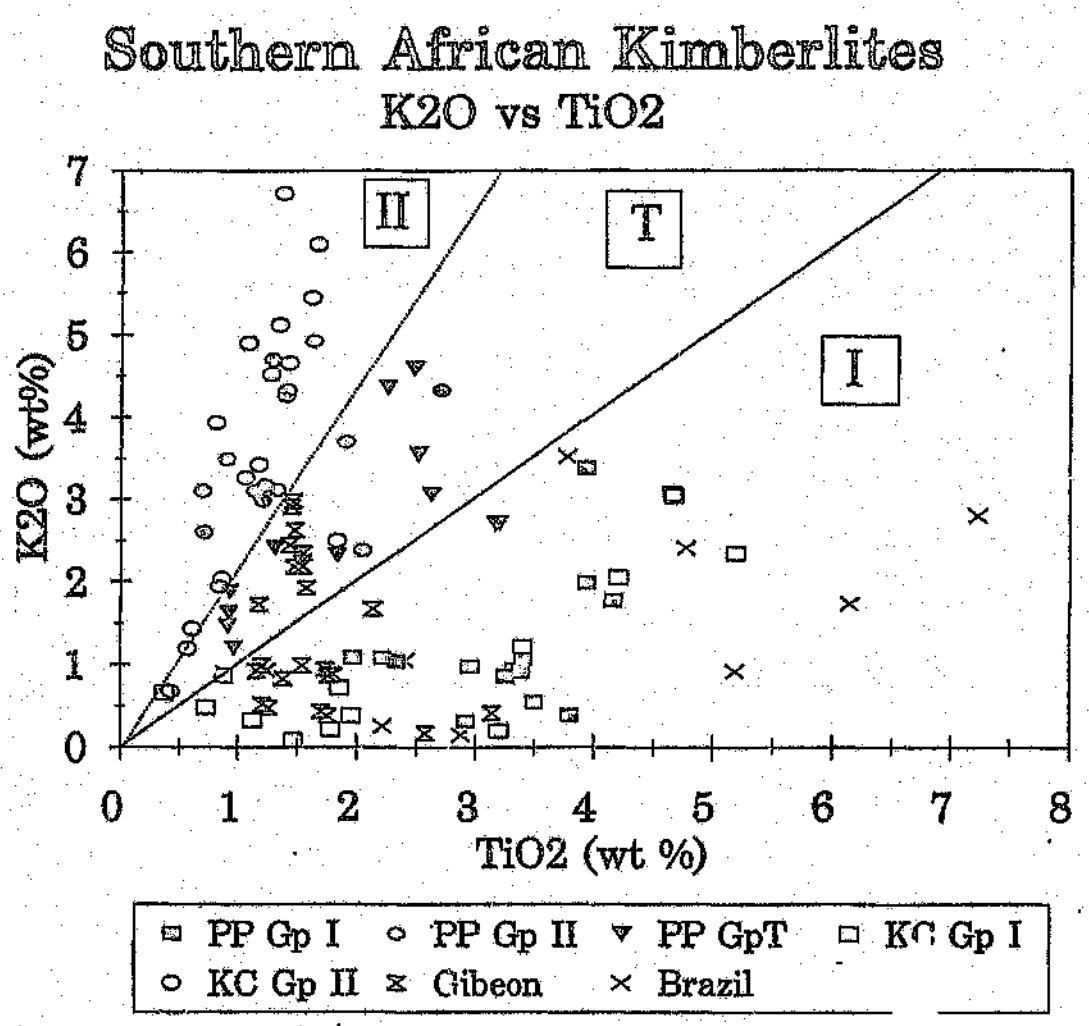

Figure 5.4 : K_2O vs TiO_2

Note that boxed text within the graph are labels for :-

- I = Group I
- II = Group II
- T = transitional kimberlites

Note that some Group II kimberlites plot within the "T" field - these tend to be more altered samples. Some of the Gibeon kimberlites also plot within this field - these are the K2 kimberlite samples.

5.4 Trace Element Geochemistry

5.4.1. Compatible Elements

Compatible elements consist of the first group of transition elements and the siderophile/chalcophile elements. These elements are found within spinel, olivine, perovskite, sulphides and diopside (Mitchell, 1986).

The Prieska Province kimberlites fall within the range for "average kimberlites" given by Mitchell (1986, see his Figure 8). The trends shown by the Prieska Province kimberlites analysed in this study are shown in Table 5.2 below :

Table 5.2 : Compatible Element Trends for the Prieska Province

ELEMENT	TREND
V	M < T < M* < NM
Cr	NM < M* < T < M
Ni	M* < NM < T < M
Co	M* < NM < M < T
Cu	M < M* < NM < T
Zn	M* < T < M < NM

Key to Table 5.2

M = micaceous, NM = non-micaceous, T = transitional

M* = weathered micaceous kimberlite samples

As can be seen from these trends, the transitional kimberlites fall between the values obtained for the non-micaceous and micaceous types for the elements V, Cr and Ni.

There is a strong positive correlation between Ni and Cr, with the Prieska Province kimberlites plotting between Ni/Cr = 0.5 and 1.0. This appears to agree well with the Kimberley group of kimberlites (Figure 7.6, p. 289, Mitchell, 1986 Micaceous and non-micaceous kimberlites plot as separate fields, with non-micaceous kimberlites displaying higher Ni/Cr ratios than the micaceous types. The transitional kimberlites fall between these trends.

5.4.2. Incompatible Elements

Incompatible elements are those elements with solid/liquid distribution coefficients of approximately zero. They are removed from the liquid only during the late stages of groundmass crystallisation and their inter-element relationships generally remain unaffected by alteration and crustal contamination (Mitchell, 1986). This is not true, however, for Rb, U and La which can be very susceptible to alteration effects. Whole-rock trace element analyses therefore provide valuable information regarding the source area characteristics of the magma from which they were derived.

Figure 5.5 shows a plot of the incompatible elements (normalised against primitive mantle) for both the Prieska Province kimberlites and the Kaapvaal Craton kimberlites. Micaceous and non-micaceous types show similar patterns, but differ in their elemental abundances. Transitional types, for many of the elements, plot between these two trends. The widest separation occurs for the most incompatible

elements (Ba, K, Nb, La, Ce and Nd). Distinct troughs occur with the elements K and Sr. The incompatible element patterns for the Prieska Province kimberlites mimic those of the cratonic kimberlites.

The different petrographic kimberlites from the Prieska Province show similar Ba/Sr ratios (around 1) to the reported values for South African kimberlites. The Group I kimberlites tend to have lower Ba than either the transitional or Group II types. No trends are discernable between Ba and Rb. Nb and Ta contents are controlled essentially by perovskite, but enrichment of these elements could also be due to the presence of large amounts of macrocrystal ilmenite (Mitchell, 1986). Micaceous kimberlites contain lower abundances of Nb and Ta than the other kimberlite groups, but Nb/Ta ratios are different for the various groups. Non-micaceous kimberlites generally show the lowest Nb/Ta ratio (13.4) with transitional types intermediate (Nb/Ta=14.6) and micaceous varieties with the highest Nb/Ta ratio (17.9).

Figure 5.6 shows the chondrite normalised rare-earth element plot for the averages of the Prieska Province and Kaapvaal Craton kimberlites. It can be seen that all the kimberlite samples are typically LREE enriched. Micaceous and non-micaceous types are widely separated for the cratonic types but very similar trends are apparent for the Prieska Province rocks. The transitional types show closer affinity with the micaceous types with respect to the LREE, but plot closer to the non-micaceous trend for the HREE. No Eu-anomaly is present. The trends in all cases follow the same pattern. Rare-earth elements are therefore not of use in defining source regions for the different kimberlite types.

There is a positive correlation between Ba/Nb and La/Nb (Figure 5.7). The distinction between Group I and II kimberlite types is very apparent from this diagram. With respect to the transitional

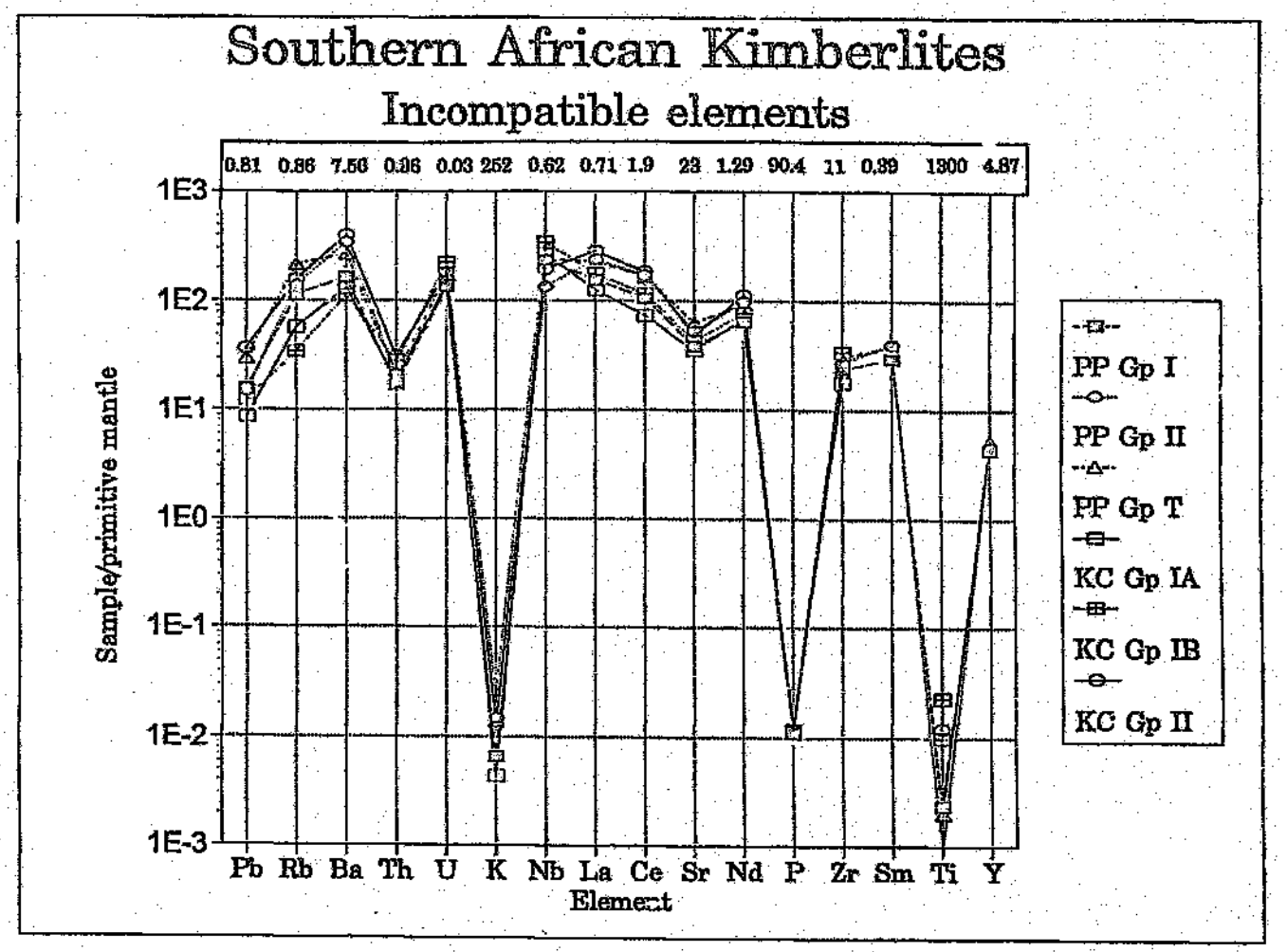

Figure 5.5 : Primitive Mantle Normalised Incompatible Element Plot

Normalising values shown at top of graph in box below title - values are those used by Smith et al. (1985).

kimberlites, two localites are plotted in this diagram - Droogfontein (2 samples) and Sweetput-Soutput (3 samples), in which the sample points for each locality cluster together. It can be seen that the Droogfontein samples plot within the Group I field, whilst the Sweetput-Soutput locality plots in the Group II field. A similar trend is seen in Figure 5.8 which shows Ba/Nb vs Zr/Nb.

There is a positive correlation between La and Nb in Group II kimberlites, and these kimberlites tend to have higher La/Nb ratios relative to the Group I rocks (Figure 5.9). A large amount of scatter is evident for the La/Nb ratio of Group II kimberlites. Positive correlations are evident between Th and Sm as well as Zr and Hf, although no separations into the various kimberlite groupings are evident.

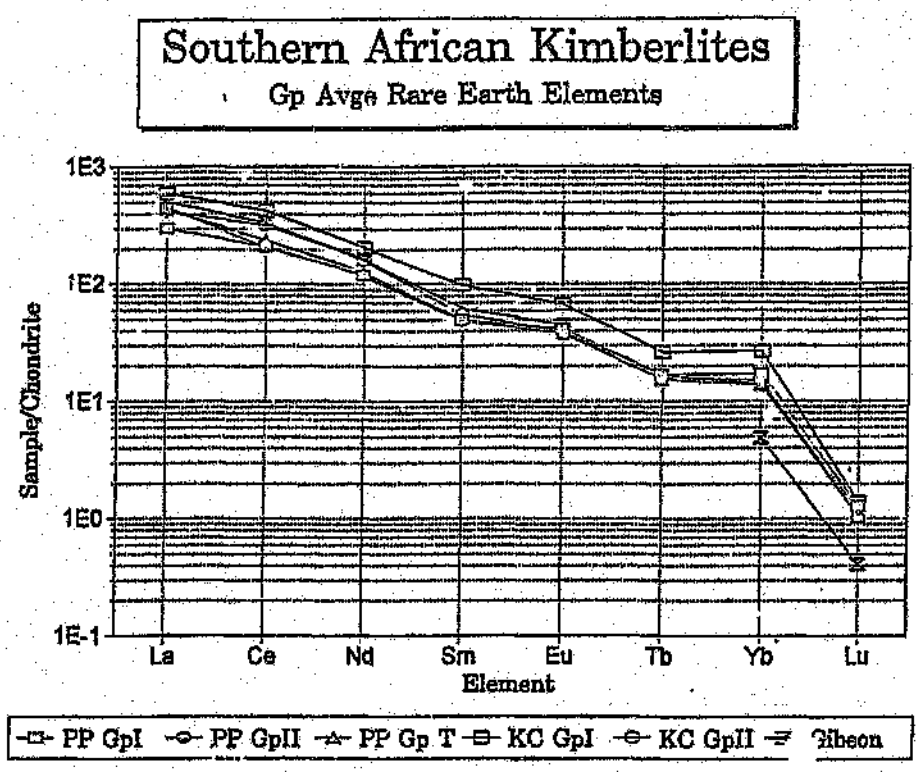

Figure 5.6 : Rare Earth Element Plot

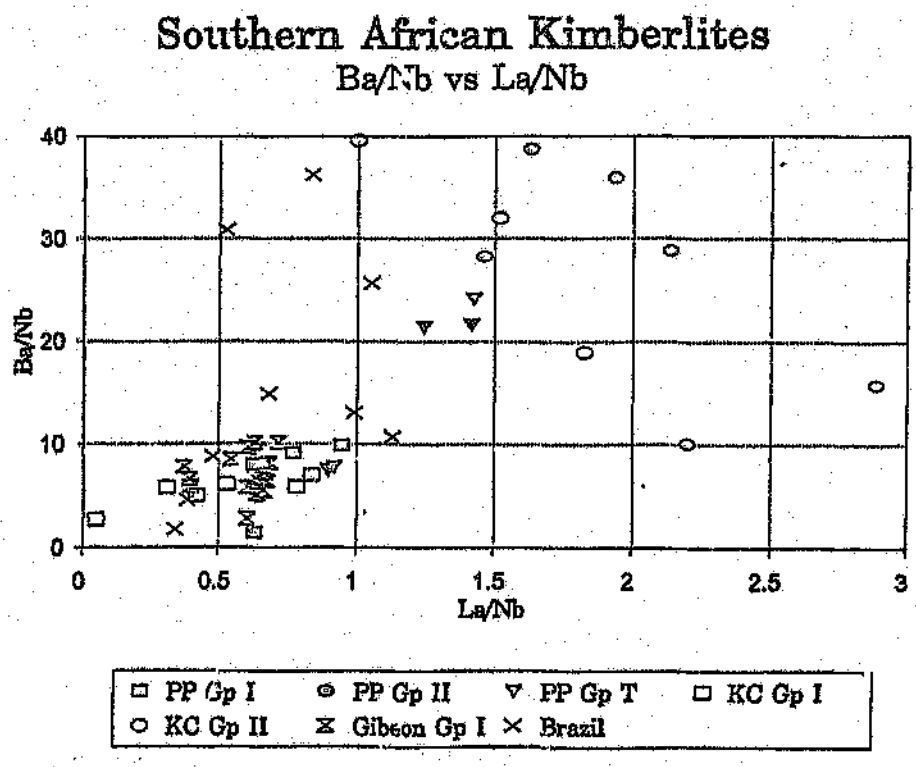

Figure 5.7 : Ba/Nb vs La/Nb

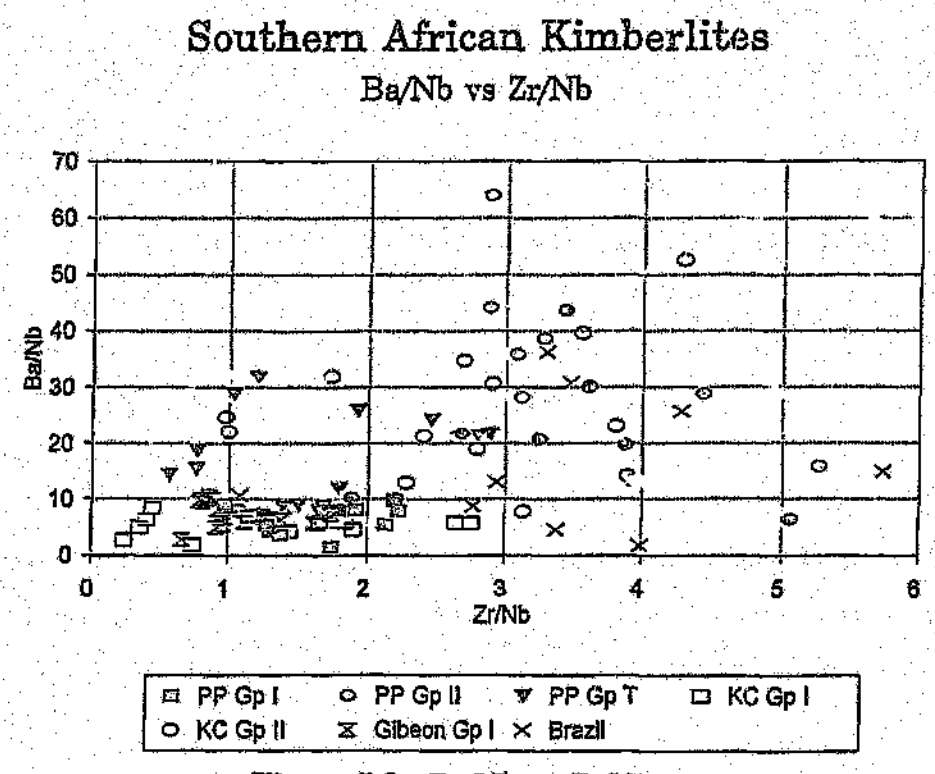

Figure 5.8 : Ba/Nb vs Zr/Nb

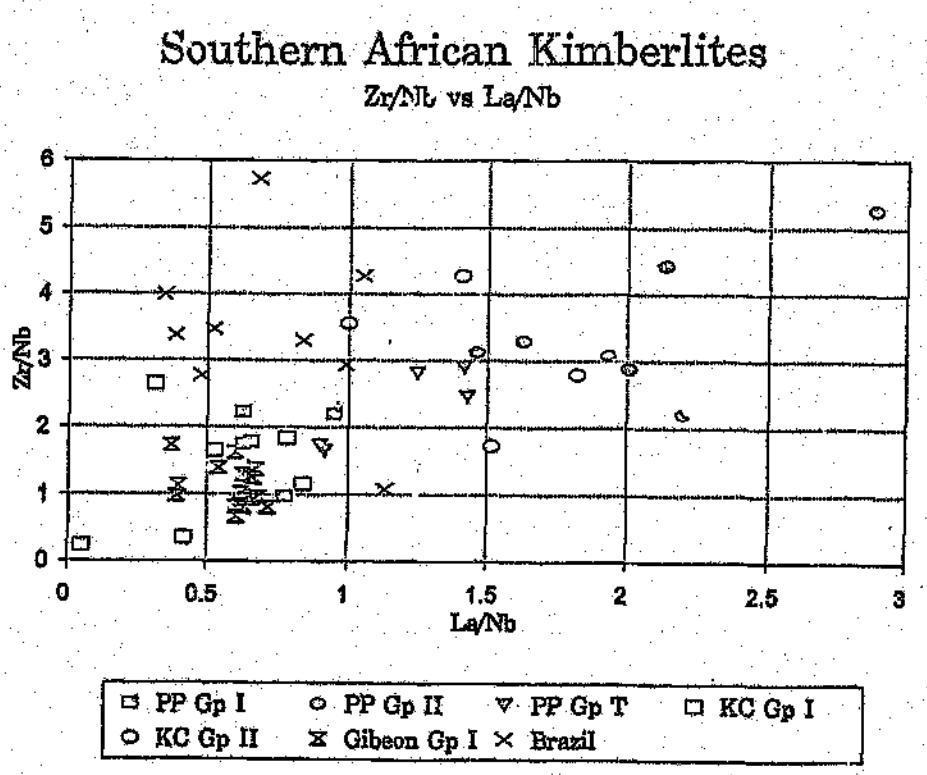

Figure 5.8 : Zr/Nb vs La/Nb

5.5 Discussion

From the results presented in previous chapters as well as above, it can be seen that the isotopic definition of kimberlite correlates well with the petrographic distictions, and also correlates reasonably well to the distinctions in geochemical character. Comparing the averaged data presented by Smith et al. (1985) to that presented in this chapter reveals some differences. Firstly the Group IA kimberlites show much lower SiO_2 than the Prieska Province kimberlites. MgO is lower for Group IA than for the Prieska Province Group I's, but MgO is lower for the Prieska Province Group II's relative to the cratonic Group II's. The Prieska Province Group I's also show far higher K_2O than the cratonic Group I's.

For many of the major elements, the transitional kimberlites also reflect a transitional chemistry, but can also show aspects of one or the other kimberlite type. From the rare earth and incompatible element plots, the similarities of the different kimberlite types in both tectonic settings must reflect similar processes operating in the source regions. The differences in abundances of certain elements (eg Pb, Ba Rb, K_2O and the HREE) is probably due to different source compositions (eg enrichment events) to explain the Group II kimberlites.

5.6 Summary

1. Major element abundances for the Prieska Province kimberlites fall within the ranges previously recorded for southern African kimberlites.

2. Comparisons to cratonic kimberlites show that the Prieska Province kimberlites are broadly similar in terms of major elements. Some differences seen in the Prieska Province relative to their cratonic counterparts include lower abundances of SiO_2 and higher MgO and K_2O in the Group I kimberlites and lower MgO in the Group II kimberlites.

3. Compatible element abundances for the Prieska Province kimberlites fall within the range of average kimberlites as recorded by Mitchell (1986). Relative differences between Group I and II types seen in the Prieska Province data correlate to the differences shown by Smith et al. (1985).

4. Incompatible element patterns for the Prieska Province are broadly similar to those seen for cratonic kimberlites. Relative abundances are significantly different for the elements Rb, Pb, Ba, Nb, La, Ce, Sr, Nd and Sm. The greatest differences appear to be with the Group I kimberlites in the two tectonic regimes, whilst the Group II kimberlites are similar from both areas.

5. There is a definite correlation between geochemistry and isotopes with the petrographic distinctions for non-micaceous (isotopic Group I) and micaceous (isotopic Group II) kimberlites.

6. Transitional kimberlite varieties have not been previously recorded from southern Africa. These transitional kimberlites show a broad geochemical similarity to Group II (micaceous) kimberlites, but are distinctive, particularly with respect to K_2O and TiO_2 contents. This is due to the transitional kimberlites containing minerals common to both Group I and II kimberlite types. However petrographically transitional kimberlites do not

correlate to either Group I or II types and care should be exercised in the terminology of micaceous kimberlites, until geochemical or isotopic determinations have been made.

7. The source regions of the kimberlites in the two tectonic areas appear to be fairly similar based on the geochemical signatures of the kimberlites investigated.

Chapter 6

Geochemistry of Perovskite

6.1 Introduction

During the petrographic examination of the kimberlites from the study area, it was noted that relatively coarse-grained perovskite occurred as an accessory mineral in many of the samples investigated. In some cases this perovskite was present in large quantities, and an attempt was made to liberate sufficient quantities of this mineral using whole-rock dissolution and electromagnetic methods in order to analyse the mineral fractions for U-Pb age determinations. Poor recoveries of perovskite using this technique led to the abandonment of conventional TIMS in favour of age determinations using the SHRIMP ion microprobe (see Smith et al., in press and Chapter 3 (this thesis) for age data obtained using this technique).

The petrographic examination also revealed that perovskites from different petrographic kimberlite types were noticeably different from one another by virtue of colour and size. This led to the belief that there may be discernible chemical differences (particularly with respect to the rare earth element abundances) between the perovskites from the different kimberlite types. Eight of the localities discussed in previous chapters were therefore selected for the analysis of perovskite based on the freshness, abundance and colour of the perovskite. The electron microprobe was selected as the tool with which to analyse the samples (see Appendix B5 for analytical details) and major elements, some minor elements and the LREE were determined. The objectives for analysing these minerals were to compare the REE patterns of the

whole-rock and the perovskite contents and discuss the control this mineral has on the whole-rock composition. Comments on the accuracy of the electron microprobe technique are made.

6.2 Kimberlitic Perovskite

Perovskite ($CaTiO_3$) is a ubiquitous accessory phase in kimberlite and is a major carrier of the rare earth elements (REE), Sr, Nb, U and Pb (Mitchell, 1986; Mitchell et al., 1988; Boctor and Boyd, 1978; Jones and Wyllie, 1984; Heaman, 1989; Smith et al., 1989). Jones and Wyllie (1984) and Mitchell et al. (1988) have suggested that perovskite compositions and abundances are the principal control of REE distributions found in the kimberlite whole-rock.

In general, kimberlitic perovskite is present in trace quantities, but may be present in modal abundances of up to 10 weight percent and rarely up to 25 weight percent, such as in the case of the Benfontein sill (Mitchell, 1986). It commonly occurs as discrete, euhedral to subhedral crystals up to 0.2mm in diameter, scattered throughout the groundmass but may also be concentrated with spinel. It may also be seen as a simple mantle around ilmenite or may be involved in a complex mantling around other opaque mineral assemblages (Mitchell, 1986). Colours range from yellow-brown to reddish-brown. Perovskite crystallises after olivines and spinels but prior to monticellite, phlogopite, serpentine and calcite (Mitchell, 1986).

Previous analyses of the REE contents of this mineral have mostly been performed utilising the electron microprobe (Boctor and Boyd, 1978, 1980 ; Wyllie and Jones, 1984). However, there has been some

discussion regarding the accuracy of the data obtained utilising this technique (Mitchell et al., 1988) as the technique suffers from high detection limits (± 200 ppm - Reed, 1986; 65-200 ppm - Jones and Wyllie, 1984). The determination of heavy REE in particular suffers from this problem due to their low concentrations in perovskite. One of the main criticisms appears to be that data of Boctor and Boyd (1979, 1980, 1981, 1982) do not plot as smooth curves when plotted on a chondrite-normalised diagram, which Mitchell (1988) believes is an indication of poor data. Mitchell et al. (1988), analysed perovskite from kimberlites and alnoites using the ion microprobe and were able to detect ten of the REE at the ppm level. These authors concluded that the data obtained using this technique are far superior to that obtained by the electron microprobe at the levels of REE found in the perovskites studied. Data plotted as smooth curves on the chondrite-normalised diagram.

Perovskite, due to its high concentration of U and Pb has also been used in attempts to provide age data for kimberlites (Allsopp and Kramers, 1977; Smith, 1983; Kramers and Smith, 1983; Heaman, 1988). However, numerous difficulties arise due to the extremely small size of these minerals and hence the difficulties in separating sufficient quantities for isotopic use. Furthermore, this mineral is resistant to chemical dissolution which poses problems with the chemical method employed to obtain the elements of interest. As stated above, attempts were made to separate perovskite from the Prieska Province kimberlites for isotopic analysis, but the poor yields were probably a function of the technique used to recover the perovskite.

Heaman (1988) was able to separate perovskite from finely ground whole-rock using magnetic separation and hand picking methods. This produced a fairly pure perovskite mineral fraction, from which isotopic

data were obtained. This mechanical method of mineral separation was not attempted due to time constraints imposed on this research.

6.3 The Prieska Province Perovskites

Perovskite is common in many of the localities under investigation. Typically, they are found as discrete euhedral (cubic) grains varying in size from 0.04mm to 0.16mm. In general, perovskites from non-micaceous kimberlites are larger in size than those occurring in micaceous varieties. Colours vary from light yellow-brown to reddish-brown to chocolate-brown. Perovskites from micaceous kimberlites are usually yellowish in colour, whereas non-micaceous kimberlitic perovskite shows dominantly brown varieties. Transitional kimberlitic perovskites are distinctly yellow in colour. In many cases, the perovskites are seen mantling opaque phases (magnetite), or occasionally occur as cores within such opaque phases. Perovskite is zoned in some cases with cores being lighter in colour than edges. Alteration is not evident, although some grains have small inclusions (see Plates 6.1, and 6.2).

A summary of the data obtained are given in Table 6.1 and all analytical data are presented in Appendix C4. The data reveal that the abundance of the LREE (La, Ce, Pr, Nd, Sm) varies from 2.07 to 9.28 weight percent, with the Group II kimberlite perovskites showing, on average, the greatest amount of LREE (8.57 weight percent), with Group I kimberlites containing 4.11 weight percent and the transitional types with the least amount of LREE (3.58 weight percent). There is no

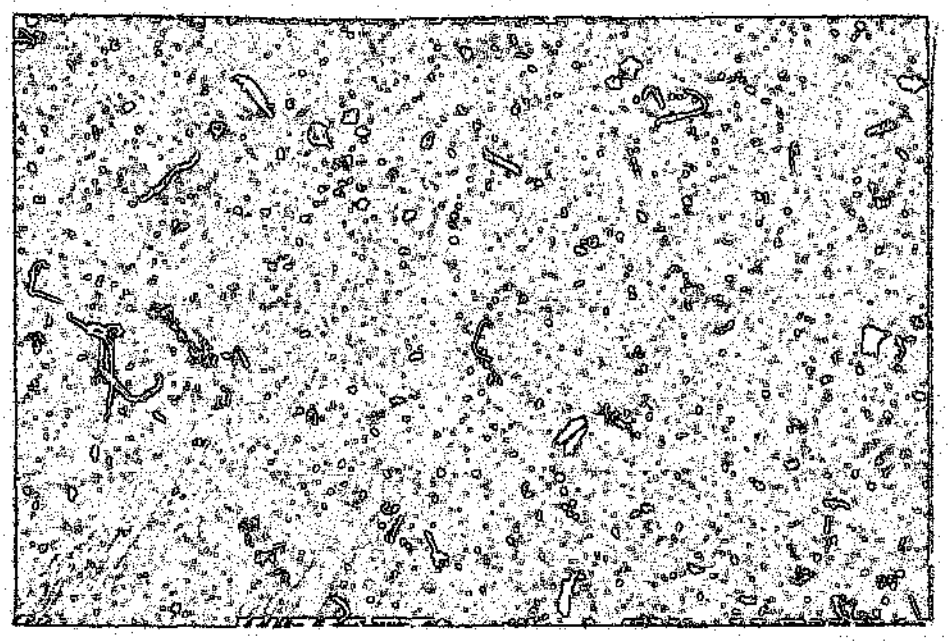

Plate 6.1 : Perovskite in Transitional Kimberlite Sweetput-Soutput
PPL , FOV = 0.4 mm *Note the large size and distinctive colour*

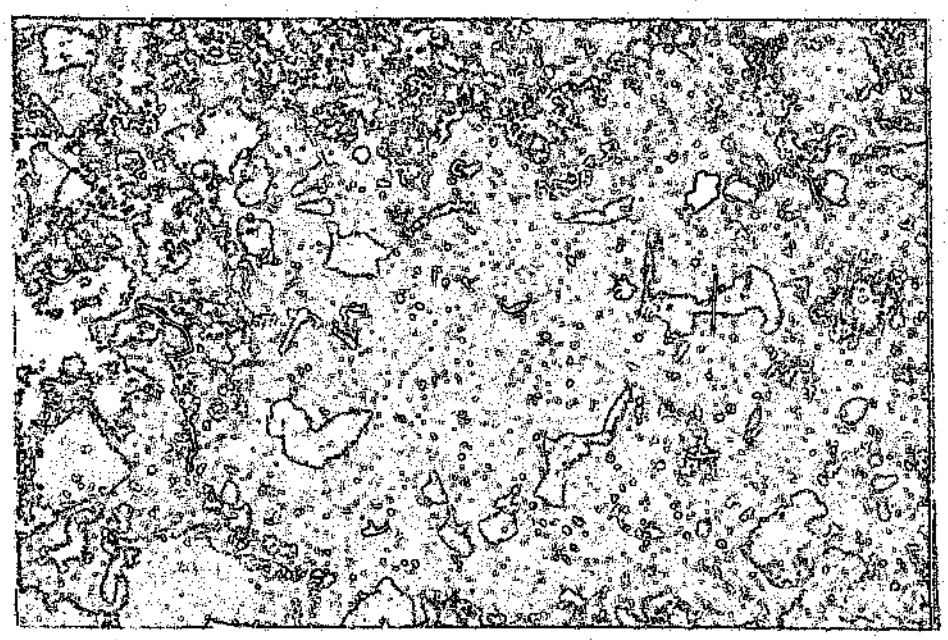

Plate 6.2 : Perovskite in Non-Micaceous Kimberlite Haartebeesfontein
PPL , FOV = 0.4 mm *Note intimate association to opaque oxide, different colour, size and shape*

appreciable difference in abundances of any elements analysed from the cores or edges of the grains analysed, in spite of the fact that some of the crystals are seen to be optically zoned. TiO_2 and CaO concentrations for the Prieska Province perovskites are typical for kimberlitic perovskite compositions previously recorded.

Jones and Wyllie (1984) point out that perovskite differs from the ideal composition of $CaTiO_3$ by addition of minor amounts of many elements with different charges (such as K, Na, Ba, Sr, REE, Sr, Si and Nb). FeO is present in small quantities (1.3 to 2.3 weight percent). The LREE are concentrated in preference to the HREE in perovskite (Jones and Wyllie, 1984) and the LREE probably replace Ca in the perovskite lattice (Boynton, 1975). From Table 6.1, the Group II perovskites (which contain the greatest abundance of LREE) also contain less CaO compared to Group I types, whilst the transitional varieties contain the least amount of LREE and the greatest abundance of CaO, indicating that the LREE substitute for Ca as Boynton (1975) pointed out.

There is a significant difference in the concentrations of Cr_2O_3 in perovskite from the different kimberlite types. Group I kimberlitic perovskites are extremely poor in this oxide relative to the Group II types (0.03 and 0.57 weight percent respectively), with the transitional types containing only slightly less than the Group II types (0.48 weight percent). MnO was only detected in Group I types. Similar amounts of ZrO_2 (0.08 to 0.25 weight percent), SrO (0.17 to 0.58 weight percent) and Nb_2O_5 (0.41 to 1.05 weight percent) were found to those reported by Jones and Wyllie (1984). It is clear that the Group II types have greater abundances than the Group I types. Ce is in all cases the most abundant REE oxide, and Sm the least abundant, which may reflect the greater abundance of LREE relative to the HREE.

Table 6.1 : PEROVSKITE MICROPROBE ANALYSES

Averages for each locality and group

	GROUP I PEROVSKITES				GROUP II PEROVSKITES					TRANSITIONAL		
	1	2	3	GP AV	4	5	6	6	GP AV	7	8	GP AVE.
SiO2	0.000	0.029	1.158	0.396	0.394	0.040	0.070	0.018	0.131	0.073	0.000	0.037
TiO2	54.923	53.138	49.891	52.651	51.351	49.542	49.724	49.800	50.104	53.579	54.423	54.601
Al2O3	0.244	0.153	0.265	0.221	0.232	0.112	0.171	0.166	0.168	0.200	0.186	0.193
Cr2O3	0.042	0.010	0.040	0.031	0.844	0.424	0.540	0.491	0.575	0.415	0.513	0.464
FeO	0.965	1.200	1.578	1.248	2.112	2.319	2.281	2.153	2.217	1.431	1.273	1.352
MnO	0.032	0.000	0.037	0.023	0.000	0.000	0.000	0.000	0.000	0.000	0.003	0.002
MgO	0.046	0.027	1.558	0.544	0.299	0.057	0.100	0.056	0.128	0.049	0.013	0.031
CaO	39.567	35.583	36.056	37.072	35.353	33.238	34.117	33.952	34.165	37.621	39.410	38.516
Na2O	0.364	0.994	0.590	0.649	0.556	0.881	0.724	0.713	0.714	0.392	0.250	0.321
K2O	0.020	0.010	0.024	0.018	0.154	0.044	0.052	0.048	0.075	0.086	0.021	0.054
SrO	0.122	0.221	0.170	0.171	0.817	0.529	0.457	0.442	0.561	0.550	0.456	0.503
ZrO2	0.129	0.065	0.239	0.144	0.102	0.300	0.277	0.329	0.250	0.095	0.085	0.090
Nb2O5	0.500	1.174	1.313	0.996	0.539	1.318	1.228	1.113	1.050	0.479	0.349	0.414
La2O3	0.879	0.965	0.828	0.724	1.476	1.736	1.655	1.622	1.622	0.920	0.729	0.825
Ce2O3	1.044	2.989	2.345	2.126	3.612	5.034	4.858	4.789	4.573	2.048	1.650	1.849
Pr2O3	0.189	0.378	0.268	0.262	0.395	0.565	0.570	0.580	0.528	0.223	0.236	0.230
Nd2O3	0.450	1.341	0.965	0.885	1.210	1.778	1.866	1.915	1.692	0.697	0.591	0.644
Sm2O3	0.057	0.176	0.101	0.111	0.190	0.163	0.175	0.174	0.153	0.041	0.029	0.035
Th2O	0.[illegible]1	0.403	0.180	0.262	0.271	1.019	0.970	0.872	0.783	0.194	0.113	0.154
TOT REE	2.07	5.35	4.41	4.11	6.79	9.28	9.12	9.08	8.57	3.93	3.24	3.58
TOTAL	99.22	98.87	97.51	98.53	99.79	99.10	99.84	99.22	99.49	99.09	100.31	99.70

Recalculation to elemental abundances

Si	0.000	0.021	0.839	0.285	0.277	0.028	0.049	0.013	0.091	0.052	0.000	0.026
Ti	50.696	48.629	46.372	48.576	46.245	44.482	44.347	44.727	44.947	49.152	49.442	49.298
Al	0.199	0.124	0.217	0.180	0.176	0.089	0.135	0.132	0.133	0.162	0.149	0.156
Cr	0.044	0.010	0.042	0.032	0.867	0.434	0.550	0.503	0.588	0.434	0.532	0.483
Fe	1.155	1.424	1.902	1.492	2.467	2.700	2.638	2.507	2.578	1.702	1.499	1.600
Mn	0.038	0.000	0.044	0.027	0.000	0.000	0.000	0.000	0.000	0.000	0.004	0.002
Mg	0.043	0.025	1.457	0.505	0.271	0.051	0.090	0.051	0.115	0.045	0.012	0.028
Ca	43.539	38.831	39.952	40.775	37.958	35.578	36.274	36.353	36.538	41.144	42.683	41.917
Na	0.416	1.126	0.679	0.741	0.597	0.379	0.799	0.792	0.792	0.445	0.281	0.363
K	0.026	0.013	0.031	0.023	0.192	0.055	0.064	0.060	0.093	0.109	0.026	0.068
Sr	0.159	0.285	0.223	0.223	1.038	0.670	0.575	0.560	0.710	0.712	0.584	0.648
Zr	0.147	0.073	0.274	0.164	0.113	0.333	0.305	0.354	0.276	0.108	0.073	0.090
Nb	0.538	1.253	1.423	1.071	0.566	1.380	1.277	1.166	1.098	0.512	0.370	0.441
La	0.428	1.256	1.095	0.950	1.891	2.217	2.099	2.072	2.070	1.200	0.942	1.071
Ce	1.372	3.895	3.104	2.793	4.632	6.437	6.170	6.125	5.842	2.676	2.135	2.404
Pr	0.183	0.493	0.355	0.344	0.507	0.723	0.725	0.742	0.674	0.292	0.306	0.299
Nd	0.594	1.755	1.150	1.168	1.558	2.283	2.380	2.460	2.171	0.914	0.768	0.841
Sm	0.076	0.232	0.135	0.148	0.130	0.211	0.225	0.225	0.197	0.054	0.038	0.046
Th	0.272	0.545	0.245	0.355	0.358	1.341	1.268	1.148	1.030	0.261	0.150	0.205
TOT REE	2.72	7.63	5.84	5.40	8.72	11.87	11.60	11.62	10.96	5.14	4.19	4.66
TOTAL	99.99	99.99	99.54	99.85	99.84	99.99	99.97	99.99	99.94	99.98	99.99	99.98

KEY:

1 : Haartebeesfontein
2 : Vioolkraal
3 : Witberg Pipe
4 : Brandewynskuil
5 : Jonkerwater
6 : Markt
7 : Droogfontein
8 : Sweetput-Soutput

Figure 6.1 shows the chondrite-normalised plot for the REE in perovskite (average REE content of perovskite in each kimberlite type). Note that the data define smooth curves, with convex-up trends. It is very clear from this graph that the Group II kimberlitic perovskites have much greater abundances of the REE's than the Group I perovskites. A positive Ce anomaly is present in both Group I and II types of perovskite, with Ce > La in both types, whilst for the transitional types La > Ce.

Figure 6.2 shows the REE plot (chondrite-normalised) for both the whole-rocks and perovskites. The whole-rock data was obtained using INAA (see Chapter 5). Note that the two trends are broadly similar, except for the trend between Nd and Sm, which for the whole-rock is not as steep as for the perovskite. In addition, for the whole-rocks, La > Ce, which is opposite to that for the perovskites. Note that in the whole-rock trend, the transitional kimberlites are more akin to the Group II kimberlites in the range La-Sm. For the perovskites, this trend is reversed. The REE patterns for the whole-rock changes from Sm-Lu, such that the transitional varieties show a pattern similar to the Group I whole-rock trend.

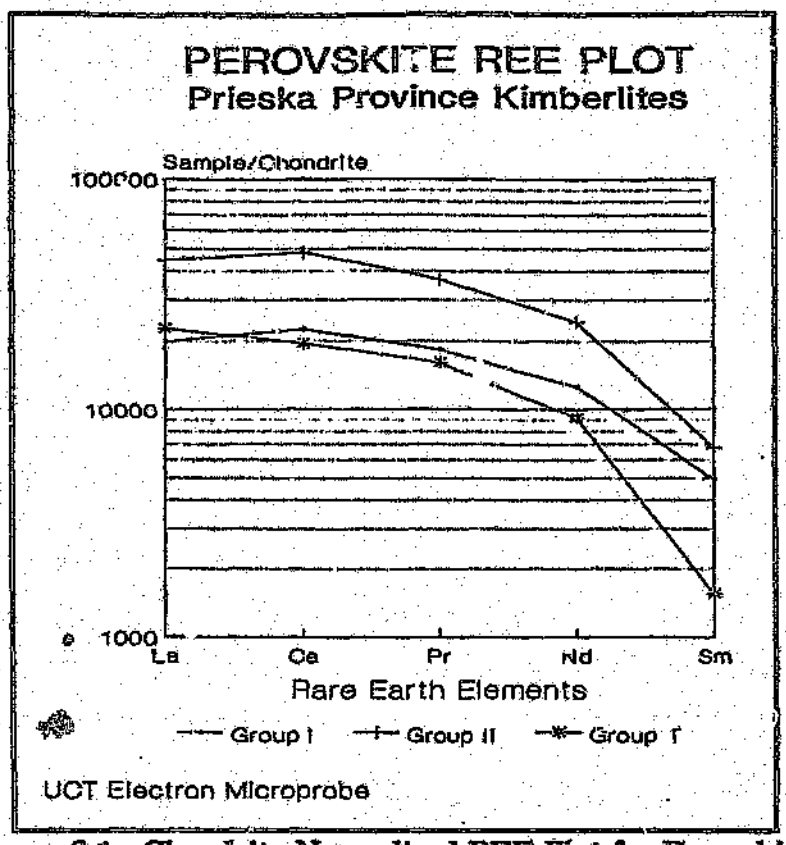

Figure 6.1 : Chondrite Normalised REE Plot for Perovskite

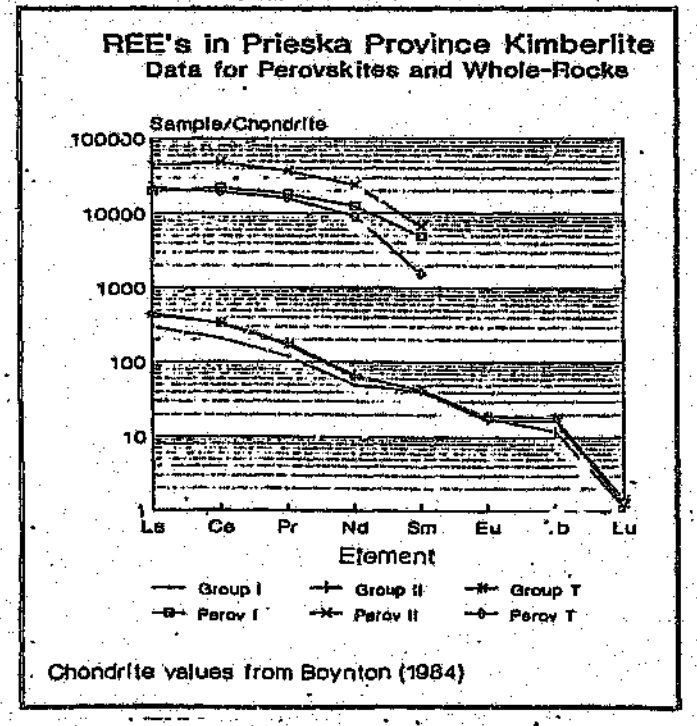

Figure 6.2 : Perovskite and Whole-Rock REE Plots

6.4 Discussion

Jones and Wyllie (1984) report that there is an expected correlation between perovskite and whole-rock REE patterns. This study confirms this and it can be concluded that perovskite is the dominant control on the REE patterns observed in kimberlite. Other phases that may also influence the REE pattern include clinopyroxene and apatite, but it is not believed that these minerals are as significant as perovskite. However, Mitchell et al. (1988) show that the higher La/Yb ratios of perovskite relative to those of the whole-rock kimberlite implies that other factors than perovskite have a bearing on the REE patterns of the kimberlite whole-rock composition. Such factors would have to increase the amounts of the HREE in order to reduce the La/Yb ratios of the whole-rocks.

One possibility discussed by Mitchell et al. (1988) that might be responsible for the elevated La/Yb ratios in kimberlite whole-rocks is crustal contamination. The Premier kimberlite is one example cited by these authors where crustal contamination can be invoked to explain this. In the case of the Prieska Province kimberlites, crustal contamination is not considered to be significant (see Chapter 5) and cannot be invoked to explain this trend.

The data acquired using the electron microprobe are considered to be accurate as shown by the smooth rare earth element plots of the data. However, the electron microprobe is not suitable for the determination of the HREE due to the extremely low concentrations of the HREE in perovskite. The advent of the SHRIMP ion microprobe makes it possible to acquire emplacement age determinations from perovskite, which implies that laborious and time consuming mineral separations

which implies that laborious and time consuming mineral separations are avoided. However, perovskite in the Prieska Province kimberlites is characterised by high contents of common lead, which can lead to high errors on the age result obtained (Smith et al., in press).

6.5 Summary

1. Perovskite occurs as a common accessory mineral in many of the kimberlites from the Prieska Province.

2. There are discernable differences in the appearance of perovskite from Group I, II and transitional kimberlites in terms of size. Group I perovskites tend to be larger than those of Group II kimberlites, but the transitional kimberlite perovskites are far larger than those of Group II types and in some cases are larger than Group I types.

3. Colour differences are marked between non-micaceous kimberlites (creamy brown) and micaceous kimberlites (yellow).

4. Perovskites were successfully analysed for their major, some minor and rare earth element abundances using the electron microprobe. The data aquired are considered to be reliable and the REE data plot as smooth (convex up) curves.

5. There are discernible differences in the geochemistry of the perovskites from different kimberlite types, corroborating the first order observations noted in 2 and 3 above.

the whole-rock kimberlite. The rare earth element signature of perovskite and kimberlite whole-rockss indicate derivation of kimberlite from a LREE enriched source region.

Chapter 7

Discussion

7.1. The Prieska Region as a Province

This investigation has shown that both Group I and II isotopic varieties (as previously defined by Smith (1983b)) of kimberlite are present in the study area. In addition, a variety of kimberlites transitional to the known isotopic kimberlite types are present, which can be defined petrographically, isotopically and geochemically. This is the first recorded occurrence of such transitional kimberlites from southern Africa.

Although the database for the transitional variety of kimberlite defined here is small, it is considered that the results are not due to fortuitous sampling or alteration effects. Important preliminary conclusions can be made regarding the source regions of the transitional kimberlites analysed thus far. Further studies on any other transitional occurrences will enable a more definitive characterisation of their source areas to be made.

The kimberlites occurring in the area are collectively referred to as the Prieska Province kimberlites in this research. The term Province is justified, as according to the definitions given by Mitchell (1986), a kimberlite province consists of one or more kimberlite fields. Kimberlite fields comprise geographically and genetically related groups (clusters) of kimberlites with similar ages. Previously, Mitchell (1986) referred to the kimberlites of this area as the Central Cape Field which, based on

available information at the time, were believed to have been emplaced at 70 Ma. Clearly, as demonstrated in this work, a complex emplacement age history (Chapter 3 and below) is apparent. Inspection of the attached plan shows that there are numerous groupings of kimberlite occurrences within the study area. A similar map presented by Skinner et al. (1991) shows these groupings in relation to "tectonic domains" and it is seen that the groupings of kimberlite within different domains are comprised of similar petrographic varieties, which are likely to constitute "fields" as per Mitchell's definition.

7.2. Prieska Province Kimberlite Age Distribution

7.2.1. Reliability of Emplacement Age Determinations

Smith et al. (in press) note that it is important to make estimates of the reliability of emplacement age data when considering the detailed chronological events of an area. For this purpose, four criteria are used, namely:

1. data quality (sample freshness, contaminants, analytical precision);
2. model ages should agree with isochron ages;
3. similar ages shown by more than one kimberlite; and
4. equivalent results for one locality by different techniques.

The first two criteria are critical to the interpretation, as these indicate that no analytical bias is present in the results. Criterion 3 is highly dependant on the information available at the time. Therefore, if a new age is obtained that is not represented elsewhere (eg. 108 Ma age of Witberg), then the age is considered valid, providing the first two

criteria are fulfilled. Criterion 4 is difficult to assess in cases where there is no agreement between techniques. For kimberlites, the U-Pb dating technique appears to be subject to greater uncertainty than the Rb-Sr whole-rock/phlogopite system, and unless the U-Pb technique is the only one available, then it is considered that ages obtained with this technique should be viewed with caution until other analyses become available that corroborate the U-Pb data.

Smith et al., (1985a) discussed the "best age dating method" for kimberlites and considered that the Rb-Sr method on whole-rock and mica analyses was the most reliable method available for determining kimberlite emplacement ages. Data obtained using this method (and fulfilling criterion 1 above) can "stand alone". With respect to the Prieska Province, only the Meltonwold and Skietkop emplacement ages are questionable at this stage. These ages were obtained by the U-Pb method on perovskite and some uncertainty is apparent from the data due to high common lead contents. However, where the Rb-Sr age dating technique cannot be used due to the lack of phlogopite, data obtained using other techniques are still valuable, but fulfillment of all the criteria presented above should be taken into account in assessing the reliability of the age information obtained.

7.2.2. Kimberlite Age Distribution for the Prieska Province

The emplacement ages of the Prieska Province kimberlites generally overlap with those for kimberlites situated on the Kaapvaal Craton, and a more complex emplacement age distribution for southern Africa is clear from the addition of these results to the known database at this time (Smith et al., in press and table 7.1 below).

Table 7.1 : Summary of Emplacement Ages for the Prieska Province

LOCALITY	AGE (Ma)	INITIAL-Sr
Britstown	74 ± 1	0.7040 ± 1
Haartebeesfontein	74 ± 1	0.7040 ± 2
Pampoenpoort	103 ± 1	0.7046 ± 1
Witberg Pipe	108 ± 1	0.7050 ± 2
Lushof	68 - 78	Zircon U-Pb
Uintjiesberg	101 ± 1	0.7043 ± 2
Eendekuil	±110	Model Age
Kaakput	114 - 117	Zircon U-Pb
Jonkerwater	116 ± 1	0.7093 ± 2
Markt	117 ± 1	0.7085 ± 2
Middelwater 01	118 ± 1	0.7082 ± 2
Sanddrift	125 ± 3	0.7074 ± 26
Welgevonden	116 ± 0.2	0.7088 ± 4
Witberg East (dyke)	118 ± 1	0.7085 ± 2
Droogfontein	174 ± 2	0.7063 ± 1
Meltonwold	143 ± 14	Perov U-Pb
Skietkop	140 ± 10	Perov U-Pb
Sweetput-Soutput	116 ± 1	0.7065 ± 2

As noted in chapter 3 and in Table 7.1 above (taken from Chapter 3), the main Group I kimberlite event of 86 Ma is apparently absent in the Prieska Province, whilst the 108 Ma event seen in the Prieska Province does not appear to be represented on the Kaapvaal Craton. The kimberlite emplacement age data obtained to date show that the Prieska Province Group I kimberlites are younger than the Group II kimberlites in keeping with the results of Smith (1983a,b) and Smith et al. (1985a). This division of Group I and II kimberlites by virtue of age shows that Group I kimberlites are younger than 116 Ma whereas Group II kimberlites are older than 114 Ma. An important conclusion of the restriction in time and space of the Group II kimberlites is that the source area of kimberlites must have changed over time. Only Group I kimberlites have been emplaced on a worldwide basis over a protracted

period of time, whereas Group II kimberlites are restricted to the interval of ± 210 to ± 110 Ma within South Africa.

No transitional kimberlite types were investigated in the earlier studies of Smith (1983a,b) and Smith et al. (1985). Whilst the transitional kimberlites show isotopic and geochemical characteristics that fall essentially between the previously defined Group I and II fields (with some overlap - see Chapters 4, 5 and section 7.3.2 below), ages obtained for three of the transitional kimberlites are older than the Group II kimberlites. Only one transitional kimberlite shows an age defined by Group II kimberlites.

The age data show that Group I kimberlites from the Prieska Province were emplaced at between 74 and 108 Ma in two events - one at 74 Ma and the other between 100-108 Ma. Group II kimberlites were emplaced between about 110 and 125 Ma, in three possible periods (110, 115-117 and 125 Ma). Note however that the 110 Ma age of Eendekuil is a model age and the age of 125 Ma for Sanddrift could be too high if xenolithic mica was incorporated into the sample (Smith et al., in press).

In addition, a third "variety" of kimberlite can be recognised in the study area, both petrographically, isotopically (see Chapter 4) and geochemically (Chapter 5). Whilst this variety has been called the "transitional" type of kimberlite in terms of the above criteria, the ages obtained for these samples are far older than either Group I or Group II kimberlites from the study area. All of these transitional localities have been very difficult to date and are characterised by very fine grained groundmass mica, often poikilitic in nature, from which it is difficult to obtain clean separates. Smith et al. (1985a), describes the Klipfontein kimberlite (a phlogopite-diopside kimberlite), situated near Barkly West, as another kimberlite where difficulty was experienced in

obtaining pure mica separates. In addition, the occurrence gives a fairly high age (159 ± 40 Ma) and initial-Sr of 0,7077 ± 4. Feldspathoid (nepheline) is also present (of uncertain origin) in the groundmass, although analysis of this mineral shows that it is not in isotopic equilibrium with the kimberlite. The presence of feldspathoid is evident from other kimberlites near Barkly West (Tainton and Browning, 1991) and although not directly comparable to the transitional variety of kimberlite described here, is interesting because for the Sover "kimberlite", the $^{87}Sr/^{86}Sr$ ratio of 0.7071-0.7076 (present day) is similar to those for the transitional kimberlites described here.

The dominant 86 Ma "Kimberley" Group I emplacement event is not represented in the Prieska Province, based on the information available to date. Confirmation is required for the U-Pb perovskite age of 82 Ma for Beyersfontein (R Pidgeon, unpubl. data) which occurs in the Prieska Province (Smith et al., in press). The Prieska Province Group I kimberlites were emplaced at 74 and 102 Ma. The 102 Ma event is not represented by Group I kimberlites on the Kaapvaal Craton.

The emplacement events for the Prieska Province Group II kimberlites occur at about 110Ma (Eendekuil - model age), 116 Ma (Jonkerwater, Middelwater 01 and Markt), and about 125 Ma (Sanddrift). On the Kaapvaal Craton, the dominant Group II event occurs between 114-134 Ma, with discernable peaks at 118 Ma (the dominant event) and a lesser defined peak at 126 Ma. Group II kimberlites from the Prieska Province are therefore contemporaneous with events recorded for the Kaapvaal Craton.

Skinner (1989), le Roex (1987) and Spriggs (1988) all attempt to relate kimberlite emplacement events to the passage of the continent over hot spots, now situated in the south Atlantic. The complexity of the ages

now established for southern Africa precludes a simple relationship to hot spots. Whilst there appears to be a general younging of ages from the northeast of South Africa from the Dokolwayo kimberlite (200 Ma) to Eendekuil (approximately 110 Ma) in the extreme southwest and Gibeon (about 70 Ma) in the west of the continent, not all kimberlites can be correlated perfectly with the known hot spot tracks. This has been noted in Smith et al., (in press), who also note that recent work by O'Conner and Duncan (1990) shows that hotspot tracks do not suggest a straightforward tracking of southern Africa over plumes during the early Cretaceous. Smith et al., (in press) further suggest that the 118 Ma event appears to coincide with the beginning of a magnetically quiet period of normal polarity of the Earth's magnetic field as well as the initial stages of the opening up of the South Atlantic.

7.3 Source Rock Isotope and Geochemical Character

7.3.1 Petrographic, Geochemical and Isotopic Aspects

The Prieska Province kimberlites comprise micaceous, non-micaceous, and transitional petrographic varieties of kimberlite (Chapter 2 and Appendix A). There are no major differences between the Prieska Province kimberlites and their cratonic counterparts in terms of petrography. A distinction is made between the petrographic and isotopic classifications, because the isotopic and geochemical signatures allow for constraints to be made on source regions (Smith 1983a,b ; Smith et al., 1985). Although Smith noted a good correspondence between the petrographic and geochemical/isotopic characteristics for Group I and II kimberlites, it is clear that this is not the case for the transitional varieties of kimberlite. Therefore, it is considered that care

is needed in making assumptions on source regions based on general petrographic character when reporting analytical results of kimberlites it should be noted whether the rock is being defined on petrographic, geochemical or isotopic grounds.

The mineralogical classification scheme for kimberlite would appear to warrant a further revision in light of the data obtained for these transitional varieties of kimberlite. Authors such as Mitchell (1991), Rock (1991) and Dawson (1989) have noted similarities between kimberlites and lamproites (particularly between Group II kimberlites and olivine lamproites) and Rock (1991) believes that kimberlites should be classed as part of the lamprophyre family, It is speculated that the existence of "lamprophyric" kimberlites such as those described by Tainton et al. (1991) could indicate that there is a continuum between some lamproites and Group II kimberlites. Or, as Mitchell (1986) has noted, are these kimberlites a distinct class of diamond-bearing rocks ? However, kimberlites are distinctive in their modes of emplacement (no diatreme facies lamprophyre has yet been described) as well as their mineralogical and geochemical characteristics relative to lamprophyre. Therefore, the incorporation of kimberlites into the lamprophyre clan as suggested by Rock (1991) is probably not valid technically, but rather a practical solution to the problem.

The major and trace element geochemical characteristics of the Prieska Province kimberlite are typical of other kimberlites found in the world (Group I) and South Africa (Group II). Major element compositions reflect the mineralogical characteristics of the kimberlites, with micaceous kimberlites showing elevated K_2O and Al_2O_3 (reflecting phlogopite abundance) relative to non-micaceous varieties. Non-micaceous kimberlites are enriched in CaO (reflecting calcite abundance) and Fe_2O_3 (reflecting the presence of opaque oxides) relative to the

micaceous varieties. There are no major distinctions that can be drawn between the Prieska Province kimberlites and their cratonic counterparts. Smith et al.'s (1985) use of discriminate function analysis enabled Group I kimberlites to be separated into cratonic and off-craton types using a combination of major and trace element data. However, the Monastry kimberlite (cratonic locality) was mis-classified using this method. The necessity of using this statistical tool indicates that the geochemical differences between the two tectonic settings are subtle.

It was seen that the trace element characteristics presented in Chapter 5 can also be used to distinguish the different varieties of kimberlite. The transitional varieties plot close to the micaceous kimberlite fields, indicative of their micaceous nature. However, compared to Brazil transitional kimberlites, the Prieska Province varieties appear to show a greater degree of overlap between established Group I and II fields, whereas the Brazilian kimberlites tend to show greater similarity to non-micaceous varieties. Rare earth and incompatible element patterns for the Prieska Province and Kaapvaal kimberlites show the same trends. Rare earths elements in the Group I cratonic kimberlites show the same trend but are noticeably enriched relative to the Prieska Province Group I kimberlites. The transitional kimberlite trends mirror those for the Group II with respect to the LREE but are more similar to the trends of the Group I types for the HREE. The rare earth element patterns may be indicative of small degrees of partial melting of a garnet-rich source (Ringwood, 1982).

Perovskite from the Prieska Province kimberlites were seen in Chapter 6 to be significantly different in terms of colour, size and chemical composition between the different petrographic groups of kimberlite. In addition, the REE contents show that perovskite is an important accessory phase for the incorporation of REE and incompatible elements.

The perovskites also show high U/Pb ratios and contain high contents of common Pb. The common lead content is one of the reasons that the ages obtained using the U-Pb perovskite method is subject to high errors, as the analysed points plot far from the intercept of the age line on the Terra-Wasserburg line. This problem is not as apparent with perovskites analysed from cratonic localities (Smith, pers. comm.), and could indicate that the lead contents in the two tectonic regimes are different, but the reason for this is not clear at the present time.

Chapter 4 dealt with the Rb-Sr, Sm-Nd and U-Pb isotopic signatures, where it was shown that the Prieska Province kimberlites are broadly similar in isotopic composition to the cratonic kimberlites examined by Smith (1983a,b) and Smith et al. (1985). The research has shown that both Group I and II (isotopic) varieites of kimberlite are present in the study area which can be correlated to the non-micaceous and micaceous varieties of kimberlite respectively. In addition, a number of Prieska Province kimberlites termed transitional on petrographic grounds have been shown to display isotopic signatures different to the defined Group I and II types of kimberlite analysed by Smith (1983a,b) and Smith et al. (1985). These transitional varieties of kimberlite are discussed separately in 7.3.2. below.

Interestingly, the whole-rock Pb isotope compositions of the Prieska province kimberlites relative to their cratonic counterparts contain lower $^{207}Pb/^{204}Pb$ for a given $^{206}Pb/^{204}Pb$ ratio. This could imply that the Pb incorporated into cratonic kimberlites is older than that for the Prieska Province kimberlites (Smith, pers. comm.), but further work on this aspect is required.

There is a correspondance between the isotopically distinct kimberlite types with petrographic and geochemical character for the Prieska

Province kimberlites. This was also recognised for the cratonic kimberlites by Smith et al. (1985). These authors suggested that since the isotopic character was indicative of source character, then the geochemical correspondance must indicate that geochemistry also reflects source composition. The geochemical similarity between kimberlites from the Kaapvaal and Prieska areas is considered to be indicative of similar source component compositions for the kimberlites within the subcontinental mantle for both tectonic environments.

7.3.2. The Transitional Kimberlite Problem

The Prieska Province is not the only area in which transitional varieties of kimberlite are known. Bizzi et al. (1991) has shown that in Brazil, there are kimberlites which, isotopically, are also transitional to the known Group I and II kimberlite types defined by Smith (1983a,b). Petrographically, these kimberlites are similar to non-micaceous varieties. Tainton and Browning (1991) describe another variety of kimberlite at the Sover occurrence near Barkly West in South Africa, where kimberlite sensu stricto and "lamprophyric" kimberlite occur in close proximity to one another. The major and compatible trace element character of the lamprophyric kimberlite would appear to be transitional to Group II and lamproitic signatures. The isotopic signature of these "lamprophyric" kimberlites appears to be similar to the Group II trend. Also near Barkly West, is the Klipfontein kimberlite which was analysed by Smith (1983a,b) and which contains groundmass feldspathoid (see Chapter 3). The Lace kimberlite situated near Kroonstadt in the Orange Free State of South Africa also appears to show transitional character (Smith, 1992 and pers. comm.). The Gibeon kimberlite Province consists of a number of essentially Group I kimberlites (Spriggs, 1988), but the K2 kimberlite body from this area is somewhat

unusual relative to the other kimberlites from the area, due to enrichment in Pb, Rb, Ba, K, Sr, P and isotopic character. This difference is ascribed to assimilation of older PKP type metasomatised lithosphere.

From the above, it is apparent that two "transitional" groups of kimberlite exist. Firstly there are those which are "kimberlitic" and contain minerals commonly found in Group I and II kimberlites, such as the Prieska Province kimberlites and secondly, a "lamprophyric" variety with minerals characteristic of lamproites, such as those described by Tainton and Browning (1991). It is not clear at this stage what relationships may exist between these different transitonal varieites of kimberlite.

The transitional kimberlites from the Prieska Province are almost all confined to the more southerly region (Domain V of Skinner, et al. 1991), with only one body (Sweetput-South) occurring on the craton. None of the bodies appear to be spatially associated with either Group I or Group II kimberlite bodies. Although the present database for these transitional kimberlites is small, the following first order observations can be made:

1. Their petrographic character is dominantly of Group II type, with relatively minor Group I characteristics.
2. The ages and spatial setting of these bodies precludes mixing of Group I with Group II kimberlites along emplacement conduits
3. Their T^{Nd}_{CHUR} ages vary from 271 Ma to 579 Ma, similar to those for the Group II kimberlites (388-887 Ma).
4. Geochemically, they are more akin to Group II kimberlites, in keeping with their petrographic character, but are transitional in many aspects (eg K_2O vs TiO_2).

5. Isotopically (Sr-Nd), they form a distinct, separate field adjacent to the Group II kimberlite field. The kimberlites described by Bizzi et al. (1991) also fall into the compositional gap between Group I and II types using Sr-Nd isotopes, but plot closer to the Group I field relative to the Prieska Province kimberlites.
6. On Pb-Pb plots, the transitional kimberlites overlap those of the Group II Prieska Province trend.

The Sr-Nd isotopic compositions of the transitional varieties appears to be unique in that they do not overlap the field of Group II kimberlites, but the Pb data for the transitionals overlap the field for the Group II field. Whilst it is tempting to infer a separate source area for these transitional kimberlites (as Bizzi et al. (1991) have done for the Brazilian "transitional kimberlites"), it would appear that the similarity in Pb isotopes, trace element geochemistry and petrographic characteristics to the known micaceous (Group II) kimberlites would surely argue for a modification of Group II kimberlite source areas. However, the age relationships of the transitional kimberlites and the fact that there are no Group I or II kimberlites near to these localities is strong evidence that mixing along source conduits is not feasible, but does not preclude source area mixing.

The model Nd ages for both the Group II and transitional rocks imply long residence times in the upper mantle, but those for the Group I kimberlites do not. Thus the enriched signatures of both of these rock types have occurred a long time ago. These enrichments are more commonly ascribed to metasomatic events in the subcontinental mantle beneath southern Africa (Bailey, 1982; Fraser et al., 1985 and others), although melt migration or subduction could also have played a role in the development of the isotopic signatures observed in these rocks.

7.3.3. Ages, Hotspots and Tectonic Processes

7.3.3.1. Southern African Kimberlite Age Distribution

Bailey (1992) notes nine phases of alkaline/kimberlite eruption ages across Africa from the Early Jurassic through to the Eocene. The major phase of activity is in the Cretaceous, with the well established Group I and Group II peaks correlating with other kimberlite events in Brazil, Congo and West Africa (for the Group I's) and the Early Cretaceous alkaline/carbonatite activity (for the Group II's). This, however, would appear to be a simplistic interpretation, certainly for the Kaapvaal Craton alone, as will be demonstrated below. However what exactly constitutes a kimberlite age event? Theoretically, kimberlites are emplaced instantaneously in terms of geological time. Therefore, should an age event be determined by a number of localities displaying the same age or can one kimberlite with a distinctive age (eg Dokolwayo) represent an age event? Much of this problem is obviously due to sampling as there are undoubtably many undiscovered kimberlites and/or undated kimberlites, which could corroborate single age events. In spite of these problems, the following discussion aims to show that a complex age distribution can be recognised, with some events being notably distinct, whilst others are tentative due to the scarcity of data.

Figure 7.1 shows the distribution of seventy four kimberlite and related rock emplacement events for southern Africa between 60 and 210 Ma. Emplacement age data for the Zimbabwe, Botswana and older South African kimberlite age events (e.g. 240 Ma Jwaneng, 1200 Ma Premier and 1600 Ma Kuruman kimberlites) are not shown on the diagram. It should be stressed from the outset that the interpretation of this

diagram is somewhat subjective. Note that the X-axis scale (age) is in increments of 2 Ma, which is considered necessary to compare small scale geochronological events. However, this small scale is subject to the accuracy and precision of the emplacement age data obtained. For instance, the Klipfontein kimberlite is dated at 159 Ma ± 40 Ma (Smith et al., 1985), implying that the age could vary from 119-200 Ma. In the case of isochrons, errors on the ages are generally less than 2 Ma, and the use of the scale as shown is considered to be valid.

Data and abbreviations used in Figure 7.1 are as follows :

Related Rocks - Moore et al. (1985) ; Davis (1977,1978) ;
Colgan et al. (1989)

Gp I off = off craton Group I Prieska Province kimberlites - this work
Gp II off = off craton Group II Prieska Province kimberlites - this work

Gp I on = Group I Kaapvaal Craton kimberlites (Smith et al.,1985)
Gp II on = Group II Kaapvaal Craton kimberlites (Smith et al.,1985)

GpT off = off craton transitional Prieska Province kimberlites - this work
GpT on = on craton transitional Prieska Province kimberlites - this work

Namibia = Namibian kimberlites (Spriggs, 1988)

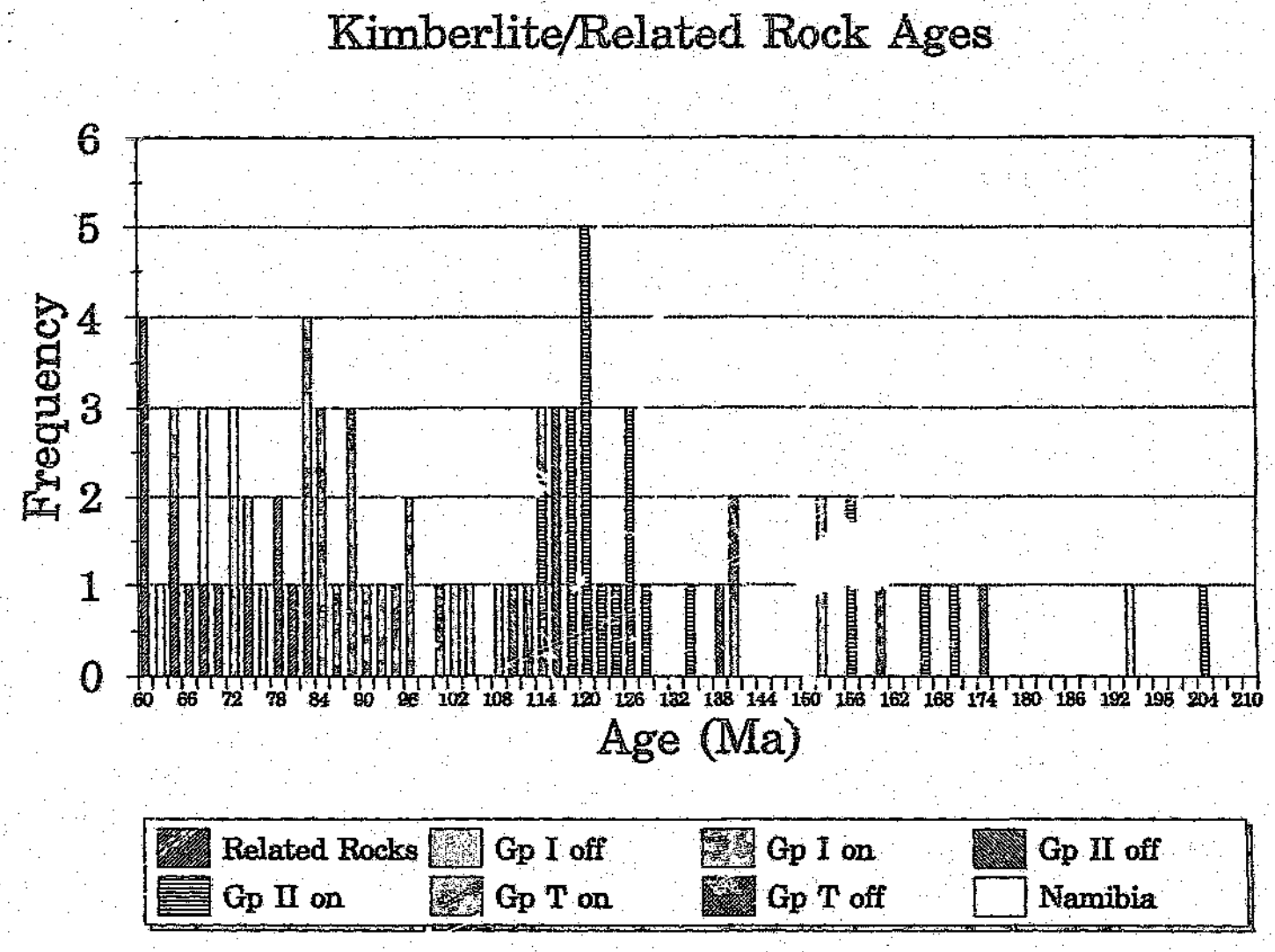

Figure 7.1 : Age Histogram of southern African Kimberlites and Related Rocks

It is clear from Figure 7.1 that the Group I and II emplacement events are fairly distinctive, with minor overlap evident between 110 and 116 Ma (caused by two of each of Group I and II kimberlites). The cratonic Group I events are very predominant between 82 and 102 Ma, and would appear to form a spectrum of fairly continuous kimberlite activity, with two and possibly three major events within this period (86, 96 and possibly 103 Ma). The off-craton Group I kimberlites do not plot in the 84-100 Ma period, but tend to be either younger or older than this. They appear to have been erupted in six events seen at 74, 82 (one locality), 102, 108 (one locality), 151 and 194 (one locality) Ma ago. Only the 82 Ma event correlates with an event on craton.

The Group II kimberlites were emplaced between 110 and 206 Ma ago. Off craton Group II's appear to be confined to a very restricted time zone of 116-118Ma (three localities) and the 110 Ma event of Eendekuil is a model age. Only one cratonic Group II occurs at 114-116 Ma, with the vast majority of the Group II kimberlites having intruded between 118 and 130 Ma ago, also in a fairly continuous period of activity. There are perhaps two peaks within this period at 120 and 126 Ma. There are nine other cratonic Group II kimberlites which show a wide spread in emplacement age data from 134 to 206 Ma. This period shows five events, but this can only be defined using one and in two cases, only two localities. This series of events is therefore not definitive until further ageas are recorded that confirm this suggestion. These five Group II age events are 134, 156, 166, 170, and 204 Ma.

The transitional kimberlites are represented on this figure by five kimberlites. Sweetput-Soutput (on-craton) falls within the earliest period of cratonic Group II activity at 116 Ma. Two kimberlites situated off craton and two cratonic kimberlites occur between 138-140 Ma, whilst the fourth off craton kimberlite was emplaced at 174 Ma. The

related rocks (olivine melilitites and melilite basalts) occur in the off-craton setting, and it is clear that they are generally younger than the Group I kimberlite emplacement events.

From the discussion above there are numerous age events that can be defined for the southern African kimberlites. It is clear that there have been a number of major protracted periods of kimberlite and related rock activity. It is considered that within these periods there have been minor peaks of activity. This is illustrated in Table 7.1 below, in which the major age period is shown in the left column, with the various eruptive peaks for the different rock types shown in the columns to the right of this. Cratonic locality ages are shown using a "x", whilst off craton ages are depicted by a "o".

Table 7.1 : Summary of Age Events for southern Africa

AGE (Ma)	Related Rocks	Group I Kimberlites	Group II Kimberlites	Transitional Kimberlites
60 - 80	o 60			
		o 64		
	o 68			
		o 72		
		o 74		
	o 80			
		o 82		
84 - 96		x 86		
		x 90		
		x 96		
100 - 108		o 102		
		x 108		
110 - 130		*Last period of Group II activity*		
			o 110	
		x 114	x 114	x 114
			o 116-118	
			x 120	
			x 126	
132 - 142			x 134	
				o 140 x 140
152 -158		o 152		
			x 156	
166 - 176			x 166	
			x 170	
				o 174
194		o 194		
204			x 204	

7.3.3.2 Hot Spots as Sources ?

The data presented in Table 7.1 show that there is a general decrease in ages of kimberlites from the interior of the Kaapvaal Craton to the southwestern edge of South Africa. This has led to suggestions that this is supportive of a hotspot model for the kimberlites generated within the southern African interior (e.g. le Roex, 1987, Skinner, 1989). However, for the Prieska Province kimberlites, a general age progression is apparent only with the inclusion of Group I and II kimberlites, which display different isotopic signatures and therefore derivation from different source regions. Furthermore, the transitional kimberlites are farthest from the craton edge and are also the oldest kimberlites within the Province. These facts clearly are not supportive of a simple hot spot model, whereby ages would young along a 'line' representing the track of a hotspot beneath the moving plate.

The volume of melt generated in the production of a kimberlite is extremely small and it is considered unlikely that a deep seated feature such as hotspots could account for any individual kimberlite body. If there is a relation of hotspots to kimberlites, it is likely to be due to the heat generated by the hotspot which could play a role in the generation or mobilisation of kimberlite melts that result in the eruption of the magma to surface.

An alternative way of generating small volume melts by a mechanism not dependant on hot spots involves decompression melting as a result of plate stresses (e.g. Bailey (1992)). Such

melts could either be omnipresent at the base of the lithosphere and erupt when suitable channelways become available to them, or the melts may be generated due to stress release in the overlying lithosphere. This suggestion appears to merit consideration, as the breakup of Gondwanaland (± 150 and 135-120 Ma) coincides with the peak of kimberlite magmatism seen in South Africa. The timing of Gondwana breakup relative to the eruption of many southern African kimberlites (particularly Group II types) strongly suggests a relationship between these events. The breakup of the continent would result in the creation of channelways created by the tensional regime operating at this time, which could allow for kimberlitic magma to erupt to the surface. Although the mechanism of stress release could cause decompression melting to occur, the old model-Nd ages of the Group II and transitional kimberlites indicates that the source from which they were derived had a long crustal residence time. Therefore, this stress release mechanism could not result in the primary generation of small degree Group II kimberlite melts, but would more probably be the trigger to the widespread eruption of kimberlites thereafter.

7.3.3.3 Alternative Source Regions

The Prieska Province kimberlites were emplaced in a relatively restricted area straddling the south-western margin of the Archaean Kaapvaal Craton. The off-craton kimberlites have intruded crustal rocks forming part of the Natal-Namaqua Mobile Belt, where higher heat flow is noted (Jones, 1992) and the underlying lithosphere is considered to be thinner than that for the Kaapvaal Craton. Compared to kimberlites from the Kaapvaal Craton, the Prieska Province kimberlites are essentially

barren of diamonds. This contrasts with cratonic kimberlites, many of which are diamondiferous. Although diamonds are xenocrysts within kimberlite, their presence, combined with studies of the numerous mantle-derived xenoliths within them, allows for some constraints to be placed on the depth of origin of cratonic kimberlites, which is difficult to do with the rocks of this study.

Therefore, the characterisation of the Prieska Province kimberlites in relation to kimberlites from cratonic environments is important since any model developed for kimberlites from the study area should be applicable to that for other areas (with some modifications due perhaps to tectonic environment, depth of origin, partial melting etc) - viz. any model for kimberlite generation should be applicable on a worldwide scale.

The subcontinental mantle environment of the Kaapvaal craton has been fairly well established due to the numerous analyses of mantle-derived rocks that are found on the craton (eg. Karoo Igneous Province) as well as the important evidence obtained from the numerous studies of mantle-derived xenoliths found within the kimberlite pipes from the cratonic environment (e.g. Nixon, 1987).

The upper mantle (extending from beneath the crust to the 650 km discontinuity) can be subdivided on the basis of geochemical and geophysical considerations into a lithospheric and asthenospheric component. The lithosphere (brittle) includes both the crust and part of the upper mantle whereas the asthenosphere (ductile) is that part of the mantle from below the lithosphere to the lower mantle. Jordan (1975, 1978, 1980), Norry

some of the stable cratonic areas of the continents, the lithosphere is thicker than that beneath mobile belts. This has lead to the concept of "continental roots" or "lithospheric keels". Estimates of the depth to the lithosphere / asthenosphere boundary beneath continents has been placed at between 150 and 200km by conventional geochemical considerations, but a number of workers (e.g. Sautter, 1991; Haggerty, 1991 and Smith, 1992) now believ that chemical and isotopic evidence from high temperature xenoliths in particular are indicative of a considerably thicker lithosphere. Geophysical estimates have placed this boundary between 250km and 400km (Jordan, 1975 and 1980 respectively). Teleseismic tomography (reviewed by Eggler, 1991) has revealed images of what are believed to be 'continental keels' which may extend to depths of several hundred kilometers beneath major cratons.

The importance of the asthenosphere/lithosphere boundary to kimberlite research is that no consensus of opinion has yet been reached as to which part of the Earth's upper mantle kimberlites have been derived from. However, it would appear that recent thoughts (eg Smith, 1992 and Ringwood, 1992) are converging towards both kimberlite types being deri [illegible] from a common source area, although these two authors di[illegible] their mantle source region (see below).

With regard to the Prieska Province, Robey (1981) showed that there is a diverse suite of lower crustal xenoliths, upper mantle xenoliths and megacrysts present in the kimberlites from this area. Upper mantle xenoliths include garnet lherzolites, lherzolites, MARID suite xenoliths and megacrysts of garnet, phlogopite, clinopyroxene and orthopyroxene. In this study,

Robey found that garnet lherzolites from Meltonwold (off craton locality) appear to be similar to the low temperature, coarse peridotites found on-craton with equilibration pressures of around 35kb, whilst garnet lherzolites and lherzolites from the nearby Haartebeesfontein kimberlite contained primary metasomatic amphibole and gave mineral equilibration pressures of 25kb. One example of a deformed peridotite was found at Haartebeesfontein. Cr-poor megacrysts were only analysed from the cratonic Lekkerfontein kimberlite and are similar to those from the Monastry kimberlite. Robey (1981) suggests on the basis of the ultrabasic xenolith compositions that the depth to the lithosphere/asthenosphere boundary is shallower than that for the Kaapvaal Craton.

From the above as well as the geochemical and isotopic characteristics presented in this study, it is believed that the subcontinental mantle beneath the Prieska Province is little different to the Kaapvaal in terms of composition. Heat flow data from the area suggest, however, that the lithosphere is thinner in this region of southern Africa relative to the cratonic portions (Jones, 1992).

Ringwood et al. (1992) suggest that low Al_2O_3 (< 4 weight percent) in kimberlites requires melting depths of at least 350 km and suggests that both kimberlite types are ultimately derived from the transition zone. These authors do not reject a subcontinental lithospheric origin for kimberlites, but believe that this type of source region requires explanantion of the high CO_2 required for kimberlite generation. The Ringwood et al. (1992) model is based on high pressure and temperature experiments performed on a theoretical kimberlite composition, in addition to assessing the

published geochemical and isotopic characteristics of kimberlites. The enriched composition of the Group II kimberlites is explained by the presence of subducted sediments that have been mixed in this zone. This model accounts for the presence of majoritic garnet in some mantle xenoliths and diamonds. However, the transition zone is a worldwide feature, implying that kimberlites should be present in the oceanic environments (Smith, pers. comm.) and it is well established that kimberlites are a continental magmatic phenomenon. In addition, the restriction of Group II kimberlites to southern Africa is not adequately handled by the model, as subduction is not restricted to southern Africa in the same manner that Group II kimberlites are.

Consideration of the various mantle source components as reviewed by Zindler and Hart (1984) shows that the Group I kimberlite sources are similar to the HIMU reservoir source composition. These authors suggest that the HIMU reservoir is present as a dispersed component within the mantle and is characterised by relatively low (about 0.7029) $^{87}Sr/^{86}Sr$ ratios and extreme Pb enrichment. Oceanic basalt islands such as St. Helena and Tubuaii display these signatures. Smith et al., (1992) show that Group I kimberlites and megacrysts can be equated to the HIMU reservoir, which they believe to be situated in the deep subcontinental lithosphere or tectosphere. They further consider that the implications of this are that kimberlites have their origins within the deep lithosphere and are not related to hotspots with respect to their material sources.

In addition to the HIMU reservoir (and other depleted mantle components) enriched mantle (EM) components must be present

islands and continental basalts that display low $^{143}Nd/^{144}Nd$, variable $^{87}Sr/^{86}Sr$, and high $^{207}Pb/^{206}Pb$ and $^{208}Pb/^{204}Pb$ at a given value of $^{206}Pb/^{204}Pb$ is taken into account. Two EM components are envisaged - EMI and EMII, with EMI showing lower $^{87}Sr/^{86}Sr$ relative to EMII. EM components are believed to have been derived from one of a number of possibilities, which include subduction of altered oceanic crust or continental sediments, subcontinental lithospheric delamination or mantle metasomatism. The Group II kimberlite trend is situated within the enriched quadrant of the Sr-Nd epsilon diagram, beyond the EMI source area towards more enriched $^{87}Sr/^{86}Sr$ compositions. West Australian lamproites are even more enriched in $^{87}Sr/^{86}Sr$ relative to Group II kimberlites (see Zindler and Hart, 1984 for further discussion).

Until the studies of kimberlites from the Prieska Province and Brazilian localities, the compositional gap between Group I and II kimberlites was very distinct. However, the incorporation of the Brazilian and transitional kimberlite data which plot within this gap, enables a trend to be discerned between Group I through transitional to Group II kimberlites. HIMU would therefore appear to be one end-member of this continuum with EMI a component along the mixing trend. However, no other endmember has yet been identified which would fit the other end of this trend. The EMII source region shows $^{143}Nd/^{144}Nd$ compositions which plot off from the "kimberlite trend". Mixing of components along this trend could then explain the different kimberlite compositions.

However, the Prieska Province is underlain by thinner lithosphere (see above), and if the HIMU and EM sources areas are only

present in the deeper parts of the subcontinental lithosphere, then the presence of kimberlites in a setting removed from the cratonic environment requires an explanantion. Moore and Verwoerd (1985) have noted a zonation of alkaline igneous activity on a regional scale from a cratonic to far off craton settings. This is recognised in eastern Siberia and southern Africa and is manifested by the presence of diamondiferous kimberlites within the cratonic interior to non-diamondiferous kimberlites in the cratonic margin to alkaline complexes, carbonatities and lamprophyres. They ascribe these changes to shallower depths of origin as one moves from the cratonic interior to the continental edges. However olivine lamproites can carry diamonds (eg Argyle diamond mine in Australia, situated in a Proterozoic mobile belt) and are likely to also have been derived from similar depths to kimberlite (Foley, 1993) .

From the above discussion, the following possibilities are put forward to explain the source area and generation of kimberlites within the Prieska Province :-

1. The Prieska Province kimberlites situated in a cratonic environment are likely to have been derived from small degrees of partial melting of a HIMU reservoir (Group I kimberlites) situated in the deep subcontinental lithosphere, whilst the Group II kimberlites would be derived by small degrees of partial melting of a more enriched mantle component at shallower levels.

2. Smith et al., (1992) suggests that the oceanic manifestations of the HIMU signature are due to lithospheric delamination during plate tectonic processes. If true, then it is considered possible that there are remnants of this 'cratonic' reservoir within the

subcontinental upper mantle of mobile belt terrains. Kimberlites could then be derived from these "off craton source areas" derived from the cratonic environment. Their non-diamondiferous nature could then be explained by having been derived from outside of the diamond stability field and therefore unable to sample diamondiferous source rock if present.

3. Transitional kimberlites, although not apparently restricted to the marginal setting, could be due to mixing of these delaminated kimberlite source components in an upper mantle where convection is likely to be more evident (shallower depth to lithospheric/asthenospheric boundary). The association of a cluster of transitional kimberlites in the off craton setting could indicate that a large segment of mixed delaminated "deep cratonic" subcontinental lithosphere is present in the region.

Model Nd ages for the Group II and transitional kimberlites imply a long residence time to explain their enriched isotopic character. The transitional varieties show model-Nd ages slightly younger than the Group II kimberlites. The main eruptive period of kimberlites in South Africa appears to coincide with the breakup of Gondwanaland. It is postulated that the tensional regime operating as a result of this tectonism was the main agent responsible for the eruption of the kimberlites at this time and that the kimberlite magmas had already developed as a result of small degrees of partial melting. Hotspots may have acted as sources of heat in the previous generation of kimberlite magmas, but they are not considered to be the material sources of such magmas.

Chapter 8

Conclusions

8.1. There is a complex distribution of kimberlite emplacement ages for the Province as a whole. Distinct emplacement events occur at 74, 80, 102, 114-120, 142? and 174? Ma. The dominant 86 Ma event recorded from the Kimberley area is not represented in the Prieska Province based on the available information. The 142 and 174 Ma Prieska Province events, although speculative at this stage, are not apparent from the Kaapvaal Craton.

8.2. There are three distinctive types of kimberlite present in the Prieska Province. These kimberlites can be defined on the basis of petrography, isotopes and in some case geochemical characteristics. A distinction is made between isotopic and petrographic varieties of kimberlite.

8.3. The isotopically defined Group I and II kimberlite types (Smith, 1983a,b) have been found to occur in the Prieska Province. These kimberlites can be correlated to the petrographic distinctions of non-micaceous and micaceous types respectively. Whilst micaceous types have been previously recorded from the study area, this is the first documented occurrence of Group II kimberlites in an off-craton setting from South Africa.

8.4. The Prieska Province Group I kimberlites have been found to be younger than the Group II types, in keeping with the trend discerned by Smith for the Kaapvaal Craton. The Group I kimberlites from the Prieska Province were emplaced between 72

and 108 Ma ago, whilst the Group II kimberlites show emplacement ages of between 110-116 Ma. The Group I Prieska Province kimberlites tend to be either younger or older than the dominant 84-96 Ma period of cratonic Group I activity.

8.5. The third type of kimberlite occurring in the study area shows petrographic characteristics that are transitional to the previously defined non-micaceous and micaceous varieties. They are essentially micaceous in nature, but also contain relatively abundant coarse-grained opaque oxides and perovskite. These minerals are usually associated with non-micaceous kimberlites.

8.6. Emplacement ages for the transitional varieties of kimberlite from the Prieska Province are generally distinctive relative to previously defined ages for southern African kimberlites. Only the locality Sweetput-Soutput shows an age previously recorded, at 116 Ma. The other transitional kimberlites show ages of 138-142 Ma (two localities) and 174 Ma (one locality).

8.7. Initial-Sr isotope ratios for the Prieska Province Group I and II kimberlites vary between 0.7040 and 0.7056 and overlap the ranges observed for the cratonic kimberlites. The transitional kimberlites show initial-Sr ratios between those for Group I and II types (varying from 0.7056-0.7073). This is the first documented example of such isotopically transitional kimberlites from South Africa.

8.8. Initial-Nd ratios for the Prieska Province kimberlites are similar to those for cratonic kimberlites. The range in initial-Nd ratios are :- Group I (0.51251-0.51270) ; Group II (0.51191-0.51214) ; Transitional (0.51214-0.51236). The transitional kimberlites have

initial-Nd ratios that are similar to Group II kimberlites, but extend to higher values.

8.9. Present-day Pb isotope ratios for the Prieska Province kimberlites (Group I $^{207}Pb/^{204}Pb$ = 15.49-15.68 ; $^{208}Pb/^{204}Pb$ = 38.93-38.98 ; Group II $^{207}Pb/^{204}Pb$ = 15.44-15.50 ; $^{208}Pb/^{204}Pb$ = 37.07-38.67 ; Transitional $^{207}Pb/^{204}Pb$ = 15.45-15.52 ; $^{208}Pb/^{204}Pb$ = 37.20-38.79) are similar to the cratonic Group I and II fields. The transitional varieties are not distinctive using Pb isotopes and plot within the Group II field.

8.10. Similarities exist between the Prieska Province kimberlites and those found to the north and northeast on the Kaapvaal craton in terms of geochemistry. In particular, rare earth element and incompatible element patterns for the kimberlites from the different tectonic settings are very similar. This indicates that similar processes have operated in both tectonic settings with respect to kimberlite generation.

8.11. The complex age distribution of the Prieska Province kimberlites is not supportive of a simple hotspot model that can be invoked for their generation. It is considered more probable that decompression melting resutling from stress release due to the breakup of Gondwanaland was the main agent responsible for the trigger to the extensive post-Karoo kimberlite magmatic events in South Africa.

8.12. The Prieska Province kimberlites are believed to have been derived from the deep lithosphere, and are the result of very small degress of partial melting of a phlogopite-bearing, carbonate-rich garnet lherzolite.

8.14. The non-diamondiferous nature of the Prieska Province kimberlites is probably due their having been derived from outside of the diamond stability field. Southern Africa diamonds are extremely old, and require a thick, ancient lithosphere for their development. This thickened lithosphere is unlikely to be present beneath the Prieska Province and in this marginal tectonic setting, the diamond stability field is probably situated at greater depths than beneath the cool cratonic lithosphere.

Appendices

A : SAMPLE DESCRIPTIONS

B : ANALYTICAL TECHNIQUES

C : DATA PRESENTATION

D : COMPARISON OF ANALYTICAL TECHNIQUES

E : AGE DATABASE

Appendix A

Sample Descriptions

A 1. Samples Analysed in this Study

In the following desriptions, sample numbers are given after the locality name and comprise four sets of numbers, separated by a "/". The first number refers to the country (in this case South Africa), the second to the 1:250 000 topographical sheet number, the third to the kimberlite number on this sheet and the last number the sample number. Where more than one sample has been collected from a locality, sample numbers are separated by commas. Terminology used for petrographic descriptions of the samples is described more fully in Chapter 1 under section 1.3.1.

A.1.1 Brandewynskuil
173/26/K6/8,11

This is a macrocrystal hypabyssal facies kimberlite with abundant shale fragments. The olivines are present as two generations and are highly serpentinised. The aphanitic groundmass is phlogopite-rich.

Petrographically, sample 8 is seen to contain numerous pellets. Two pellet types are present - one type consists of large single anhedral olivine cores surrounded by aphanitic phlogopite, whilst the other type of pellet consists of two generations of olivine and two generations of phlogopite and very fine-grained diopside needles surrounded by an extremely fine-grained matrix. Country rock fragments

consist of shale, siltstone and fine-grained dolerite. The sample is classified as a diatreme facies pelletal diopside-bearing phlogopite kimberlite.

Sample 11 is a typical hypabyssal facies kimberlite, with two generations of olivine and phlogopite. The olivines are very anhedral (corroded) and highly serpentinised, often seen with very fine-grained phlogopite selvages within the grains. The phlogopites have dark rims and lighter cores and often show evidence of strain. Diopside is present in the groundmass and opaque mineral oxides are present, but are fine-grained and sparse. Clay/sericite is occasionally present as an interstitial phase in the groundmass. The sample is classified as a hypabyssal facies macrocrystic diopside-phlogopite kimberlite.

A.1.2 Britstown
173/27/K35/16

In hand specimen, the selected sample consists of a hypabyssal, macrocrystic kimberlite, in which numerous shale fragments are present. Abundant phlogopite is present, both as macrocrystal and groundmass phases. Phlogopite constitutes 31% of the rock by volume (7% macrocrystal and 24% groundmass) which is a high proportion for a non-micaceous (Group I) kimberlite. The groundmass is rich in opaque oxides. Serpentinisation is common and the olivines are corroded. Petrographically, this kimberlite is described as a hypabyssal facies macrocrystic altered phlogopite-monticellite kimberlite.

A.1.3 Droogfontein

173/27/K19/2,3,5,10,14

This kimberlite consists of hypabyssal macrocrystic kimberlite with two generations of olivine detected in hand specimen. The groundmass is seen to be very fine-grained and phlogopite-rich. Numerous crustal xenoliths are present. Irregular patches or veins of phlogopite kimberlite pervade serpentine kimberlite.

Petrographically, the macrocrystal olivine is seen to be extensively corroded (embayed outlines) and is often serpentinised. Phlogopite is an abundant groundmass phase, equant in shape, uniform in colour and poikilitic (sometimes extremely so) in texture. Diopside is also common in the groundmass (up to 0.1mm wide). Coarse-grained (<= 0.05mm), creamy-brown perovskite is present in the groundmass and occurs both in the phlogopite and serpentine phases. There are no significant differences between different thin sections of the various samples selected. The kimberlite is classified as a hypabyssal facies diopside-serpentine-phlogopite kimberlite.

A.1.4 Eendekuil

173/18/K2/6,13

Very few macrocrysts of olivine are present in the samples studied, and where seen are completely serpentinised. Phlogopite is abundant as both macrocrystal and phenocrystal phases. Phlogopite macrocrysts are seen to be deformed and chloritised, and calcite is commonly present

along cleavage traces. Calcite is a common interstitial groundmass phase. Spinels and perovskite are fairly abundant, but are fine-grained (± 0,04 mm). Many of the olivine macrocrysts have been replaced by phlogopite. The Eendekuil kimberlite is classified as a hypabyssal facies, macrocrystic, carbonatised phlogopite kimberlite.

A.1.5 Haartebeesfontein
173/27/K1/17,19

Olivine macrocrysts are present as complex shapes and very serpentinised. Small, fresh monticellite crystals are evident and rare bleached phlogopite laths poikilitically enclosing monticellite and opaque minerals are present. Cubic spinels and creamy coloured perovskite (± 0,1 mm) are fairly abundant. Ilmenite is rare. Calcite is present as irregular patches, segregationary pools and veinlets. This kimberlite can be classified as a hypabbysal facies, macrocrystic, opaque mineral-rich phlogopite-monticellite-calcite kimberlite.

A.1.6 Jonkerwater
173/26/K51/2

Two generations of olivine are present, with the macrocrysts being anhedral in shape whilst the phenocrysts tend to be euhedral. All the olivines are serpentinised. Phlogopite is an abundant groundmass mineral and opaque minerals are numerous but fine-grained. This kimberlite is classified as a hypabyssal facies phlogopite-kimberlite.

A.1.7 Markt

173/26/K16/24

The Markt kimberlite is classified as a hypabyssal facies macrocrystic phlogopite kimberlite. Abundant fine-gained opaques (+/-0.02mm) and perovskite occur in the groundmass, and calcite is present as a secondary constituent. M. Mc Gurl (pers. comm.) notes that ilmenite was recovered from the heavy mineral analysis suggesting a transitional character.

A.1.8 Meltonwold

173/27/K9/18,20 ; JJC...

This occurrence is classified as a hypabyssal facies macrocrystal calcite-phlogopite kimberlite. Phlogopite is extremely abundant in the groundmass, forming equant stubby laths. Calcite is a ubiquitous interstitial phase. Groundmass opques are relatively abundant and slightly coarser-grained than is usual for a micaceous variety of kimberlite.

Sample JJG2165 was analysed by Smith using INAA and a whole-rock powder of this sample was used by this author for whole-rock analyses.

A.1.9 Middelwater 01

173/26/K19/13,14,15,18,21

Samples from this locality are seen to be very macrocrystic, with the olivines being anhedral in shape and highly

serpentinised. Some corrosion and recrystallisation of the olivine is evident. Phlogopite is abundant both as macrocrysts and phenocrysts but are in many cases chloritised and calcitised. The micas are equant in shape, displaying light cores and dark red-brown rims. Diopside is common in the groundmass. The kimberlite consists of a hypabyssal facies, macrocrystic, carbonatised, phlogopite kimberlite.

A.1.10 Pampoenpoort
173/27/K16/1

The sample consists of a compact hypabyssal facies kimberlite with two generations of olivine (very corroded crystals) and phlogopite present. Thin section analysis reveals this kimberlite to be an opaque mineral-rich monticellite kimberlite. Opaque oxides constitute up to 20% of the sample. Olivine macrocrysts are rounded in shape (occasional complex shape) and serpentine is present in the groundmass. Occasional perovskite is present in the groundmass.

A.1.11 Sanddrift
173/25/K5/P2

Two generations of olivine are present with the macrocrysts being very rounded and serpentinised. Phlogopite is abundant showing dark rims and strongly intergrown with opaque oxides. The groundmass contains a lot of serpentine and calcite. The Sanddrift kimberlite is classified as a hypabyssal facies, macrocrystic, phlogopite kimberlite.

A.1.12 Silvery Home

173/27/K11/2

The sample is very macrocrystic, but the olivines are very corroded, with serpentine replacement commonly seen at the edges of the grains. Serpentine and calcite are common in the groundmass and phlogopite is present poikilitically enclosing diopside. Some areas of the thin section are diopside-rich. Perovskite is common in the groundmass between 0.03 and 0.1mm in size. The kimberlite is classified as a hypabyssal facies diopside phlogopite kimberlite

A.1.13 Skietkop

173/27/K23/2

Samples from this locality were not examined petrographically by the author. No details regarding the field relationships of this occurrence were made available to the author. The kimberlite is described as a hypabyssal facies macrocrystic phlogopite kimberlite, and abundant opaque oxides and perrovskite are present in the groundmass.

A.1.14 Slypsteen 01

173/26/K24/5

Portions of the core sample obtained show evidence of flow differentiation within the dyke. Petrographically, very corroded and serpentinised olivine macrocrysts are set in a fine-grained phlogopite matrix which tend to be aligned between the olivine crystals and intergrown with diopside.

Some phlogopite macrocrysts are present. Minor opaque oxides are present and serpentinisation of the groundmass is evident. The kimberlite is described as a diopside-bearing phlogopite kimberlite.

A.1.15 Sweetput-Soutput
173/26/K40/10,12,13,20

Olivine macrocrysts are extensively corroded whilst olivine phenocrysts are commonly seen as aggregates. There is abundant groundmass phlogopite, occasional diopside, coarse-grained perovskite and accessory spinel and apatite. Phlogopite tends to be poikilitic, and the phenocrysts are equant in shape and have dark rims and light cores. Occasionally, the phlogopite is seen to be in glomerates and evidence of recrystallisation is noted. The coarse-grained perovskite (up to 0,17 mm) is optically different to perovskites present in other Prieska Province kimberlites with respect to size, colour and shape. The Sweetput-Soutput perovskites are notably yellow in colour, whilst the opaque oxides are fine-grained (< 0.1mm) but abundant. Small altered melilite crystals and secondary serpentine is occasionally observed within the groundmass.

Petrographically, this kimberlite is classified as a hypabyssal facies, macrocrystic melilite (altered) diopside-bearing phlogopite kimberlite.

A.1.16 Vioolkraal West
173/26/K46/3

The kimberlite is described petrographically as a porphyritic,

hypabyssal facies, opaque mineral-rich, phlogopite, monticellite kimberlite. Olivine is more abundant as phenocrysts and tend to be corroded. Perovskite is fairly abundant in some of the samples. Alteration of the monticellite to serpentine and calcite is common and occasional phlogopite shows normal pleochroism and evidence of strain.

A.1.17 Welgevonden
173/26/K67/14

Abundant serpentinised olivine macrocrysts (often corroded) and phenocrysts are present set in a matrix of abundant phlogopite, lesser calcite, minor spinel and accessory apatite and perovskite. Some ilmenite is also present. The kimberlite is classified as a hypabyssal facies macrocrystic phlogopite kimberlite.

A.1.18 Witberg Pipe
173/25/K10/11,13,15

The Witberg Pipe consists of a hypabyssal facies macrocrystic spinel-rich phlogopite monticellite kimberlite. Anhedral olivine macrocrysts are abundant, and serpentinisation along cracks is common. Phlogopite is present (but not abundant) as macrocrysts and phenocrysts. The phlogopites have dark rims and in some cases are slightly chloritised. The groundmass consists of ilmenite, spinel, phlogopite and monticellite. Serpentine is also present and in some cases displays triple point contacts. Alteration of monticellite to calcite is evident. Perovskite was not noted in the specimen.

A.1.19 Witberg East
173/25/K26/13,15

Serpentinised olivine macrocrysts are rare relative to the phenocrysts present. Phenocrysts of olivine are often present as glomerations. The fine-grained groundmass consists of phlogopite, lesser diopside and minor spinel. The phlogopite is very needle-like, and often rims olivine crystals. Diopside has an interlocked with the phlogopite. Opaque minerals are rare. Calcite veining and alteration to serpentine and calcite is common. In sample 15, a large country rock fragment of dolerite is noted.

The Witberg East dyke is classified as a hypabyssal facies, porphyritic, diopside-bearing phlogopite kimberlite.

A.2. Kimberlites not Analysed in this Work

Kimberlites present in the study area, but analysed by other authors are described briefly below.

A.2.1 Uintjiesburg

This is a macrocrystic, segregationary textured serpentine, calcite kimberlite. Olivine and phlogopite are present as macrocrysts and in the groundmass. Calcite is present interstitially as is serpentine. Spinel and perovskite is present in the groundmass.

A.2.2 Kalkput

The sample obtained by the author consists of a diatreme-

facies lithic TKB. The mineralogical classification is that of a carbonatised phlogopite kimberlite. Perovskite is rare, but where present, is altered and fine-grained. Occasional hypabyssal facies kimberlite autoliths are present (up to 12 cm), which contain large phlogopite macrocrysts partially altered to calcite along cleavage traces.

A.2.3 Lushof

The sample obtained from this occurrence is a diatreme-facies pelletal TKB which is classified petrographically as an opaque mineral-rich, phlogopite, monticellite kimberlite. No autoliths are present, but hypaoyssal 'patches' containing relatively fresh phlogopite and perovskite are present.

Appendix B

Analytical Methods

Introduction

Flowsheets are presented in the following pages and illustrate the overall processes employed from samp collection to sample analysis. The flowsheets are followed by separate appendices which details each step, with respe the different techniques utilised.

All isotopic work was conducted at the isotope facility at the Bernard Price Institute for Geophysical Research at the University of the Witwatersrand (Wits). XRF data were acquired on behalf of the author at the university of the O Free State by Dr W van der Westhuisen whilst INAA analyses were conducted by the author at the Schonland Centre at Wits. Microprobe analyses were obtained on behalf of the author by R Rickard at the Department of Geochemistry, University of Cape Town.

FLOWCHART 1 : SAMPLE PREPARATION

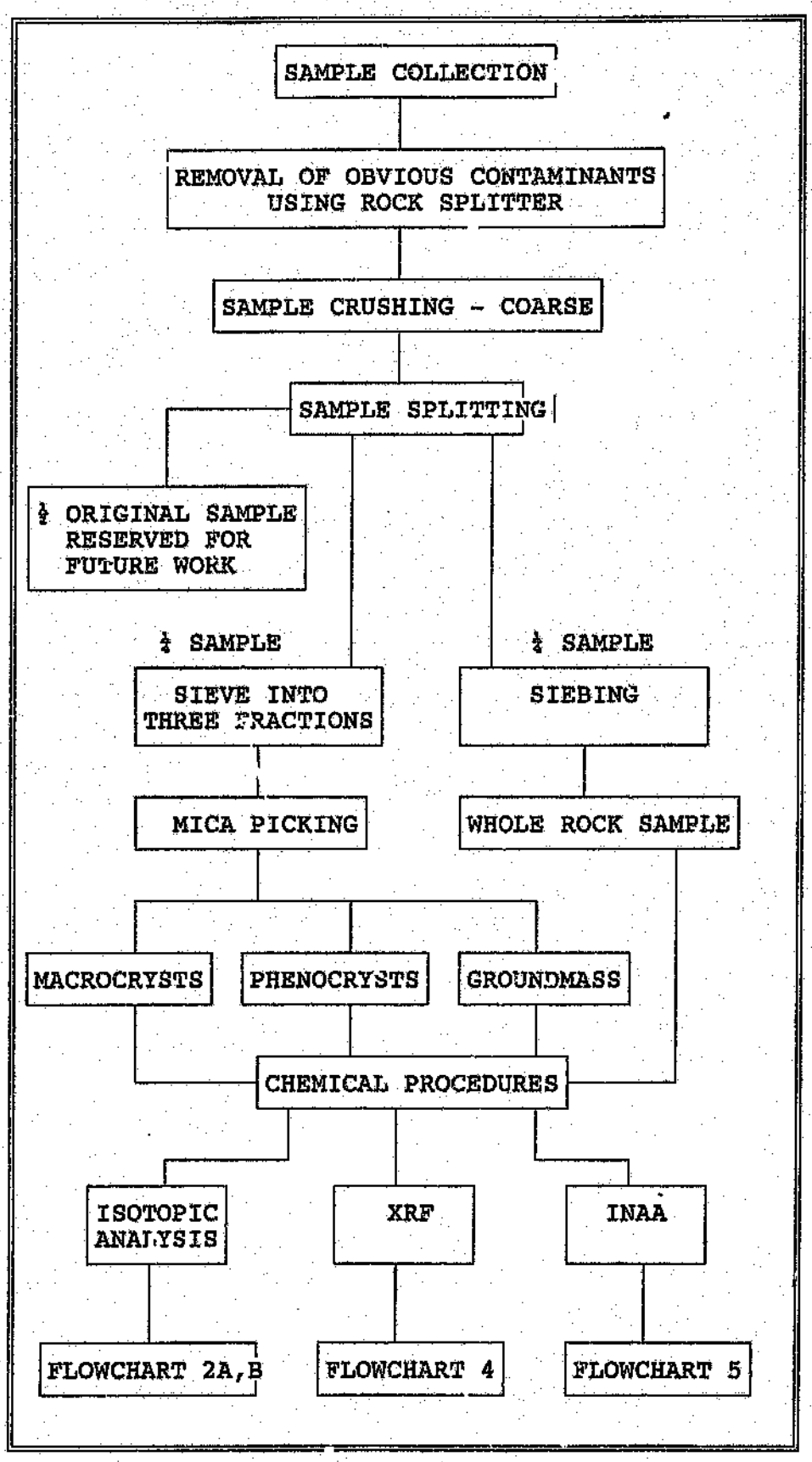

FLOWSHEET 2a : CHEMICAL PROCEDURES

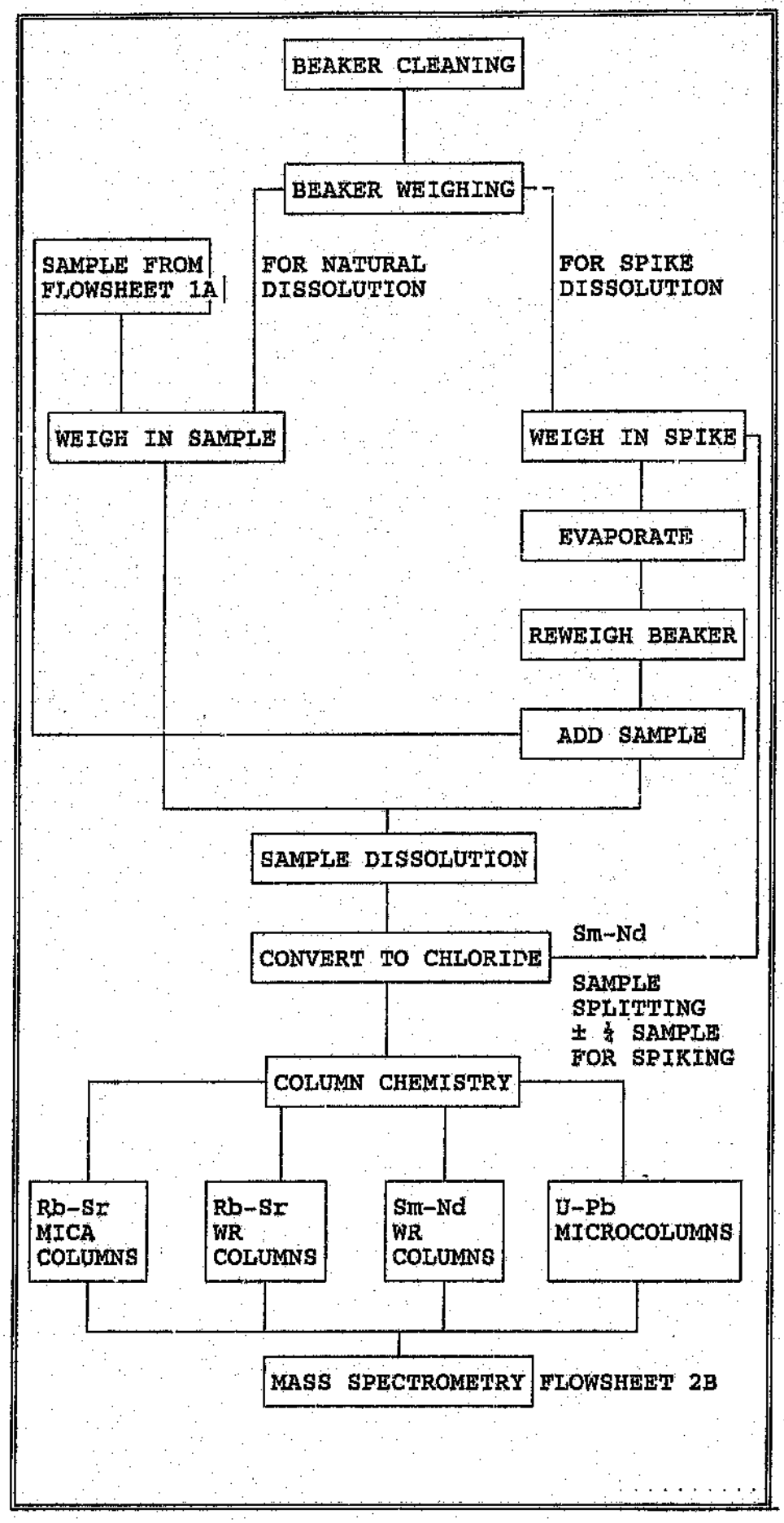

FLOWSHEET 2b : MASS SPECTROMETRY
APPENDIX B2

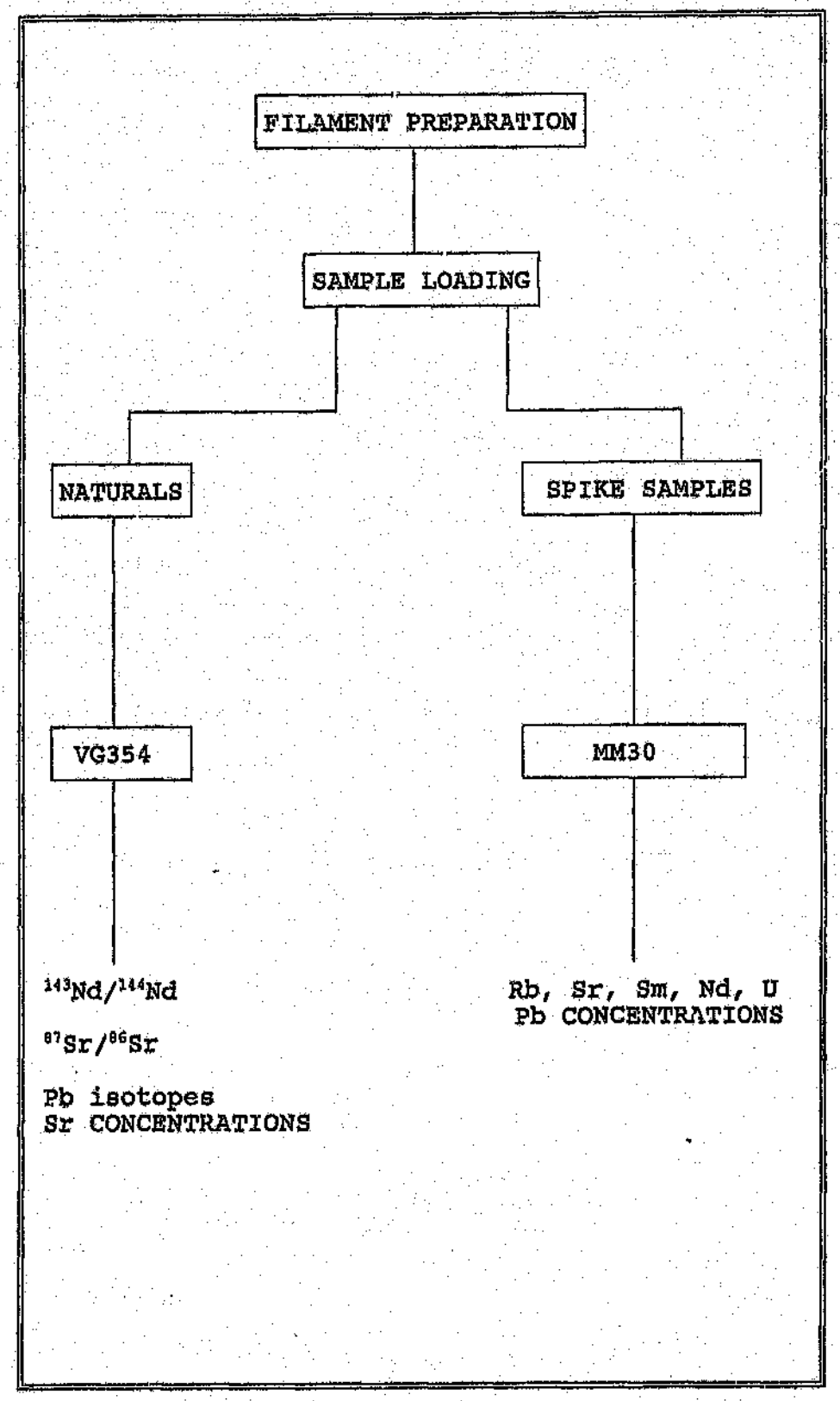

FLOWSHEET 3:
INSTRUMENTAL NEUTRON ACTIVATION ANALYSIS
APPENDIX B3

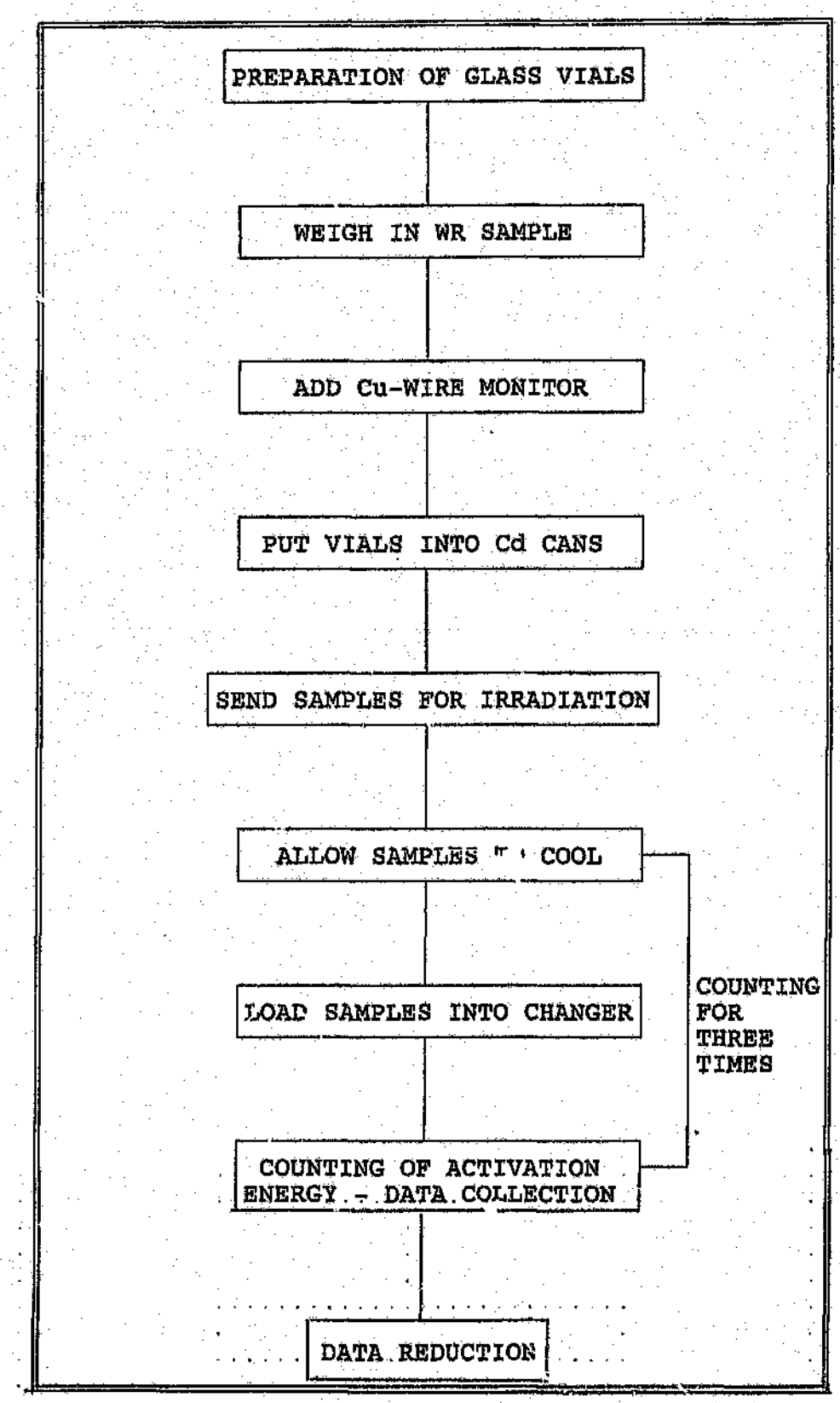

FLOWSHEET 4 : XRF ANALYSES
APPENDIX B4

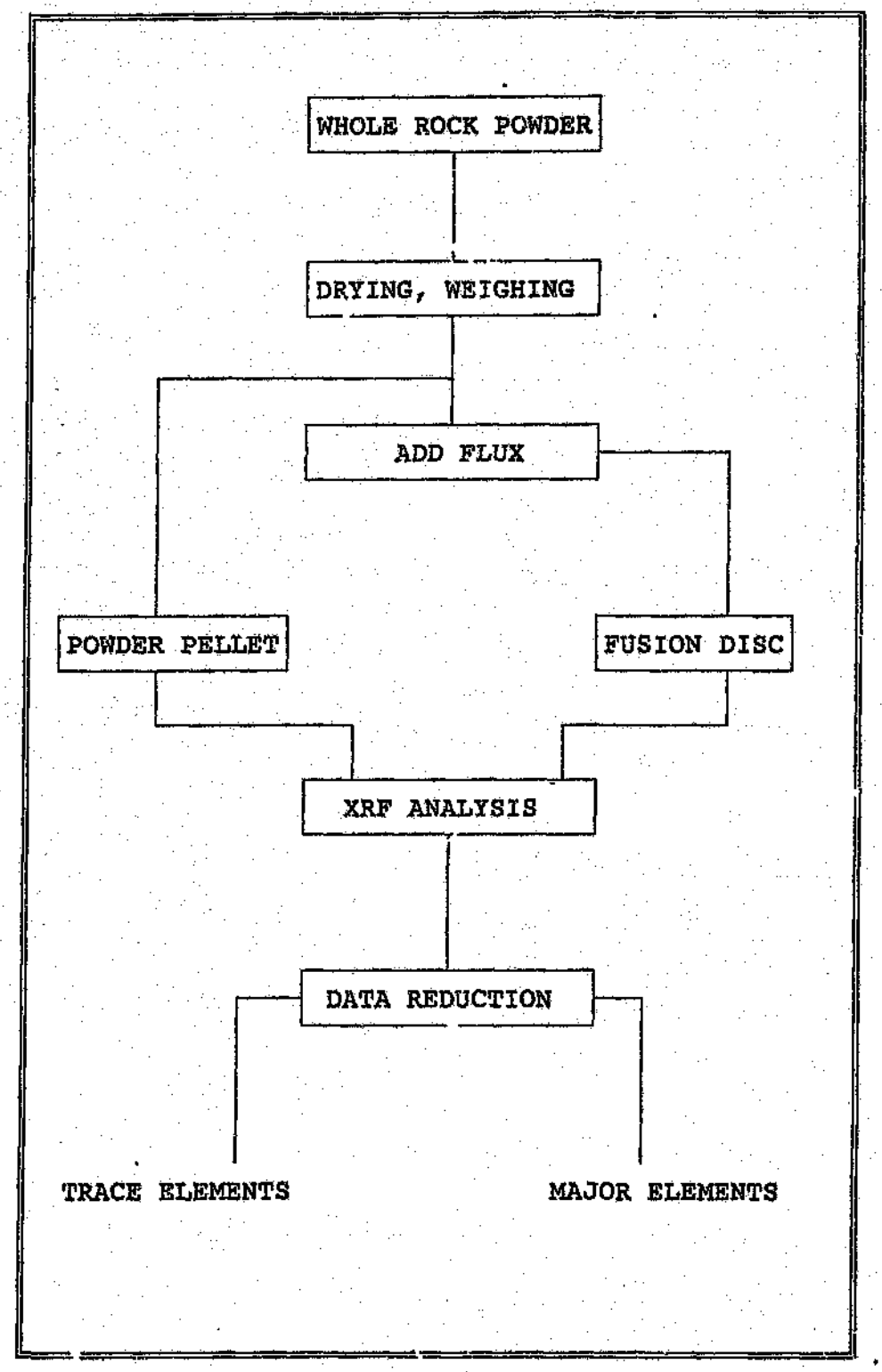

B 1. Sample Preparation

B 1.1 Introduction

All of the samples analysed isotopically in this study consist of hypabyssal' facies kimberlites. The samples were selected from large diameter (± 15 cm) drill core, obtained from the exploration activities of De Beers Consolidated Mines. Samples were, in all cases except Eendekuil, selected with due regard for obvious alteration effects, and consisted of the 'freshest- looking' pieces available. Samples from Eendekuil were extremely altered, with a clay matrix, but some samples contained notable phlogopite phenocrysts and macrocrysts.

As numerous authors have pointed out in the past (Barrett and Berg, 1975; Skinner and Clement, 1979; Smith, 1983a,b; Mitchell, 1986), kimberlite is by its very nature, difficult to analyse geochemically, due to its inherent (deuteric) alteration. Whilst petrographic examination was utilised as an aid to sample selection of the freshest material, this technique is by no means fallible. Therefore, during the geochemical analysis of the samples, 'contamination indices' were calculated for the samples, using the methods of Clement (1982) and Ilupin and Lutz (1971), as an additional aid in assessing the freshness of the samples (see Chapter 5).

B 1.2 Whole-Rock Preparation

The reader is referred to Flowsheet 1 for the techniques used in sample preparation. The samples were initially spilt utilising a hydraulic rock splitter. Extraneous material such as weathered

pieces, country rock fragments, mantle xenoliths or the outside of samples which showed grease stains (from the drilling) were removed wherever possible. The split samples were then fed into a pre-cleaned (using a wire brush, followed by distilled water and acetone) steel jaw crusher. The crushed sample, collected in a chrome-plated tray were then split into two fractions using an aluminium riffle. One of these (half the original sample) fractions was reserved for possible future work, whilst the other was spilt again into two fractions. One of these secondary splits was used for phlogopite separation and the other was prepared for powdering using a pre-cleaned (water followed by acetone) and then pre-contaminated agate Sieb mill. In some cases, due to the unavailability of the agate Sieb mill, samples had to be powdered using a pre-cleaned and pre-contaminated tungsten-carbide Sieb mill. Samples powdered with this mill were noted, so as to check the whole-rock major and trace element compositions were not contaminated (with Mn, Cr, W). Whole-rock powders are around 170 mesh in size. These samples were utilised for whole-rock isotopic, XRF and INAA techniques.

B 1.3 Mineral Separates

B 1.3.1 Phlogopite

The ¼ split sample (from above), was then sieved into three fractions using brass sieves, specially reserved for kimberlite samples. These were thoroughly cleaned prior to use utilising a nylon brush and rinsing the sieves with distilled water followed by acetone. The sizes of the sieved samples were +1 700 μm; +500/-1 700 μm; +250/-500 μm and -250 μm.

Each sieved fraction was then examined under a binocular microscope and suitable phlogopite grains were selected. This

was more easily accomplished for the two larger size fractions, but in the case of the smaller sizes, an attempt was made to pre-concentrate the mica grains, using techniques outlined by Smith (1983), notably the 'paper shaking' method. These concentrations were then further purified by hand-picking, aided by the binocular microscope.

The handpicked mica was cleaned by washing with distilled water and alcohol or acetone, agitating the mixture for a few minutes in an ultrasonic bath. The phlogopite concentrates are estimated to be at least 99% pure. Wherever possible, mica flakes that contained opaque inclusions were excluded. It is estimated that such inclusions not removed would account for less than 1% of the sample.

Previous work (Smith, 1983b; Brown, et al., 1985) has shown that leaching of phlogopite separates prior to isotopic analysis is an effective way of removing contaminants (principally calcite) and thus leads to better results in isotopic analysis. This technique was also applied to the phlogopites analyses in this work. The technique consists of adding 10 mls of cold double-distilled (1N) HCl to the phlogopite sample for about ten minutes, with around one minute of ultrasonic agitation. The leached sample was then washed (the leachate solution was discarded) using double-distilled H_2O, followed by a rinse with analytical grade acetone. This technique thus removes common Sr present in carbonate without affecting the Rb or radiogenic Sr contents.

B 1.3.2 Perovskite

In some of the thin sections examined, perovskite was noted to occur as a fairly coarse-grained and abundant groundmass

phase (notably sections of Sweetput-Soutput, Droogfontein and Markt). However, in spite of the relatively coarse size (up to 100 μm), this perovskite is extremely difficult to separate out from the rock. Smith (1983) achieved limited success in obtaining perovskite separates using the services of O.G. Garvie (Anglo American Research Laboratories). These were obtained by decomposition of the rock using concentrated HF, followed by magnetic separation of the heavy mineral fraction.

This was attempted in this work for the previously mentioned samples, but was not found to be particularly effective. This was probably due to not having enough sample available for preparation, as the concentrated acid could also have digested some of the heavy minerals (including perovskite). Therefore perovskite was analysed for REE utilising the electron microprobe in this research.

B 2. Isotope Dilution Analysis

B 2.1 Introduction

Air introduced into the isotope laboratory at the Bernard Price Institute is carefully filtered, creating a positive pressure relative to atmosphere. During the course of this investigation, refinements in the isotope laboratory took place. Earlier work consisted of solely utilising PTFE beakers, but these were later replaced by savillex beakers (with screw-top caps). Thus most Rb-Sr chemistry was performed using PTFE beakers, whereas the Sm-Nd and U-Pb chemistry was carried out using the savillex beakers.

In addition, earlier work concerning sample dissolution and drying of samples was carried out in large laminar- flow fume cupboards. These were largely replaced with small perspex boxes, whereby the filtered air passing into the laboratory, was then passed through another filter before entering the perspex box. The beakers were placed on teflon-coated aluminium blocks and heated by heat lamps in order to evaporate the solution.

Water distillation originally consisted of a first distillation using a boiling-point quartz still, followed by sub-boiling distillation in a smaller glass still. This was later replaced with a Millipore water purification system.

Originally, weighing of samples was achieved utilising a four decimal place Mettler balance. Later work utilised an electronic Mettler balance, capable of weighing samples to five decimal places. It was also noticed whilst utilising this new balance that when weighing small quantities of spike, evaporation of the spike took place. This would therefore introduce errors to the weights. In order to compensate for this, the dry cooled beaker was

weighed, and a stopwatch started once the approximate weight of spike had been introduced into the beaker. Readings were then taken at fifteen second intervals for a period of approximately three minutes (until a steady evaporation rate occurred). These data was then regressed to produce an initial weight of spike.

B 2.2 Chemical Procedures

B 2.2.1 Reagents, Spikes and Standards

Reagents such as HCl, HBr, HNO_3 and HF were bought as analytical grade. These were then double-distilled using sub-boiling point quartz glass stills, except for the HBr which was cleaned by repeatedly passing through Agl-X8 resin after dilution to 2N using double- distilled water. Reagents were then titrated in order to provide a range of suitable concentrations (0.21 N; 2,15N HCl; 2.59N HCl; 6N HCl; 5M HNO_3 and 7,5 M HNO_3). HF was not diluted after distillation. In the following descriptions, double distilled reagents are prefixed by xx.

In order to determine the concentration of an isotope in an unknown sample, it is necessary to add a known quantity of a known isotope with a known concentration (*tracer solution or spike*) to the sample under investigation. These tracer solutions had been previously made from high purity powders enriched in the desired isotope. These were dissolved with weak acids to obtain the required concentrations, and sealed in plastic or teflon dropper bottles (the top was modified by adding a teflon tip). Various spikes are used depending on which element is to be deterrmined and included ^{87}Rb (for whole-rock Rb-Sr work), ^{84}Sr (two concentration strengths of spike were used - a stronger one for whole-rock Rb-Sr and a

weaker one for phlogopite work), ^{235}U and ^{204}Pb (for U-Pb whole-rocks) and ^{149}Sm and ^{146}Nd (for Sm-Nd whole-rocks)

These spikes were periodically calibrated against gravimetric standards in order to check the concentrations, which can change over time, by evaporation and/or absorption effects of the container in which they are stored.

B 2.2.2 Beaker Cleaning

All beakers (glass, PFTE and savillex) and PTFE cover-slips and planchettes were cleaned using the following steps:

1. Heating to sub-boiling point in xx 3N HCl
2. Heating to sub-boiling point in xx H_2O
3. Heating to sub-boiling point in xx HNO_3
4. Heating to sub-boiling point in xx H_2O

These cleaned beakers were then stored in covered glass beakers or in plastic boxes (with lids). Prior to use, the beakers were filled with xx 7.5 M HNO_3 and warmed on a hotplate, followed by a rinse with xx H_2O, dried and cooled. Glass beakers were only used for the collection of Rb.

B 2.2.3 Sample Dissolution

Two types of dissolution procedures were utilised; namely natural and spike sample dissolution. In the case of Rb-Sr whole-rock compositions, spike dissolutions were performed. For Sm-Nd and U-Pb, both spike and natural dissolutions were required in order to calculate the $^{143}Nd/^{144}Nd$ (natural)

and $^{146}Nd/^{144}Nd$ (spike) and $^{208}Pb/^{204}Pb$, $^{207}Pb/^{204}Pb$ and $^{206}Pb/^{204}Pb$ compositions. For natural dissolutions, the procedure outlined below was carried out. However, for spiked sample dissolution, spikes of the various isotope desired was added to the beaker, weighed and dried prior to adding the sample and following the dissolution procedure below. For the case where samples required both natural and spike dissolutions, sample splitting was performed. In this case, dissolution of the natural sample took place first. The sample (in xx 6N HCl) was then split, with a proportion of the sample left for determining the natural concentration whilst the rest of the sample solution was added to a previously weighed 'spiked' beaker.

For dissolutions, approximately 0.1g of whole-rock powder and for phlogopite analyses, 0.02g was used in the isotope dilution analyses. The samples were dissolved in clean teflon beakers using about 6 mls xx HF, to which a few drops of xx 7.5 M HNO_3 were added (which serves as an oxidising agent to prevent the formation of insoluble fluorides). PTFE beakers were then covered with a PTFE cover-slip (savillex beakers have their own caps) and warmed on a hot plate in a laminar flow fume hood for at least two days. The solutions were then strongly heated in order to evaporate the excess HF. The dried sample was re-dissolved with xx 6N HCl and providing complete dissolution was achieved, a clear pale yellow solution was obtained. If any residue was noted, the solution was dried and the HF + HNO_3 procedure was repeated, before being taken up in HCl again. Occasionally, tiny amounts of black residues were noted, but as noted by Smith (1983b), these residues were seen to consist of opaque oxides which are unlikely to contain the elements of interest.

B 2.3 Ion Exchange Column Chemistry

In order to separate and concentrate the isotope of interest, the principles of ion-exchange chromatography were employed. Rb and Sr were separated using the method of Aldrich, (1956), Sm and Nd were separated using the methods of Richard et al. (1976), while U and Pb were separated by a variation of the method described by Strelow et al. (1966).

B 2.3.1 Rb-Sr whole-rock chemistry

The dissolved sample, to which was added xx 6N HCl (described above) was then dried in a fume cupboard (or small perspex box through which filtered air was passed). Thereafter, it was again dissolved with 2.8ml of xx 2.59 N HCl. This solution was then transferred to pre-cleaned sealable plastic tubes and centrifuged, after which it was poured onto precleaned and preconditioned cation exchange columns containing DOWEX 50W-X8 resin. These columns were specifically reserved for whole-rock Rb-Sr work. The sample was eluted with xx 2.59N HCl and the Rb and Sr fractions collected at calibrated intervals. The columns were then cleaned with 6N HCl and reconditioned with xx 2.59N HCl prior to the next sample being put through the columns. The Rb is collected in glass beakers and stored ready for analysis, whilst the collected Sr fraction is dried, following which a drop of xx HNO_3 is added to the dried sample and this is transferred to a PTFE planchette ready for mass spectrometric analysis.

B 2.3.2 Rb-Sr phlogopite chemistry

The prepared phlogopite separates are dissolved as for the

whole-rocks above. Only spike dissolutions were performed. The dried dissolution product was taken up in 2.5 ml of xx 2.15N HCl and centrifuged prior to being put onto preconditioned cation exchange columns. The Rb and Sr fractions from the dissolved sample are collected in an analogous manner to those of the whole-rocks, except that smaller cation exchange columns are used, which are specifically reserved for mineral separates (used mostly for phlogopite samples). The Rb and Sr fractions are eluted with calibrated amounts of xx 2.15N HCl and the sample is dried and stored as for the whole-rock samples.

B 2.3.3 Sm-Nd whole-rock chemistry

In order to obtain both the concentrations of Nd and Sm as well as the $^{143}Nd/^{144}Nd$ ratio for each sample, sample splitting (as described in B 2.2.3 above) were used. The natural and spike splits are treated in separate columns. The spike REE "package" is first obtained from the Rb-Sr whole-rock columns, where the REE's are eluted after the Sr fraction. This REE sample is then dried and redissolved in xx 0.21N HCl and transferred to a second set of columns containing teflon powder and used exclusively for REE separations. The sample is washed with successive aliquots of xx 0.21N HCl and the Nd fraction collected after calibrated amounts of this have been added. Sm is eluted by a change of acid normality to 3 or 6N HCl. Frequent calibration of the REE columns was necessary as the resin is sensitive to disturbance of the resin bed. The collected fractions of Sm and Nd were dried and stored in a planchette ready for analysis.

The natural REE sample is treated in a similar way, except

that specially reserved "natural" cation exchange columns were used to collect the Nd for analysis. As both Rb-Sr and Sm-Nd can be collected from one sample, later work made use of this by starting with a natural dissolution, splitting and then spiking the new set of samples. However, earlier work used separate sample dissolutions (natural and spike) for the isolation of the two isotope species.

B 2.3.4 U-Pb whole-rock chemistry

U and Pb chemistry was performed in an isolated part of the chemistry lab as the contamination levels of Pb are far greater than that for the other elements of interest. All work was performed using micro-columns made from heat-shrink teflon tubing and teflon fritts and in which a small quantity of cleaned Serva DOWEX Anion Exchange AG1-X8 200-400# resin was placed. The resin was cleaned by warming in aqua regia and rinsing with xx H_2O to get rid of the fine fractionof resin. The columns were conditioned with xx 6N HCl and xx H_2O. 0.5 ml of xxxx HBr was then added to the dissolved sample before being put into the column and calibrated quantities of xxxx 0.8 N HBr added. The Pb fraction is eluted with xx 2.59 N HCl, and the U fraction collected by adding a calibrated quantity of xx H_2O after the Pb fraction has been collected. The collected Pb fraction was then put through the columns a second time in order to further purify the Pb. The U fraction was not put through the columns twice. The collected fractions of U and Pb are then evaporated to dryness and stored on planchettes ready for analysis. The resin was discarded after use.

B 2.4 Mass Spectrometry

B 2.4.1 Loading Samples

The collected elements were then loaded onto outgassed filaments of Ta or Re ribbon which had been welded onto pins mounted in glass beads.

In the case of Sr, a drop of phosphoric acid was placed on a single Ta bead and evaporated to dryness by passing a small current through the filament. The Sr sample was then loaded onto the filament by dissolving the sample with HNO_3 and using a micro-pipette to load the Sr onto the filament. Current is then passed through the filament until the sample starts to fume, then it is cooled and stored ready for analysis.

In the case of Rb, the sample is dissolved in xx H_2O and added to the side filament of a double Ta bead assembly. The filament is heated until it glows and the dried Rb forms a white deposit. The filament is cooled ready for mass spectrometric analysis.

For Nd and Sm, the sample is dissolved in a small drop of xx 2.59 N HCl; one drop of phosphoric acid and charcoal are put onto a single Re filament and the sample loaded onto this and dried by passing a small current through the filament, following the method of Noble et al. (1989).

For Pb, the sample is dissolved in a small drop of phosphoric acid. A drop of silica gel is added to a single Re filament and almost dried. The Pb sample is then added to this drop and the mixture is then heated to dryness.

B 2.4.2. Mass Spectrometer Analysis

Two mass spectrometers were used during the course of this investigation. The Micromass 30 (MM30) and VG 354 are Niers type thermal ionisation mass spectrometers. The MM30 is a semi-automatic single collector instrument, which measures the different mass peaks by sequentially varying the magnetic field, whereas the VG 354 is a fully automated instrument with five collectors and a fixed magnetic field, measuring up to five peaks simultaneously.

All Rb concentrations, some Sr concentrations and $^{87}Sr/^{86}Sr$ ratios were obtained using the MM30 mass spectrometer. Some Sr concentrations and $^{87}Sr/^{86}Sr$ ratios were obtained using the VG 354 mass spectrometer. All Sm and Nd concentrations were obtained using the MM30, whilst the natural Nd samples were run on the VG 354. Pb ratios and concentrations were obtained using the MM30.

Appendix B 3

Instrumental Neutron Activation Analysis (INAA)

All INAA analyses were performed at the Schonland Institute for Nuclear Research, at the University of the Witwatersrand. Dr Rodger Hart supervised this author on the technique whilst Mrs L Roberts supervised on the actual sample preparation and data collection. The techniques are described in Erasmus et al. (1977).

The powdered whole-rock samples were dried overnight. The glass vials were made from 0,4 cm diameter silica glass tubing, cut into 4 cm lengths (cleaned using the methods outlined in B2.2.2 above) and the one end sealed using an acetylene torch (approximately 0,3g of sample was then loaded into a glass vial) and the other end sealed, taking care not to heat the sample by using a 'heat sink' (wet towelling wrapped around the vial).

A piece of high purity copper wire, accurately weighed, was wrapped around each vial to act as a flux monitor. Six vials were then loaded into a cadmium can (using gloves), comprising five kimberlite samples and one standard sample per can.

The cans were then sent to the nuclear reactor at Pelindaba, where they were placed in the 'poolside' position and irradiated for 48 hours in a thermal flux of 5×10^{12} ncm $^{-2}$ s^{-1}. The samples were returned in Pb-cans and allowed to cool for five days. The sample vials were then transferred from these cans (all work at this stage performed behind a Pb-cage and sample manipulation by use of tongs) and the copper wire monitor removed. The vial and monitor are then placed into a foam rubber insert, which fitted into a plastic bottle, with the Cu-wire monitor and sample vial in

separate bottles.

The samples were then placed into the automated loader, which, by use of compressed air, fed the sample bottles to the counting device. This device consisted of a planar low-energy photon spectrometer. Counts were taken for each sample four times, separated by one week, in order to determine the decay of each element.

Standards enabled concentration curves to be calculated, from which concentration values for each "unknown" sample could be calculated.

Appendix B4

X-Ray Fluorescence Spectrometry

The techniques of Norrish and Fitton (1969) were followed, with calibration using international standards. Major element analyses were obtained using the fusion technique, whilst pressed powder pellets were made in order to analyse for trace elements.

Samples were analysed using a Phillips PW1404 X-ray fluorescence spectrometer. Running parameters for major elements were 50 kV, 50 mA for major elements and between 60 and 70 kv and 30-40 mA for minor and trace elements.

Appendix B5

Microprobe Analyses

Microprobe analyses were performed on behalf of the author by R Rickard at the Geochemistry Department of the University of Cape Town. Probe sections of the various samples selected were analysed using a Cameca electron microprobe using a method developed by R Rickard base on the methods presented by Heaman (1988).

Appendix B 6

Standards and Duplicates

Numerous errors can be encountered in the isotopic analysis of rock samples and comprise two types - geological or analytical errors. Geological errors are mainly due to sample selection, in that the freshest sample is required for analysis, and in the case of kimberlites, hypabyssal facies types are the only types suitable for analysis. Analytical errors are largely preventable through careful work. However, in order to monitor these effects, standard samples and duplicate dissolutions need to be analysed periodically to help monitor geological and analytical errors with respect to precision and accuracy. Sources of analytical error are numerous and include weighing errors, incorrect spike calibrations, sample inhomogeneity, incomplete sample dissolution, cross contamination between beakers on the hotplates, reagant impurities, mass spectrometric uncertainties, isotope dilution error magnification and contamination through clothing, human hair, and imperfectly filtered air. These topics are addressed more fully in Smith (1983b) and will not be repeated here.

In order to monitor analytical uncertainties due to contamination, "blank" samples, were run for the various reagants as well as for the different exchange columns. "Total method blanks" were also routinely run, particularly for Pb, in order to monitor the total contamination expected for a batch of samples being analysed. For mica total method blanks, results showed less than 1 ng for Sr and Rb, whilst for whole-rocks total method blanks were less than 2 ng for Sr and Rb. In one instance, a mica column blank revealed contamination as shown by the high blanks recorded (up to 21 ng

for Sr) and required a long period of cleaning in order to bring this contamination level down. Nd column blanks tended to be less than 1 ng and Pb blanks were generally less than 60 pg/ml, but occassionally were up to 600 pg/ml. The introduction of the "clean boxes" in the different labs helped to bring blank levels down over the course of the research.

International rock standards were routinely run by users of the isotope laboratory. SRM 987 was used to check the $^{87}Sr/^{86}Sr$ ratio measured on the mass spectrometers. The internationally accepted value of $^{87}Sr/^{86}Sr = 0.71025 \pm 7$, but no corrections to the Sr data obtained was made, as the results for this standard were close to the accepted value (0.710226 for 30 analytical runs). Internal corrections were made by the computer software for the $^{88}Sr/^{86}Sr$ ratio. The standard SRM607 (K-Feldspar) was run and gave results of 65.49 ppm Sr and 522.10 ppm Rb. A natural Rb standard to check the $^{85}Rb/^{87}Rb$ ratio was run and gave an acceptable value of 2.6234 ± 8.

SRM 981 was run with every turret of six samples in order to monitor Pb fractionation. The values obtained for $^{208}Pb/^{204}Pb$, $^{207}Pb/^{204}Pb$, and $^{208}Pb/^{204}Pb$ over a period of time were then normalised to the accepted values of 16.937, 15.491, and 36.721 respectively (January to February 1990 - 14 runs). For the Pb data presented in Appendix C1.4, normalising factors of 1.00195, 1.00246, and 1.00391 were used for the $^{206}Pb/^{204}Pb$, $^{207}Pb/^{204}Pb$, and $^{208}Pb/^{204}Pb$ ratios respectively.

For Nd, samples of the Rhon basalt were analysed, giving a $^{143}Nd/^{144}Nd$ ratio of 0.512864 for three runs. This compares to the accepted values of 0.512861 ± 6. Internal corrections were made by the computer program for the $^{146}Nd/^{144}Nd$ ratio. Another standard (the J&M standard) was used as an in-house Nd

standard. One analysis of this sample gave 0.511844 ± 12, compared to an average of 0.511811 ± 12 for twenty runs by various lab users.

Duplicate dissolutions were also performed on whole-rock samples in order to check precision and accuracy. Duplicate runs showed a percentage difference of 0.04 % on the $^{87}Sr/^{86}Sr$ ratio for three duplicate samples run, one with a 0.03 % difference and one with a 0.15 % difference, which was due to a poor mass spectrometric run. Total Sr concentration percentage differences on these duplicates was less than 1 %, whilst Rb gave up to 8 % for one sample (Sweetput-Soutput), but was less than 1 % for the others.

No duplicate dissolutions were performed on phlogopite seperates as micas are extremely variable with respect to Rb and Sr ratios. Kimberlites themselves are difficult to duplicate due mostly to the mica contents, which cause problems in the grinding of the whole-rock. This can produce inhomogeneities in the powders produced.

Appendix C

DATA PRESENTATION

Calculations Used in Isotopic Analysis

The reader is referred to Faure (1977) for the basic principles of isotope systematics. In order to obtain initial-ratios and epsilon values, it is necessary to calculate these values from isotope equations using the obtained measured isotope ratios as follows :-

1. *Initial Ratios*

$$(^{143}Nd/^{144}Nd)_m = \{(^{147}Sm/^{144}Nd) \times (e^{\lambda t} - 1)\} + (^{143}Nd/^{144}Nd)_i$$

$$(^{87}Sr/^{86}Sr)_m = \{(^{87}Rb/^{86}Sr) \times (e^{\lambda t} - 1)\} + (^{87}Sr/^{86}Sr)_i$$

where :-

$\lambda\ (^{147}Sm) = 6.54 \times 10^{-12}\ y^{-1}$

$\lambda\ (^{87}Rb) = 1.42 \times 10^{-11}\ y^{-1}$

$(\text{isotope ratio})_m$ = measured isotope ratio

$(\text{isotope ratio})_i$ = initial isotope ratio at time t (Ma)

2. Epsilon Notation

The epsilon (ε) notation is a way of representing Sr and Nd isotope ratios for a sample formed at time t (Ma) relative to a reservoir at the same time (Hawkesworth and van Calsteren, 1984). The reservoir used for Nd isotopes is CHUR, whilst the Bulk Earth (BE) or Uniform Reservoir (UR) is used for Sr. Thus,

$$\varepsilon(Nd) = [\{(^{143}Nd/^{144}Nd)^{t}_{sample} / (^{143}Nd/^{144}Nd)^{t}_{CHUR}\} - 1] \times 10^{4}$$

$$\varepsilon(Sr) = [\{(^{87}Sr/^{86}Sr)^{t}_{sample} / (^{86}Sr/^{86}Sr)^{t}_{UR}\} - 1] \times 10^{4}$$

where :-

t = age (in Ma)

$^{143}Nd/^{144}Nd)_{CHUR} = 0.51264$

$(^{147}Sm/^{144}Nd)_{CHUR} = 0.1967$

$(^{86}Sr/^{86}Sr)_{UR} = 0.7047$

$(^{87}Rb/^{86}Sr)_{UR} = 0.0847$

In the whole-rock data presentation, errors on the measured isotopic ratios are 2 sigma, epsilon is calculated at 0 Ma for Rb, and for Nd, both 0 Ma and 100 Ma epsilon values are given.

Appendix C 1.1 : Rb-Sr Phlogopite Data

Locality Name	Sample Number	Rb ppm	Sr ppm	$^{87}Rb/^{86}Sr$ atomic	$^{87}Sr/^{86}Sr$ measured	2Std error
Britstown	16M	162	13	36.1	0.86187	8
Britstown	16P	644	13	140.5	0.85180	8
Britstown	16G	579	43	39.4	0.75146	5
Droogfontein	Mica A #	451	63.27	20.7	0.75770	4
Droogfontein	Mica B #	404	214.8	5.4	0.71974	3
Droogfontein	Mica C #	430	151.7	8.2	0.72492	4
Haartebeesfontein	17M	683	51.14	38.6	0.73993	5
Haartebeesfontein	17P	553	55.12	29.1	0.73488	4
Haartebeesfontein	19M	607	33.58	52.6	0.74001	14
Haartebeesfontein	19P	597	[illegible]	32.5	0.74435	44
Haartebeesfontein	19G	505	38.4	38.1	0.74435	6
Jonkerwater	2M	523	23	66.3	0.81980	5
Jonkerwater	2P	494	25	58.6	0.80520	4
Jonkerwater	2G	462	126	10.6	0.72690	5
Markt	10 x 1L	374	101.8	10.7	0.73007	81
Markt	10 x 2L	402	168.9	6.9	0.73100	207
Markt	10LB	302	67.14	13.0	0.73733	88
Markt	10LB-D	387	91.28	12.3	0.72932	6
Markt	10DB	352	291.1	3.5	0.71497	14
Markt	10DB-D	393	239.1	4.8	0.71751	5
Markt	10BR	410	186.6	6.4	0.72008	55
Markt	10BR-D	445	208.4	6.2	0.72070	5
Markt	Mac A #	311	18.18	49.9	0.79176	3
Markt	Mac B #	300	52.92	16.5	0.73587	3
Markt	Mac C #	299	51.77	16.8	0.73628	3
Middelwater 01	13M	585	21.17	81.1	0.84225	22
Middelwater 01	14M	580	29.08	58.3	0.80588	16
Middelwater 01	15M	533	58.51	26.5	0.75258	50
Middelwater 01	18M	553	22.9	70.7	0.82615	56
Middelwater 01	21M	541	29.06	54.3	0.80061	16
Pampoenpoort	1TM	416	17.2	70.6	0.80452	995
Pampoenpoort	1G	444	17.19	75.6	0.81749	13
Pampoenpoort	6M	595	14.87	117.6	0.87665	5
Pampoenpoort	6P	550	17.26	93.3	0.84123	70
Pampoenpoort	6G	441	40.77	31.4	0.75035	4
Sanddrift	E1 A #	512	19.79	75.9	0.84276	30
Sanddrift	E1 B #	502	17.47	84.4	0.86410	11
Sanddrift	E1 C #	541	13.38	119.7	0.94330	2
Sweetput-Soutput	12G-SS3#	502	28.52	51.3	0.77875	8
Sweetput-Soutput	12G-SS2#	374	30.6	35.6	0.76367	2
Sweetput-Soutput	A Mica #	467	32.18	42.3	0.77692	6
Sweetput-Soutput	B Mica #	368	30.6	35.0	0.76367	2
Sweetput-Soutput	C Mica #	493	28.52	50.4	0.77875	8

Appendix C 1.1 : Rb-Sr Phlogopite Data

Locality Name	Sample Number	Rb ppm	Sr ppm	87Rb/86Sr atomic	87Sr/86Sr measured	2Std error
Sweetput-Soutput	D Mica #	435	33.34	38.0	0.76942	4
Sweetput-Soutput	E Mica #	468	31.4	43.4	0.77792	7
Sweetput-Soutput	F Mica #	458	21.68	61.8	0.80800	4
Welgevonden	Welg A #	378	6.07	185.6	1.01508	4
Welgevonden	Welg B #	369	4.38	253.9	1.12740	6
Welgevonden	Welg C #	385	11.39	99.4	0.87332	5
Welgevonden	Welg D #	385	10.23	110.8	0.89186	4
Welgevonden	14M	418	24.69	49.4	0.79444	27
Welgevonden	14P	na	13.2	0.0	0.85417	81
Witberg East	Mica A #	532	30.75	50.5	0.79318	3
Witberg East	Mica B #	556	30.58	53.1	0.79705	3
Witberg East	Mica C #	549	31.31	51.2	0.79406	3
Witberg Pipe	Wit 2 #	810	10.18	238.4	1.07197	4
Witberg Pipe	Wit 3 #	775	7.766	301.6	1.16754	5
Witberg Pipe	Wit 4 #	804	9.503	253.9	1.09470	4
Witberg Pipe	Wit 5 #	804	10.66	225.5	1.05191	4
Witberg Pipe	Wit 7 #	828	8.076	310.4	1.18040	4
Witberg Pipe	Wit 8 #	844	8.845	287.9	1.14602	4
Witberg Pipe	11M	779	10.5	222.2	1.06429	78
Witberg Pipe	11M-R	770	10.16	226.8	1.06974	49
Witberg Pipe	15M	811	10.53	231.0	1.07695	659

KEY TO TABLE

Suffix Meanings :- M=Macrocryst, P=Phenocryst, G=Groundma

Sa.No. suffixed by -R = Repeat on same dissolution

Sa.No. suffixed by -D = Duplicate sample

Sa.No. suffixed by # = Sample run by CBS

Appendix C 1.2 : Rb-Sr Whole-Rock Data

Locality Name	Sample Number	Rb ppm	Sr ppm	87Rb/86Sr atomic	87Sr/86Sr measured	± Std error	Initial Sr ratio	ε (0 Ma)
Brandewynskuil	11W *	110	1476	0.215	0.70858	2	0.7083	53.2
Britstown	16W	162	1252	0.373	0.70443	5	0.7040	-8.2
Droogfontein	2W	na	1644	-	0.70706			
Eendekuil	2W	211	1507	0.406	0.70797		0.7073	39.3
Eendekuil	13W	na	1407	-	0.70785		0.7079	46.6
Haartebeesfontei	16W	127	1212	0.302	0.70433		0.7040	-8.5
Jonkerwater	2W	72	1892	0.110	0.70852	6	0.7084	55.1
Jonkerwater	2W *	-	1899	-	0.70829	1		
Markt	24W	86	1774	0.140	0.70881	6	0.7086	56.9
Markt	24W *	na	1775	-	0.70853	1		
Markt	24W -R	na	1782	-	0.70846	3		
Markt	25W	77	2289	0.098	0.70866	10	0.7085	55.8
Markt	25W *	na	2306	-	0.70880	1		
Markt	25W-*R	na	2309	-	0.70876	2		
Meltonwold	18W *	91	791	0.334	0.70696	2	0.7065	27.1
Meltonwold	2165 *	143	1062	0.389	0.70634	2	0.7058	17.1
Meltonwold	20W *	na	660	-	0.70732	2	0.7073	38.8
Middelwater 01	21W	204	964	0.614	0.70942	4	0.7084	54.5
Middelwater 01	15W	139	770	0.523	0.70950	6	0.7086	57.7
Middelwater 01	13W	190	878	0.625	0.70918	4	0.7081	50.8
Pampoenpoort	6W	56	861	0.186	0.70493	5	0.7047	1.2
Pampoenpoort	6W-D	55	853	0.188	0.70600	7		
Pampoenpoort	6W *	na	867	-	0.70540	6		
Pampoenpoort	6W-*R	na	869	-	0.70480	3		
Sanddrift	P2W *	88	595	0.427	0.70831	1	0.7076	42.9
Silvery Home	2W *	121	990	0.354	0.70852	1	0.7080	48.7
Skietkop	3W *	161	1318	0.354	0.70680	1	0.7063	24.3
Skietkop	2W *	94	449	0.603	0.70765	2	0.7068	31.5
Slypsteen 01	5W *	na	1138	-	0.70908	1		
Sweetput-Soutput	13W	199	1461	0.410	0.70717	4	0.7067	28.5
Sweetput-Soutput	20W	158	1501	0.318	0.70720	8	0.7064	29.7
Sweetput-Soutput	10W	185	1532	0.364	0.70706	5	0.7065	27.8
Sweetput-Soutput	10W-D	200	1544	0.375	0.70732	9		
Vioolkraal West	3W *	na	1675	-	0.70357	25		
Welgevonden	14W	124	1111	0.323	0.70909			
Welgevonden	14W	na	1163		0.70918	14		
Welgevonden	14W-R	na	1164		0.70913	5	0.7091	64.4
Witberg East	11W	148	704	0.610	0.70947			
Witberg Pipe	11W *	na	630		0.70947	1		
Witberg Pipe	15W *	82	570	0.415	0.70562	3	0.7049	5.4

KEY TO TABLE
Sa.No. = Sample Number
Suffix Meanings :- W=Whole Rock
Sa.No. suffixed by -D = Duplicate sample
Sa.No. suffixed by * = 87Sr/86Sr + Sr concentration from VG354
Sa.No. suffixed by -R = Sample rerun on VG354
na = not analysed

Appendix C1.3 : Sm/Nd Whole-Rock Analyses

LOCALITY NAME	Sample Number	Nd ppm	Sm ppm	Sm/Nd atomic	143/144Nd measured	+/-	Ro	ε	ε 100	T(Nd) chur
Pampoenpoort	6W	79.0	11.5	0.0880	0.512571	6	0.51251	0.1	0.0	97.0
Witberg Pipe	15W	64.0	9.0	0.0747			0.51260	1.9	1.8	-
Vicolkraal West	3W		39.7	0.09	0.512697	7	0.51264	2.5	2.5	-81.7
Britstown	16W	105.9	16.3	0.0930	0.512697	7	0.51265	2.1	2.8	-84.1
Haartebeesfontein	16W	71.2	12.0	0.1016	0.512754	6	0.51270	3.1	3.8	-183.3
Slypsteen 01	5W	92.6	12.3	0.0801	0.511961	6	0.51191	-11.8	-11.7	887.7
Brandewynskuil	11W	116.0	13.0	0.0677	0.511987	7	0.51194	-11.1	-11.1	772.3
Markt	24W	139.2	17.7	0.0769	0.512015	7	0.51196	-10.4	-10.8	795.9
Jonkerwater	2W	194.4	25.2	0.0783	0.512026	6	0.51196	-10.2	-10.6	791.1
Middelwater 01	15W	57.4	7.8	0.0825	0.512036	64	0.51197	-10.1	-10.5	806.5
Welgevonden	14W	102.2	13.7	0.0811	0.512098	14	0.51204	-8.9	-9.2	715.0
Sanddrift	P2	65.5	7.8	0.0717	0.512097	7	0.51204	-8.6	-9.2	662.8
Eendekuil	13W	122.6	17.0	0.0841	0.512099	6	0.51204	-9.0	-9.2	732.8
Eendekuil	2W	120.8	16.9	0.0843	0.512109	7	0.51205	-8.8	-9.0	720.9
Witberg East	11W	61.3		0.0000	0.512140	9	0.51214	-6.8	-7.2	388.2
Silvery Home	2W	-	9.0	0.08	0.512197	8	0.51214	-7.2	-7.1	579.3
Droogfontein	2W-R	126.0	17.0	0.0816	0.512238	10	0.51215	-5.3	-7.1	532.9
Droogfontein	2W	135.2	18.5	0.0825	0.512257	6	0.51216	-4.9	-6.8	512.0
Skietkop	2W	79.6	10.1	0.0764	0.512217	7	0.51215	-6.1	-7.1	536.9
Sweetput-Soutput	10W	99.3	13.6	0.0826	0.512220	7	0.51216	-6.7	-6.8	561.9
Sweetput-Soutput	20W	97.6	13.6	0.0843	0.512237	8	0.51218	-6.4	-6.5	547.1
Meltonwold	18W	65.4	8.7	0.0800	0.512386	7	0.51231	-2.8	-3.9	332.5
Meltonwold	2165	84.6	11.4	0.0813	0.512435	7	0.51236	-1.9	-2.9	271.4

Appendix C1.4 : Pb Data

	206/204	2 σ-	207/204	2 σ-	208/204	2 σ-	Pb ppm
Brandewynskuil 11W	19.342	8	15.565	8	39.233	9	6.9
Britstown 16W	21.295	6	15.760	6	40.289	7	10.2
Droogfontein 2W	18.024	5	15.572	6	38.552	6	12.0
Eendekuil 13W	17.680	5	15.551	5	38.462	7	11.7
Jonkerwater 2W	17.634	5	15.526	6	37.992	7	13.4
Markt 24W	17.653	11	15.559	12	38.271	13	12.8
Meltonwold 2165	17.264	23	15.517	25	37.359	27	7.7
Middelwater 01 15W	18.327	6	15.577	6	38.972	6	14.5
Sanddrift P2	17.496	65	15.514	57	37.935	58	
Skietkop 2W	17.456	12	15.521	13	37.487	15	2.9
Slypsteen 5W	18.285	11	15.594	15	39.096	19	7.7
Sweetput-Soutput 13W	17.686	8	15.550	7	38.376	7	8.4
Vioolkraal West 3W	18.070	6	15.576	7	38.349	7	7.6

Appendix C 2 : XRF Whole-Rock Data

Key to Data Presented :

1: Britstown 16
2: Haartebeesfontein 16
3: Pampoenpoort 6
4: Vioolkraal West 3
5: Witberg Pipe 11
6: Witberg Pipe 15
7: Brandewynskuil 8
8: Jonkerwater 2
9: Markt 24
10: Middelwater 01 - 13
11: Middelwater 01 - 15
12: Middelwater 01 - 21
13: Sanddrift P2
14: Welgevonden 14
15: Brandewynskuil 11
16: Eendekuil 6
17: Eendekuil 13
18: Slypsteen 5
19: Witberg East 11
20: Droogfontein 2
21: Droogfontein 5
22: Meltonwold 2165
23: Meltonwold 18
24: Meltonwold 20
25: Silvery Home 2
26: Skietkop 2
27: Skietkop 3
28: Sweetput-Soutput - 13
29: Sweetput-Soutput - 20
30: Sweetput-Soutput - 10

CI = Contamination Index
Si/Mg = Contamination Index
- see Chapter 5 for discussion

All XRF and INAA data given in ppm

	GROUP I KIMBERLITES					
Oxide	1	2	3	4	5	6
SiO2	34.16	29.29	30.27	28.29	30.72	30.06
TiO2	3.95	3.94	1.98	3.26	2.23	2.34
Al2O3	5.64	3.95	2.22	3.96	2.50	2.65
Fe2O3	11.64	13.07	10.11	14.86	12.42	12.25
MnO	0.19	0.20	0.18	0.30	0.27	0.27
MgO	19.78	25.01	30.77	18.93	30.11	28.89
CaO	9.04	11.62	9.33	13.79	7.28	8.00
Na2O	0.63	0.12	0.06	0.06	0.05	0.04
K2O	3.39	1.99	1.08	0.85	1.08	1.04
P2O5	1.10	1.11	0.84	1.94	0.96	0.93
H2O-	1.57	0.76	0.71	1.17	0.87	0.89
LOI	8.80	8.93	12.37	12.40	11.38	12.49
TOTAL	99.89	99.99	99.92	99.81	99.87	99.85
CI	1.52	1.15	0.99	1.57	1.03	1.06
Si/Mg	1.34	0.91	0.76	1.16	0.79	0.81
Element	1	2	3	4	5	6
Ba	1915.0	1092.0	1144.0	1671.0	985.0	998.0
Rb	172.00	115.00	54.00	38.00	79.00	79.00
Sr	1234.0	1045.0	824.0	1565.0	497.0	547.0
Y	31.00	25.00	15.00	59.00	13.00	13.00
Zr	204.00	305.00	255.00	397.00	221.00	220.00
Nb	209.00	137.00	116.00	309.00	123.00	123.00
V	231.00	233.00	128.00	212.00	132.00	136.00
Cr	698.0	1060.0	1474.0	725.0	1104.0	1015.0
Co	84.00	87.00	109.00	61.00	103.00	99.00
Cu	95.00	81.00	42.00	78.00	76.00	76.00
Zn	88.00	86.00	73.00	160.00	85.00	82.00
Ni	625.0	691.0	1322.0	395.0	1043.0	969.0
U	17.0	11.0	9.0	26.0	6.0	8.0
Th	20.0	6.0	8.0	25.0	8.0	7.0
Pb	23.0	10.0	10.0	22.0	8.0	8.0

	GROUP II KIMBERLITES							
Oxide	7	8	9	10	11	12	13	14
SiO2	41.36	31.98	34.58	39.25	38.56	38.61	35.86	33.18
TiO2	1.42	0.84	0.70	1.29	0.91	1.64	0.71	1.15
Al2O3	6.38	2.94	3.68	3.80	3.01	4.19	2.77	2.88
Fe2O3	8.16	7.51	7.33	9.14	8.22	9.41	7.53	8.62
MnO	0.13	0.16	0.15	0.17	0.17	0.18	0.18	0.17
MgO	21.39	27.01	27.75	24.75	26.56	24.04	28.75	26.18
CaO	7.12	9.72	8.33	4.60	5.04	5.42	5.32	7.47
Na2O	0.17	0.03	0.05	0.11	0.11	0.13	0.04	0.10
K2O	4.33	1.95	3.10	4.70	3.49	4.92	2.60	3.10
P2O5	1.35	1.91	1.17	0.95	0.68	1.27	0.04	0.94
H2O-	2.30	0.71	0.65	1.74	1.53	1.65	1.80	1.87
LOI	5.66	14.25	12.39	9.43	11.51	8.37	14.30	14.37
TOTAL	99.77	99.01	99.88	99.93	99.79	99.83	99.90	100.03
CI	1.59	1.13	1.13	1.26	1.24	1.27	1.14	1.12
Si/Mg	1.50	0.92	0.97	1.23	1.13	1.24	0.97	0.98
Element	7	8	9	10	11	12	13	14
Ba	6521.0	5431.0	3307.0	2004.0	1781.0	1890.0	1793.0	1126.0
Rb	147.00	73.00	85.00	193.00	139.00	205.00	82.00	124.00
Sr	1102.0	1818.0	1673.0	857.0	743.0	948.0	558.0	1111.0
Y	22.00	29.00	22.00	18.00	11.00	24.00	5.00	18.00
Zr	295.00	355.00	284.00	222.00	151.00	296.00	141.00	374.00
Nb	102.00	123.00	92.00	71.00	46.00	91.00	41.00	71.00
V	102.00	177.00	62.00	182.00	127.00	248.00	50.00	84.00
Cr	1599.0	1620.0	1404.0	1694.0	1717.0	1547.0	1988.0	1361.0
Co	81.00	90.00	84.00	102.00	112.00	87.00	108.00	89.00
Cu	27.00	26.00	22.00	36.00	29.00	42.00	12.00	30.00
Zn	68.00	61.00	56.00	74.00	71.00	83.00	55.00	80.00
Ni	1047.0	1164.0	1181.0	1324.0	1524.0	1047.0	1643.0	1160.0
U	11.0	18.0	14.0	8.0	5.0	12.0	2.0	10.0
Th	20.0	31.0	21.0	9.0	5.0	14.0	3.0	14.0
Pb	11.0	35.0	20.0	20.0	16.0	24.0	2.0	15.0

	WEATHERED GROUP II KIMBERLITES				
Oxide	15	16	17	18	19
SiO2	41.01	26.84	30.17	44.27	43.94
TiO2	1.24	2.05	2.71	1.91	1.34
Al2O3	6.43	4.72	5.95	6.26	6.19
Fe2O3	7.67	8.70	10.27	9.38	9.66
MnO	0.11	0.30	0.18	0.14	0.16
MgO	20.40	9.06	11.23	18.23	17.73
CaO	6.15	23.95	17.96	7.02	6.84
Na2O	0.36	0.08	0.08	0.68	0.36
K2O	3.17	2.38	4.33	3.70	3.12
P2O5	1.06	0.37	0.77	1.09	0.81
H2O-	3.97	1.12	0.78	1.66	2.58
LOI	8.42	20.36	15.50	5.51	7.20
TOTAL	99.99	99.93	99.93	99.85	99.93
CI	1.79	2.29	1.82	2.00	2.11
Si/Mg	1.56	2.30	2.08	1.88	1.92
Element	15	16	17	18	19
Ba	1929.0	908.0	1314.0	1479.0	1476.0
Rb	110.00	138.00	213.00	155.00	148.00
Sr	1445.0	858.0	1327.0	1072.0	704.0
Y	23.00	29.00	36.00	19.00	12.00
Zr	297.00	199.00	242.00	291.00	177.00
Nb	67.00	90.00	128.00	75.00	49.00
V	131.00	166.00	185.00	231.00	242.00
Cr	1412.0	343.0	485.0	1267.0	1830.0
Co	77.00	48.00	61.00	69.00	87.00
Cu	28.00	28.00	29.00	54.00	62.00
Zn	76.00	67.00	77.00	86.00	79.00
Ni	972.0	231.0	301.0	676.0	931.0
U	12.0	11.0	14.0	12.0	7.0
Th	17.0	15.0	20.0	12.0	5.0
Pb	14.0	18.0	23.0	23.0	16.0

	TRANSITIONAL KIMBERLITES										WTHD
Oxide	20	21	22	23	24	25	26	27	28	29	30
SiO2	36.07	35.98	33.29	35.24	35.47	35.05	39.32	33.45	35.37	36.13	36.31
TiO2	3.20	3.17	1.32	0.93	0.92	1.84	0.97	2.63	2.26	2.48	2.52
Al2O3	6.70	6.48	3.03	2.39	2.37	2.34	3.23	3.99	5.47	6.28	5.90
Fe2O3	10.20	10.14	8.71	8.60	8.76	9.87	9.15	10.67	9.21	10.10	10.48
MnO	0.17	0.18	0.15	0.15	0.15	0.15	0.17	0.21	0.18	0.18	0.15
MgO	22.25	22.69	28.67	32.01	31.01	29.60	34.54	25.96	19.70	18.52	18.85
CaO	7.68	7.42	8.17	[illegible]	4.42	4.54	5.74	6.68	9.91	9.69	9.59
Na2O	0.05	0.04	0.01	[illegible]	0.03	0.04	0.07	0.03	0.71	0.77	0.71
K2O	2.72	2.71	2.42	[illegible]	1.47	2.33	1.20	3.07	4.37	4.60	3.56
P2O5	2.03	2.00	0.81	0.36	0.55	1.76	0.19	1.98	0.86	0.98	0.93
H2O-	1.49	1.50	0.45	0.09	0.73	1.54	1.00	0.47	1.33	1.10	1.28
LOI	7.34	7.50	12.92	13.43	14.09	10.85	4.09	10.73	10.44	9.04	9.53
TOTAL	99.90	99.81	99.95	99.78	99.97	99.91	99.87	99.87	99.81	99.87	99.81
CI	1.55	1.51	1.08	1.07	1.12	1.09	1.16	1.17	1.46	1.56	1.65
Si/Mg	1.26	1.23	0.90	0.85	0.89	0.92	0.89	1.00	1.39	1.51	1.49
Element	20	21	22	23	24	25	26	27	28	29	30
Ba	1727.0	1640.0	2721.0	2827.0	2995.0	3648.0	1267.0	4926.0	2195.0	2244.0	2117.0
Rb	158.00	160.00	133.00	84.00	69.00	172.00	83.00	160.00	211.00	219.00	198.00
Sr	1557.0	1586.0	1004.0	729.0	610.0	943.0	436.0	1225.0	1404.0	1435.0	1465.0
Y	32.00	32.00	14.00	10.00	8.00	15.00	11.00	24.00	22.00	26.00	23.00
Zr	369.00	382.00	135.00	107.00	108.00	272.00	192.00	194.00	224.00	295.00	284.00
Nb	223.00	220.00	176.00	89.00	104.00	141.00	107.00	342.00	91.00	105.00	98.00
V	148.00	174.00	96.00	73.00	105.00	93.00	38.00	192.00	180.00	220.00	156.00
Cr	1236.0	1193.0	1544.0	1918.0	1976.0	1615.0	1935.0	2239.0	884.0	964.0	904.0
Co	93.00	95.00	99.00	123.00	129.00	112.00	123.00	90.00	77.00	72.00	80.00
Cu	84.00	91.00	63.00	53.00	51.00	65.00	22.00	93.00	21.00	55.00	61.00
Zn	95.00	93.00	61.00	65.00	63.00	66.00	61.00	81.00	123.00	138.00	73.00
Ni	951.0	981.0	1326.0	1658.0	1721.0	1491.0	1735.0	936.0	642.0	591.0	657.0
U	16.0	18.0	11.0	5.0	5.0	8.0	6.0	16.0	15.0	15.0	16.0
Th	21.0	19.0	16.0	8.0	11.0	7.0	12.0	45.0	12.0	11.0	10.0
Pb	24.0	24.0	7.0	5.0	7.0	6.0	4.0	17.0	23.0	33.0	18.0

Note "WTHD" for sample No. 30 = weathered sample

Appendix C3 : INAA Whole-Rock Data

	GROUP I KIMBERLITE				GROUP II KIMBERLITES							TRANSITIONAL KIMBERLITES				
Element	1	2	3	4	5	6	7	8	9	10	11	12	13	14	15	16
K	31300	20500	11900	8600	19700	29900	37900	26400	114600	26900	36500	26500	30700	35200	45400	38500
Na	9700	5700	5500	5200	5500	5100	5800	5800	18800	9100	4000	5200	5100	13100	13200	12700
Ba	1903	1195	1091	904	5658	3108	1940	1733	1106	1750	1894	1663	1545	2308	2376	2251
Ni	579	669	1256	879	1011	1037	1255	1372	1110	854	313	932	896	646	585	650
Cr	799	966	1566	1072	1510	1395	1608	1545	1320	1389	627	1359	1328	1013	916	1033
U	6.4	2.9	3.6	2.4	6.4	2.6	3.7	2.4	5.8	2.6	2.7	6.0	5.7	3.9	4.4	4.2
Rb	164	125	61	81	70	85	187	143	124	107	210	156	144	213	209	199
Th	28	12	14	14	31	22	13	9	17	18	30	27	25	16	16	16
Co	75	77	92	83	71	65	77	82	71	58	63	79	75	67	63	69
Zr	225	300	318	200	388	307	294	236	365	309	186	521	365	252	264	330
Ta	12.4	11.6	9.0	10.1	5.9	5.1	4.2	2.7	4.2	4.2	8.7	15.2	14.9	6.7	6.9	7.1
Cs	7.3	2.4	1.7	0.6	3.3	4.4	3.5	2.7	2.9	1.7	4.6	3.4	3.2	3.0	3.3	3.9
Hf	4.6	8.1	6.0	5.1	8.7	6.4	5.5	3.6	9.3	7.3	4.7	9.8	9.3	5.9	7.6	7.1
W	1.5	0.9	1.4	0.7	17.0	nd	nd	nd	nd	nd	7.0	nd	nd	nd	nd	nd
As	7.9	3.2	8.5	2.5	5.0	6.9	2.9	4.2	8	1.9	2.6	2.3	2.2	3.8	1.8	1.7
Sb	0.5	0.3	0.2	0.2	0.2	0.4	0.2	0.2	0.7	0.2	0.4	0.2	0.2	0.2	0.2	0.2
Au	0.8	0.3	0.5	5.0	0.6	0.7	1.0	0.9	1.7	1.8	1.9	2.7	0.8	0.3	nd	nd
Sc	24	21	17	17	26	22	18	12	17	19	20	17	16	21	24	23
La	162	86	110	81	247	178	104	75	205	143	198	205	198	130	131	139
Ce	326	137	180	132	499	369	175	126	239	296	404	416	393	275	220	292
Nd	109	88	79	64	170	143	104	57	109	116	154	157	126	105	106	110
Sm	16	11	11	9	24	17	11	8	19	13	17	18	17	13	13	13
Eu	4.5	3.6	3.2	2.8	5.3	4.2	2.8	1.9	3.2	3.2	4.0	4.8	4.4	3.1	3.5	3.3
Tb	1.3	1.0	0.9	0.8	1.3	1.1	0.8	0.6	1.0	0.9	1.2	1.4	1.3	0.9	1.0	1.0
Yb	5.3	4.6	3.8	3.8	3.9	3.0	2.5	1.7	2.5	2.9	4.1	6.5	6.1	3.2	3.6	3.5
Lu	0.8	0.4	0.5	0.3	0.7	0.4	0.5	0.3	0.5	0.4	0.4	0.8	0.6	0.5	0.5	0.5

KEY:

1 : Britstown 16
2 : Haartebeesfontein 16
3 : Pampoenpoort 6
4 : Witberg Pipe 15
5 : Jonkerwater 2
6 : Markt 2
7 : Middelwater 01 13
8 : Middelwater 01 15
9 : Welgevonden 14
10 : Brandewynskuil 11
11 : Eendekuil 6
12 : Droogfontein 2
13 : Droogfontein 5
14 : Sweetput-Soutput 13
15 : Sweetput-Soutput 20
16 : Sweetput-Soutput 11

Appendix C4 : Perovskite Microprobe Analyses

MARKT 173/26/K15/25

POINT ANALYSED	SiO2	TiO2	Al2O3	Cr2O3	FeO	MnO	MgO	CaO	Na2O	K2O	SrO	ZrO2	Nb2O5	La2O3	Ce2O3	Pr2O3	Nd2O3	Sm2O3	ThO2	TOTAL
46/359	0.021	49.320	0.162	0.491	2.248	0.000	0.058	33.310	0.780	0.068	0.430	0.373	1.312	1.641	4.990	0.591	1.984	0.162	1.099	99.040
42/351	0.014	50.010	0.166	0.514	2.048	0.000	0.042	34.190	0.656	0.034	0.450	0.288	0.930	1.631	4.701	0.575	1.867	0.167	0.675	98.958
42/351 edge	0.055	50.090	0.164	0.459	2.127	0.000	0.068	34.500	0.630	0.060	0.430	0.309	0.915	1.561	4.567	0.524	1.809	0.187	0.507	98.962
156/356	0.000	49.980	0.167	0.482	2.182	0.000	0.055	33.910	0.740	0.035	0.452	0.313	1.190	1.673	4.854	0.588	1.939	0.169	0.958	99.687
111/345	0.000	49.600	0.172	0.508	2.161	0.000	0.055	33.850	0.759	0.042	0.446	0.313	1.220	1.605	4.831	0.624	1.975	0.186	1.123	99.470
AVERAGES	0.018	49.800	0.166	0.491	2.153	0.000	0.056	33.952	0.713	0.048	0.442	0.319	1.113	1.622	4.789	0.580	1.915	0.174	0.872	99.223

DROOGFONTEIN 173/27/K19/3

POINT ANALYSED	SiO2	TiO2	Al2O3	Cr2O3	FeO	MnO	MgO	CaO	Na2O	K2O	SrO	ZrO2	Nb2O5	La2O3	Ce2O3	Pr2O3	Nd2O3	Sm2O3	ThO2	TOTAL
266/424	0.000	52.840	0.269	0.503	1.679	0.000	0.048	37.290	0.366	0.081	0.462	0.116	0.402	1.094	2.575	0.266	0.904	0.091	0.274	99.260
216/459	0.000	53.010	0.235	0.593	1.543	0.000	0.040	37.290	0.365	0.051	0.520	0.083	0.397	1.136	2.626	0.292	0.886	0.093	0.287	99.447
206/463	0.035	52.770	0.280	0.545	1.616	0.000	0.054	36.860	0.362	0.064	0.517	0.085	0.377	1.239	2.906	0.302	0.982	0.080	0.309	99.383
130/420	0.019	53.110	0.274	0.502	1.652	0.000	0.054	37.230	0.394	0.061	0.506	0.103	0.389	1.136	2.683	0.299	0.924	0.000	0.280	99.616
110/415 core	0.014	53.080	0.269	0.495	1.584	0.000	0.049	37.100	0.379	0.060	0.486	0.119	0.398	1.185	2.687	0.285	0.902	0.064	0.298	99.454
110/415 edge	0.229	55.560	0.078	0.274	0.992	0.000	0.105	38.700	0.373	0.027	0.676	0.071	0.639	0.531	0.879	0.081	0.280	0.000	0.022	99.517
101/407 core	0.039	52.460	0.285	0.471	1.782	0.000	0.053	36.920	0.408	0.060	0.484	0.174	0.434	1.094	2.658	0.287	0.915	0.077	0.294	98.895
101/407 edge	0.059	55.110	0.050	0.326	0.857	0.000	0.023	38.650	0.446	0.052	0.710	0.061	0.730	0.531	0.947	0.107	0.300	0.000	0.042	99.001
199/462 core	0.285	53.010	0.198	0.294	1.416	0.000	0.052	37.730	0.367	0.253	0.431	0.073	0.351	0.722	1.543	0.197	0.542	0.000	0.092	97.556
199/462	0.052	54.840	0.059	0.148	1.187	0.000	0.015	38.440	0.463	0.149	0.709	0.061	0.670	0.535	0.976	0.113	0.337	0.000	0.045	98.799
AVERAGES	0.073	53.579	0.200	0.415	1.431	0.000	0.049	37.621	0.392	0.086	0.550	0.095	0.479	0.920	2.048	0.223	0.697	0.041	0.194	99.093

SWEETPUT-SOUTPUT 173/26/K40/10

POINT ANALYSED	SiO2	TiO2	Al2O3	Cr2O3	FeO	MnO	MgO	CaO	Na2O	K2O	SrO	ZrO2	Nb2O5	La2O3	Ce2O3	Pr2O3	Nd2O3	Sm2O3	ThO2	TOTAL
circle 6	0.000	55.670	0.210	0.540	1.300	0.000	0.000	39.420	0.270	0.019	0.415	0.000	0.325	0.760	1.720	0.212	0.615	0.000	0.125	101.60
circle 5	0.000	54.060	0.190	0.690	1.270	0.000	0.011	39.410	0.220	0.018	0.420	0.031	0.322	0.702	1.807	0.190	0.657	0.068	0.139	100.21
circle 4 core	0.000	54.140	0.190	0.570	1.290	0.000	0.008	39.420	0.240	0.016	0.399	0.031	0.331	0.744	1.765	0.230	0.632	0.071	0.143	100.22
circle 4 edge	0.000	54.730	0.140	0.300	1.080	0.018	0.033	39.590	0.260	0.019	0.456	0.037	0.374	0.604	1.178	0.163	0.375	0.000	0.051	99.408
circle 3 core	0.000	54.110	0.190	0.500	1.300	0.000	0.016	39.440	0.260	0.017	0.658	0.031	0.338	0.695	1.601	0.173	0.732	0.000	0.109	100.17
circle 3 edge	0.000	53.970	0.190	0.440	1.410	0.000	0.015	39.230	0.260	0.048	0.462	0.260	0.351	0.738	1.675	0.474	0.581	0.000	0.096	100.20
circle 2	0.000	54.280	0.190	0.550	1.260	0.000	0.007	39.360	0.240	0.013	0.381	0.067	0.402	0.858	1.801	0.212	0.548	0.066	0.127	100.36
AVERAGES	0.000	54.423	0.186	0.513	1.273	0.003	0.013	39.410	0.250	0.021	0.456	0.065	0.349	0.729	1.650	0.236	0.591	0.029	0.113	100.31

BRANDEWYNSKUIL 173/26/K6/12

POINT ANALYSED	SiO2	TiO2	Al2O3	Cr2O3	FeO	MnO	MgO	CaO	Na2O	K2O	SrO	ZrO2	Nb2O5	La2O3	Ce2O3	Pr2O3	Nd2O3	Sm2O3	ThO2	TOTAL
279/464	0.135	50.400	0.152	0.983	1.991	0.000	0.035	35.590	0.476	0.097	0.739	0.135	0.472	1.507	3.807	0.401	1.295	0.099	0.294	98.608
240/453	0.073	51.160	0.144	1.019	1.983	0.000	0.039	35.870	0.470	0.081	0.812	0.096	0.506	1.518	3.708	0.419	1.286	0.118	0.273	99.575
165/392	0.142	51.150	0.148	0.821	2.315	0.000	0.049	35.500	0.566	0.208	0.785	0.134	0.576	1.524	3.627	0.408	1.195	0.080	0.265	99.493
101/417	0.147	50.300	0.154	1.041	2.189	0.000	0.045	35.740	0.493	0.147	0.751	0.119	0.489	1.422	3.685	0.405	1.244	0.096	0.280	98.747
43/409	1.791	52.180	0.710	0.766	2.023	0.000	1.688	34.300	0.486	0.336	0.927	0.077	0.581	1.367	3.144	0.350	0.990	0.087	0.228	102.03
130/531	0.048	51.540	0.105	0.258	2.231	0.000	0.028	34.790	0.678	0.117	0.861	0.109	0.568	1.548	4.071	0.430	1.368	0.121	0.312	99.183
52/389	0.399	52.670	0.171	0.782	1.843	0.000	0.186	35.760	0.624	0.092	0.885	0.075	0.626	1.430	3.298	0.361	1.062	0.096	0.249	100.61
235/445	0.417	51.410	0.194	1.080	2.325	0.000	0.321	35.300	0.491	0.154	0.779	0.074	0.491	1.494	3.558	0.383	1.242	0.106	0.264	100.08
AVERAGES	0.394	51.351	0.222	0.844	2.113	0.000	0.299	35.356	0.536	0.154	0.817	0.102	0.539	1.476	3.612	0.395	1.210	0.100	0.271	99.791

JONKERWATER 173/26/K51/2

POINT ANALYSED	SiO2	TiO2	Al2O3	Cr2O3	FeO	MnO	MgO	CaO	Na2O	K2O	SrO	ZrO2	Nb2O5	La2O3	Ce2O3	Pr2O3	Nd2O3	Sm2O3	ThO2	TOTAL
268/413	0.000	49.340	0.103	0.456	2.288	0.000	0.048	33.330	0.928	0.038	0.566	0.398	1.428	1.683	4.921	0.580	1.799	0.155	1.163	99.224
181/420	0.123	49.940	0.135	0.384	2.313	0.000	0.071	33.500	0.795	0.044	0.609	0.260	1.233	1.737	4.922	0.547	1.773	0.170	0.733	99.289
51/376	0.000	49.500	0.102	0.470	2.237	0.000	0.050	32.760	0.972	0.027	0.579	0.286	1.361	1.753	5.175	0.555	1.924	0.174	1.323	99.248
254/337	0.028	49.210	0.106	0.459	2.377	0.000	0.058	33.010	0.906	0.055	0.282	0.279	1.357	1.741	5.155	0.563	1.635	0.162	1.194	98.577
268/350	0.049	49.720	0.112	0.353	2.378	0.000	0.057	33.590	0.805	0.056	0.608	0.279	1.210	1.767	4.995	0.581	1.761	0.155	0.684	99.160
AVERAGES	0.040	49.542	0.112	0.424	2.319	0.000	0.057	33.238	0.881	0.044	0.529	0.300	1.318	1.736	5.034	0.565	1.778	0.163	1.019	99.100

MARKT 173/26/K15/24

POINT ANALYSED	SiO2	TiO2	Al2O3	Cr2O3	FeO	MnO	MgO	CaO	Na2O	K2O	SrO	ZrO2	Nb2O5	La2O3	Ce2O3	Pr2O3	Nd2O3	Sm2O3	ThO2	TOTAL
circle 1	0.000	52.000	0.190	0.480	2.340	0.000	0.046	35.330	0.581	0.037	0.466	0.256	0.986	1.635	4.710	0.553	1.838	0.151	0.496	102.10
circle 2	0.000	49.900	0.170	0.560	2.140	0.000	0.045	34.330	0.727	0.044	0.455	0.235	1.164	1.641	4.865	0.565	1.822	0.163	1.012	99.838
large clear perov	0.488	48.330	0.160	0.550	2.330	0.000	0.407	32.990	0.790	0.057	0.432	0.294	1.376	1.671	4.933	0.600	1.899	0.177	1.233	98.717
large sq perov	0.000	49.200	0.170	0.550	2.250	0.000	0.053	33.970	0.753	0.038	0.473	0.299	1.374	1.645	4.835	0.603	1.884	0.180	1.130	99.407
perov (5)	0.000	49.690	0.170	0.560	2.250	0.000	0.051	34.270	0.728	0.042	0.457	0.278	1.179	1.645	4.805	0.553	1.848	0.155	0.939	99.620
perov (6)	0.000	49.880	0.170	0.520	2.340	0.000	0.045	34.430	0.715	0.055	0.461	0.270	1.140	1.682	4.867	0.559	1.853	0.197	0.799	99.983
perov next to mica	0.000	49.070	0.170	0.560	2.320	0.000	0.055	33.500	0.771	0.093	0.455	0.308	1.378	1.667	4.994	0.556	1.919	0.199	1.184	99.199
AVERAGES	0.070	49.724	0.171	0.540	2.281	0.000	0.100	34.117	0.724	0.052	0.457	0.277	1.228	1.655	4.858	0.570	1.866	0.175	0.970	99.837

HAARTEBEESFONTEIN 173/27/K1/16

POINT ANALYSED	SiO2	TiO2	Al2O3	Cr2O3	FeO	MnO	MgO	CaO	Na2O	K2O	SrO	ZrO2	Nb2O5	La2O3	Ce2O3	Pr2O3	Nd2O3	Sm2O3	ThO2	TOTAL
circle 3	0.000	55.000	0.230	0.044	0.940	0.031	0.048	39.280	0.392	0.009	0.128	0.103	0.532	0.423	1.273	0.158	0.595	0.085	0.066	99.337
circle 4 core	0.000	54.770	0.250	0.036	0.960	0.028	0.051	38.910	0.467	0.017	0.114	0.103	0.627	0.471	1.558	0.205	0.729	0.108	0.386	99.790
circle 4 edge	0.000	54.990	0.290	0.023	0.970	0.023	0.026	40.900	0.160	0.037	0.158	0.243	0.487	0.252	0.364	0.057	0.082	0.000	0.051	99.113
core (4)	0.000	54.490	0.260	0.038	1.010	0.035	0.051	38.770	0.479	0.015	0.120	0.096	0.643	0.480	1.597	0.188	0.741	0.094	0.439	99.546
edge (5)	0.000	55.690	0.210	0.039	0.820	0.037	0.046	40.390	0.287	0.048	0.115	0.110	0.386	0.317	0.645	0.065	0.217	0.000	0.051	99.473
circle 2 core	0.000	55.570	0.200	0.077	1.010	0.039	0.048	40.180	0.357	0.007	0.128	0.139	0.469	0.299	0.670	0.101	0.235	0.000	0.051	99.580
circle 2 edge	0.000	55.890	0.200	0.053	1.060	0.035	0.043	40.330	0.276	0.006	0.120	0.096	0.384	0.305	0.560	0.052	0.166	0.000	0.051	99.627
core (8)	0.000	54.800	0.250	0.043	0.970	0.031	0.046	39.050	0.424	0.015	0.104	0.095	0.589	0.431	1.387	0.204	0.646	0.088	0.224	99.397
edge (9)	0.000	54.640	0.290	0.032	0.880	0.025	0.033	40.690	0.174	0.024	0.133	0.232	0.473	0.257	0.372	0.053	0.086	0.000	0.051	98.445
circle 2 core	0.000	53.940	0.280	0.023	1.070	0.035	0.060	38.370	0.521	0.014	0.102	0.130	0.679	0.444	1.543	0.229	0.757	0.115	0.672	98.984
dark area circle 2	0.000	54.280	0.250	0.037	1.010	0.034	0.052	38.610	0.451	0.017	0.116	0.099	0.630	0.470	1.457	0.209	0.694	0.105	0.322	98.843
same grain edge	0.000	55.020	0.229	0.053	0.880	0.025	0.046	39.320	0.382	0.028	0.127	0.106	0.095	0.399	1.099	0.145	0.453	0.093	0.051	98.542
AVERAGES	0.000	54.923	0.244	0.042	0.965	0.032	0.046	39.567	0.364	0.020	0.122	0.129	0.500	0.379	1.044	0.139	0.450	0.057	0.201	99.223

VIOOLKRAAL WEST 173/26/K46/3

POINT ANALYSED	SiO2	TiO2	Al2O3	Cr2O3	FeO	MnO	MgO	CaO	Na2O	K2O	SrO	ZrO2	Nb2O5	La2O3	Ce2O3	Pr2O3	Nd2O3	Sm2O3	ThO2	TOTAL
195/424	0.000	53.370	0.158	0.018	1.195	0.000	0.027	36.060	0.881	0.021	0.232	0.055	0.929	0.905	2.730	0.325	1.214	0.156	0.251	98.437
181/478	0.000	52.720	0.159	0.014	1.204	0.000	0.025	35.170	1.096	0.007	0.234	0.054	1.171	1.048	3.329	0.426	1.470	0.193	0.644	98.964
179/479	0.018	53.270	0.142	0.000	1.241	0.000	0.025	35.620	1.037	0.006	0.213	0.068	1.310	0.913	2.919	0.370	1.368	0.187	0.412	99.119
179/479 edge	0.023	53.330	0.159	0.000	1.306	0.000	0.032	35.880	0.962	0.000	0.225	0.074	1.233	1.005	3.011	0.386	1.281	0.168	0.199	99.274
195/424	0.000	53.280	0.142	0.015	1.108	0.000	0.023	35.470	0.952	0.019	0.219	0.059	1.027	0.944	2.944	0.341	1.310	0.170	0.29	98.313
272/394	0.133	52.860	0.157	0.012	1.235	0.000	0.030	35.360	1.035	0.009	0.204	0.082	1.374	0.923	3.002	0.417	1.404	0.180	0.64	99.057
AVERAGES	0.029	53.138	0.153	0.010	1.200	0.000	0.027	35.593	0.994	0.010	0.221	0.065	1.174	0.956	2.989	0.378	1.341	0.176	0.406	98.861

WITBERG PIPE 173/25/K10/13

POINT ANALYSED	SiO2	TiO2	Al2O3	Cr2O3	FeO	MnO	MgO	CaO	Na2O	K2O	SrO	ZrO2	Nb2O5	La2O3	Ce2O3	Pr2O3	Nd2O3	Sm2O3	ThO2	TOTAL
18/350	0.000	55.170	0.148	0.047	0.918	0.000	0.046	38.440	0.510	0.021	0.180	0.066	0.593	0.624	1.567	0.163	0.556	0.079	0.078	99.208
179/397	0.016	54.150	0.173	0.039	1.285	0.000	0.066	37.600	0.615	0.030	0.164	0.044	0.565	0.673	1.899	0.236	0.718	0.088	0.365	98.726
35/342	0.023	49.960	0.401	0.027	1.536	0.000	0.077	35.310	0.853	0.024	0.144	0.663	2.920	1.135	3.300	0.380	1.277	0.160	0.222	98.412
40/328	0.056	54.940	0.246	0.049	1.049	0.000	0.042	39.650	0.266	0.008	0.192	0.069	0.561	0.071	0.903	0.106	0.285	0.000	0.08	98.573
90/472	0.000	53.750	0.183	0.031	1.112	0.000	0.061	37.320	0.669	0.034	0.153	0.042	0.577	0.724	2.031	0.267	0.758	0.087	0.411	98.210
67/474	0.723	47.880	0.477	0.047	2.593	0.260	0.280	32.960	0.830	0.014	0.169	0.651	2.983	1.105	3.282	0.372	1.263	0.159	0.059	96.107
297/334	7.285	33.390	0.229	0.038	2.551	0.000	10.331	31.110	0.387	0.036	0.186	0.139	0.993	1.461	3.430	0.350	1.197	0.136	0.044	93.293
AVERAGES	1.158	49.891	0.265	0.040	1.578	0.037	1.558	36.056	0.590	0.024	0.170	0.239	1.313	0.828	2.345	0.268	0.865	0.101	0.180	97.504

Appendix D

Comparison of Analytical Techniques

D 1.1 Introduction

Trace elements have been analysed both by XRF and INAA techniques. This allows for the comparison of the two techniques for elements of overlap. In the case where elements were also obtained by isotope dilution, comparisons may also be made. In addition, some samples analysed by Smith et al (1985) at the Max Plank Institute for INAA, were also analysed by this author by INAA at the Schonland Centre at the University of the Witwatersrand. This allows for interlaboratory comparison.

D 1.2 XRF versus INAA

Data obtained using XRF are presented in Appendix C2, whilst INAA data are presented in Appendix C3. Overlapping trace element data from the two techniques include Ba, Rb, Zr, Co, Ni, U and Th. The data are plotted in the figures below.

It is clear that there is a reasonable agreement between the techniques for the elements Ba, Rb, Cr and Ni, although there is some scatter evident for Cr and Ni. There is a fair amount of scatter about the 1:1 line for the element Zr, with generally higher values being obtained by INAA than by XRF. For the elements Co, Th and U, a poor correlation is noted. In the case of Co, the data fall on two distinct trends of higher XRF values relative to

INAA values. For Th, INAA values are consistently higher than for XRF data, whilst for U, XRF data is very much higher than that for INAA.

In particular, one sample that shows the most scatter is the altered sample Eendekuil 6W. On the Cr plot, this sample plots far from the 1:1 correlation line with noticeably lower Cr concentrations obtained by INAA, whilst on the Rb plot XRF values are particularly low relative to INAA for this sample. On the Ba plot, INAA results are nearly twice that obtained for XRF, whilst on the Co plot a significant discrepancy is seen, with the INAA data giving a much higher concentration than that obtained by XRF. It is unclear as to exactly why this altered sample should plot off from the main trend shown by the rest of the data. It is possible that for this sample, inhomogeneities may be present - since it is extremely weathered, there are a lot of clay minerals present, which are notoriously difficult to pulverise during whole-rock preparation. This again highlights the need to analyse material that is as fresh as possible during geochemical studies.

For the most part, inconsistencies are probably due to calibration problems associated with the particular technique (eg XRF data for U and Th are rarely accurate in routine analyses of whole-rocks) and interferences may also play a part in obtaining such inconsistencies. It is considered that for the elements presented above, data for Th and U is more accurate using INAA, whilst for the other elements either technique gives reasonable data.

COMPARISON OF XRF vs INAA DATA
Data for Ba (ppm)

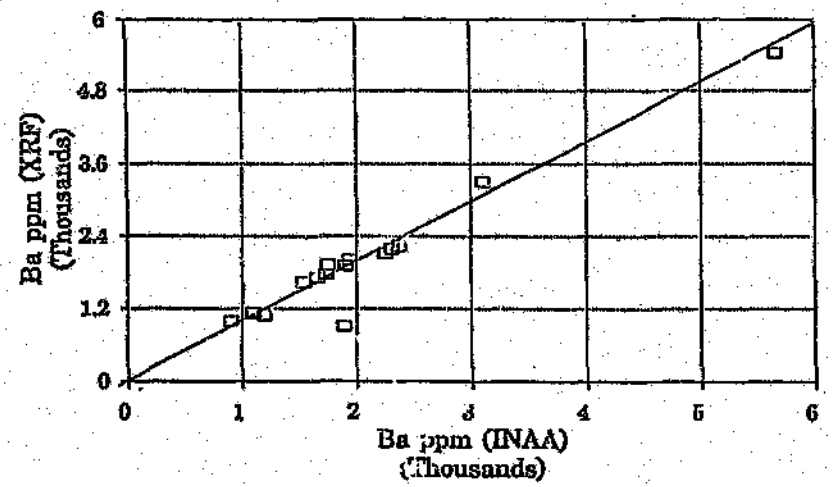

COMPARISON OF XRF vs INAA DATA
Data for Rb (ppm)

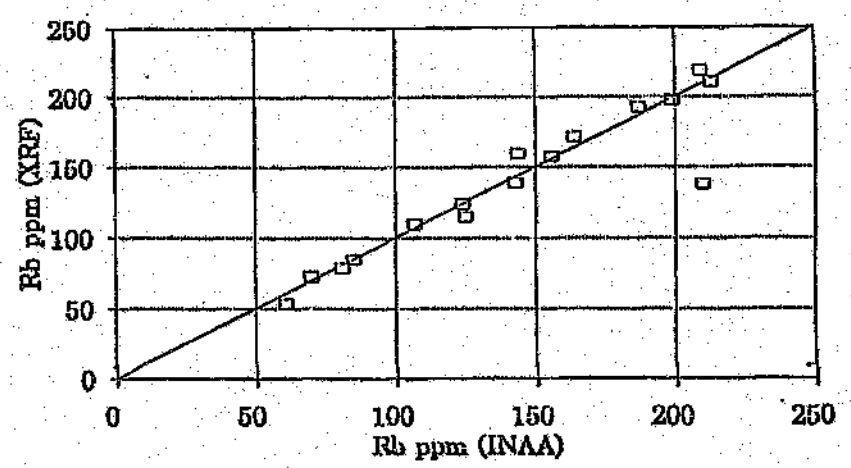

COMPARISON OF XRF vs INAA DATA
Data for Zr (ppm)

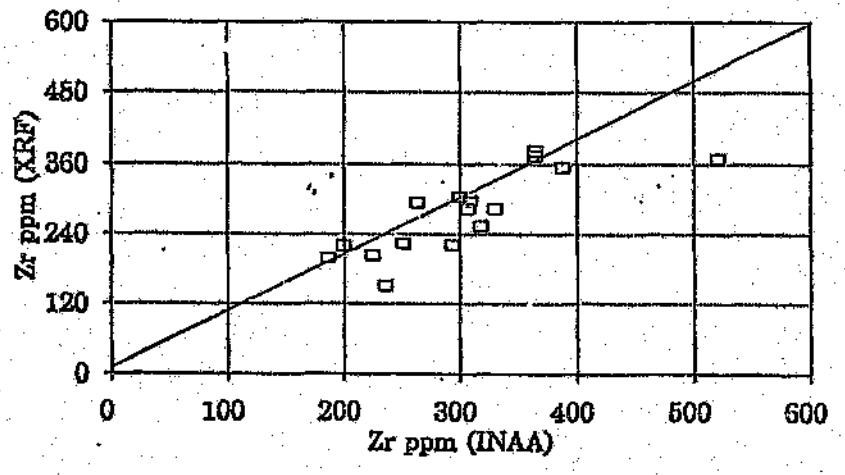

COMPARISON OF XRF vs INAA DATA
Data for Co (ppm)

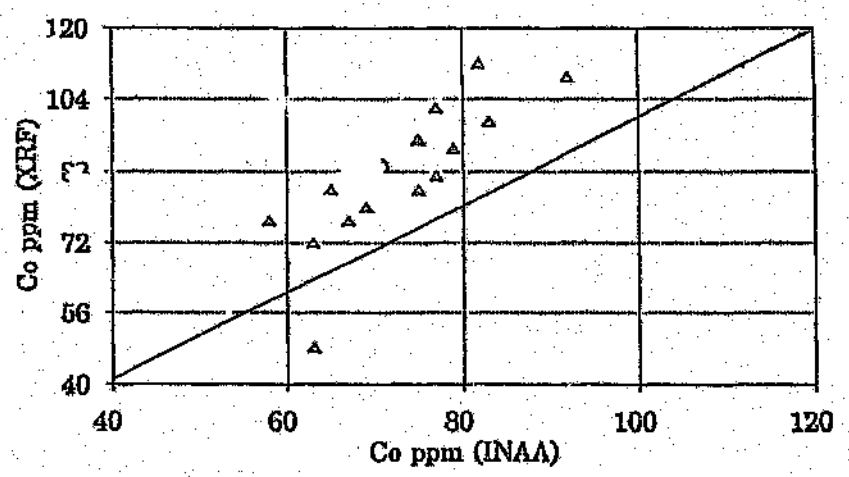

COMPARISON OF XRF vs INAA DATA
Data for Ni (ppm)

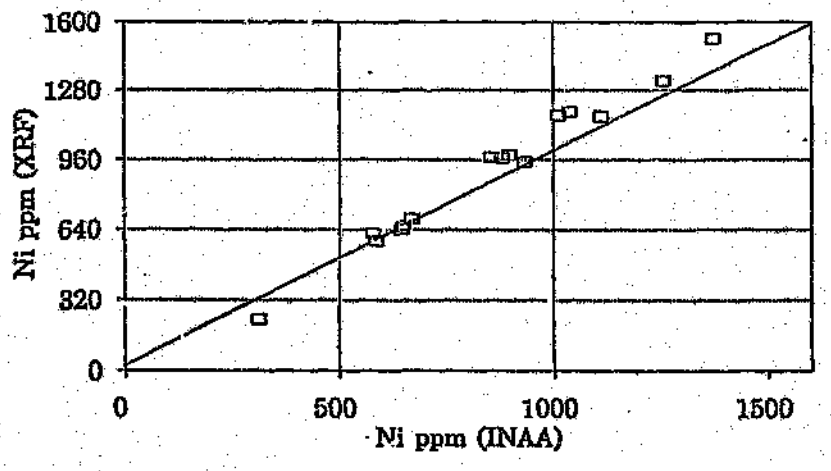

COMPARISON OF XRF vs INAA DATA
Data for Cr (ppm)

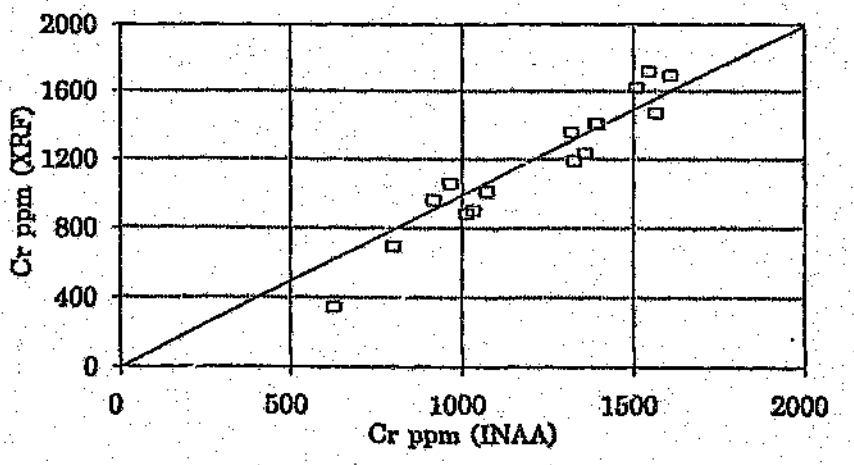

COMPARISON OF XRF vs INAA DATA
Data for Th (ppm)

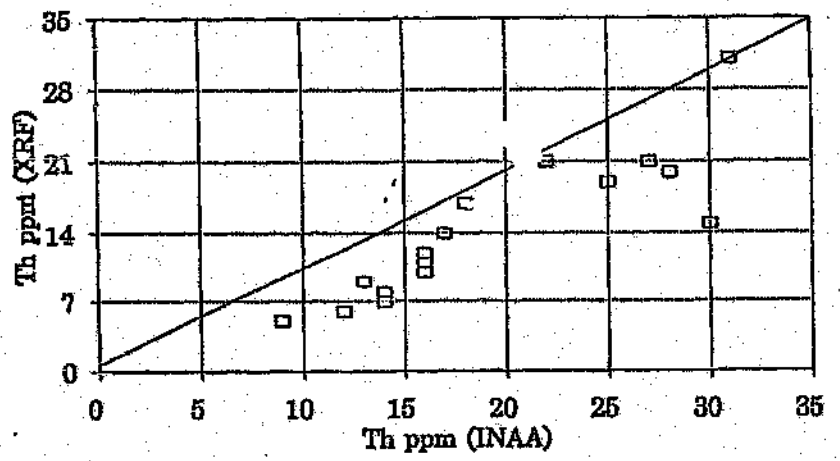

COMPARISON OF XRF vs INAA DATA
Data for U (ppm)

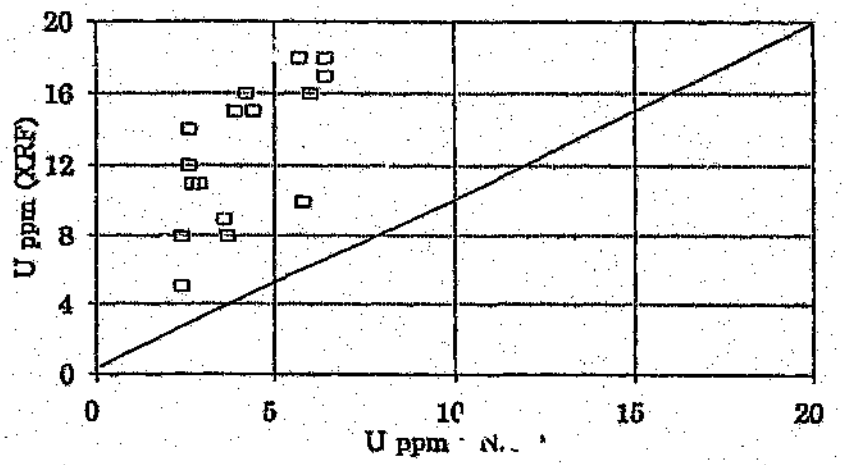

D 1.2 INAA Interlaboratory Correlation

A number of samples analysed by Smith et al (1985) at the Max Plank Institute using INAA were also analysed by this author using INAA at the Schonland Centre as internal controls on the data acquired for the Prieska Province kimberlites. The data obtained for two of these samples are plotted in Figures D8 and D9 below, to show the correspondance between the two labs for different elements. Only those elements for which there is poor correlation are labelled on these figures.

It can be seen from these plots that there is excellent agreement for the data obtained at the two different laboratories. Elements that do not correlate well include Yb, Lu, Sb, Ir, Na, K and Au, which give consistently higher concentration values in the Schonland dataset. Au and Ir show the greatest discrepancy, and two factors may be responsible for this. One is that these elements are present in very low concentrations in kimberlite and analytical uncertainty cannot be ruled out. The other reason is that gold jewelry (eg wedding bands) can cause severe contamination if not removed during the preparation of the whole-rock powder. In the case of K, sample FINSCH B is a very micaceous variety of kimberlite, and K would be dominantly held in this mineral. The difficulties in obtaining homogeneous whole-rock powders could have played a role in this discrepancy. Other samples analysed show very similar results and are therefore not displayed here. In spite of these few poor correlations, the agreement for the majority of elements is well within the analytical uncertainties, and the importance of selecting the correct standards to analyse at the same time as one's own samples is crucial to obtaing reproducible data.

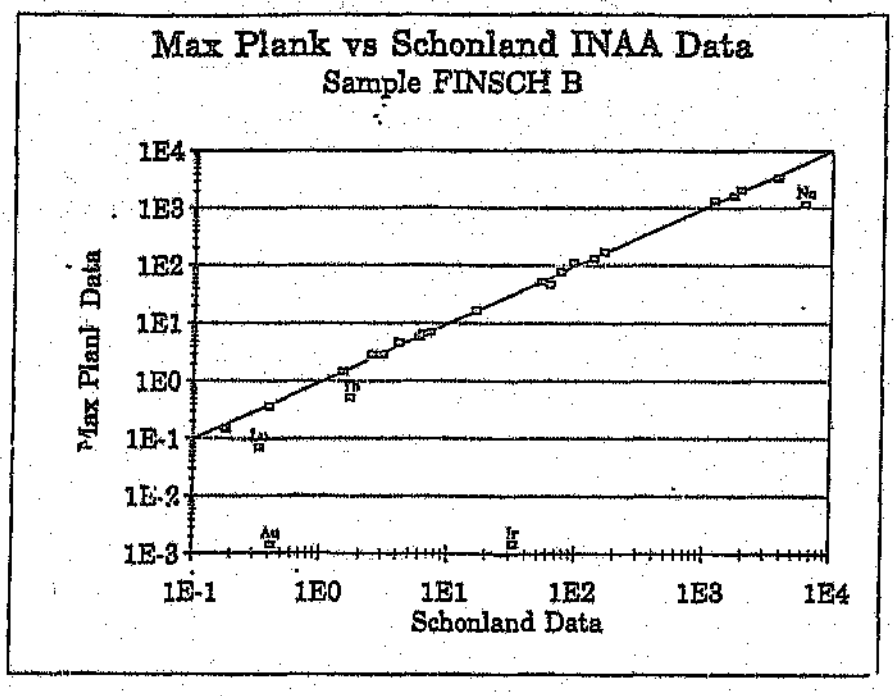

Figure D8 : Interlaboratory Correlation for Sample FINSCH B

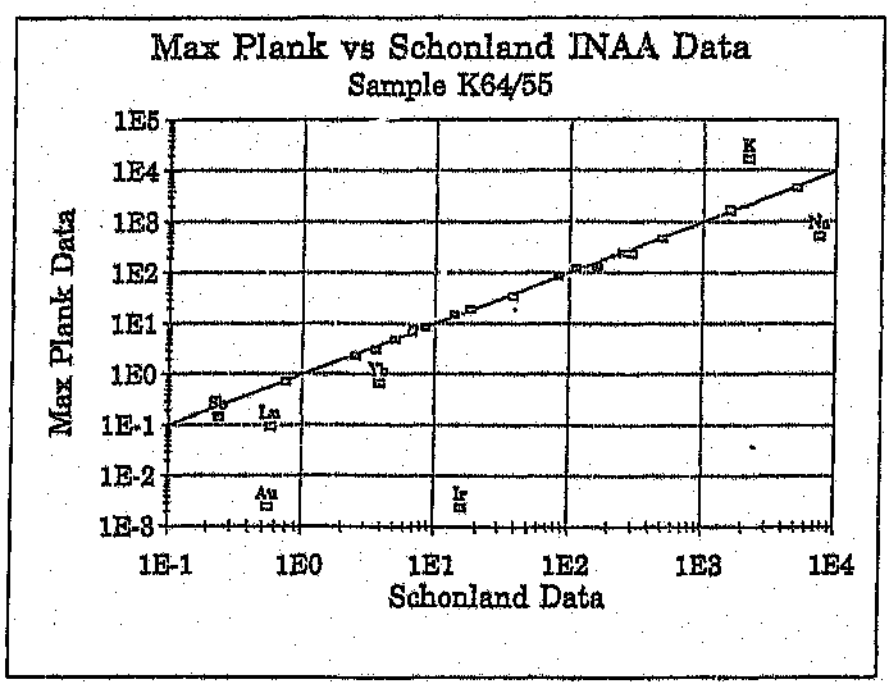

Figure D9: Interlaboratory Correlation for Sample K64/55

Appendix E

Southern African Kimberlite and Related Rock Age Database

The following table summarises age data for southern African kimberlites and some related rocks in the age interval of 60-204 Ma.

The columns contain the following information :

Column 1 - Locality Name
Column 2 - Age in Ma
Column 3 - Error on Age where known
Column 4 - Rock Type
- OM = Olivine Melilitite
- MB = Melilite Basalt
- I = Group I Kimberlite
- II = Group II Kimberlite
- T = Transitional Kimberlite

Column 5 - Method used to obtain age
Column 6 - Author Reference

Kimberlite Age Database - South Africa

Dikdoring	38		OM	OFF	K-Ar whole rock	Kroner (1973)
Braidfontein	54.1		OM	OFF	U-Pb zircon	Davis (1977b)
Bleskeafontein	56	3	OM	OFF	K-Ar whole rock	Moore & Verwoerd (1985)
Spinnkop	59.3		OM	OFF	K-Ar whole rock	Moore & Verwoerd (1985)
Spiegel River	62.6	1	MB	OFF	K-Ar whole rock	Duncan et al (1978)
Melkfontein	63.4		I	OFF	U-Pb zircon	Davis (1977b)
Robertson	63.7	1.3	MB	OFF	K-Ar whole rock	Duncan et al (1978)
Boksputs	64.2			OFF	U-Pb zircon	Davis (1978)
Platbakkies	66.7		OM	OFF	U-Pb zircon	Davis (1977b)
Boksputs	67.9		OM	OFF	U-Pb zircon	Davis (1978)
Riembreck	69		OM	OFF	U-Pb zircon	Davis (1978)
Rietfontein (Cape)	71.9		I	OFF	U-Pb zircon	Davis (1977b)
Lushof	72		I	OFF	U-Pb zircon	Davis (1977b)
Salpeterkop	72.5	1.2	MB		K-Ar biotite	Duncan et al (1978)
Hartebeesfontein	74	1	I	OFF	Rb/Sr Isochron	Smith et al. (in press)
Brittstown	74.4	0.8	I	OFF	Rb/Sr Isochron	Smith et al. (in press)
Swartheuwel	77	3	OM	OFF	K-Ar whole rock	Moore & Verwoerd (1985)
Sutherland	78	1.2	OM	OFF	K-Ar whole rock	Duncan et al (1978)
Tembani ranch	80		OM	OFF	Rb/Sr phlogopite	Colgan et al (1989)
McKenzies Post	80.4		I	OFF	U-Pb zircon	Davis (1977b)
Hoolkombo	81		OM	OFF	Rb-Sr phlogopite	Allsopp (unpubl.)
Wesselton	81	4	I	ON	Rb-Sr mica	Allsopp & Barrett (1975)
Beyersfontein	81.5	1	I	OFF	U-Pb zircon	(in) Skinner et al. (1991)
Bultfontein	84	3	I	ON	Rb-Sr mica	Allsopp & Barret (1975)
De Beers	84	3	I	ON	Rb-Sr phlogopite	Allsopp & Barret (1975)
Dutoitspan	84	3	I	ON	Rb/Sr Phlogopite	Allsopp & Barrett (1975)
Jagersfontein	85.6	1	I	ON	Rb/Sr whole rock	Allsopp et al (1989)
Saulpaas	86.5	2	I	ON	Rb/Sr ? mica	Allen (1990)
Kimberdam	86.9		I	ON	U/Pb zircon	Davis (1977)
Monastery	88	4	I	ON	Rb-Sr phlogopite	Allsopp & Barrett (1975)
Wesselton Sills	88.6		I	ON	Stratigraphy	Shee & Clement (1991)
Koffiefontein	90.4		I	ON	U/Pb zircon	Davis (1978)
Leicester	92.4		I	ON	U/Pb zircon	Davis (1978)
Kimberley Pool	94.9		I	ON	U/Pb zircon	Davis (1978)
Rietfontein	95	4	I	OFF	Rb/Sr micas	Allsopp et al (1989)
Droogfontein (GP 1)	100	25	T	OFF	Ion Probe Perovskite	Smith et al. (in press)
Goedgevonden	100		I	ON	Rb-Sr phlogopite, WR	Kramers & Smith (1983)
Uintjiesberg	100.7	1	I	OFF	Rb/Sr phlogopite	Smith et al (1985)
Pampoenpoort	103	1	I	OFF	Rb/Sr isochron	Smith et al. (in press)
Witberg Pipe	108		I	ON	Rb/Sr mica	Smith et al. (in press)
Randekuil	109		II	OFF	Rb-Sr phlogopite	Allsopp (1989)
Last Hope	111.5		I	ON	U-Pb zircon	Davis (1978)
Frank Smith	113.7	1	I	ON	Rb/Sr phlogopite	Smith et al (1985)
Newlands	114	1.6	II	ON	Rb/Sr mica W.R.	Smith et al (1985)
Sweetput-Stoutput	114	1	T	ON	Rb/Sr mica & W.R.	Smith et al. (in press)
Kalkput	115		II	OFF	U-Pb zircon	Davis (1978)
Markt	116	3	II	OFF	Rb/Sr isochron	Smith et al. (in press)
Welgevonden	116		II	OFF	Rb/Sr mica	Smith et al. (in press)
Mayeng	117		II	ON	Rb/Sr mica	Apter et al (1984)
Witberg dyke	117		II	ON	Rb/Sr isochron	Smith et al. (in press)
Middelwater	118	3	II	ON	Rb/Sr isochron	Smith et al. (in press)
Erasmus	118.4	2	II	ON	Rb/Sr mica W.R.	Smith et al (1985)
Bellsbank	118.8	2.8	II	ON	Rb-Sr phlogopite	Smith et al (1985)
Finsch	118.8	2.8	II	ON	Rb-Sr phlogopite	Smith et al (1985)
Jonkerwater	119	2	II	ON	Rb/Sr isochron	Smith et al. (in press)
Poortjie	119		II	ON	Rb-Sr phlogopite	Smith et al (1985)
Mokgonyane	121	2	II	ON	Rb/Sr phlogopite	Brown (1985)
Star	124		II	ON	K/Ar phlogopite	McIntyre & Dawson (1976)
Zout en Zuur	125		II	ON	K/Ar phlogopite	McIntyre & Dawson (1976)
New Elands	125.7	2	II	ON	Rb/Sr isochron W.R.	Allsopp et al (1989)
Sandrift	126	2	II	ON	Rb/Sr mica & W.R.	Smith et al. (in press)
Roberts Victor	127	3	II	ON	Rb-Sr phlogopite	Allsopp & Barrett (1975)
Bultmwbosch	133	27	II	ON	Rb/Sr phlogopite	Smith et al (1985)
Skietkop	136	9	T	OFF	Ion probe perovskite	Smith et al. (in press)
Mehlomveld	138	14	T	OFF	Ion probe perovskite	Smith et al. (in press)
Lace	140		T ?	ON	Rb/Sr phlogopite	
Bannisellise	150.0		I	OFF	U-Pb zircon	Davis (1977b)
Mazongwana	152	3	I	OFF	Rb/Sr phlogopite	Smith et al (1985)
Helam (Swartruggens)	156	13	II	ON	Rb/Sr phlogopite	Smith et al (1985)
Swartruggens	153	13	II	ON	Rb-Sr phlogopite	Smith et al (1985)
Klipfontein	159	40	?	ON	Rb/Sr phlogopite	Smith et al (1985)
Middelputs	165		II	ON	Rb/Sr phlogopite	Allsopp (1989)
Skietkop	167	8	T	OFF	Ion probe perovskite	Smith et al. (in press)
Blondskloof	170		II	ON	Rb-Sr phlogopite	Smith et al (1985)
Droogfontein	174		T	OFF	Ion Probe Perovskite	Smith et al. (in press)
Clarkton	193.9		I	OFF	U/Pb zircon	Davis (1978)
Dokolwayo	203	7	II	ON	Rb-Sr phlogopite	Allsopp & Roddick (1984)

References

Aldridge, L.T., 1956. Measurement of Radioactive Ages of Rocks. *Science*, V.123, pp.871-875.

Allsopp, H.L., Nicolaysen, L.O. and Hahn-Weinheimer, P., 1969. Rb\K ratios and Sr-isotopic compositions of minerals in eclogitic and periotitic rocks. *E.P.S.L.*, v. 5, 231-244.

Allsopp, H.L. and Barrett, D.R. 1975. Rb-Sr age determinations on South African Kimberlite Pipes. *Phys. Chem. Earth.*, v. 9, 605-617.

Allsopp, H.L. and Kramers, J.D., 1977. Rb-Sr and U-Pb age determinations of southern African kimberlite pipes. *In: Extended Abstracts, 2IKC.*, New Mexico.

Allsopp, H.L., Köstlin, E.O., Welke, H.J., Burger, A.J., Kröner, A. and Blignault, H.J., 1979. Rb-Sr and U-Pb Geochronology of Late Precambrian-Early Palaeozoic Igneous Activity in the Richtersveld (South Africa) and southern South West Africa. *T.G.S.S.A.*, v. 82, 185-204.

Allsopp, H.L., and Roddick, J.C., 1984. Rb-Sr and 40Ar-39Ar age determinations on phlogopite micas from the pre-Lebombo group Dokolwayo kimberlite pipe. *Spec. Publ. geol. Soc. S. Afr.*, v. 13, 267-271.

Allsopp, H.L., Bristow, J.W., Smith, C.B., Brown, R., Gleadow, A.J.W., Kramers, J.D. and Garvie, O.G., 1989. A summary of radiometric dating methods applicable to

kimberlites and related rocks. *In : Kimberlites and Related Rocks, Volume 1,* 4IKC., Perth, pp.343-357.

Altermann, W. and Hälbich, I.W., 1991. Structural history of the southwestern corner of the Kaapvaal Craton and the adjacent Namaqua realm : new observations and a re-appraisal. *Precambrian Research,* 52, 133-166.

Atkinson, W.J., Highes, F.E. and Smith, C.J., 1984. A review of the kimberlitic rocks of Western Australia. In : Kornprobst, J. (ed.), *Kimberlites I : Kimberlites and Related Rocks,* pp. 195-224. Elsevier, Amsterdam.

Bailey, D.K., 1982. Mantle metasomatism - continuing chemical change within the Earth. *Nature,* v. 296, no. 5857, 525-530.

Bailey, D.K., 1992. Petrogenetic implications of the timing of alkaline, carbonatite, and kimberlite igneous activity in Africa. *In : Ext. Abs., 24th Geological Conference,* Bloemfontein South Africa, pp.20-21.

Barrett, D.R. and Berg, G.W., 1975. Complementary petrographic and strontium-isotope ratio studies of South African kimberlite. *Phys. Chem. Earth.,* v. 9, 619-635.

Berg, G.W. and Allsopp, H.L., 1972. Low 87/86 Sr ratios in fresh South African kimberlites. *E.P.S.L.,* v. 16, 27-30.

Bizzi, L.A., Smith, C.B., de Wit, M.J., Armstrong, R.A., and Meyer, H.O.A., 1991. Mesozoic kimberlites and related alkalic rocks in south-western Sao Francisco Craton, Brazil : a case for local mantle reservoirs and their interaction. In :

Ext. Abs., 5IKC, Araxa, Brazil, pp. 17-19.

Boctor, N.Z. and Boyd, F.R., 1978. Distribution of rare earth elements in perovskite from kimberlites. *C.I.W.Yb,* 78-79, N. 1790, 572-574.

Boctor, N.Z. and Boyd, F.R., 1980. Oxide minerals in layered kimberlite-carbonate sills from Benfontein, South Africa. *Contrib. Min. Petrol.,* V. 76, 253-259.

Bristow, J.W., and Hatton, C.J., 1992. Setting of Basalts and Alkaline Rocks in Relation to the Cratonic Structure of southern Africa. *In : Ext. Abs., 24th Geological Conference,* Bloemfontein South Africa, pp.57-58.

Brown, R.W., Allsopp, H.L., Bristow, J.W., and Smith, C.B., 1989. Improved precision of Rb-Sr dating of kimberlitic micas : An assessment of a leaching technique. *Chemical Geology (Isotope Geoscience Section),* V.79, pp.125-136.

Clement, C.R., 1982. A comparative geological study of some major kimberlite pipes in the northern Cape and Orange Free State. Ph.D. thesis (unpubl.), University of Cape Town.

Clement, C.R. and Skinner, E.M.W., 1985. A textural- genetic classification of kimberlites. *T.G.S.S.A.,* v. 88, 403-409.

Colgan, E.A., Clark, T.C., Bristow, J.W. and Allsopp, H.L., 1989. Geological setting, petrography and petrogenesis of olivine melilitites of the Natal coast, South Africa. In: *Proc. 4I.K.C.,* Perth, 419-435.

Daniels, L.R.M., and Gurney, J.J., 1989. The chemistry of the garnets, chromites and diamond inclusions of the Dokolwayo kimberlite, Kingdom of Swaziland. *In : Kimberlites and Related Rocks*, Volume 2, 4IKC, Perth, 1986, pp. 1012-1021.

Davis, G.L., 1977. The ages and contents of zircons from kimberlites and associated rocks. In: *Extended abstracts, 2IKC.*, New Mexico.

Davis, G.L., 1978. Zircons from the mantle. In: Short papers, 4th Int. Conf. Geochron, Cosmochron, *Isotope Geol.*, 86-88.

Dawson, J.B., 1967. Geochemistry and origin of kimberlite. In: *Ultramafic and Related Rocks* (Ed. P.J. Wyllie) Wiley, New York, p. 241-251.

Dawson, J.B., 1971. Advances in Kimberlite Geology. *Earth Sci. Rev.*, V.7, p.187-214.

Dawson, J.B., 1972. Kimberlites and their relationship to the upper mantle. *R. Soc. London Philos. Trans. Ser.*, A 271, p.297-311.

Dawson, J.B., 1980. *Kimberlites and their Xenoliths.* Springer-Verlag, New York, 252 pp.

Dawson, J.B. 1989. Geographic and Time Distribution of Kimberlites and Lamproites: Relationships to Tectonic Processes. In: *Kimberlites and Related Rocks*, Volume 1, 4IKC, Perth, 1986, pp. 323-342.

Dupre, B., and Allegre, C.J., 1983. Pb-Sr isotope variation in Indian Ocean basalts and mixing phenomena. *Nature*, V.303, pp142-146.

Eggler, D.H. and Wendlandt, R.F. 1977. Phase relations of a kimberlite composition. *C.I.W.Y.*, v. 77, n. 1755, 751-756.

Eggler, D.H. 1989. Kimberlites: how do they form ? *In : Kimberlites and Related Rocks*, Volume 1, 4IKC, Perth, 1986, pp. 489-504.

Egglington, B.M.,, and Harmer, R.E., 1991. *GEODATE: A Program for the Processing and Regression of Isotope Data using IBM-Compatible Microcomputers*, CSIR Manual EMA-H 9102, 70pp.

Erasmus, C.S., Fesq, H.W., Kable, E.J.D., Rasmussen, S.E. and Selschopp, J.P.F., 1977. The NIMROC samples as reference materials for neutron activation. *J. Radio. Anal. Chem.*, V.39, pp.323-329.

Fesq, H.W., Kable, E.J.D. and Gurney, J.J., 1975. Aspects of the geochemistry of kimberlites from the Premier Mine and other South African occurrences, with particular reference to the rare earth elements. *Phys. Chem. Earth*, V.9, pp. 687-707.

Foley, S.F. 1993. An experimental study of olivine lamproite:First results from the diamond stability field. *Geochimica et Cosmochimica Acta*, V.57, pp.483-489.

Fraser, K.J., Hawkesworth, C.J., Erlank, A.J., Mitchell, R.H. and Scott-Smith, B.H., 1985. Sr, Nd and Pb isotope and minor

element geochemistry of lamproites and kimberlites. *E.P.S.L.*, v. 76, 57-70.

Fraser, K.J., 1987. Petrogenesis of Kimberlites from South Africa and Lamproites fr ⁻ : Western Australia and North America. Ph.D. thesis (unpubl.), Open University.

Harmer, R.E. and Eglington, B.M., 1990. A review of the statistical principles of geochronometry : towards a more consistent approach for reporting geochronological data. '..A.J.G., 93, (5/6), 845-856.

Harris, P.G. and Middelmost, E.A.K., 1969. The Evolution of Kimberlites. *Lithos*, V.3, p.77-88.

Heaman, L.M., 1989. The nature of the subcontinental mantle from Sr-Nd-Pb isotopic studies on kimberlitic perovskite. *E.P.S.L.*, 92, 323-334.

Hawkesworth, C.J., and van Calsteren, P., 1984. Radiogenic Isotopes - some geological applications. *In: Rare Earth Element Geochemistry*. (Ed: P. Henderson), Elsevier, Oxford, pp.375-421.

Hawthorne, J.B. 1975. Model of a kimberlite pipe. *Phys. Chem. Earth.*, v. 9, 1-15.

Ilupin, I.P., and Lutz, B.G., 1971. The chemical composition of kimberlite and questions on the origin of kimberlite magmas. *Sovetskaya Geol.*, V.6., 61-73.

Jacobs, J., Thomas, R.J., and Weber, K., 1993. Accretion and

indentation tectonics at the southern edge of the Kaapvaal caron during the Kibaran (Grenville) orogeny. *Geology,* V.21, p.203-206.

Jones, A.P. and Wyllie, P.J., 1984. Minor elements in perovskite from kimberlites and distribution of the rare earth elements : an electron probe study. *E.P.S.L.,* 69, 128-140.

Jordan, T.H., 1975. The continental tectosphere. *Review of Geophysics and Space Physics,* v. 13, n. 3, 1-12.

Jordan, T.H., 1978. Composition and development of the continental tectosphere. *Nature,* v. 274, 544-548.

Jordan, T.H., 1988. Structure and formation of the continental tectosphere. J. Petrol.

Kramers, J.D., 1977. Lead and strontium isotopes in Cretaceous kimberlites and mantle-derived xenolithe from southern Africa. *E.P.S.L.,* v. 34, 419-431.

Kramers, J.D., and Smith, C.B., 1983. A feasibility study of U-Pb and Pb-Pb dating of kimberlites using groundmass mineral fractions and whole-rock samples. *Isotope Geoscience,* 1, 23-38.

le Roex, A.P. 1987. Geochemical correlation between southern African kimberlites and South Atlantic hotspots. *Nature,* v. 324, 243-245.

Lock, B.E., 1980. Flat plate subduction and the Cape Fold Belt of South Africa. *Geology,* V.8, pp.35-39

Macintyre, R.W., and Dawson, J.B., 1976. Age and significance of some South African kimberlites. *4th Eur. Colloq. Geochron. Cocmochron Isotope Geol.* Amsterdam, Abst. 66.

Marsh, J.S., Sweeney, R.J., and Armstrong, R.A., 1992. New Pb, Sr and Nd Isotopic Data from the Karoo Province. *In: Ext. Abs., 24th Geological Conference,* Geol. Soc. S.A., Bloemfontein, pp.262-264.

McCulloch, M.T., Jaques, A.L., Nelson, D.R. and Lewis, J.D. 1983. Nd and Sr isotopes in kimberlites and lamproites from western Australia : an enriched mantle origin. *Nature,* v. 302, 400-403.

McKenzie, D. 1985. The extraction of magma from the crust and mantle. *E.P.S.L.,* v. 74, 81-91.

Mitchell, R.H., 1972. Composition of perovskite in kimberlite. *Am. Mineral.,* 57, 1748-1753.

Mitchell, R.H. 1986. *Kimberlites : mineralogy, geochemistry and petrology.* Plenum press, New York.

Mitchell, R.H. 1989. Aspects of the petrology of kimberlites and lamproites : some definitions and distinctions. *In: Kimberlites and Related Rocks,* Volume 1, 4th IKC, Perth, 1986, pp.7-45.

Mitchell, R.H. and Reed, S.J.B., 1988. Ion microprobe determination of rare earth elements in perovskite from kimberlites and alnöites. Min. Mag., v. 52, 331-339.

Moore, A.E. and Verwoerd, W.J. (1985). The olivine melilitite

- 'kimberlite' - carbonatite suite of Namaqualand and Bushmanland, South Africa. *T.G.S.S.A.*, 88, 281-294.

Nixon, P.H. 1973. *Lesotho kimberlites.* Lesotho Natl. Dev. Co., Maseru. 350pp.

Nixon, P.H., Rogers, N.W., Gibson, I.L. and Grey, A., 1981. Depleted and fertile mantle xenoliths from South African kimberlites. *Ann. Rev. Earth Planet. Sci.*, 9, 285-309.

Nixon, P.H., Boyd, F.R. and Boctor, N.Z., 1983. East Griqualand kimberlites. *T.G.S.S.A.*, v. 86, 221-236.

Noble, S.R., Lightfoot, P.C., and Sharer, U., 1989. A new method for single filament isotope analysis of Nd using insitu reduction. *Chem. Geol. (Iso. Geosci.)*, V. 79, 15-19.

O'Hara, M.J., and Yoder, H.S., 1967. Formation and Fractionation of Basic Magmas at High Pressure. *Scottish J. Geol.*, V.3, p.67-117.

Potts, P.J., Williams Thorpe, P., Isaacs, M.C. and Wright, D.W., 1985. High-precision instrumental neutron-activation analysis of geological samples employing simultaneous counting with both planar and coaxial detectors. *Chemical Geology*, 48, 145-155.

Richardson, S.H., Gurney, J.J., Erlank, A.J. and Harris, J.W., 1984. Origin of diamonds in old enriched mantle. *Nature*, v. 310, 198-202.

Robey, J.v A., 1981. Kimberlites of the Central Cape Province, R.S.A., Ph.D. thesis (unpubl.), University of Cape Town.

Rock, N.M.S., 1991. *Lamprophyres.* Blackie, Glasgow, 275pp.

Rogers, N.W. 1977. Granulite xenoliths from Lesotho kimberlites and the composition of the lower continental crust. *Nature* (London), 270, 681-684.

Skinner, E.M.W. and Clement, C.R. 1979. Mineralogical classifi[illegible] [illegible]uthern African kimberlites. *In* : Boyd, F.R. and M[illegible] [illegible]eds.). *Kimberlites, diatremes and diamonds* [illegible] *petrology and geochemistry.* AGU, washington, [illegible]

Skinner, E.M.W. 1989. Contrasting Group 1 and Group 2 kimberlite petrology : towards a genetic model for kimberlites. *In : Kimberlites and Related Rocks,* Volume 1, 4IKC, Perth, 1986, pp. 528-544.

Skinner, E.M.W., Viljoen, K.S., Clark, T.C., and Smith, C.B., 1991. The Petrography, Tectonic Setting and Emplacement Ages of Kimberlites in the South Western Border Region of the Kaapvaal Craton, Prieska Area, RSA. In : Ext Abst., 5IKC, Araxa, Brazil, p.373-375.

Smith, C.B., 1983a. Pb, Sr and Nd isotopic evidence for sources of southern African Cretaceous kimberlites. *Nature,* V.304, N.5921, pp. 51-54.

Smith, C.B., 1983b. Rubidium-Strontium, Uranium-Lead and

Samarium-Neodymium Isotopic Studies of Kimberlite and Selected Mantle-Derived Xenoliths. Ph.D. thesis (unpubl.), University of the Witwatersrand.

Smith, C.B., Allsopp, H.L., Kramers, J.D., Hutchinson, G. and Roddick, J.C. 1985a. Emplacement ages of Jurassic-Cretaceous South African kimberlites by the Rb-Sr method on phlogopite and whole-rock samples. *T.G.S.S.A.*, 88, 249-266.

Smith, C.B., Gurney, J.J., Skinner, E.M.W., Clement, C.R., and Ebrahim, N., 1985. Geochemical Character of southern African Kimberlites: A New Approach Based on Isotopic Constraints. *T.G.S.S.A.*, V. 88, N.2, pp.267-280.

Smith, C.B., Allsopp, H.L., Garvie, O.G., Kramers, J.D., Jackson, P.F.S., and Clement, C.R. 1989. Note on the U-Pb perovskite method for dating kimberlites : Examples from the Wesselton and De Beers mines, South Africa and Somerset Island, Canada. *Chemical Geology (Isotope Geoscience Section)*, 79, 137-145.

Smith, C.B., Clark, T.C., Barton, E.B., and Bristow, J.W., (in press). Emplacement Ages of Kimberlite Occurrences in the Prieska Region, Southwest Border of the Kaapvaal Crator. *Chem. Geol.*

Smith, C.B., Schulze, D.J., Viljoen, K.S., and Barton, E.B., 1992. The origins of the subcalcic megacryst suite in kimberlite : Implications for the origins of kimberlite and constitution of the deep subcontinental lithosphere. *In : Ext. Abst., 24th Geological Conference,* Geol. Soc. S.A., Bloemfontein, p.379-381.

Spriggs, A.J., 1988. An Isotopic and Geochemical Study of Kimberlites and Associated Alkaline Rocks from Namibia. Ph.D. thesis (unpubl.), University of Leeds.

Strelow, F.W.E., and Torien, F. von S., 1966. Separation of Lead (II) from Bismuth (III), Thallium (III), Cadmium (II), Mercury (II), Gold (III), Platinum (IV), Palladium (II) and other elements by ion exchange chromatography. *Anal. Chem.*, V.38, pp. 545-548.

Tainton, K.M. and Browning, P., 1991. The Group-2-Kimberlite-Lamproite Connection: Some Constraints from the Brakly-West District, northern Cape Province, South Africa. *In: Ext. Abs., 5IKC*, Araxa, Brazil, pp.405-407.

Tankard, A.J., Jackson, M.P.A., Eriksson, K.A., Hobday, D.K., Hunter, D.R. and Minter W.E.L., 1982. *Crustal Evolution of Southern Africa : 3.8 billion years of Earth History.* Springer-Verlag, New York.

Viljoen, K.S., 1988. *Petrology of the Sutherland Commonage Melilitite Intrusives*, MSc thesis (unpubl.), University of Cape Town.

Wagner, P.A., 1914. *The Diamond Fields of Southern Africa.* C. Struik (Pty.) Ltd., Cape Town. 355pp.

Wyllie, P.J., 1980. The origin of kimberlite. *J. Geophys. Res.*, V.85, p. 6902-6910.

York, D., 1969. Least squares fitting of a straight line with correlated errors. *E.P.S.L.*, V. 5, p. 320-324.

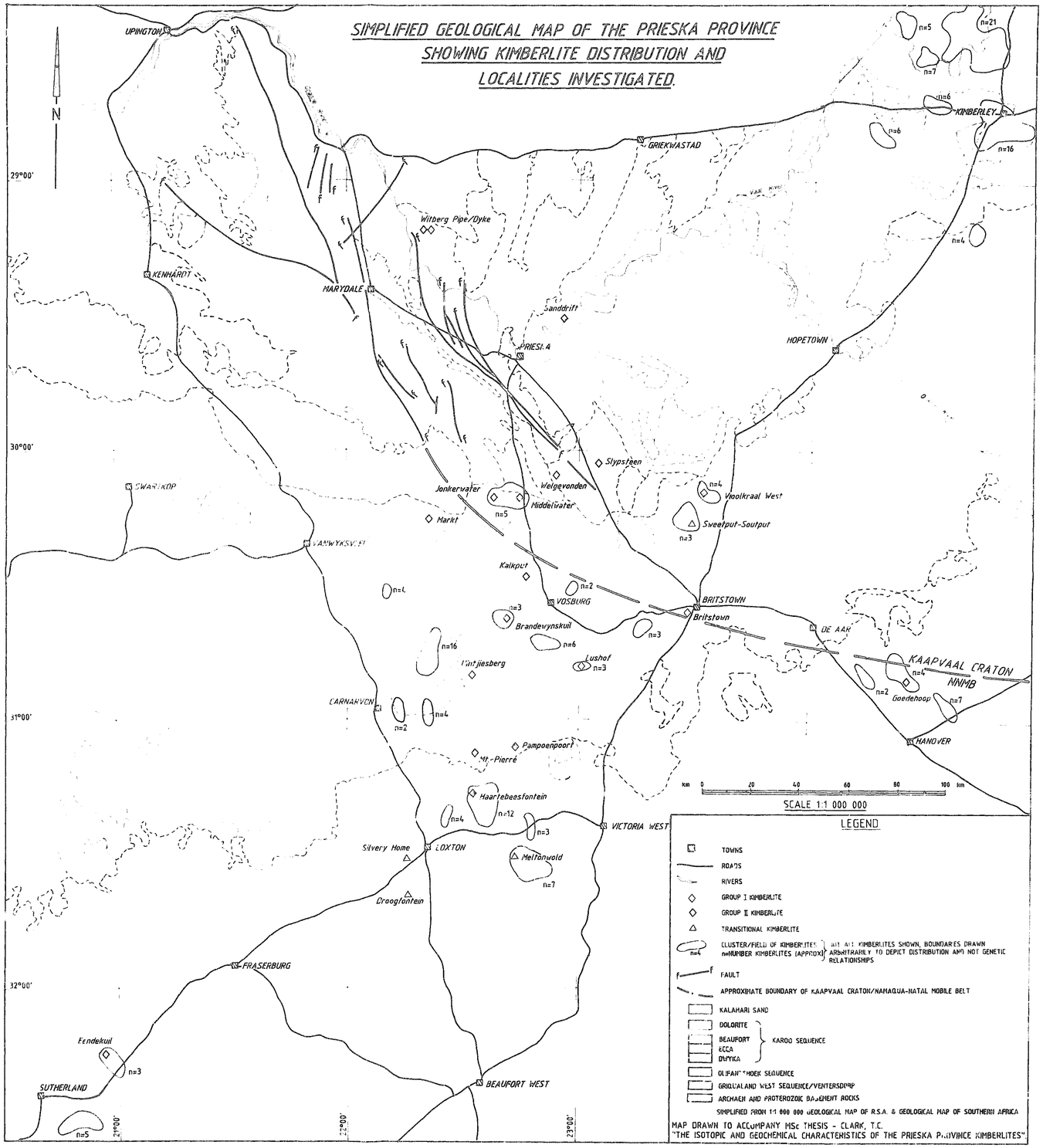
SIMPLIFIED GEOLOGICAL MAP OF THE PRIESKA PROVINCE
SHOWING KIMBERLITE DISTRIBUTION AND
LOCALITIES INVESTIGATED.
N
29°00'
30°00'
31°00'
32°00'
21°00'
22°00'
23°00'
UPINGTON
KENHARDT
MARYDALE
GRIEKWASTAD
KIMBERLEY
HOPETOWN
PRIESKA
SWARTKOP
VAN WYKSVLEI
CARNARVON
VOSBURG
BRITSTOWN
DE AAR
HANOVER
VICTORIA WEST
LOXTON
FRASERBURG
SUTHERLAND
BEAUFORT WEST
KAAPVAAL CRATON
NMMB
Witberg Pipe/Dyke
Sanddrift
Slypsteen
Welgevonden
Middelwater
Jonkerwater
Markt
Kalkput
Brandewynskuil
Lushof
Vintjiesberg
Pampoenpoort
Mt-Pierré
Haartebeesfontein
Meltonwold
Silvery Home
Droogfontein
Fendekuil
Vaalkraal West
Sweetput-Soutput
Goedehoop
n=5
n=21
n=7
n=6
n=16
n=4
n=3
n=2
n=12
km 0 20 40 60 80 100 km
SCALE 1:1 000 000
LEGEND
TOWNS
ROADS
RIVERS
GROUP I KIMBERLITE
GROUP II KIMBERLITE
TRANSITIONAL KIMBERLITE
CLUSTER/FIELD OF KIMBERLITES
n=NUMBER KIMBERLITES (APPROX)
ALL ALL KIMBERLITES SHOWN, BOUNDARIES DRAWN ARBITRARILY TO DEPICT DISTRIBUTION AND NOT GENETIC RELATIONSHIPS
FAULT
APPROXIMATE BOUNDARY OF KAAPVAAL CRATON/NAMAQUA-NATAL MOBILE BELT
KALAHARI SAND
DOLORITE
BEAUFORT
ECCA
DWYKA
KAROO SEQUENCE
OLIFANTSHOEK SEQUENCE
GRIQUALAND WEST SEQUENCE/VENTERSDORP
ARCHAEAN AND PROTEROZOIC BASEMENT ROCKS
SIMPLIFIED FROM 1:1 000 000 GEOLOGICAL MAP OF R.S.A. & GEOLOGICAL MAP OF SOUTHERN AFRICA
MAP DRAWN TO ACCOMPANY MSc THESIS - CLARK, T.C.
"THE ISOTOPIC AND GEOCHEMICAL CHARACTERISTICS OF THE PRIESKA PROVINCE KIMBERLITES"

FILING 7702

Author: Clark Trevor Charles.
Name of thesis: An integrated geochemical and isotopic study of the Prieska Province Kimberlites from the Republic of South Africa.

PUBLISHER:
University of the Witwatersrand, Johannesburg
©2015

LEGALNOTICES:

Copyright Notice: All materials on the University of the Witwatersrand, Johannesburg Library website are protected by South African copyright law and may not be distributed, transmitted, displayed or otherwise published in any format, without the prior written permission of the copyright owner.

Disclaimer and Terms of Use: Provided that you maintain all copyright and other notices contained therein, you may download material (one machine readable copy and one print copy per page)for your personal and/or educational non-commercial use only.

The University of the Witwatersrand, Johannesburg, is not responsible for any errors or omissions and excludes any and all liability for any errors in or omissions from the information on the Library website.